

Challenges and current research status of vertigo/vestibular diseases, volume II

Edited by

Andrea Castellucci, Daogong Zhang, Wenyan Li, Hubertus Axer, Nicolas Perez-Fernandez and Sulin Zhang

Coordinated by

Jun Wang

Published in

Frontiers in Neurology
Frontiers in Neuroscience



FRONTIERS EBOOK COPYRIGHT STATEMENT

The copyright in the text of individual articles in this ebook is the property of their respective authors or their respective institutions or funders. The copyright in graphics and images within each article may be subject to copyright of other parties. In both cases this is subject to a license granted to Frontiers.

The compilation of articles constituting this ebook is the property of Frontiers.

Each article within this ebook, and the ebook itself, are published under the most recent version of the Creative Commons CC-BY licence. The version current at the date of publication of this ebook is CC-BY 4.0. If the CC-BY licence is updated, the licence granted by Frontiers is automatically updated to the new version.

When exercising any right under the CC-BY licence, Frontiers must be attributed as the original publisher of the article or ebook, as applicable.

Authors have the responsibility of ensuring that any graphics or other materials which are the property of others may be included in the CC-BY licence, but this should be checked before relying on the CC-BY licence to reproduce those materials. Any copyright notices relating to those materials must be complied with.

Copyright and source acknowledgement notices may not be removed and must be displayed in any copy, derivative work or partial copy which includes the elements in question.

All copyright, and all rights therein, are protected by national and international copyright laws. The above represents a summary only. For further information please read Frontiers' Conditions for Website Use and Copyright Statement, and the applicable CC-BY licence.

ISSN 1664-8714
ISBN 978-2-8325-4909-4
DOI 10.3389/978-2-8325-4909-4

About Frontiers

Frontiers is more than just an open access publisher of scholarly articles: it is a pioneering approach to the world of academia, radically improving the way scholarly research is managed. The grand vision of Frontiers is a world where all people have an equal opportunity to seek, share and generate knowledge. Frontiers provides immediate and permanent online open access to all its publications, but this alone is not enough to realize our grand goals.

Frontiers journal series

The Frontiers journal series is a multi-tier and interdisciplinary set of open-access, online journals, promising a paradigm shift from the current review, selection and dissemination processes in academic publishing. All Frontiers journals are driven by researchers for researchers; therefore, they constitute a service to the scholarly community. At the same time, the *Frontiers journal series* operates on a revolutionary invention, the tiered publishing system, initially addressing specific communities of scholars, and gradually climbing up to broader public understanding, thus serving the interests of the lay society, too.

Dedication to quality

Each Frontiers article is a landmark of the highest quality, thanks to genuinely collaborative interactions between authors and review editors, who include some of the world's best academicians. Research must be certified by peers before entering a stream of knowledge that may eventually reach the public - and shape society; therefore, Frontiers only applies the most rigorous and unbiased reviews. Frontiers revolutionizes research publishing by freely delivering the most outstanding research, evaluated with no bias from both the academic and social point of view. By applying the most advanced information technologies, Frontiers is catapulting scholarly publishing into a new generation.

What are Frontiers Research Topics?

Frontiers Research Topics are very popular trademarks of the *Frontiers journals series*: they are collections of at least ten articles, all centered on a particular subject. With their unique mix of varied contributions from Original Research to Review Articles, Frontiers Research Topics unify the most influential researchers, the latest key findings and historical advances in a hot research area.

Find out more on how to host your own Frontiers Research Topic or contribute to one as an author by contacting the Frontiers editorial office: frontiersin.org/about/contact

Challenges and current research status of vertigo/vestibular diseases, volume II

Topic editors

Andrea Castellucci — ENT Unit, Department of Surgery, Azienda USL – IRCCS di Reggio Emilia, Italy

Daogong Zhang — Shandong Provincial ENT Hospital, China

Wenyan Li — Fudan University, China

Hubertus Axer — Jena University Hospital, Germany

Nicolas Perez-Fernandez — University Clinic of Navarra, Spain

Sulin Zhang — Huazhong University of Science and Technology, China

Topic coordinator

Jun Wang — Huazhong University of Science and Technology, China

Citation

Castellucci, A., Zhang, D., Li, W., Axer, H., Perez-Fernandez, N., Zhang, S., Wang, J., eds. (2024). *Challenges and current research status of vertigo/vestibular diseases, volume II*. Lausanne: Frontiers Media SA. doi: 10.3389/978-2-8325-4909-4

Table of contents

- 04 **Editorial: Challenges and current research status of vertigo/vestibular diseases, volume II**
Jun Wang, Andrea Castellucci, Hubertus Axer and Sulin Zhang
- 07 **Changes in functional connectivity among vestibulo-visuo-somatosensory and spatial cognitive cortical areas in persistent postural-perceptual dizziness: resting-state fMRI studies before and after visual stimulation**
Chihiro Yagi, Yuka Morita, Tatsuya Yamagishi, Shinsuke Ohshima, Shuji Izumi, Kuniyuki Takahashi, Masaki Watanabe, Kosuke Itoh, Yuji Suzuki, Hironaka Igarashi and Arata Horii
- 21 **Characteristics of spontaneous nystagmus and its correlation to video head impulse test findings in vestibular neuritis**
Xueqing Zhang, Qiaomei Deng, Yao Liu, Shanshan Li, Chao Wen, Qiang Liu, Xiaobang Huang, Wei Wang and Taisheng Chen
- 29 **Case report: MRI changes of the inner ear in an MD patient with suspected immune dysfunction**
Yurun Chen, Pengfei Zhao, Xin Ma, Tongxiang Diao and Lisheng Yu
- 33 **The auditory function in migraine model rats induced by postauricular nitroglycerin injection**
Rongxiang Qi, Jilei Zhang, Tongxiang Diao and Lisheng Yu
- 39 **Weak nystagmus in the dark persists for months after acute unilateral vestibular loss**
Chih-Chung Chen, Anand K. Bery and Tzu-Pu Chang
- 44 **Bilateral vestibulopathy: a clinical update and proposed diagnostic algorithm**
Lisa van Stiphout, David J. Szmulewicz, Nils Guinand, Angélica Pérez Fornos, Vincent Van Rompaey and Raymond van de Berg
- 52 **The effectiveness of the modified Epley maneuver for the treatment of posterior semicircular canal benign paroxysmal positional vertigo**
Xiaosu Chen, Jiesheng Mao, Hua Ye, Luping Fan, Qiaowen Tong, Hehui Zhang, Chengcheng Wu and Xiaokai Yang
- 60 **Three-dimensional characteristics of nystagmus induced by low frequency in semicircular canals of healthy young people**
Xiaobang Huang, Xueqing Zhang, Qiaomei Deng, Shanshan Li, Qiang Liu, Chao Wen, Wei Wang and Taisheng Chen
- 70 **Multi-frequency VEMPs improve detection of present otolith responses in bilateral vestibulopathy**
F. Lucieer, M. van der Lubbe, L. van Stiphout, M. Janssen, V. Van Rompaey, E. Devocht, A. Perez-Fornos, N. Guinand and R. van de Berg
- 78 **Associations between benign paroxysmal positional vertigo and seven mental disorders: a two-sample Mendelian randomization study**
Shihan Liu, Lingli Zhang, Dan Deng and Wenlong Luo



OPEN ACCESS

EDITED AND REVIEWED BY
Michael Strupp,
Ludwig Maximilian University of
Munich, Germany

*CORRESPONDENCE

Sulin Zhang
✉ sulin_zhang@hust.edu.cn
Hubertus Axer
✉ hubertus.axer@med.uni-jena.de
Andrea Castellucci
✉ andrea.castellucci@ausl.re.it

RECEIVED 29 March 2024

ACCEPTED 15 April 2024

PUBLISHED 02 May 2024

CITATION

Wang J, Castellucci A, Axer H and Zhang S
(2024) Editorial: Challenges and current
research status of vertigo/vestibular diseases,
volume II. *Front. Neurol.* 15:1409139.
doi: 10.3389/fneur.2024.1409139

COPYRIGHT

© 2024 Wang, Castellucci, Axer and Zhang.
This is an open-access article distributed
under the terms of the [Creative Commons
Attribution License \(CC BY\)](https://creativecommons.org/licenses/by/4.0/). The use,
distribution or reproduction in other forums is
permitted, provided the original author(s) and
the copyright owner(s) are credited and that
the original publication in this journal is cited,
in accordance with accepted academic
practice. No use, distribution or reproduction
is permitted which does not comply with
these terms.

Editorial: Challenges and current research status of vertigo/vestibular diseases, volume II

Jun Wang¹, Andrea Castellucci^{2*}, Hubertus Axer^{3*} and
Sulin Zhang^{1*}

¹Department of Otorhinolaryngology, Union Hospital, Tongji Medical College, Huazhong University of Science and Technology, Wuhan, China, ²ENT Unit, Department of Surgery, Azienda USL-IRCCS, Reggio Emilia, Italy, ³Department of Neurology, Jena University Hospital, Jena, Germany

KEYWORDS

vertigo, vestibular disorders, benign paroxysmal positional vertigo (BPPV), bilateral vestibulopathy (BV), Meniere's disease, persistent postural-perceptual dizziness (PPPD)

Editorial on the Research Topic

Challenges and current research status of vertigo/vestibular diseases, volume II

Vertigo and vestibular diseases are prevalent among middle-aged and older adults, posing an increased risk of falls and thereby significantly contributing to injury and disability. These conditions also exert a notable impact on individuals' psychological wellbeing. Management can be particularly challenging, as symptoms are often nonspecific and may indicate various underlying causes. The ten published articles in this Research Topic encompass clinical and basic research on common vertigo disorders, as well as reviews and case reports.

This topic includes two articles on Benign Paroxysmal Positional Vertigo (BPPV), which is the most common cause of vertigo. [Chen X. et al.](#) conducted a comparative analysis between the modified Epley maneuver and the traditional method for treating posterior semicircular canal BPPV. Their research unveiled that, compared to the traditional method, the modified Epley maneuver significantly enhanced repositioning success rates and reduced instances of canal switching. Previous research has suggested a link between BPPV and various mental disorders, but due to methodological constraints, the results remain contentious. Therefore, [Liu et al.](#) employed the Mendelian randomization method to investigate the association between BPPV and seven mental disorders. They did not find a significant causal relationship between BPPV and bipolar disorder, depression, anxiety disorder, schizophrenia, or suicidal tendencies. But they conclude that neuroticism and mood swings may be risk factors for BPPV.

There are two articles on Bilateral Vestibulopathy (BVP) in this Research Topic. BVP is known for its diverse clinical manifestations and multiple underlying causes, contributing to its heterogeneous and chronic nature. [van Stiphout et al.](#) conducted a narrative review focusing on key insights and advancements concerning the clinical presentation of BVP. Additionally, they introduced a novel diagnostic algorithm and discussed current and prospective therapeutic approaches. Moreover, variability exists in the reported presence or

absence of Vestibular Evoked Myogenic Potentials (VEMPs) among studies involving BVP patients. [Lucieer et al.](#) showcased that multi-frequency testing yielded a higher incidence of otolith responses. Cervical VEMPs (cVEMPs) were more frequently present than ocular VEMPs (oVEMPs). Notably, the majority of present VEMP responses were detected during testing at 500, 750, and 1,000 Hz, with fewer occurrences at 2,000 Hz, which also exhibited significantly higher thresholds (for cVEMPs).

Additionally, three articles focus on the application of nystagmus in this topic. Spontaneous nystagmus (SN) serves as a prevalent clinical indicator of peripheral vestibular disorders ([1, 2](#)). It commonly manifests as horizontal or horizontal-torsional, direction-fixed movements, accentuated by the removal of visual fixation. Furthermore, its slow phase velocity (SPV) adheres to Alexander's law, wherein the nystagmus amplitude intensifies when the eye moves in the direction of the fast phase ([2](#)). [Huang et al.](#) elucidated the three-dimensional features of nystagmus elicited by various semicircular canal combinations in healthy young individuals. Additionally, they established an initial reference range for the SPV and its asymmetry in nystagmus induced by the vertical semicircular canal. This research serves to deepen understanding of the mechanisms underlying semicircular canal-induced nystagmus and enhance the diagnostic precision of nystagmus in patients with otogenic vertigo. [Zhang et al.](#) demonstrated a positive correlation between the SPV of horizontal and torsional components of SN in vestibular neuritis (VN) patients and the angular vestibulo-ocular reflex (aVOR) gain asymmetry observed in the video head impulse test (vHIT). Additionally, they found that the direction of SN aligns with the plane of the affected semicircular canals. Superior VN typically presents with horizontal-vertical upward-torsional nystagmus, while total VN exhibits horizontal nystagmus with a prominent torsional component but no vertical component. Weak nystagmus, observed upon fixation removal, may occur in both normal individuals and during recovery from unilateral vestibular disturbances, yet its clinical relevance remains unclear in patients experiencing dizziness. [Chen C-C. et al.](#) conducted a comparison of nystagmus characteristics at different stages following unilateral vestibular loss. Their findings suggest that nystagmus with visual fixation may diminish as early as 1 week after the onset of acute unilateral vestibular loss. Conversely, nystagmus in the absence of visual input persisted at a subdued level for several months, with its direction predominantly aligning with the anticipated pattern of paralytic nystagmus.

In a case report, MRI follow-ups depicted the evolving transition from an initial inflammatory response to the development of endolymphatic hydrops within the inner ear ([Chen Y. et al.](#)). [Chen Y. et al.](#) detailed these progressive changes, observed from labyrinthitis to endolymphatic hydrops, as visualized in inner ear MRI scans of a patient diagnosed with Meniere's disease (MD) and suspected immune dysfunction. This visual representation highlights the correlation between MD and inflammation, offering valuable insights into its pathogenesis to inform treatment decisions. [Qi et al.](#) demonstrated that employing postauricular injection of nitroglycerin provides a safer and more effective approach for modeling migraine in rats compared to intraperitoneal injection. This novel method of establishing a migraine animal model not only confirms the impact of

migraine on hearing but also establishes a groundwork for future clinical research.

Persistent postural-perceptual dizziness (PPPD) typically arises following conditions that disrupt balance or manifest as acute or episodic vertigo, unsteadiness, or dizziness ([Yagi et al.](#)). An essential characteristic of PPPD warranting further investigation is its exacerbation upon exposure to moving or complex visual stimuli. [Yagi et al.](#) discovered that vestibular inputs may not be fully integrated within the vestibulo-visuo-somatosensory network. They observed an increase in functional connectivity (FC) between visuospatial and spatial cognitive areas even in healthy individuals following visual stimuli. Therefore, these results showing heightened FC from visual areas to spatial cognitive and prefrontal areas subsequent to visual stimuli may contribute to explaining the prolonged symptoms experienced after visual exacerbation in PPPD.

In a nutshell, this Research Topic, consisting of 10 articles covering diverse subjects within the realm of vertigo or vestibular diseases, unveiled the significant potential of this area of research and facilitated advancements in this challenging field of study.

Author contributions

JW: Writing – original draft. AC: Writing – review & editing. HA: Writing – review & editing. SZ: Writing – review & editing.

Funding

The author(s) declare that financial support was received for the research, authorship, and/or publication of this article. This work was supported by grants from the National Key Research and Development Program of China (grant nos. 2023YFC2500185 and 2023YFC2508403), the National Natural Science Foundation of China (grant nos. 82371168 and 82171152), and the Hubei Provincial Key Research and Development Program (grant no. 2023BCB027).

Conflict of interest

The authors declare that the research was conducted in the absence of any commercial or financial relationships that could be construed as a potential conflict of interest.

The author(s) declared that they were an editorial board member of Frontiers, at the time of submission. This had no impact on the peer review process and the final decision.

Publisher's note

All claims expressed in this article are solely those of the authors and do not necessarily represent those of their affiliated organizations, or those of the publisher, the editors and the reviewers. Any product that may be evaluated in this article, or claim that may be made by its manufacturer, is not guaranteed or endorsed by the publisher.

References

1. Yang TH, Lee JH, Oh SY, Kang JJ, Kim JS, Dieterich M. Clinical implications of head-shaking nystagmus in central and peripheral vestibular disorders: is perverted head-shaking nystagmus specific for central vestibular pathology? *Eur J Neurol.* (2020) 27:1296–303. doi: 10.1111/ene.14161
2. Hegemann S, Straumann D, Bockisch C. Alexander's law in patients with acute vestibular tone asymmetry—evidence for multiple horizontal neural integrators. *J Assoc Res Otolaryngol.* (2007) 8:551–61. doi: 10.1007/s10162-007-0095-6



OPEN ACCESS

EDITED BY

Daogong Zhang,
Shandong Provincial ENT Hospital, China

REVIEWED BY

Eugen Constant Ionescu,
Hospices Civils de Lyon, France
Qing Zhang,
Xinhua Hospital, Shanghai Jiaotong University
School of Medicine, China
Yameng Gu,
The Ohio State University, United States

*CORRESPONDENCE

Chihiro Yagi
✉ c-yagi@med.niigata-u.ac.jp

RECEIVED 01 May 2023

ACCEPTED 22 June 2023

PUBLISHED 24 July 2023

CITATION

Yagi C, Morita Y, Yamagishi T, Ohshima S,
Izumi S, Takahashi K, Watanabe M, Itoh K,
Suzuki Y, Igarashi H and Horii A (2023) Changes
in functional connectivity among vestibulo-
visuo-somatosensory and spatial cognitive
cortical areas in persistent postural-perceptual
dizziness: resting-state fMRI studies before and
after visual stimulation.
Front. Neurol. 14:1215004.
doi: 10.3389/fneur.2023.1215004

COPYRIGHT

© 2023 Yagi, Morita, Yamagishi, Ohshima,
Izumi, Takahashi, Watanabe, Itoh, Suzuki,
Igarashi and Horii. This is an open-access
article distributed under the terms of the
[Creative Commons Attribution License \(CC BY\)](https://creativecommons.org/licenses/by/4.0/).
The use, distribution or reproduction in other
forums is permitted, provided the original
author(s) and the copyright owner(s) are
credited and that the original publication in this
journal is cited, in accordance with accepted
academic practice. No use, distribution or
reproduction is permitted which does not
comply with these terms.

Changes in functional connectivity among vestibulo-visuo-somatosensory and spatial cognitive cortical areas in persistent postural-perceptual dizziness: resting-state fMRI studies before and after visual stimulation

Chihiro Yagi^{1*}, Yuka Morita¹, Tatsuya Yamagishi¹,
Shinsuke Ohshima¹, Shuji Izumi¹, Kuniyuki Takahashi²,
Masaki Watanabe³, Kosuke Itoh³, Yuji Suzuki³, Hironaka Igarashi³
and Arata Horii¹

¹Department of Otolaryngology Head and Neck Surgery, Niigata University Graduate School of Medical and Dental Sciences, Niigata, Japan, ²Department of Otolaryngology Head and Neck Surgery, Faculty of Medicine, University of Miyazaki, Miyazaki, Japan, ³Center for Integrated Human Brain Science, Brain Research Institute, Niigata University, Niigata, Japan

Introduction: Persistent postural-perceptual dizziness (PPPD) is a functional chronic vestibular syndrome with symptom exacerbation by upright posture, motion, and complex visual stimuli. Among these exacerbating factors, visual exacerbation is the most specific characteristic of PPPD requiring further investigation. We hypothesized that stimulus-induced changes occur in the functional connectivity (FC) rather than simple neural activation that is involved in visual stimulation. The present study aimed to identify the neural basis of PPPD by investigating FC before and after visual stimulation.

Methods: Eleven patients with PPPD and 11 age- and sex-matched healthy controls (HCs) underwent resting-state fMRI (rs-fMRI) before and after task-based fMRI with visual stimuli.

Results: At pre-stimulus, FC between the vestibular cortex and visual areas was low, while that between the somatosensory and visual areas was high in PPPD compared with that in HCs. FC between the visuospatial (parahippocampal gyrus) and spatial cognitive areas (inferior parietal lobule) was elevated in PPPD even in the pre-stimulus condition, which no longer increased at post-stimulus as observed in HCs. In the post-stimulus condition, FC between the visual and spatial cognitive areas and that between the visual and prefrontal areas increased compared with that in the pre-stimulus condition in PPPD. Task-based fMRI demonstrated that no brain regions showed different activities between the HC and PPPD groups during visual stimulation.

Discussion: In PPPD, vestibular inputs may not be fully utilized in the vestibulo-visuo-somatosensory network. Given that the FC between visuospatial and spatial cognitive areas increased even in HCs after visual stimuli, elevated status of this

FC in combination with the high FC between the somatosensory and visual areas would be involved in the visual exacerbation in PPPD. An increase in FC from the visual areas to spatial cognitive and prefrontal areas after visual stimuli may account for the prolonged symptoms after visual exacerbation and anxious status in PPPD.

KEYWORDS

persistent postural-perceptual dizziness, resting-state functional magnetic resonance imaging, functional connectivity, visual stimuli, vestibular system, chronic dizziness

1. Introduction

Persistent postural-perceptual dizziness (PPPD) is a functional vestibular disorder characterized by chronic vestibular symptoms lasting over 3 months. The core symptoms are dizziness, unsteadiness, and non-spinning vertigo that are exacerbated by three factors: upright posture or walking, active or passive movement, and exposure to moving or complex visual stimuli (1).

Persistent postural-perceptual dizziness is usually preceded by conditions that disrupt balance or cause acute or episodic vertigo, unsteadiness, or dizziness. The most common preceding conditions are peripheral or central vestibular disorders (1, 2). Posture is maintained by three sensory inputs: visual, vestibular, and somatosensory information. Preceding vestibular disorders disrupt balance and posture, leading to two reactions: first, heightened vigilance as expressed by postural stiffness during standing and walking, which is also observed in healthy individuals when standing on elevated or unstable surfaces (3–5), and second, increased reliance on visual and/or somatosensory information (6, 7). Generally, these two conditions return to normal with the recovery of the preceding disease. However, the psychological trend of patients with PPPD involving neuroticism or introversion (8, 9) could influence the persistence of these conditions (10). Sustained heightened vigilance

and increased reliance on visual and/or somatosensory information cause persistent dizziness and exacerbation by visual stimuli and motions (11). Ultimately, these processes may alter the spatial orientation (12) and impair postural control in complex environments (13, 14).

Recent neuroimaging studies on PPPD have gradually revealed the neural mechanisms that account for the abovementioned pathophysiological models. Resting-state functional MRI (rs-fMRI) and voxel-based morphometry have shown reduced functional connectivity (FC) and decreased gray matter volume, respectively, in multimodal vestibular cortical areas of patients with PPPD compared with those of healthy controls (HCs) (15, 16). Among three exacerbating factors, visual exacerbation is the most specific characteristic of PPPD (17) and requires further investigation. Therefore, we focused on the neural mechanisms underlying visual exacerbation in this study. Once symptom exacerbation by visual stimuli occurs, it persists for hours or more, suggesting that the stimulus-induced changes occur in FC rather than the simple neural activation that is involved in the visual stimulation. Hence, we performed rs-fMRI on patients with PPPD and normal volunteers before and after visual stimulation. In addition, task-based fMRI analysis was also performed during visual stimulation.

2. Methods

2.1. Patients

Eleven patients with PPPD were enrolled in this study between October 2020 and September 2021. As a control group, 11 healthy volunteers who were matched for age, sex, and handedness to patients with PPPD were included. All healthy volunteers had no history of vertigo or dizziness and no serious medical diseases.

Persistent postural-perceptual dizziness was diagnosed using the diagnostic criteria of the Barany Society (1). The Japanese version of the dizziness handicap inventory (DHI) (18, 19) was used to assess the severity of vestibular symptoms, the Hospital Anxiety and Depression Scale (HADS) (20) to evaluate anxiety and depression levels, the Japanese version of the Ten Item Personality Inventory (TIPI-J) (21, 22) to assess personality, the Visual Analog Scale (VAS) to evaluate the degree and changes in vestibular symptoms before and after the visual stimuli, and the Simulator Sickness Questionnaire (SSQ) (23) to evaluate visual stimulation-induced symptoms.

To assess the patients' vestibular function, bithermal caloric testing, rotatory chair test (RCT), video head impulse test (vHIT),

Abbreviations: PPPD, persistent postural-perceptual dizziness; FC, functional connectivity; HCs, healthy controls; rs-fMRI, resting-state fMRI; DHI, dizziness handicap inventory; HADS, hospital anxiety and depression scale; TIPI-J, the Japanese version of the Ten Item Personality Inventory; VAS, visual analog scale; SSQ, simulator sickness questionnaire; RCT, rotatory chair test; vHIT, video head impulse test; cVEMP, cervical vestibular evoked myogenic potentials; oVEMP, ocular vestibular-evoked myogenic potential; SVV, subjective visual vertical; CP, canal paresis; VOR, vestibulo-ocular reflex; CUS, catch-up saccades; IAARs, interaural asymmetry ratios; 3D-FSPGR, three-dimension spoiled gradient recalled echo; TR, repetition time; FOV, field of view; TE, echo time; MNI, Montreal neurological institute; FWHM, fullwidth at half-maximum; PIVC, parieto-insular vestibular cortex; PIC, posterior insular cortex; ICC, intracalcarine cortex; SCC, supracalcarine cortex; LG, lingual gyrus; CC, cuneal cortex; PostCG, post-central gyrus; aPaHC and pPaHC, anterior/posterior parahippocampal gyrus; HC, hippocampus; FWE, family-wise error; IQR, interquartile ranges; AUVP, acute unilateral vestibulopathy; BPPV, benign paroxysmal positional vertigo; toMTG/toITG, temporooccipital part of middle/inferior temporal gyrus; pSMG/AG, posterior division of supramarginal gyrus/angular gyrus; FP, frontal pole; PCG, paracingulate gyrus; SFG, superior frontal gyrus; sLOC, superior division of lateral occipital cortex; MidFG, middle frontal gyrus; pSMG, posterior supramarginal gyrus.

cervical and ocular vestibular-evoked myogenic potential (cVEMP and oVEMP, respectively), and subjective visual vertical (SVV) test were conducted. Bithermal caloric testing was performed by stimulating each external auditory canal twice with air at 26°C and 45°C for 60 s at 5-min intervals. The maximum slow phase velocity was measured using an electronystagmography and canal paresis (CP; %) was calculated using Jongkee's index formula (24). RCT was done with a rotatory chair to which a pendulum-like rotation was applied, so that the maximum head angular velocity was 50°/s at a stimulation frequency of 0.1 Hz. The eye movements were monitored using an electronystagmography and vestibulo-ocular reflex (VOR) gain was calculated. vHIT was conducted using EyeSeeCam® (Interacoustics, Denmark) to assess the VOR gain and corrective catch-up saccades (CUS) during a rapid high-velocity head turn. cVEMP and oVEMP using the Neuropack System® (Nihon Kohden, Japan) were performed to evaluate the otolithic function, and the interaural asymmetry ratios (IAARs) of the cVEMP and oVEMP were used as indicators of saccular and utricular function, respectively. SVV test was also conducted to assess otolithic function using the SVV examination system (UNIMEC, Japan). CP greater than 25%, VOR gain less than 0.3 in RCT (25), VOR gain less than 0.8 with CUS in vHIT (26), IAAR greater than 32% (27, 28), and SVV greater than 2.5 degrees (29) were considered abnormal values.

All participants underwent static posturography on a solid or foam rubber surface using Gravicoda® (ANIMA Corp., Japan) with eyes open and in closed conditions. The elliptical balance area (cm²) was adopted as a representative index of the degree of postural sway. Pure tone audiometry, blood pressure measurement, and blood routine tests were performed if indicated.

2.2. Experimental design and visual stimuli

Rs-fMRI was acquired before (pre-stimulus) and after (post-stimulus) visual stimulation for 320 s each (Figure 1). The data from the initial 20 s were discarded to ensure a steady state. The visual stimulation task designed and used in this study consisted of five different visual stimuli. Each block consisted of 180 s, and the data for the initial 30 s were discarded to ensure a steady state. The rest and task were administered alternately for 30 s each.

The visual stimuli used in this study were created with the After Effects software (Adobe Inc., San Jose, CA, United States) by attempting to reproduce the stimuli of scenes that are likely to exacerbate symptoms in patients with PPPD in daily life, such as flashing lights on TV, scenery flowing sideways when viewed from inside a train, and scenery flowing from front to back when riding in a passenger car. In the experiments, visual stimuli consisted of (i) a checkerboard pattern stimulus comprising 8 rows × 12 columns of squares reversed in contrast (100%) at 0.5 Hz, (ii) a checkerboard pattern stimulus comprising 2 rows × 2 columns of squares reversed in contrast (100%) at 12 Hz, (iii) a checkerboard pattern stimulus comprising 8 rows × 12 columns of squares reversed in contrast (100%) at 12 Hz, (iv) optokinetic stimulus by 12 black-and-white vertical stripes sweeping across a screen at 6°/s, and (v) radial optic flow stimulus with moving white dots (size: 0.1–1.1 degrees of visual angle, speed: 3°/s with a flat speed gradient) on a black background expanding from the center of the screen. For visual stimuli (i), (ii), and (iii), a checkerboard pattern comprising 2 rows × 2 columns of squares reversed in contrast (100%) at 0.5 Hz was presented as rest. For visual stimuli (iv) and (v), the respective static images were presented as rest.

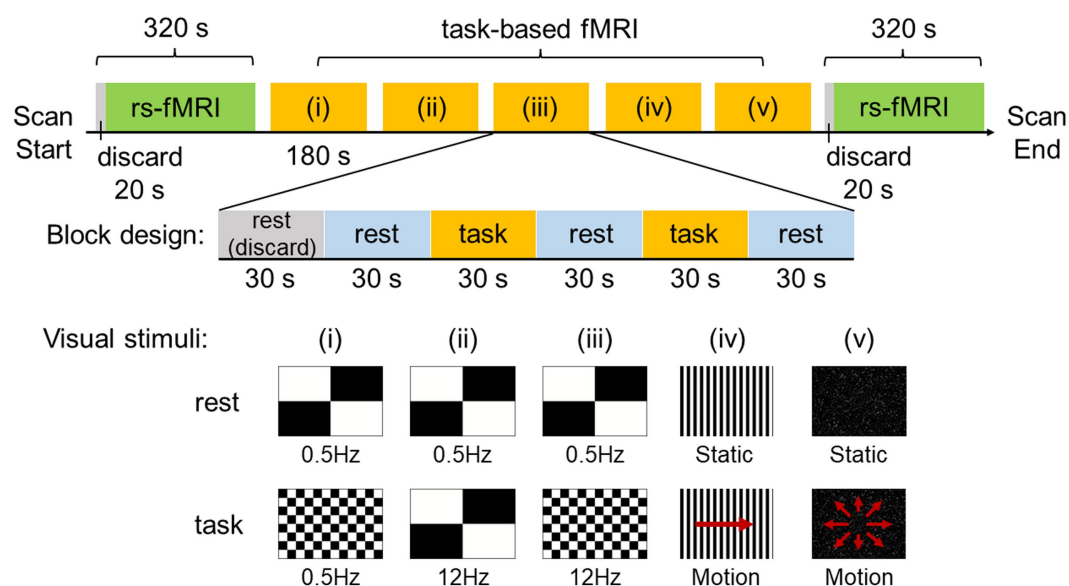


FIGURE 1

Experimental design and visual stimuli. Resting-state functional MRI (rs-fMRI) was acquired before and after visual stimulation for 320 s each and the data for the initial 20 s was discarded to ensure a steady state. The visual stimulation task used in this study utilized a block design and consisted of five different visual stimuli. One block consisted of 180 s, with the data for the initial 30 s discarded to ensure a steady state. Rest and task were administered alternately for 30 s each.

2.3. Imaging

All imaging data were acquired on the Signa LX 3.0-Tesla (GE Medical System) imaging system with an 8-channel head coil. During image acquisition, the participants were instructed to relax, stay awake, and focus on the middle of the screen throughout the experiment. As a general quality assurance procedure, functional scans were checked for head movements with a translation not exceeding 0.6 mm in any axis during each run. If a head movement exceeding 0.6 mm was observed, the run was re-performed. The structural images were recorded using a three-dimension spoiled gradient recalled echo (3D-FSPGR) sequence [repetition time (TR), 7.4 ms; field of view (FOV), $200 \times 200 \text{ mm}^2$; voxel size, $0.781 \times 0.781 \times 1.5 \text{ mm}^3$; matrix, 256×256 ; echo time (TE), 3.04 ms; flip angle, 20° ; slice thickness, 1.5 mm; slice spacing, 1.5 mm]. The functional images were obtained using gradient-echo echo-planar pulse sequence (TR, 1000 ms; FOV, $200 \times 200 \text{ mm}^2$; voxel size, $3.125 \times 3.125 \times 7.5 \text{ mm}^3$; matrix, 64×64 ; TE, 30 ms; flip angle, 70° ; slice thickness, 5 mm; slice spacing, 7.5 mm).

2.4. Preprocessing

2.4.1. rs-fMRI

The rs-fMRI images were preprocessed using Statistical Parametric Mapping 12 (SPM12, Wellcome Department of Cognitive Neurology, United Kingdom) and the CONN toolbox (version 21a; <http://www.nitrc.org/projects/conn>) working on MATLAB R2022a (MathWorks, Inc., Natick, United States). The preprocessing and quality assurance of functional and structural MRI data were performed according to the default pipeline implemented in CONN as follows: (a) realignment and unwarp, (b) slice timing correction, (c) outlier detection with conservative settings (95th percentile of the normative sample), (d) segmentation and normalization (transform to the Montreal Neurological Institute [MNI] space), and (e) smoothing using a 6-mm fullwidth at half-maximum (FWHM) Gaussian kernel. After the preprocessing, time points were identified as outliers if movement from a preceding image exceeded a 0.5 mm deviation or global mean signal intensity exceeded 3 standard deviations. These time points were included as regressors along with principal components extracted from anatomical noise regions and realignment parameters during a denoising step. Finally, a band-pass filter was applied to the functional data with a frequency window of 0.008–0.09 Hz.

2.4.2. Task-based fMRI

The task-based fMRI images were preprocessed using the SPM12 software. Functional images were realigned to the first image in the series to correct for within-scan head motions, performed slice timing correction to correct for temporal misalignment of slices, coregistered with the T1-weighted structural image for each subject, normalized to the MNI space, and spatially smoothed by an 8-mm FWHM Gaussian kernel.

2.5. Data analysis

2.5.1. Demographic and clinical characteristics

To compare the demographic and clinical characteristics between the HC and PPPD groups, the Mann–Whitney *U* test was performed

for HADS, TIPI-J, SSQ, and posturographic data. Statistical significance was set at $p < 0.05$. Statistical analyses were performed using GraphPad Prism version 9 (GraphPad Software, San Diego, CA, United States).

2.5.2. rs-fMRI analysis

We performed seed-to-voxel resting-state FC analysis using priori-defined seed regions related to the vestibular, visual, somatosensory, and spatial cognitive regions of the brain. For the vestibular cortex, we selected the parieto-insular vestibular cortex (PIVC) and posterior insular cortex (PIC). The seed regions were determined as spheres with a radius of 5 mm, according to the latest structural study (30): $x = -36$, $y = -25$, $z = 18$ for the left PIVC; $x = 36$, $y = -22$, $z = 17$ for the right PIVC; $x = -46$, $y = -33$, $z = 24$ for the left PIC; and $x = 51$, $y = -27$, $z = 28$ for the right PIC. For the visual cortex, we selected the intracalcarine cortex (ICC), supracalcarine cortex (SCC), lingual gyrus (LG), and cuneal cortex (CC) bilaterally. For the somatosensory cortex, we selected the post-central gyrus (PostCG) bilaterally. For the visuospatial and spatial cognitive regions, we selected the anterior/posterior parahippocampal gyrus (aPaHC and pPaHC) and hippocampus (HC), respectively. The above seeds related to visual, somatosensory, and spatial cognition were determined from the atlas, which consists of cortical or subcortical regions of interest from the FSL Harvard–Oxford Atlas and is included by default in CONN.

To infer clusters of voxels functionally connected to each seed region, two thresholds were sequentially applied based on the random field theory method, used with a cluster-forming threshold of uncorrected $p < 0.001$ and cluster-level threshold of $p < 0.05$ corrected for multiple comparisons by using family-wise error (FWE).

To compare the base FC conditions between patients with PPPD and HCs, a two-sample *t*-test was performed on the pre-stimulus data.

For comparisons between pre- and post-stimulus in the PPPD group, data from only patients in whom dizziness symptoms were exacerbated by the visual stimuli, confirmed by an increase in the VAS score compared with that of pre-stimulus, were used. Differences in FC between pre- and post-stimulus in HCs or PPPD were tested using a paired *t*-test.

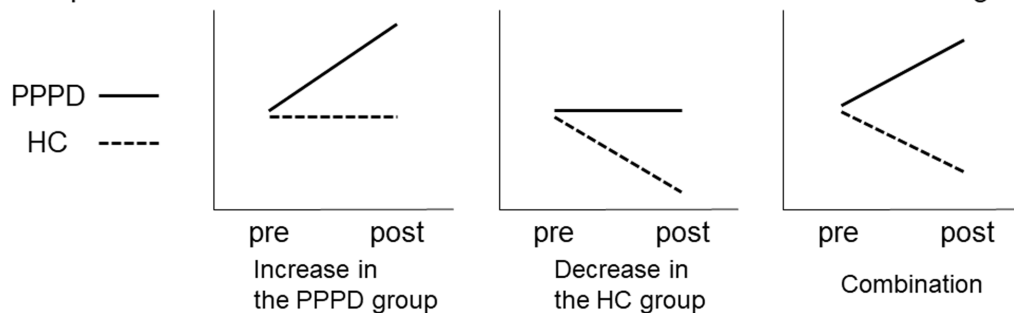
To detect regions showing a significant change in FC after visual stimuli in the PPPD group, differences between pre- and post-stimulus were evaluated relative to those of the HC group. This was tested using a 2×2 mixed ANOVA interaction. The patterns of changes in PPPD/HC group showed significant differences between the pre- and post-stimulus conditions in the PPPD group relative to the HC group (Figure 2). When the patterns of the relative increase in FC are observed after visual stimuli in the PPPD group, the following three possibilities may be included: increase in the PPPD group, decrease in the HC group, and a combination of both (the upper row). Similarly, when the patterns of the relative decrease in FC are observed after visual stimuli in the PPPD group, the following three possibilities may be included: decrease in the PPPD group, increase in the HC group, and a combination of both (the lower row).

For all group analyses, we used FWE-corrected values for multiple comparisons, and $p < 0.05$ was considered to indicate statistical significance.

2.5.3. Task-based fMRI analysis

For the first-level analysis, the onsets and durations of the task were modeled, and the change in brain activity during the task relative

The patterns of relative increase in FC after visual stimuli in the PPPD group



The patterns of relative decrease in FC after visual stimuli in the PPPD group

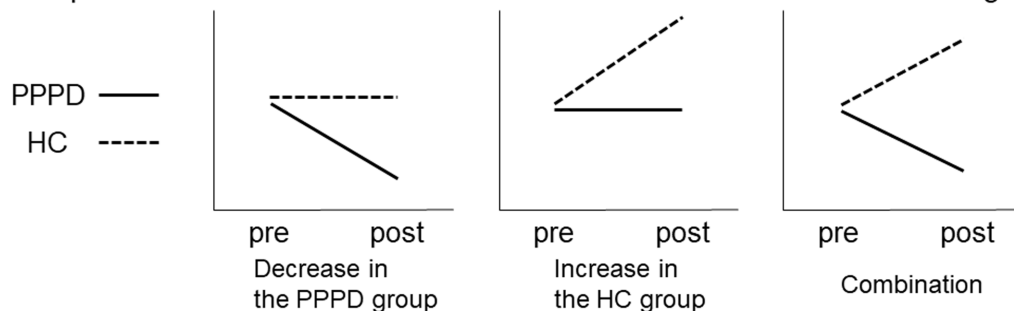


FIGURE 2

Relative increase or decrease in FC after visual stimuli in the PPPD group. Patterns of changes in PPPD/HC group showed significant differences between the pre- and post-stimulus conditions in the PPPD group relative to the HC group. The upper and lower row shows the patterns of relative increase or decrease after visual stimulation in the PPPD group, respectively. FC, functional connectivity; HC, hippocampus; PPPD, persistent postural-perceptual dizziness.

to that during rest was set as a contrast. For the second-level analysis, the group analyses with unpaired *t*-tests comparing the HC and PPPD groups were performed with a significant threshold at FWE-corrected $p < 0.05$.

2.6. Ethics statement

This study was approved by the institutional review board of Niigata University Medical and Dental Hospital (Niigata city, Japan; #2019-0021). All procedures performed in this study were in accordance with the ethical standard of the 1964 Helsinki Declaration. Informed consent was obtained from all participants at the time of inclusion in the study, authorizing the anonymous use of data for further studies.

3. Results

3.1. Demographic and clinical characteristics

Table 1 summarizes the demographic and clinical data of the HC and PPPD groups. Two males and nine females were included in each group. All participants were right-handed. There was no significant difference in age between the two groups. As shown in Table 1, the Mann–Whitney *U* test demonstrated that the HADS score (total

score) and the neuroticism score of the TIPI-J were significantly higher in the PPPD group than in the HC group. There was no significant difference in the elliptical balance area (with eyes open) between the two groups, while the elliptical balance area (with eyes closed, eyes open on foam rubber, eyes closed on foam rubber) of the PPPD group was significantly larger than that of the HC group. The SSQ score of the PPPD group was significantly higher than that of the HC group.

Table 2 summarizes the demographic data of each patient with PPPD. The median duration of disease was 32 months (interquartile ranges [IQR]: 14 months), and the preceding diseases were acute unilateral vestibulopathy (AUV) in 6 patients, benign paroxysmal positional vertigo (BPPV) in 4 patients, and chronic anxiety disorders in 1 patient. The median DHI score was 34 (IQR: 48). Of the 11 patients with PPPD, 5 were taking escitalopram or venlafaxine. Eight of 11 patients had exacerbation of dizziness symptoms by visual stimulation, which was confirmed by an increase in the VAS score compared with that of pre-stimulus data. Data from only these eight exacerbated patients were used for comparisons between pre- and post-stimulus in the PPPD group. In contrast, no participant in the HC group complained of dizziness symptoms during/after visual stimuli.

Vestibular test results for patients with PPPD are shown in Supplementary Table 1. Some patients (P01, P06, and P09) showed results deviating from the normal range; however, no cases of obvious peripheral vestibular dysfunction were found based on the overall findings of the examination.

3.2. Pre-stimulus FCs in PPPD and HCs

The PPPD group showed several significant differences in FC compared with the HC group at pre-stimulus. FC between the left

TABLE 1 Demographic profiles and characteristics of the healthy controls (HCs) and patients with persistent postural-perceptual dizziness (PPPD).

Variables	HCs	PPPD	Value of <i>p</i> (Mann–Whitney <i>U</i> test)
Sample size (male/female)	11 [2/9]	11 [2/9]	
Age, years	46 (8)	42 (4)	0.30
HADS (total score)	9 (7)	16 (14)	<0.01**
TIPI-J Extraversion	4.5 (3.0)	2.5 (3.5)	0.07
Agreeableness	5.0 (1.5)	4.5 (2.5)	0.39
Conscientiousness	4.0 (2.0)	4.0 (1.5)	0.66
Neuroticism	3.5 (2.0)	6.0 (2.5)	<0.01**
Openness	3.5 (3.0)	4.0 (2.5)	0.21
Elliptical balance area, cm ² Eyes open	3.3 (3.7)	6.1 (3.9)	0.19
Eyes closed	4.5 (3.8)	9.3 (7.9)	0.02*
Eyes open on foam rubber	6.1 (2.5)	9.6 (5.1)	<0.01**
Eyes closed on foam rubber	10.6 (5.6)	17.6 (15.6)	<0.01**
SSQ (total score)	3.7 (18.7)	44.9 (78.5)	<0.01**

*Values indicate statistical significance. **p* < 0.05; ***p* < 0.01.

Values are reported as median and interquartile range.

HADS, Hospital Anxiety and Depression Scale; HCs, healthy controls; PPPD, persistent postural-perceptual dizziness; SSQ, Simulator Sickness Questionnaire; TIPI-J, Ten Item Personality Inventory.

PostCG and the right temporooccipital part of the middle/inferior temporal gyrus (toMTG/toITG), right aPaHC and the right posterior division of supramarginal gyrus/angular gyrus (pSMG/AG), and the right HC and the left frontal pole (FP) in the PPPD group was significantly higher than that in the HC group at pre-stimulus (Figure 3; Table 3). Conversely, FC between the right PostCG and the left FP, the right PIVC and the bilateral LG, and the left PIVC and the left FP/paracingulate gyrus/superior frontal gyrus (FP/PCG/SFG) in the PPPD group was significantly lower than those in the HC group (Figure 3; Table 3).

3.3. Differences between pre- and post-stimulus FCs

As shown in Figure 4 and Table 4, FC between the right PIVC and left LG and that between the right SCC and left pSMG significantly increased in the post-stimulus condition than those in the pre-stimulus condition in the PPPD group. FC between the right PostCG and right pSMG and that between the right CC and left pMTG significantly decreased in the post-stimulus condition than those in the pre-stimulus condition in the PPPD group. No FC other than these 4 FCs showed significant changes after the stimulus compared with those before the stimulus in PPPD.

As shown in Figure 5 and Table 5, FC between the right aPaHC and right pSMG, which was significantly lower in the HC group than in the PPPD group before the stimulus (Figure 3; Table 3), significantly increased in the post-stimulus condition than those in the pre-stimulus condition in the HC group. FC between the right CC and left FP significantly increased, whereas FC between the right ICC and right superior division of lateral occipital cortex (sLOC) was significantly decreased in the post-stimulus condition than that in the pre-stimulus condition in the HC group.

TABLE 2 Demographic characteristics of patients with persistent postural-perceptual dizziness (PPPD).

Patient no.	Age (years)	Sex (M/F)	Duration (months)	Preceding disease	DHI	Medication	VAS (before→after)/ Exacerbation (+ or −)
P01	43	F	32	AUVP	10	Escitalopram	5 → 7/(+)
P02	41	F	27	BPPV	82	(−)	3 → 8/(+)
P03	42	F	7	AUVP	34	(−)	2 → 6/(+)
P04	42	F	33	AUVP	12	Venlafaxine	3 → 3/(−)
P05	45	M	34	BPPV	50	(−)	6 → 6/(−)
P06	39	F	5	BPPV	74	(−)	5 → 7/(+)
P07	41	F	50	AUVP	48	Escitalopram	0 → 2/(+)
P08	47	M	73	AUVP	26	(−)	4 → 7/(+)
P09	32	F	23	AUVP	64	Venlafaxine	7 → 9/(+)
P10	44	F	35	BPPV	30	Escitalopram	1 → 1/(−)
P11	40	F	6	Chronic anxiety disorders	16	(−)	4 → 5/(+)

AUVP, acute unilateral vestibulopathy; BPPV, benign paroxysmal positional vertigo; DHI, Dizziness Handicap Inventory; F, female; HADS, Hospital Anxiety and Depression Scale; M, male; PPPD, persistent postural-perceptual dizziness; VAS, visual analog scale.

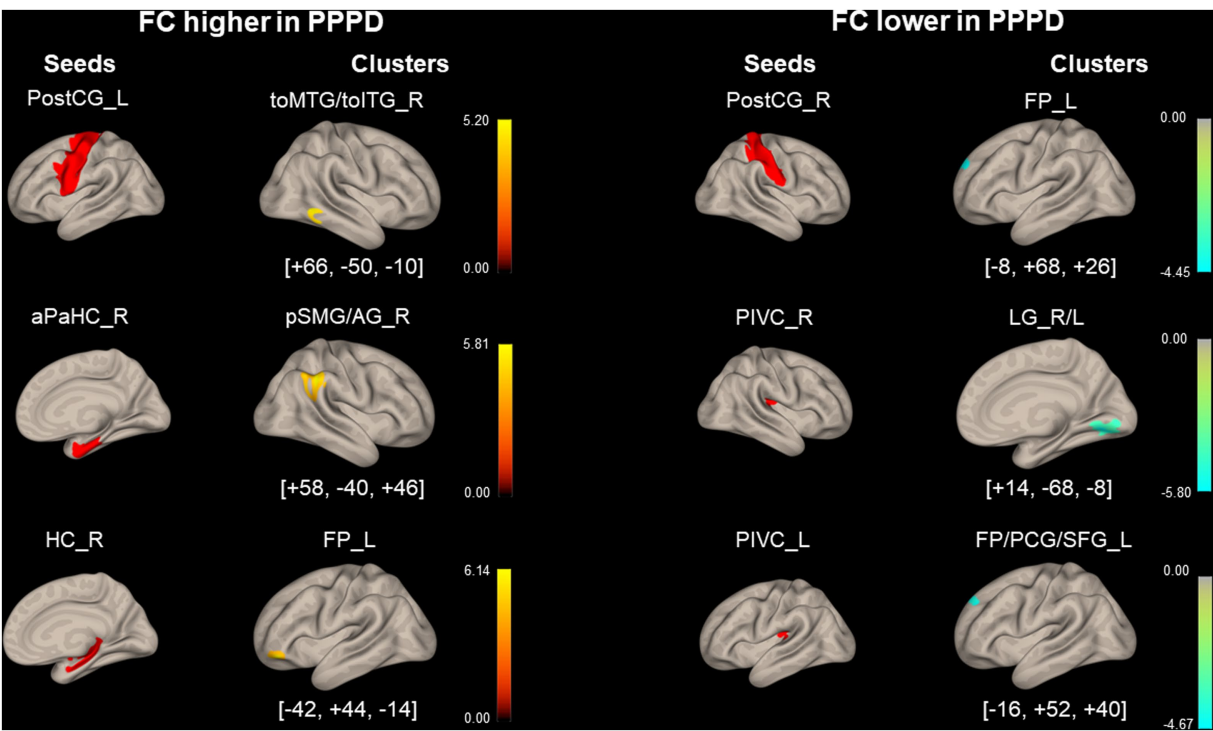


FIGURE 3 Significantly different functional connectivity between patients with persistent postural-perceptual dizziness and healthy controls under the pre-stimulus condition. Seed regions are shown in red, higher functional connectivity (FC) is indicated by yellow bars, and lower FC is indicated by green bars. The color bar represents *T* scores. The [x, y, z] values indicate the Montreal Neurological Institute (MNI) coordinates. aPaHC, anterior parahippocampal gyrus; FP, frontal pole; FP/PCG/SFG, frontal pole/paracingulate gyrus/superior frontal gyrus; HC, hippocampus; LG, lingual gyrus; PIVC, parieto-insular vestibular cortex; PPPD, persistent postural-perceptual dizziness; pMTG, posterior middle temporal gyrus; postCG, post-central gyrus; pSMG/AG, posterior supramarginal gyrus/angular gyrus; toMTG/toITG, temporooccipital middle/inferior temporal gyrus.

TABLE 3 Significantly different functional connectivity (FC) between patients with persistent postural-perceptual dizziness (PPPD) and healthy controls (HCs) in the pre-stimulus condition.

Seed region	Cluster coordinates (x, y, z)	Cluster size	Cluster regions	Cluster value of <i>p</i> (FWE)
<i>Higher FC in PPPD</i>				
Postcentral Gyrus_L	+ 66– 50– 10	138	Middle/Inferior Temporal Gyrus, temporooccipital part_R	0.015
Parahippocampal Gyrus, anterior division_R	+ 58– 40+ 46	589	Supramarginal Gyrus, posterior division_R/Angular Gyrus_R	<0.001
Hippocampus_R	– 42+ 44– 14	215	Frontal Pole_L	<0.001
<i>Lower FC in PPPD</i>				
Postcentral Gyrus_R	– 8+ 68+ 26	145	Frontal Pole_L	<0.01
PIVC_R	+ 14– 68– 8	738	Lingual Gyrus_R/L	<0.001
PIVC_L	– 16+ 52+ 40	140	Frontal Pole_L/Paracingulate Gyrus_L/Superior Frontal Gyrus_L	<0.01

R/L, bilateral; FC, functional connectivity; FWE, family-wise error; HCs, healthy control; L, left; PIVC, parieto-insular vestibular cortex; PPPD, persistent postural-perceptual dizziness; R, right.

3.4. Differences between pre- and post-stimulus FCs in PPPD relative to HCs

Figure 6 and Table 6 show the FCs modulated by visual stimulation in the PPPD group relative to the HC group. FC

between the right ICC and the left pSMG, the right SCC and the left middle frontal gyrus (MidFG), and the right CC and the right MidFG significantly increased in the post-stimulus condition in the PPPD group relative to the HC group. It should be noted that this was an increase relative to that in the HC group. Since these three

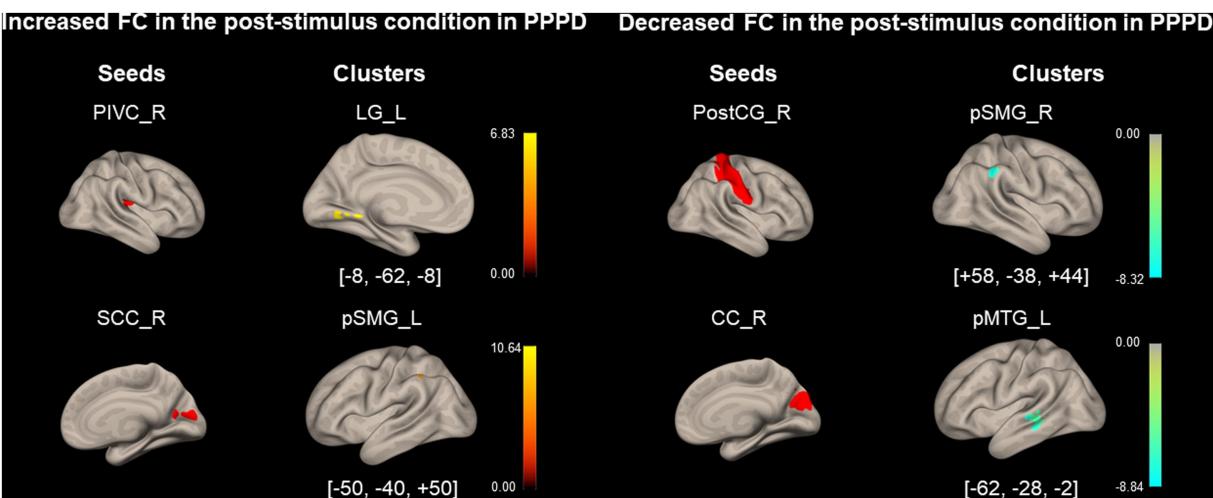


FIGURE 4 Significantly modified functional connectivity under the post-stimulus condition in the persistent postural-perceptual dizziness group. Seed regions are shown in red, increased functional connectivity (FC) is indicated by yellow bars, and decreased FC is indicated by green bars. The color bar represents *T* scores. The [x, y, z] values indicate the Montreal Neurological Institute (MNI) coordinates. CC, calcarine cortex; LG, lingual gyrus; PIVC, parieto-insular vestibular cortex; PPPD, persistent postural-perceptual dizziness; pMTG, posterior middle temporal gyrus; postCG, post-central gyrus; pSMG, posterior supramarginal gyrus; SCC, supracalcarine cortex.

TABLE 4 Significantly modified functional connectivity (FC) in the post-stimulus condition in the persistent postural-perceptual dizziness (PPPD) group.

Seed region	Cluster coordinates (x, y, z)	Cluster size	Cluster regions	Cluster value of <i>p</i> (FWE)
<i>Increased FC</i>				
PIVC_R	-8 -62 -8	98	Lingual Gyrus_L	<0.001
Supracalcarine Cortex_R	-50 -40 +50	77	Supramarginal Gyrus, posterior division_L	<0.01
<i>Decreased FC</i>				
Postcentral Gyrus_R	+58 -38 +44	99	Supramarginal Gyrus, posterior division_R	<0.01
Cuneal Cortex_R	-62 -28 -2	119	Posterior Middle Temporal Gyrus_L	<0.001

FC, functional connectivity; PPPD, persistent postural-perceptual dizziness; FWE, family-wise error; L, left; PIVC, parieto-insular vestibular cortex, R, right.

FCs neither occurred in the list of increased FC after visual stimulus in the PPPD group (Figure 4; Table 4) nor in that of decreased FC after visual stimulus in the HC group (Figure 5; Table 5), increase in these FCs could be derived from the combination of increase and decrease in FC of the PPPD and HC groups, respectively (See Methods and Figure 2). FC between the left PostCG and the right toMTG/toITG, the right aPaHC and the right pSMG/AG, and the

left aPaHC and the right toMTG/AG/pSMG significantly decreased in the PPPD group compared with that in the HC group (Figure 6; Table 6). Among these, FC between the right aPaHC and the right pSMG/AG was higher in the PPPD group than that in the HC group in the pre-stimulus condition (Figure 3; Table 3). There were no significant changes in this FC between pre- and post-stimulus conditions in the PPPD group (Figure 4; Table 4), while this FC significantly increased in the post-stimulus than in the pre-stimulus condition in the HC group (Figure 5; Table 5). In summary, the relative decrease in FC observed in the post-stimulus condition of PPPD may imply that this FC increased after visual stimulation in the HC group; however, it could no longer occur in the PPPD group, perhaps this FC had already been fully facilitated even in the pre-stimulus condition.

3.5. Brain activity during visual stimulation in PPPD: task-based fMRI analysis

No areas were significantly activated/inhibited during all five visual stimulations in the PPPD group compared with those in the HC group (data not shown).

4. Discussion

4.1. Demographic and clinical characteristics of PPPD

As shown in Table 1, the PPPD group had higher total scores for HADS and neuroticism scores for TIPI-J than the HC group. These psychiatric trends of patients with PPPD, i.e., anxiety/depression and neuroticism are consistent with those in previous reports (8, 31).

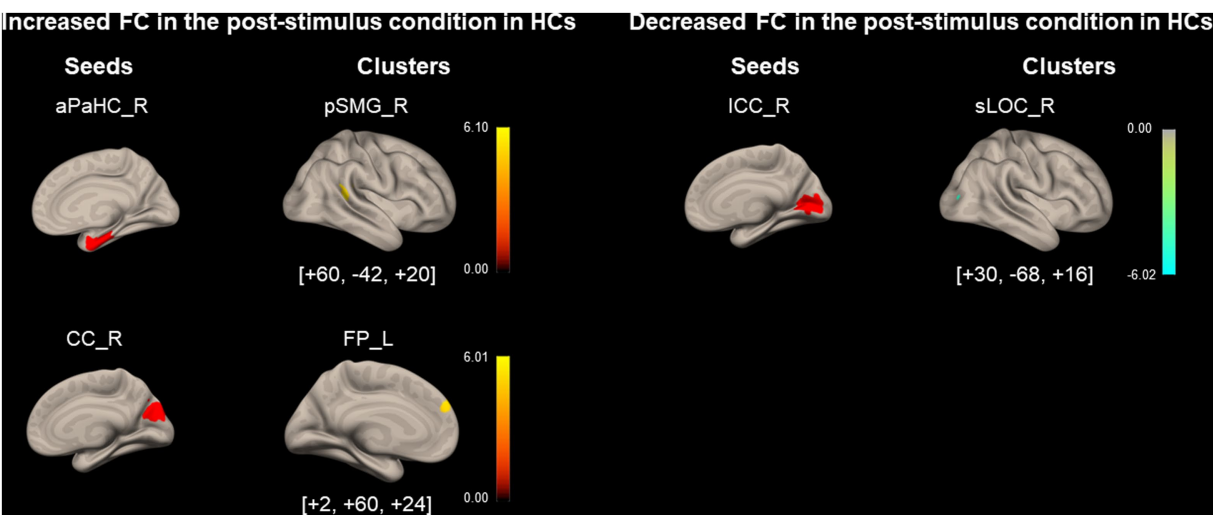


FIGURE 5 Significantly modified functional connectivity under the post-stimulus condition in the healthy control group. Seed regions are shown in red, increased functional connectivity (FC) is indicated by yellow bars, and decreased FC is indicated by green bars. The color bar represents *T* scores. The [x, y, z] values indicate the Montreal Neurological Institute (MNI) coordinates. aPaHC, anterior parahippocampal gyrus; CC, calcarine cortex; FP, frontal pole; HC, healthy control; ICC, intracalcarine cortex; pSMG, posterior supramarginal gyrus; sLOC, superior division of lateral occipital cortex.

TABLE 5 Significantly modified functional connectivity (FC) in the post-stimulus condition in the healthy controls (HCs).

Seed region	Cluster coordinates (x, y, z)	Cluster size	Cluster regions	Cluster value of <i>p</i> (FWE)
<i>Increased FC</i>				
Parahippocampal Gyrus, anterior division_R	+60–42+20	113	Supramarginal Gyrus, posterior division_R	<0.01
Cuneal Cortex_R	+2+60+24	68	Frontal Pole_L	0.048
<i>Decreased FC</i>				
Intracalcarine Cortex _R	+30–68+16	134	Lateral Occipital Cortex, superior division_R	<0.01

FC, functional connectivity; HCs, healthy controls; FWE, family-wise error; L, left; R, right.

The PPPD group had broader elliptical balance areas on posturography than the HC group under the eyes closed, eyes open on foam rubber, and eyes closed on foam rubber conditions. These posturography results are consistent with previous outcomes (13, 14), showing no significant differences under the eyes open condition compared with that in the HC group, but significantly poorer performance under challenging conditions such as the eyes closed or standing on foam rubber conditions. Therefore, postural stability, which is barely maintained under the eyes open condition, would be easily disrupted by mild stimulation in patients with PPPD.

Regarding the vestibular function, the comprehensive findings of the examination revealed no cases of obvious unilateral or bilateral vestibular dysfunction, consistent with previous reports (32, 33) that described a deficit of specific laboratory findings.

SSQ (total score) was significantly higher in the PPPD group, indicating that patients with PPPD were more likely to be affected by motion sickness symptoms by visual stimuli (Table 1). Vestibular symptoms in patients with PPPD were considered to be exacerbated by visual stimuli and symptoms such as nausea and disorientation also occurred in conjunction with the exacerbation.

In summary, although the number of participants in this study was relatively small; the demographic and clinical features of patients with PPPD, e.g., anxious/depressive, neurotic, unstable posture, almost normal canal function, and susceptibility to visual stimuli were consistent with those of previous studies.

4.2. Comparison of FCs between PPPD and HCs at rest

Regarding the visuo- and vestibulo-spatial cognitive processes, the right hemisphere may be the dominant hemisphere (34, 35). As shown in Figure 3 and Table 3, significant differences in FC with seeds of PIVC, aPaHC, and HC of the dominant hemisphere were observed between the HC and PPPD groups: FC between right PIVC and bilateral LGs, that between the right aPaHC and right inferior parietal lobule (pSMG/AG), and that between the right HC and left FP.

Significantly lower FC was found in the PPPD group than in the HC group between the right PIVC, vestibular cortex, and bilateral LGs, the visual areas (Figure 3; Table 3). This is consistent with

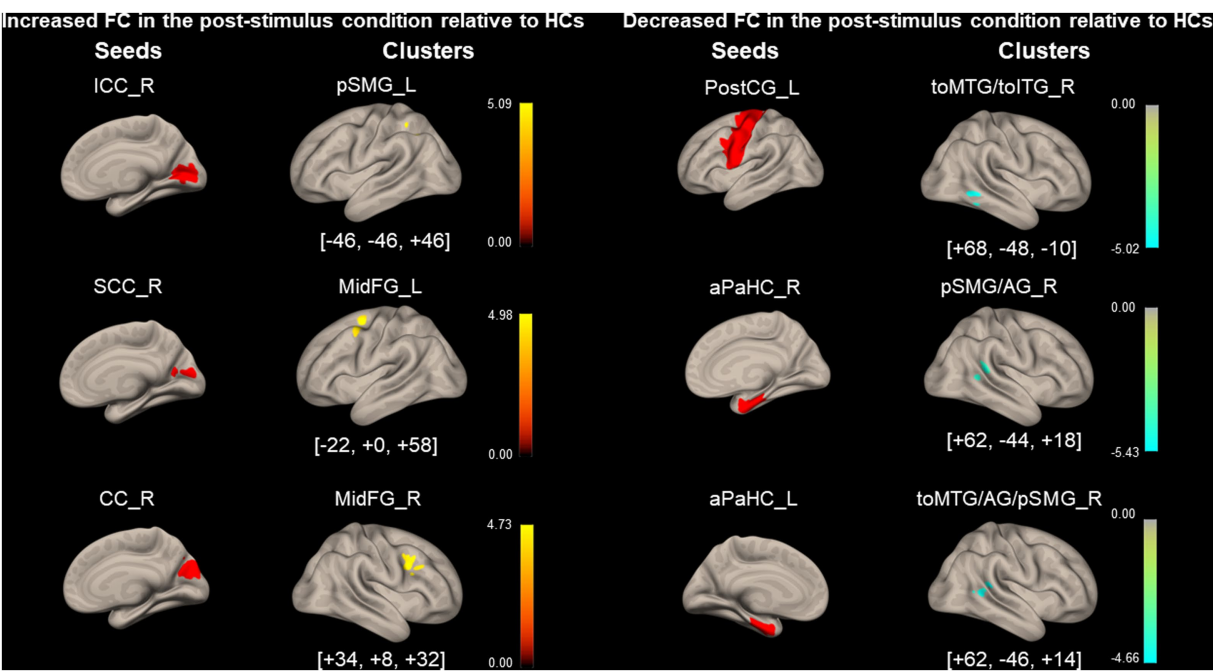


FIGURE 6 Significantly modified functional connectivity under the post-stimulus condition in patients with persistent postural-perceptual dizziness relative to that of healthy control. Seed regions are shown in red, increased functional connectivity (FC) is indicated by yellow bars, and decreased FC is indicated by green bars. The color bar represents *F* scores. The [x, y, z] values indicate the Montreal Neurological Institute (MNI) coordinates. aPaHC, anterior parahippocampal gyrus; CC, calcarine cortex; ICC, intracalcarine cortex; MidFG, middle frontal gyrus; PostCG, post-central gyrus; PPPD, persistent postural-perceptual dizziness; pSMG/AG, posterior supramarginal gyrus/angular gyrus; SCC, supracalcarine cortex; toMTG/toITG, temporooccipital middle/inferior temporal gyrus.

TABLE 6 Significantly modified functional connectivity (FC) in the post-stimulus condition in persistent postural-perceptual dizziness (PPPD) relative to healthy controls (HCs).

Seed region	Cluster coordinates (x, y, z)	Cluster size	Cluster regions	Cluster value of <i>p</i> (FWE)
<i>Increased FC</i>				
Intracalcarine Cortex_R	− 46 − 46 + 46	96	Supramarginal Gyrus, posterior division_L	0.047
Supracalcarine Cortex_R	− 22 + 0 + 58	168	Middle Frontal Gyrus_L	<0.01
Cuneal Cortex_R	+ 34 + 8 + 32	105	Middle Frontal Gyrus_R	0.026
<i>Decreased FC</i>				
Postcentral Gyrus_L	+ 68 − 48 − 10	118	Middle/Inferior Temporal Gyrus, temporooccipital part_R	0.017
Parahippocampal Gyrus, anterior division_R	+ 62 − 44 + 18	167	Supramarginal Gyrus, posterior division_R/Angular Gyrus_R	<0.01
Parahippocampal Gyrus, anterior division_L	+ 62 − 46 + 14	111	Middle Temporal Gyrus, temporooccipital part_R/Angular Gyrus_R/Supramarginal Gyrus, posterior division_R	0.022

FC, functional connectivity; L, left; PPPD, persistent postural-perceptual dizziness; R, right; HCs, healthy control; FWE, family-wise error.

previous reports where decreased FC was found between the vestibular cortex, represented by the posterior perisylvian regions, and visual areas such as the extrastriate areas when evaluating FC in patients with PPPD or predecessors of PPPD relative to HCs (36, 37). Moreover, in our study, a higher FC was observed between the PostCG of the left dominant side (38), a somatosensory cortex, and toMTG/

toITG of the right dominant side (39), upstream of the visual pathway (Figure 3; Table 3). Li et al. (40) also found a similar increase in FC between the post-central gyrus and the occipital pole visual network in PPPD. These findings suggest that vestibular inputs are not fully utilized in the vestibulo-visuo-somatosensory network, and the somatosensory and visual inputs would compensate for the vestibular

inputs, leading to visually and somatosensory-dependent maintenance of spatial orientation in PPPD.

The PPPD group showed significantly higher FC between the right aPaHC and the right inferior parietal lobule (pSMG/AG) than the HC group (Figure 3; Table 3). The inferior parietal lobule including pSMG/AG is a spatial cognitive area that aggregates and integrates multiple types of sensory information and regulates the spatial interrelationship between the body and the external environment (41, 42), while the aPaHC is involved in visuospatial processing (43). Therefore, visual inputs are more likely facilitated in patients with PPPD than in HCs to maintain spatial cognition.

FC between the right HC and the left FP was significantly higher in the PPPD group than in the HC group (Figure 3; Table 3). Since HC and FP are the central areas for spatial cognition and mood control, respectively, the facilitation of this FC would account for changes in mood, e.g., anxiety, induced by tasks that require the spatial cognitive processes in patients with PPPD.

FCs between the right PostCG and the left FP and that between the left PIVC and the left FP/PCG were significantly lower in the PPPD group than in the HC group under the pre-stimulus condition (Figure 3; Table 3). Although the finding was significant, the role of differences in FCs from these non-dominant seed regions (right PostCG and left PIVC) should be treated with caution.

4.3. Brain activity during visual stimulation in PPPD

Task-based fMRI demonstrated that there were no brain regions that showed significantly different activities between the HC and PPPD groups during all five visual stimulations (data not shown), suggesting that there was no difference in the visual processing in PPPD and HCs. Consistent with our results, Riccelli et al. (44) found no significant difference in brain activity between the HC and PPPD groups assessed by fMRI when presented with virtual-reality rollercoaster stimuli in the motion vs. static conditions, whereas when vertical vs. horizontal motion conditions were compared, they found greater activation in the third short insular gyrus and adjacent Rolandic operculum in the HC group than that in the PPPD group. Although some studies previously demonstrated visually activated/inhibited areas in PPPD (45, 46), our results failed to reveal significant areas that were affected during visual stimuli relative to that in HCs. This could be attributed to the fact that although five types of visual stimuli were used in this study, the degree of symptom exacerbation by each stimulus would vary from patient to patient, and the diversity of symptoms within the disease group, which is also observed in real clinical practice, may have prevented the demonstration of the significant areas.

4.4. FCs in HCs and PPPD after visual stimulations

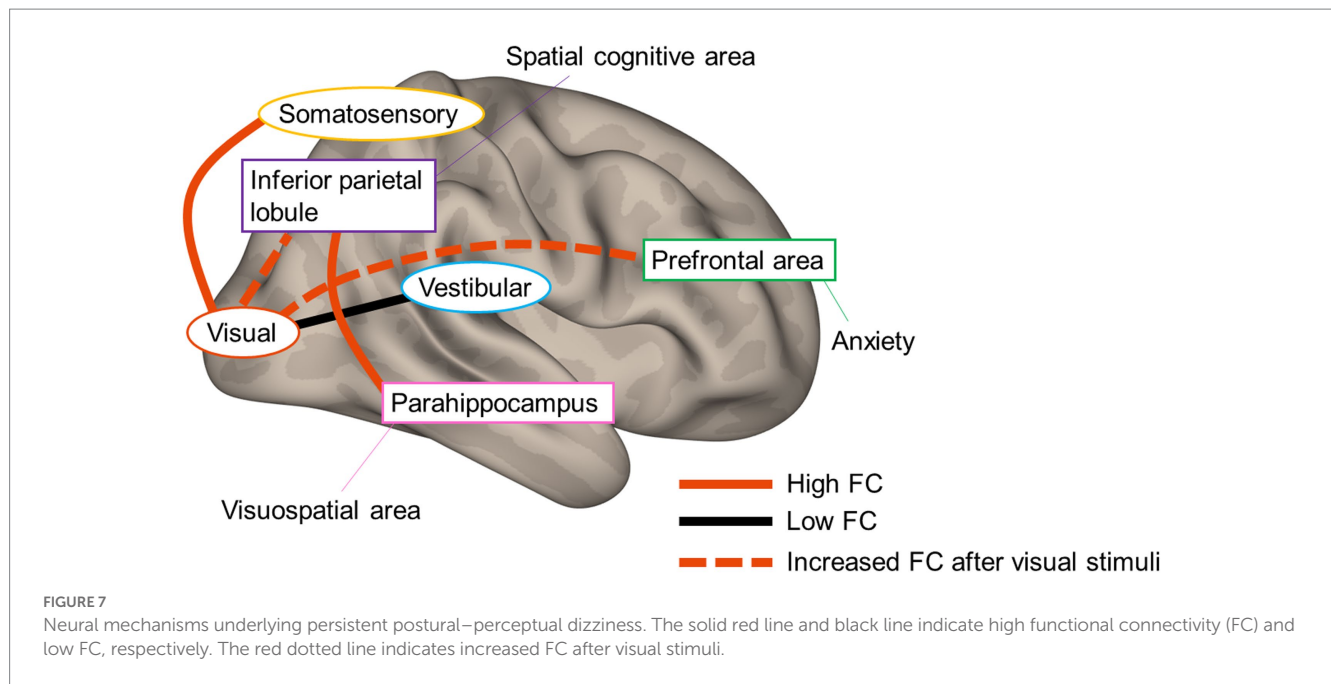
FC between the right aPaHC and right pSMG, which was higher in the PPPD group than in the HC group under the pre-stimulus condition (Figure 3; Table 3), increased under the post-stimulus condition in the HC group (Figure 5; Table 5). In contrast, this FC could no longer be increased under the post-stimulus condition in the

PPPD group (Figure 4; Table 4); rather, it decreased relative to that in the HC group (Figure 6; Table 6), perhaps because this FC had already been elevated under the pre-stimulus condition in the PPPD group. An increase in this FC under the post-stimulus condition in the HC group suggests that visuospatial pathways were facilitated in the spatial cognitive processes even in HCs after visual stimulation. Given that the vestibular symptoms were never induced in the HC group during/after visual stimulation, enhancement of only this FC was not sufficient to account for visually dependent spatial orientation nor visual exacerbation of symptoms. Additional facilitation of FC between somatosensory (PostCG) and visual (toMTG/toITG; Figure 3; Table 3) areas to that between aPaHC and pSMG/AG might be responsible for the visual exacerbation in PPPD.

FCs from several seed regions of visual areas of the dominant side (47), e.g., right ICC/SCC/CC, increased under the post-stimulus condition in the PPPD group compared with that in the HC group. FC between the right ICC and the left pSMG increased under the post-stimulus condition compared with that under the pre-stimulus condition in the PPPD group relative to the HC group (Figure 6; Table 6). Since ICC and pSMG were the centers for visual processing and spatial cognition, respectively, it is suggested that visuospatial pathways were facilitated in PPPD after visual stimulation. FC between the right SCC/CC and the left/right MidFG, the prefrontal responsible area for emotion and mood disorders (48, 49), also increased under the post-stimulus condition in the PPPD group relative to the HC group (Figure 6; Table 6). Popp et al. (45) and Passamonti et al. (50) also reported an increase in FC by visual stimulations between the visual and prefrontal areas in PPPD. All these results would account for the prolonged symptoms after a visual exacerbation and anxious status in patients with PPPD.

FC between the left PostCG and the right toMTG/toITG, which was higher in the PPPD group than in the HC group under the pre-stimulus condition (Figure 3; Table 3), significantly decreased under the post-stimulus condition in the PPPD group relative to the HC group (Figure 6; Table 6). Since changes of this FC were not observed in the HC group (Figure 5; Table 5), it is suggested that visual stimulation would weaken the somatosensory (postCG) to visual (toMTG/toITG) circuit of spatial orientation, which was heightened even at rest in patients with PPPD. In clinical settings, this may imply that the vestibular rehabilitation that promotes habituation to visual stimuli would effectively affect this point in the treatment of PPPD.

Significance of changes observed under the post-stimulus condition in the PPPD group, e.g., an increase in FC between the vestibular (PIVC) and visual (LG) areas and that between the visual (SCC) and spatial cognitive (pSMG) areas and a decrease in FC among the visual areas (CC and pMTG; Figure 4; Table 4), disappeared when analyzed relative to HCs (Figure 6; Table 6). Therefore, these data must be interpreted carefully. FC between the left aPaHC and the right toMTG/AG/pSMG decreased under the post-stimulus condition in the PPPD group relative to the HC group (Figure 6; Table 6). FC between the right PostCG and the right pSMG also decreased under the post-stimulus condition compared with that under the pre-stimulus condition in the PPPD group. Although the results were significant, the role of differences in FCs from these non-dominant seed regions (left aPaHC and right PostCG) should be treated with caution.



4.5. Neural mechanisms underlying PPPD

Figure 7 summarizes the current results and possible neural mechanisms underlying PPPD. At rest, while FC between vestibular and visual cortices is low, that between somatosensory and visual cortices is high, suggesting that vestibular inputs are not fully utilized in the vestibulo-visuo-somatosensory network. A heightened FC between parahippocampal visuospatial and spatial cognitive areas of the inferior parietal lobe in combination with visually and somatosensory-dependent spatial orientation strategy would be involved in the visual exacerbation in PPPD. An increase in FC from visual areas to spatial cognitive and prefrontal areas after visual stimuli may account for the prolonged symptoms after a visual exacerbation and anxious status in PPPD. Overall, the study presents the underlying neural mechanisms involved in PPPD and will promote better management of the patients.

4.6. Limitations

There are several limitations in this study. First, the psychological factors were not controlled due to the small sample size. Second, patients on antidepressants were included (51–53). Third, the possibility that brain regions other than the seed region used in this analysis may be implicated in the pathogenesis of PPPD cannot be denied. Lastly, it was difficult to determine whether the FC changes observed in this study were a cause or a consequence. To better elucidate the pathogenesis of PPPD, it is necessary to interpret not only the results of fMRI studies but also combine them with the results of clinical tests, such as the sensory organization test, subjective visual vertical test, eye-tracking test, or spatial cognition test.

5. Conclusion

In PPPD, vestibular inputs may not be fully utilized in the vestibulo-visuo-somatosensory network. The FC between visuospatial and spatial cognitive areas was increased even in HCs after visual stimuli. Hence, the elevated status of this FC in combination with the high FC between the somatosensory and visual areas would be involved in the visual exacerbation in PPPD. An increase in FC from the visual areas to spatial cognitive and prefrontal areas after visual stimuli may account for the prolonged symptoms after a visual exacerbation and anxious status in PPPD.

Data availability statement

The raw data supporting the conclusions of this article will be made available by the authors, without undue reservation.

Ethics statement

The studies involving human participants were reviewed and approved by the institutional review board of Niigata University Medical and Dental Hospital. The patients/participants provided their written informed consent to participate in this study.

Author contributions

CY: conceptualization, methodology, formal analysis, investigation, data curation, writing—original draft, writing—review and editing, project administration, and funding acquisition. YM, TY,

SO, SI, KT: resources, writing—review and editing. MW: software, investigation, and resources. KI: methodology, formal analysis, investigation, writing—original draft, and writing—review and editing. YS: methodology, formal analysis, investigation, writing—review and editing, and project administration. HI: writing—review and editing, and supervision. AH: conceptualization, resources, writing—original draft, writing—review and editing, supervision, and funding acquisition. All authors contributed to the article and approved the submitted version.

Funding

This work was partly supported by Grants-in-Aid from the Ministry of Education, Culture, Sports, Science, and Technology of Japan [19K18799] (for CY) and [21H03084] (for AH).

Acknowledgments

We would like to thank Editage (www.editage.com) for English language editing.

References

1. Staab JP, Eckhardt-Henn A, Horii A, Jacob R, Strupp M, Brandt T, et al. Diagnostic criteria for persistent postural-perceptual dizziness (PPPD): consensus document of the committee for the classification of vestibular disorders of the Barany society. *J Vestib Res.* (2017) 27:191–208. doi: 10.3233/VES-170622
2. Azzi JL, Khoury M, Séguin J, Rourke R, Hogan D, Tse D, et al. Characteristics of persistent postural perceptual dizziness patients in a multidisciplinary dizziness clinic. *J Vestib Res.* (2022) 32:285–93. doi: 10.3233/VES-190749
3. Wuehr M, Kugler G, Schniepp R, Eckl M, Pradhan C, Jahn K, et al. Balance control and anti-gravity muscle activity during the experience of fear at heights. *Physiol Rep.* (2014) 2:e00232. doi: 10.1002/phy2.232
4. Schniepp R, Wuehr M, Huth S, Pradhan C, Brandt T, Jahn K. Gait characteristics of patients with phobic postural vertigo: effects of fear of falling, attention, and visual input. *J Neurol.* (2014) 261:738–46. doi: 10.1007/s00415-014-7259-1
5. Wuehr M, Brandt T, Schniepp R. Distracting attention in phobic postural vertigo normalizes leg muscle activity and balance. *Neurology.* (2017) 88:284–8. doi: 10.1212/WNL.0000000000003516
6. Cousins S, Cutfield NJ, Kaski D, Palla A, Seemungal BM, Golding JF, et al. Visual dependency and dizziness after vestibular neuritis. *PLoS One.* (2014) 9:e105426. doi: 10.1371/journal.pone.0105426
7. Okumura T, Horii A, Kitahara T, Imai T, Uno A, Osaki Y, et al. Somatosensory shift of postural control in dizzy patients. *Acta Otolaryngol.* (2015) 135:925–30. doi: 10.3109/00016489.2015.1040172
8. Chiarella G, Petrolo C, Riccelli R, Giofrè L, Olivades G, Gioacchini FM, et al. Chronic subjective dizziness: analysis of underlying personality factors. *J Vestib Res.* (2016) 26:403–8. doi: 10.3233/VES-160590
9. Yan Z, Cui L, Yu T, Liang H, Wang Y, Chen C. Analysis of the characteristics of persistent postural-perceptual dizziness: a clinical-based study in China. *Int J Audiol.* (2017) 56:33–7. doi: 10.1080/14992027.2016.1211763
10. Trindade A, Harman P, Stone J, Staab JP, Goebel JA. Assessment of potential risk factors for the development of persistent postural-perceptual dizziness: a case-control pilot study. *Front Neurol.* (2021) 11:601883. doi: 10.3389/fneur.2020.601883
11. Staab JP. Persistent postural-perceptual dizziness. *Semin Neurol.* (2020) 40:130–7. doi: 10.1055/s-0039-3402736
12. Breinbauer HA, Contreras MD, Lira JP, Guevara C, Castillo L, Rüdelinger K, et al. Spatial navigation is distinctively impaired in persistent postural perceptual dizziness. *Front Neurol.* (2019) 10:1361. doi: 10.3389/fneur.2019.01361
13. Söhsten E, Bittar RS, Staab JP. Posturographic profile of patients with persistent postural-perceptual dizziness on the sensory organization test. *J Vestib Res.* (2016) 26:319–26. doi: 10.3233/VES-160583
14. McCaslin DL, Shepard NT, Hollman JH, Staab JP. Characterization of postural sway in patients with persistent postural-perceptual dizziness (PPPD) using wearable motion sensors. *Otol Neurotol.* (2022) 43:e243–51. doi: 10.1097/MAO.0000000000003393
15. Indovina I, Passamonti L, Mucci V, Chiarella G, Lacquaniti F, Staab JP. Brain correlates of persistent postural-perceptual dizziness: a review of neuroimaging studies. *J Clin Med.* (2021) 10:4274. doi: 10.3390/jcm10184274
16. Castro P, Bancroft MJ, Arshad Q, Kaski D. Persistent postural-perceptual dizziness (PPPD) from brain imaging to behaviour and perception. *Brain Sci.* (2022) 12:753. doi: 10.3390/brainsci12060753
17. Yagi C, Morita Y, Kitazawa M, Nonomura Y, Yamagishi T, Ohshima S, et al. A validated questionnaire to assess the severity of persistent postural-perceptual dizziness (PPPD): the Niigata PPPD questionnaire (NPQ). *Otol Neurotol.* (2019) 40:e747–52. doi: 10.1097/MAO.0000000000002325
18. Jacobson GP, Newman CW. The development of the dizziness handicap inventory. *Arch Otolaryngol Head Neck Surg.* (1990) 116:424–7. doi: 10.1001/archotol.1990.01870040046011
19. Goto F, Tsutsumi T, Ogawa K. The Japanese version of the dizziness handicap inventory as an index of treatment success: exploratory factor analysis. *Acta Otolaryngol Japanese version.* (2011) 131:817–25. doi: 10.3109/00016489.2011.565423
20. Zigmond AS, Snaith RP. The hospital anxiety and depression scale. *Acta Psychiatr Scand.* (1983) 67:361–70. doi: 10.1111/j.1600-0447.1983.tb09716.x
21. Gosling SD, Rentfrow PJ, Swann WB Jr. A very brief measure of the big-five personality domains. *J Res Pers.* (2003) 37:504–28. doi: 10.1016/S0092-6566(03)00046-1
22. Oshio A, Abe S, Cutrone P. Development, reliability, and validity of the Japanese version of ten item personality inventory (TIPI-J). *Jpn J Pers.* (2012) 21:40–52. doi: 10.2132/personality.21.40
23. Kennedy RS, Lane NE, Berbaum KS, Lilienthal MG. Simulator sickness questionnaire: an enhanced method for quantifying simulator sickness. *Int J Aviat Psychol.* (1993) 3:203–20. doi: 10.1207/s15327108ijap0303_3
24. Jongkees LB, Maas JP, Philipszoon AJ. Clinical nystagmography; a detailed study of electro-nystagmography in 341 patients with vertigo. *Pract Otorhinolaryngol.* (1962) 24:65–93. doi: 10.1159/000274383
25. Kao AC, Nanda A, Williams CS, Tinetti ME. Validation of dizziness as a possible geriatric syndrome. *J Am Geriatr Soc.* (2001) 49:72–5. doi: 10.1046/j.1532-5415.2001.49012.x
26. Curthoys IS, McGarvie LA, MacDougall HG, Burgess AM, Halmagyi GM, Rey-Martinez J, et al. A review of the geometrical basis and the principles underlying the use and interpretation of the video head impulse test (vHIT) in clinical vestibular testing. *Front Neurol.* (2023) 14:1147253. doi: 10.3389/fneur.2023.1147253
27. Blakley BW, Wong V. Normal values for cervical vestibular-evoked myogenic potentials. *Otol Neurotol.* (2015) 36:1069–73. doi: 10.1097/MAO.0000000000000752
28. Shahnaz N, David EA. Normal values for cervical and ocular vestibular-evoked myogenic potentials using EMG scaling: effect of body position and electrode montage. *Acta Otolaryngol.* (2021) 141:440–8. doi: 10.1080/00016489.2021.1887517

Conflict of interest

The authors declare that the research was conducted in the absence of any commercial or financial relationships that could be construed as a potential conflict of interest.

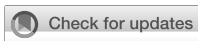
Publisher's note

All claims expressed in this article are solely those of the authors and do not necessarily represent those of their affiliated organizations, or those of the publisher, the editors and the reviewers. Any product that may be evaluated in this article, or claim that may be made by its manufacturer, is not guaranteed or endorsed by the publisher.

Supplementary material

The Supplementary material for this article can be found online at: <https://www.frontiersin.org/articles/10.3389/fneur.2023.1215004/full#supplementary-material>

29. Piscicelli C, Pérennou D. Visual verticality perception after stroke: a systematic review of methodological approaches and suggestions for standardization. *Ann Phys Rehabil Med.* (2017) 60:208–16. doi: 10.1016/j.rehab.2016.02.004
30. Indovina I, Bosco G, Riccelli R, Maffei V, Lacquaniti F, Passamonti L, et al. Structural connectome and connectivity lateralization of the multimodal vestibular cortical network. *NeuroImage.* (2020) 222:117247. doi: 10.1016/j.neuroimage.2020.117247
31. Bittar RS, Lins EM. Clinical characteristics of patients with persistent postural-perceptual dizziness. *Braz J Otorhinolaryngol.* (2015) 81:276–82. doi: 10.1016/j.bjorl.2014.08.012
32. Kitazawa M, Morita Y, Yagi C, Takahashi K, Ohshima S, Yamagishi T, et al. Test batteries and the diagnostic algorithm for chronic vestibular syndromes. *Front Neurol.* (2021) 12:768718. doi: 10.3389/fneur.2021.768718
33. Yagi C, Morita Y, Kitazawa M, Yamagishi T, Ohshima S, Izumi S, et al. Subtypes of persistent postural-perceptual dizziness. *Front Neurol.* (2021) 12:652366. doi: 10.3389/fneur.2021.652366
34. Dieterich M, Brandt T. Chapter 6. The parietal lobe and the vestibular system. *Handb. Clin. Neurol.* (2018):119–40. doi: 10.1016/B978-0-444-63622-5.00006-1
35. Jahn K, Wagner J, Deutschländer A, Kalla R, Hüfner K, Stephan T, et al. Human hippocampal activation during stance and locomotion: fMRI study on healthy, blind, and vestibular-loss subjects. *Ann N Y Acad Sci.* (2009) 1164:229–35. doi: 10.1111/j.1749-6632.2009.03770.x
36. Indovina I, Riccelli R, Chiarella G, Petrolo C, Augimeri A, Giofrè L, et al. Role of the insula and vestibular system in patients with chronic subjective dizziness: an fMRI study using sound-evoked vestibular stimulation. *Front Behav Neurosci.* (2015) 9:334. doi: 10.3389/fnbeh.2015.00334
37. Lee JO, Lee ES, Kim JS, Lee YB, Jeong Y, Choi BS, et al. Altered brain function in persistent postural perceptual dizziness: a study on resting state functional connectivity. *Hum Brain Mapp.* (2018) 39:3340–53. doi: 10.1002/hbm.24080
38. Gotts SJ, Jo HJ, Wallace GL, Saad ZS, Cox RW, Martin A. Two distinct forms of functional lateralization in the human brain. *Proc Natl Acad Sci U S A.* (2013) 110:E3435–44. doi: 10.1073/pnas.1302581110. [Epub 2013 Aug 19]
39. Diekmann V, Jürgens R, Becker W. Deriving angular displacement from optic flow: a fMRI study. *Exp Brain Res.* (2009) 195:101–16. doi: 10.1007/s00221-009-1753-1
40. Li K, Si L, Cui B, Ling X, Shen B, Yang X. Altered intra- and inter-network functional connectivity in patients with persistent postural-perceptual dizziness. *NeuroImage Clin.* (2020) 26:102216. doi: 10.1016/j.nicl.2020.102216
41. Kandel E, Schwartz J, Jessell T, Siegelbaum S, Hudspeth AJ. (editors). Chapter 28. High-level visual processing: cognitive influences In: *Principles of Neural Science*, vol. V. 5th ed (McGraw-Hill companies, Inc.) (2012). 621–37.
42. Kandel E, Schwartz J, Jessell T, Siegelbaum S, Hudspeth AJ. (editors). Chapter 38. Voluntary movement: the parietal and premotor cortex In: *Principles of Neural Science*, vol. VI. 5th ed (McGraw-Hill companies, Inc.) (2012). 865–93.
43. Connor CE, Knierim JJ. Integration of objects and space in perception and memory. *Nat Neurosci.* (2017) 20:1493–503. doi: 10.1038/nn.4657
44. Riccelli R, Passamonti L, Toschi N, Nigro S, Chiarella G, Petrolo C, et al. Altered insular and occipital responses to simulated vertical self-motion in patients with persistent postural-perceptual dizziness. *Front Neurol.* (2017) 8:529. doi: 10.3389/fneur.2017.00529
45. Popp P, Zu Eulenburg PZ, Stephan T, Bögle R, Habs M, Henningsen P, et al. Cortical alterations in phobic postural vertigo—a multimodal imaging approach. *Ann Clin Transl Neurol.* (2018) 5:717–29. doi: 10.1002/acn3.570
46. Roberts RE, Ahmad H, Patel M, Dima DI, Ibitoye R, Sharif M, et al. An fMRI study of visuo-vestibular interactions following vestibular neuritis. *NeuroImage Clin.* (2018) 20:1010–7. doi: 10.1016/j.nicl.2018.10.007
47. Hougaard A, Jensen BH, Amin FM, Rostrup E, Hoffmann MB, Ashina M. Cerebral asymmetry of fMRI-BOLD responses to visual stimulation. *PLoS One.* (2015) 10:e0126477. doi: 10.1371/journal.pone.0126477
48. Koenigs M, Grafman J. The functional neuroanatomy of depression: distinct roles for ventromedial and dorsolateral prefrontal cortex. *Behav Brain Res.* (2009) 201:239–43. doi: 10.1016/j.bbr.2009.03.004
49. Myers-Schulz B, Koenigs M. Functional anatomy of ventromedial prefrontal cortex: implications for mood and anxiety disorders. *Mol Psychiatry.* (2012) 17:132–41. doi: 10.1038/mp.2011.88
50. Passamonti L, Riccelli R, Lacquaniti F, Staab JP, Indovina I. Brain responses to virtual reality visual motion stimulation are affected by neurotic personality traits in patients with persistent postural-perceptual dizziness. *J Vestib Res.* (2018) 28:369–78. doi: 10.3233/VES-190653
51. Anand A, Li Y, Wang Y, Gardner K, Lowe MJ. Reciprocal effects of antidepressant treatment on activity and connectivity of the mood regulating circuit: an FMRI study. *J Neuropsychiatry Clin Neurosci.* (2007) 19:274–82. doi: 10.1176/appi.neuropsych.19.3.274
52. Yang R, Zhang H, Wu X, Yang J, Ma M, Gao Y, et al. Hypothalamus-anchored resting brain network changes before and after sertraline treatment in major depression. *Biomed Res Int.* (2014) 2014:915026. doi: 10.1155/2014/915026
53. Dichter GS, Gibbs D, Smoski MJ. A systematic review of relations between resting-state functional-MRI and treatment response in major depressive disorder. *J Affect Disord.* (2015) 172:8–17. doi: 10.1016/j.jad.2014.09.028



OPEN ACCESS

EDITED BY

Daogong Zhang,
Shandong Provincial ENT Hospital, China

REVIEWED BY

Mayada Elsherif,
Alexandria University, Egypt
Jorge Kattah,
University of Illinois at Chicago, United States
Alexandre Bisdorff,
Hospital Center Emile Mayrisch, Luxembourg

*CORRESPONDENCE

Wei Wang
✉ wwei1106@hotmail.com
Taisheng Chen
✉ fch_cts@asina.com

RECEIVED 21 June 2023

ACCEPTED 08 August 2023

PUBLISHED 22 August 2023

CITATION

Zhang X, Deng Q, Liu Y, Li S, Wen C, Liu Q,
Huang X, Wang W and Chen T (2023)
Characteristics of spontaneous nystagmus and
its correlation to video head impulse test
findings in vestibular neuritis.
Front. Neurosci. 17:1243720.
doi: 10.3389/fnins.2023.1243720

COPYRIGHT

© 2023 Zhang, Deng, Liu, Li, Wen, Liu, Huang,
Wang and Chen. This is an open-access article
distributed under the terms of the [Creative
Commons Attribution License \(CC BY\)](#). The
use, distribution or reproduction in other
forums is permitted, provided the original
author(s) and the copyright owner(s) are
credited and that the original publication in this
journal is cited, in accordance with accepted
academic practice. No use, distribution or
reproduction is permitted which does not
comply with these terms.

Characteristics of spontaneous nystagmus and its correlation to video head impulse test findings in vestibular neuritis

Xueqing Zhang^{1,2,3,4,5}, Qiaomei Deng^{1,2,3,4,5}, Yao Liu^{1,2,3,4,5},
Shanshan Li^{1,2,3,4,5}, Chao Wen^{1,2,3,4,5}, Qiang Liu^{1,2,3,4,5},
Xiaobang Huang^{1,2,3,4,5}, Wei Wang^{1,2,3,4,5*} and
Taisheng Chen^{1,2,3,4,5*}

¹Department of Otorhinolaryngology Head and Neck Surgery, Tianjin First Central Hospital, Tianjin, China, ²Institute of Otolaryngology of Tianjin, Tianjin, China, ³Key Laboratory of Auditory Speech and Balance Medicine, Tianjin, China, ⁴Key Medical Discipline of Tianjin (Otolaryngology), Tianjin, China, ⁵Quality Control Centre of Otolaryngology, Tianjin, China

Objective: To explore the direction and SPV (slow phase velocity) of the components of spontaneous nystagmus (SN) in patients with vestibular neuritis (VN) and the correlation between SN components and affected semicircular canals (SCCs). Additionally, we aimed to elucidate the role of directional features of peripheral SN in diagnosing acute vestibular syndrome.

Materials and methods: A retrospective analysis was conducted on 38 patients diagnosed with VN in our hospital between 2022 and 2023. The direction and SPV of SN components recorded with three-dimensional videonystagmography (3D-VNG) and the video head impulse test (vHIT) gain of each SCC were analyzed as observational indicators. We examined the correlation between superior and inferior vestibular nerve damage and the direction and SPV of SN components, and vHIT gain values in VN patients.

Results: The median illness duration of between symptom onset and moment of testing was 6 days among the 38 VN patients (17 right VN and 21 left VN). In total, 31 patients had superior vestibular neuritis (SVN), and 7 had total vestibular neuritis (TVN). Among the 38 VN patients, all had horizontal component with an SPV of $(7.66 \pm 5.37)^\circ/\text{s}$, 25 (65.8%) had vertical upward component with a SPV of $(2.64 \pm 1.63)^\circ/\text{s}$, and 26 (68.4%) had torsional component with a SPV of $(4.40 \pm 3.12)^\circ/\text{s}$. The vHIT results in the 38 VN patients showed that the angular vestibulo-ocular reflex (aVOR) gain of the anterior (A), lateral (L), and posterior (P) SCCs on the ipsilesional side were 0.60 ± 0.23 , 0.44 ± 0.15 and 0.89 ± 0.19 , respectively, while the gains on the opposite side were 0.95 ± 0.14 , 0.91 ± 0.08 , and 0.96 ± 0.11 , respectively. There was a statistically significant difference in the aVOR gain between the A-, L-SCC on the ipsilesional side and the other SCCs ($p < 0.001$). The aVOR gains of A-, L-, and P-SCC on the ipsilesional sides in 31 SVN patients were 0.62 ± 0.24 , 0.45 ± 0.16 , and 0.96 ± 0.10 , while the aVOR gains on the opposite side were 0.96 ± 0.13 , 0.91 ± 0.06 , and 0.98 ± 0.11 , respectively. There was a statistically significant difference in the aVOR gain between the A-, L-SCC on the ipsilesional side and the other SCCs ($p < 0.001$). In 7 TVN patients, the aVOR gains of A-, L-, and P-SCC on the ipsilesional side were 0.50 ± 0.14 , 0.38 ± 0.06 , and 0.53 ± 0.07 , while the aVOR gains on the opposite side were 0.93 ± 0.17 , 0.90 ± 0.16 , and 0.89 ± 0.09 , respectively. There was a statistically significant difference in the aVOR gain between the A-, L-, and P-SCC on the

ipsilesional side and the other SCCs ($p < 0.001$). The aVOR gain asymmetry of L-SCCs in 38 VN was 36.3%. The aVOR gain asymmetry between bilateral A-SCCs and bilateral P-SCCs for VN patients with and without a vertical upward component was 12.8% and 8.3%, which was statistically significant ($p < 0.05$). For VN patients with and without a torsional component, the aVOR gain asymmetry of bilateral vertical SCCs was 17.0% and 6.6%, which was statistically significant ($p < 0.01$). Further analysis revealed a significant positive correlation between the aVOR gain asymmetry of L-SCCs and the SPV of the horizontal component of SN in all VN patients ($r = 0.484$, $p < 0.01$), as well as between the asymmetry of bilateral vertical SCCs and the SPV of torsional component in 26 VN patients ($r = 0.445$, $p < 0.05$). However, there was no significant correlation between the aVOR gains asymmetry of bilateral A-SCCs and P-SCCs and the SPV of the vertical component in 25 VN patients.

Conclusion: There is a correlation between the three-dimensional direction and SPV characteristics of SN and the aVOR gain of vHIT in VN patients. These direction characteristics can help assess different SCCs impairments in patients with unilateral vestibular diseases.

KEYWORDS

spontaneous nystagmus, vHIT, vestibular neuritis, semicircular canals, nystagmus direction

1. Introduction

Spontaneous nystagmus (SN) is a common clinical sign of peripheral vestibular disorders. SN is typically horizontal or horizontal-torsional, direction-fixed, and enhanced by removing visual fixation, and its SPV follows Alexander's law (Liu et al., 2017). It is an objective indicator of asymmetric static tension in the bilateral vestibular system (Liu et al., 2017). Vestibular neuritis (VN) is a vestibular syndrome caused by acute unilateral vestibulopathy and is the second leading cause of peripheral vestibular vertigo: with the first being benign paroxysmal positioning vertigo (BPPV) (Le et al., 2019). There is unambiguous evidence of reduced aVOR function on the side opposite to the direction of the fast phase of the SN in VN (Aw et al., 2001; Baier et al., 2008; Bachmann et al., 2018). Unidirectional horizontal-torsional SN beats to the healthy side, and the SPV weakens with the establishment of vestibular compensation (Lacour et al., 2016). In 1996, Fetter and Dichgans (1996) studied the three-dimensional (3D) properties of aVOR in 16 VN patients using 3D magnetic search coil eye movement recording and quantified the dynamic asymmetries. A large body of research has shown that VN is not a complete unilateral vestibular lesion; instead, it most commonly affects only the upper branch of the vestibular nerve innervating the anterior (A)-semicircular canal (SCC), L-SCC, the utricle, and their afferents (Sando et al., 1972; Buki and Ward, 2021). Therefore, patients with unilateral VN show significantly reduced aVOR gain values of A- and L-SCCs on the ipsilesional side and present with covert or overt saccades (Psillas et al., 2022). This study aimed to investigate impairments in SCCs and explore the relationship between the direction characteristics of SN and various SCCs impairments. This was achieved by analyzing the 3D direction and SPV of SN in patients with unilateral VN and combining them with the aVOR gain and aVOR gain asymmetry in vHIT. This study's

findings will assist in further evaluating different SCCs impairments in patients with unilateral vestibular diseases.

2. Materials and methods

2.1. Participants

This retrospective study involved the assessment of 38 patients with unilateral VN or acute unilateral vestibulopathy (AUVP) patients, examined at the Ear, Nose, and Throat (ENT) Department of MY Hospital, Tianjin First Central Hospital between 2022 and 2023. Of 38 patients, 31 had superior vestibular neuritis (SVN), and seven had total vestibular neuritis (TVN). All the subjects provided informed consent to be included in the study. The study procedures were approved by the Ethics Committee of Tianjin First Central Hospital.

We included patients diagnosed with AUVP or VN according to the multidisciplinary experts' consensus on vestibular neuritis (Professional Committee on Vertigo, 2020) and the diagnostic criteria of AUVP or VN (Strupp et al., 2022).

We exclude patients with unclear diagnoses or diagnostic controversies. Additionally, we excluded patients with coexistence of other diseases, such as BPPV, Meniere disease, sudden deafness with vertigo, Ramsay Hunt syndrome, labyrinthitis, as well as head trauma, vestibular migraine, stroke, and other central vestibular vertigo and balance disorders.

2.2. Study procedure

We obtained a detailed medical history of the onset of symptoms and their severity, illness duration, and associated factors. VN and

AUVP were diagnosed with the results of SN, vHIT, and caloric test. The lesion side, superior or inferior vestibular nerve damage, and associated SCCs were determined. SN, vHIT, caloric test, and corresponding parameters were observed and recorded using 3D-VNG (VertiGoggles-M, ZEHNIT Medical Technology-VNG-II, Shanghai, China).

The VOR gain of vHIT is the ratio of eye velocity to head velocity, with a normal values range of 0.8–1.2 for L-SCCs and 0.7–1.2 for vertical SCCs. Unilateral weakness (UW) $\geq 25\%$ and directional preponderance (DP) $\geq 30\%$ indicate an abnormal caloric test.

2.3. Analysis

The main measures in vHIT are the aVOR gain, aVOR gain asymmetry, and the presence or absence of compensatory saccades. The aVOR gain assesses the function of the SCCs and their corresponding nerves on both sides. The aVOR gain asymmetry is a good sensitivity and specificity test for the early diagnosis of VN associated with acute vertigo. We analyzed the 3D direction and SPV (slow phase velocity) of SN and the aVOR gain of vHIT in patients with unilateral VN. The horizontal component of SN is caused by the imbalance of aVOR in the bilateral L-SCCs, while the vertical and torsional components are the comprehensive vectors of bilateral A- and P-SCCs effects.

The formula for calculating the aVOR gain asymmetry of vHIT is as follows:

- 1) The aVOR gain asymmetry of L-SCCs:

$$|(L_{ipsilesional} - L_{opposite}) / (L_{ipsilesional} + L_{opposite})| * 100\%$$

- 2) The aVOR gain asymmetry between bilateral A-SCCs and bilateral P-SCCs:

$$|[(A_{ipsilesional} + A_{opposite}) - (P_{ipsilesional} + P_{opposite})] / [A_{ipsilesional} + A_{opposite} + P_{ipsilesional} + P_{opposite}]| * 100\%$$

- 3) The aVOR gains asymmetry of bilateral vertical SCCs:

$$|[(A_{ipsilesional} + P_{ipsilesional}) - (A_{opposite} + P_{opposite})] / [A_{ipsilesional} + P_{ipsilesional} + A_{opposite} + P_{opposite}]| * 100\%$$

IBM SPSS Statistics 22 (IBM SPSS, Turkey) and JASP 0.16.3 (JASP, Netherlands) were used for statistical analyses. The quantitative data are presented as mean \pm SD values and plotted using GraphPad Prism version 5 (GraphPad, San Diego, CA, United States). The strength of

correlation (r) was calculated, and a p -value < 0.05 was considered statistically significant.

3. Results

3.1. General demographic characteristics of subjects

The ages of the 38 patients with VN (26 male and 12 female) ranged from 18–68 years (mean 42.21). Seventeen of the 38 patients had right-VN (13 male and 4 female) and their ages ranged from 20–62 years (mean 42.76), while 21 patients had left-VN (13 male and 8 female) with age ranges from 18–68 years (mean 41.76). Thirty one patients had superior-VN (22 male and 9 female), and their ages ranged from 18–68 years (mean 40.68); 7 patients had total-VN (4 male and 3 female) with ages ranging from 43–62 years (mean 49.00). Demographic data for VN are shown in Table 1. There were no significant differences in age or sex ratio between groups ($p > 0.05$). All VN patients had a median illness duration of between symptom onset and moment of testing of 6 days. And the illness duration was negatively correlated with the horizontal and torsional components, respectively, but not with the vertical components (Figures 1A–C).

3.2. Direction and SPV of spontaneous nystagmus of VN

The 3D direction and SPV of SN in the 38 VN patients were recorded and analyzed. The direction of the horizontal component was toward the opposite side, and the SPV was $7.66 \pm 5.37^\circ/\text{s}$. About 65.7% (25/38) of the patients had a vertical upward component with a SPV of $2.64 \pm 1.63^\circ/\text{s}$, and 68.4% (26/38) had a torsional component with a SPV of $4.40 \pm 3.12^\circ/\text{s}$. Among the 17 RVN patients, all cases had a left horizontal component with a SPV of $11.30 \pm 5.42^\circ/\text{s}$, 12 cases had a vertical upward component with a SPV of $3.47 \pm 1.78^\circ/\text{s}$, and 13 cases had a torsional component with the direction of upper pole of the eye beating toward the right ear (from patients' perspective) with a SPV of $5.46 \pm 3.72^\circ/\text{s}$. Among the 21 LVN cases, 21 had a right horizontal component with a SPV of $4.70 \pm 3.05^\circ/\text{s}$, 13 cases had a vertical upward component with a SPV of $1.87 \pm 1.02^\circ/\text{s}$, and 13 cases had a torsional component with the direction of upper pole of the eye beating toward the left ear (from patients' perspective) with a SPV of $3.35 \pm 2.01^\circ/\text{s}$. Of the 31 SVN patients, the SPV of the horizontal component was $7.38 \pm 5.49^\circ/\text{s}$, 23 cases had a vertical upward component with a SPV of $2.64 \pm 1.67^\circ/\text{s}$, and 19 cases had a torsional component with a SPV of $4.41 \pm 3.19^\circ/\text{s}$. In the 7 TVN patients, all cases had a horizontal and torsional components with SPV of

TABLE 1 Demographic features of subjects in the vestibular neuritis groups.

Group feature	R-VN	L-VN	SVN	TVN	VN
Number	17	21	31	7	38
Age (years)*	42.76 \pm 13.25	41.76 \pm 14.11	40.68 \pm 14.05	49.00 \pm 8.93	42.21 \pm 13.55
Sex (M:F)*	13:4	13:8	22:9	4:3	26:12

VN, vestibular neuritis; RVN, right VN; LVN, left VN; SVN, superior VN; TVN, total VN; M, male; F, female; * $p > 0.05$.

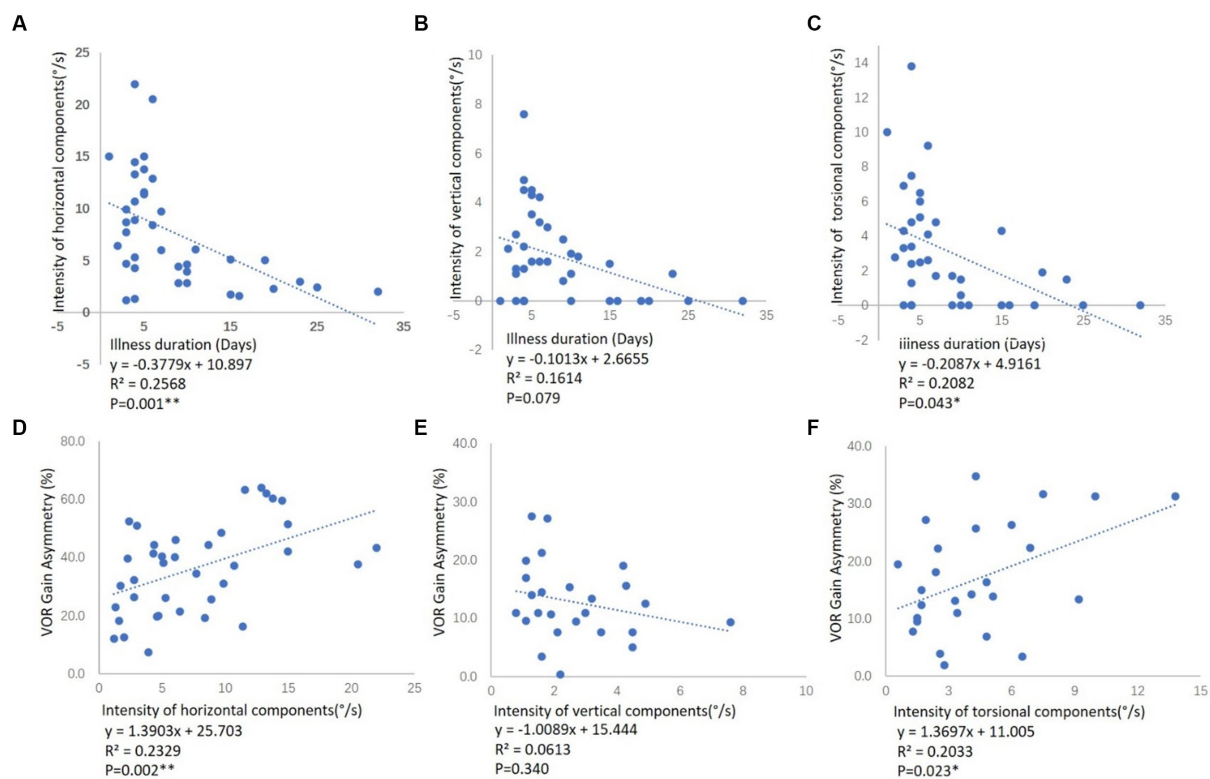


FIGURE 1

Correlation between the illness duration and the SPV of SN components in VN patients, and correlation between the SPV of SN components and aVOR gain asymmetry of vHIT in VN patients. **(A)** The correlation between the illness duration and the SPV of the horizontal component among all the VN patients. **(B)** The correlation between the illness duration and the SPV of the vertical component among 25 VN patients. **(C)** The correlation between the illness duration and the SPV of a torsional component among 26 VN patients. Illness duration means the time between symptom onset and moment of testing. The illness duration was negatively correlated with the horizontal and torsional components, respectively, but not with the vertical components. **(D)** The correlation between the aVOR gain asymmetry of L-SCCs and the SPV of the horizontal component among all the VN patients. **(E)** The correlation between the aVOR gain asymmetry of bilateral A- and P-SCCs and the SPV of the vertical component among 25 VN patients. **(F)** The correlation between the aVOR gain asymmetry of bilateral vertical SCCs and the SPV of a torsional component among 26 VN patients. R^2 represents the goodness of fit, and $p < 0.05$ indicates a significant correlation between aVOR gain asymmetry and the SPV of SN components.

$8.87 \pm 4.98^\circ/\text{s}$ and $5.54 \pm 2.61^\circ/\text{s}$ respectively, and 2 case had vertical component with SPV of $2.50 \pm 1.41^\circ/\text{s}$ (Table 2).

3.3. Characteristics of vHIT and caloric test in VN

The aVOR gain and aVOR gain asymmetry of vHIT were analyzed in all 38 VN cases. The aVOR gains of the A-, L- and P-SCCs on the ipsilesional side were 0.60 ± 0.23 , 0.44 ± 0.15 , 0.89 ± 0.19 , and those on the opposite side were 0.95 ± 0.14 , 0.91 ± 0.08 , 0.96 ± 0.11 , respectively. There were significant differences between the gains of the A- and L-SCCs on the ipsilesional side and those of the other SCCs ($p < 0.001$). In the 17 RVN patients, the gains of A-, L-, and P-SCCs on the right side were 0.51 ± 0.21 , 0.35 ± 0.11 , and 0.85 ± 0.21 , and those on the left side were 0.99 ± 0.12 , 0.94 ± 0.08 , and 0.89 ± 0.09 , respectively. There were significant differences between the gains of the A- and L-SCCs on the right side and those of the other SCCs ($p < 0.001$). In the 21 LVN patients, the gains of A-, L-, and P-SCCs on the right side were 0.92 ± 0.14 , 0.88 ± 0.07 , and 1.02 ± 0.10 , and those on the left side were 0.67 ± 0.22 , 0.51 ± 0.15 , and 0.91 ± 0.17 , respectively. There were significant differences between the gains of the A- and L-SCCs on the left side and those of the other SCCs ($p < 0.001$). In the 31 SVN patients, the gains of A-, L-, and P-SCCs on the

ipsilesional side were 0.62 ± 0.24 , 0.45 ± 0.16 , 0.96 ± 0.10 , and those on the opposite were 0.96 ± 0.13 , 0.91 ± 0.06 , and 0.98 ± 0.11 , respectively. There were significant differences between the gains of the A- and L-SCCs on the ipsilesional side and those of the other SCCs ($p < 0.001$). Among the 7 TVN patients, the gains of A-, L-, and P-SCCs on the ipsilesional side were 0.50 ± 0.14 , 0.38 ± 0.06 , and 0.53 ± 0.07 , and those on the opposite were 0.93 ± 0.17 , 0.90 ± 0.16 , and 0.89 ± 0.09 , respectively. There were significant differences between the gains of the A-, L-, and P-SCCs on the ipsilesional side and those of the other SCCs ($p < 0.001$) (Figure 2).

The caloric test showed decreased aVOR function of L-SCCs on the ipsilesional side at low frequency (0.003 Hz) in all the VN patients and DP to the opposite side ($UW = 58.51 \pm 22.89 > 25$, $DP = 83.37 \pm 25.65 > 30$). The UW and DP were (47.60 ± 20.69) and (89.00 ± 27.11) in the 17 RVN patients and were (66.70 ± 22.02) and (79.15 ± 25.04) in the 21 LVN patients, respectively, consistent with previous research results (Molnar et al., 2023).

3.4. Correlation between SN and vHIT gain in VN

All patients with VN had SN directed toward the opposite side (Figure 3). We analyzed the aVOR gain asymmetry of different SCCs

in vHIT. The aVOR gain asymmetry of L-SCCs in 38 VN was 36.3%. For VN patients with a vertical upward component (65.8%, 25/38), the aVOR gain asymmetry between bilateral A-SCCs and bilateral P-SCCs was 12.8%, while the asymmetry for those without a vertical component was 8.3%, and these differences were statistically significant ($p < 0.05$). For VN patients with a torsional component (68.4%, 26/38), the aVOR gain asymmetry of bilateral vertical SCCs was 17.0%, while the asymmetry for those without a vertical component was 6.6%, and these differences were statistically significant ($p < 0.01$).

We further analyzed the correlation between the aVOR gain asymmetry of SCCs in vHIT and the SPV of 3D components of SN in VN patients (Figures 1D–F). There was a significant positive correlation between the aVOR gain asymmetry of L-SCCs and the SPV of the horizontal component among all the VN patients ($r = 0.484$, $p < 0.01$), as well as the asymmetry of bilateral vertical SCCs and the SPV of torsional component in 26 VN patients ($r = 0.445$, $p < 0.05$). However, no significant correlations were found in asymmetry of

bilateral A- and P-SCCs and the SPV of vertical component among 25 VN patients.

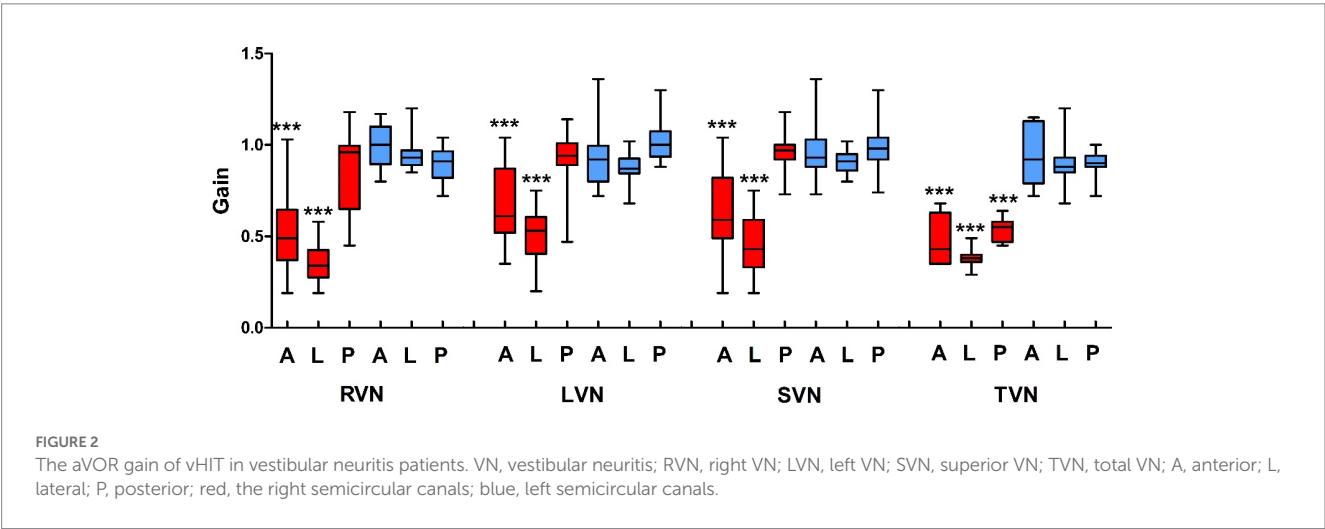
4. Discussion

Spontaneous nystagmus (SN)—present in a static state with the head upright and looking straight forward without any inducing condition—is common in acute unilateral vestibular dysfunction, which is spontaneous, unilateral and caused by asymmetric hypo-function of the angular vestibulo-ocular reflex (aVOR) (WenYu et al., 2017; Ling et al., 2023). In the diagnosis, treatment, and rehabilitation of vestibular diseases, SN has the following clinical significance as a routine physical examination indication: (1) it identifies a central or peripheral disease based on the fixation inhibition test and changes in the direction and SPV of nystagmus during left and right fixation (Alexander’s law); (2) it indicates the side of the peripheral vestibular lesion. The direction of the SN

TABLE 2 The direction and SPV of spontaneous nystagmus in 38 VN patients.

Comp.	Direction and SPV	Direction	R-VN (17 cases)	L-VN (21 cases)	SVN (31cases)	TVN (7 cases)	VN (38 cases)
H	Direction	Left	17	0	13	4	17
		Right	0	21	18	3	21
		/	0	0	0	0	0
	SPV (°/s)		11.30 ± 5.42	4.70 ± 3.05	7.38 ± 5.49	8.87 ± 4.98	7.66 ± 5.37
V	Direction	Upward	12	13	23	2	25
		Downward	0	0	0	0	0
		/	5	8	8	5	13
	SPV (°/s)		3.47 ± 1.78	1.87 ± 1.02	2.64 ± 1.67	2.50 ± 1.41	2.64 ± 1.63
T	Direction	Right	13	0	9	4	13
		Left	0	13	10	3	13
		/	4	8	12	0	12
	SPV (°/s)		5.46 ± 3.72	3.35 ± 2.01	4.41 ± 3.19	5.54 ± 2.61	4.40 ± 3.12

Comp., component; H, horizontal component; V, vertical component; T, torsional component; left/right, upward/downward, right/left (upper pole of the eye beating toward the right/left ear from patients’ perspective), the direction of a component; /, no nystagmus.



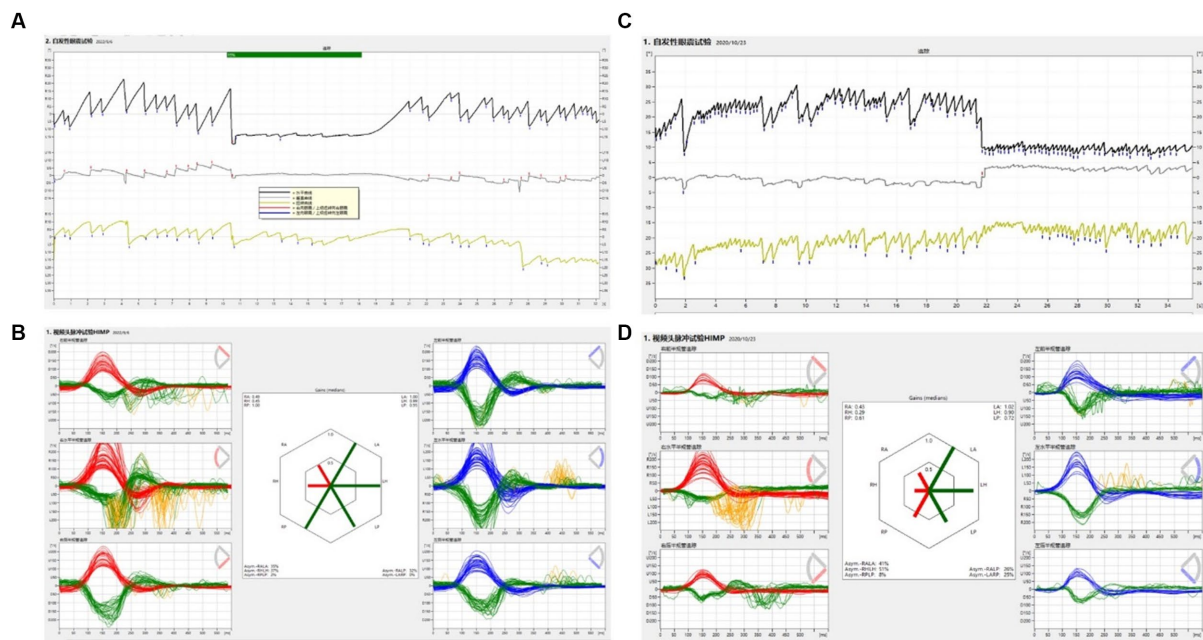


FIGURE 3

The SN and vHIT in SVN and TVN patients. (A) The SN of a SVN patient. Left horizontal (black), upward vertical (gray), and torsional (yellow) components. Nystagmus decreased after fixation. (B) vHIT of a SVN patient. Low aVOR gain in the A- and L-SCCs on the right side with overt and covert saccades, and normal gain and no saccade in other SCCs. (C) The SN of a TVN patient. Left horizontal (black), no vertical (gray), and torsional (yellow) components. Nystagmus decreased after fixation. (D) vHIT of a TVN patient. Low aVOR gains in both the A-, L- and P-SCCs on the right side, accompanied by overt and covert saccades, and normal gain and no saccade in Left SCCs.

points toward the higher tension side of the bilateral vestibule, which is usually the healthy side. For example, a right SN indicates a left peripheral vestibular lesion; (3) it evaluates the status of compensation. Patients with SN often indicate that vestibular static compensation has not been established; (4) it affects other vestibular examination results. SN of a certain SPV often affects the results of visual eye movement tests and caloric tests (Liu et al., 2017; Xie et al., 2021); (5) based on the theory of vestibular frequency, SN is a common sign of vestibular lesion at various frequencies (Deng et al., 2023); and (6) it traces the lesion of SCCs. Vestibular SN is a sign of SCCs pathway damage, but its relationship with SCCs lesions is not fully understood.

Ewald's law, derived from animal experiments, reveals the physiological effects of endolymph flowing in a single SCC, including the plane, direction, and SPV of nystagmus. One of its main connotations is that the direction of nystagmus is the same as the plane of the stimulated SCCs. The law helps in understanding the physiological and pathological characteristics of human SCCs. Nystagmus induced by unilateral L-SCC stimulation was mainly the horizontal component accompanied by a weak vertical upward component. By contrast, nystagmus induced by unilateral P-SCC stimulation was chiefly vertical, upward, and torsional, accompanied by a weak horizontal component. Meanwhile, nystagmus induced by unilateral A-SCC stimulation was vertical, downward, and torsional nystagmus (Eggers et al., 2019). The nystagmus induced by BPPV follows the physiological effects of endolymph flowing in a single SCC. Previous studies have shown that the characteristics of

nystagmus in horizontal semicircular canal canalolithiasis (HSC-Can) (Zhang et al., 2021, 2022) and posterior semicircular canal canalolithiasis (PSC-Can) (Liu et al., 2022) align with Ewald's law and can be used as excellent physiological stimulation model of SCCs in humans.

However, peripheral vestibular diseases represented by VN in clinical often involve two or more SCCs pathways, resulting in a combined vector feature of multiple SCCs effects in the direction of SN. This interplay makes it challenging for clinicians to observe and understand SN and its intrinsic pathology. 3D-VNG technology can help analyze the combined vector features of SN. According to Ewald's law, analyzing the characteristics of SN components using 3D-VNG technology and tracing the damage to the affected SCCs pathway is a new perspective for the clinical diagnosis of vestibular disease. Our study focuses on patients with a confirmed diagnosis of VN or AUVP and combines vHIT with 3D-VNG technology to explore the 3D characteristics of nystagmus after different SCCs aVOR injuries.

VN is a unilateral vestibular lesion mainly affecting the superior division of the vestibular nerve (Chang et al., 2022; Paris et al., 2022)—injuries to both the superior and inferior vestibular nerves are rare, whereas the inferior vestibular nerve is most often spared (Lee et al., 2019). Studies have shown that SN in SVN is horizontal, vertical, and torsional, whereby L-SCC afferent nerve dysfunction leads to the horizontal component, while A-SCC afferent nerve dysfunction leads to the torsional and weak vertical upward components (Fetter and Dichgans, 1996; Yagi et al., 2010). In the current study, the results of the vHIT and the caloric test

demonstrated that the superior vestibular nerve was affected in 31 of the 38 VN patients, while both the superior and inferior vestibular nerves were affected in 7 of the 38 patients. The median illness duration of between symptom onset and moment of testing was 6 days. Static compensation had not yet been established, and SN was present in all patients. And the illness duration was negatively correlated with the horizontal and torsional components, respectively, but not with the vertical components (Figures 1A–C). All 38 VN patients in this study had a horizontal component toward the opposite side, 65.8% (25/38) had a vertical upward component, 68.4% (26/38) had a torsional component, and no patient had a vertical downward component. The results of vHIT showed significantly reduced aVOR gain values on the ipsilesional L-SCC with normal aVOR gain in the opposite L-SCC, and the asymmetry of L-SCCs was 36.3%. For VN patients with a vertical upward component, the aVOR gain asymmetry between bilateral A-SCCs and bilateral P-SCCs was 12.8%, while the asymmetry was 8.3% for those without a vertical component, and these differences were statistically significant ($p < 0.05$). And for VN patients with a torsional component, the aVOR gains asymmetry of bilateral vertical SCCs was 17.0%, while the asymmetry was 6.6% for those without a vertical component, and these differences were statistically significant ($p < 0.01$).

Further analysis of the correlation between the aVOR gain asymmetry and the SPV of SN components revealed a significant positive correlation between the aVOR gain asymmetry of L-SCCs and the SPV of horizontal component among the 38 VN patients ($r = 0.484$, $p < 0.01$), as well as between the asymmetry of bilateral vertical SCCs (analysis in Materials and methods) and the SPV of torsional component in 26 VN patients ($r = 0.445$, $p < 0.05$), while there was no significant correlations in asymmetry of bilateral A- and P-SCCs and the SPV of vertical component. However, no effective correlation analysis could be conducted due to the small sample size. Additionally, the intensities of SN components induced by the A- and P-SCCs were 30% and 10% of that of the L-SCCs, respectively (Aw et al., 1998); the vertical components have low weights in nystagmus such that weak nystagmus values cannot show a significant correlation with vHIT gain.

In this study, patients with SVN had significantly lower vHIT gains of the A- and L-SCCs on the ipsilesional side than other SCCs. The aVOR of the L-SCC on the ipsilesional side was lower than that on the opposite side, and the aVOR of the A-SCC on the ipsilesional side was lower than that of the other vertical SCCs. The direction characteristics of SN included a horizontal component toward the opposite side, a vertical upward component, and a torsional component (upper pole of the eye beating toward the right ear in RVN and upper pole of the eye beating toward the left ear in LVN). In patients with TVN, the vertical components of the A- and P-SCCs cancel or partially cancel each other, while the torsional components are added up with a stronger SPV than that of SVN (Table 2), so that the SN appears as a horizontal-torsional component. Patients with IVN were not involved in this study. According to the results of this study and Ewald's law, the afferent nerve of the affected P-SCC is dysfunctional, the aVOR of the affected P-SCC is lower than that of other vertical SCCs, and the direction of SN is a vertical downward with torsional component (upper pole of the eye beating toward the right ear in RVN and upper pole of the eye beating toward the left ear in LVN).

Among the VN patients included in this study, the superior vestibular nerve was affected in 31, while both the superior and inferior vestibular nerves were affected in 7. The number of cases was relatively small, and there was a lack of patients with a dysfunctional inferior vestibular nerve. It is impossible to describe and analyze the SN characteristics of a single P-SCC lesion. Therefore, the SN characteristics of a single P-SCC lesion and its correlation with VHIT gain need further study. In addition, the lack of VEMPs results makes it impossible to evaluate the impact of otolith damage on SN in VN patients. In contrast to vHIT and caloric testing, VEMPs are much less relevant for the diagnosis of VN/AUVP (Fife et al., 2017; Strupp et al., 2022), while it is necessary to improve the evaluation of otolith damage on SN in VN patients in the future.

In conclusion, we analyzed the correlation between the direction and SPV of SN components and vHIT gain. The results showed that the SPV of the SN horizontal components and torsional components in VN patients were positively correlated with the aVOR gain asymmetry of vHIT, and the direction of SN corresponded to the plane of the excitable SCCs. There is a horizontal-vertical upward-torsional nystagmus in SVN, while horizontal nystagmus with a strong torsional component is found with no vertical component in TVN (upper pole of the eye beating toward the right ear in RVN, upper pole of the eye beating toward the left ear in LVN). Combining Ewald's law and observing the 3D direction of SN in patients with VN/AUVP, it is of great clinical significance to locate the damaged SCCs and trace the target of the lesion. This study provides an objective basis for investigating the relationship between the SN direction and SCC lesions. It also clarifies the significance of the directional characteristics of vestibular peripheral SN components in diagnosing acute vestibular syndrome through medical history and examination.

Data availability statement

The original contributions presented in the study are included in the article/Supplementary material, further inquiries can be directed to the corresponding author/s.

Author contributions

WW and TC performed the study design. XZ and QD acquired and analyzed the data. XZ and TC drafted the manuscript. YL, SL, QL, CW, and XH revised the manuscript. All authors read and approved the final manuscript.

Funding

This study was supported by the Tianjin Key Medical Discipline Construction Project (TJYXZDXK-046A), Tianjin Applied Basic Research Multiple Investment Fund Project (21JCQNJC01780 and 21JCQNJC01670), and Tianjin Health Research Project (TJWJ2022QN027, TJWJ2022QN028, and TJSJMYXYC-D2-021).

Conflict of interest

The authors declare that the research was conducted in the absence of any commercial or financial relationships that could be construed as a potential conflict of interest.

Publisher's note

All claims expressed in this article are solely those of the authors and do not necessarily represent those of their affiliated

organizations, or those of the publisher, the editors and the reviewers. Any product that may be evaluated in this article, or claim that may be made by its manufacturer, is not guaranteed or endorsed by the publisher.

Supplementary material

The Supplementary material for this article can be found online at: <https://www.frontiersin.org/articles/10.3389/fnins.2023.1243720/full#supplementary-material>

References

- Aw, S. T., Fetter, M., Cremer, P. D., Karlberg, M., and Halmagyi, G. M. (2001). Individual semicircular canal function in superior and inferior vestibular neuritis. *Neurology* 57, 768–774. doi: 10.1212/wnl.57.5.768
- Aw, S. T., Haslwanter, T., Fetter, M., Heimberger, J., and Todd, M. J. (1998). Contribution of the vertical semicircular canals to the caloric nystagmus. *Acta Otolaryngol.* 118, 618–627. doi: 10.1080/00016489850183089
- Bachmann, K., Sipos, K., Lavender, V., and Hunter, L. L. (2018). Video head impulse testing in a pediatric population: normative findings. *J. Am. Acad. Audiol.* 29, 417–426. doi: 10.3766/jaaa.17076
- Baier, B., Bense, S., and Dieterich, M. (2008). Are signs of ocular tilt reaction in patients with cerebellar lesions mediated by the dentate nucleus? *Brain* 131, 1445–1454. doi: 10.1093/brain/awn086
- Buki, B., and Ward, B. K. (2021). Length of the narrow bony channels may not be the sole cause of differential involvement of the nerves in vestibular neuritis. *Otol. Neurotol.* 42, e918–e924. doi: 10.1097/MAO.00000000000003161
- Chang, C. M., Lo, W. C., Young, Y. H., Liao, L. J., Wu, P. H., Cheng, P. C., et al. (2022). Galvanic vestibular-evoked myogenic potentials in evaluating damaged sites of vestibular neuritis. *Laryngoscope Investig Otolaryngol* 7, 506–514. doi: 10.1002/lio2.745
- Deng, Q., Zhang, X., Wen, C., Liu, Q., Liu, Y., and Chen, T. (2023). Further exploration of the classification and clinical value of head-shaking nystagmus. *Lin Chung Er Bi Yan Hou Tou Jing Wai Ke Za Zhi* 37, 473–477. doi: 10.13201/j.issn.2096-7993.2023.06.013
- Eggers, S. D. Z., Bisdorff, A., von Brevern, M., Zee, D. S., Kim, J. S., Perez-Fernandez, N., et al. (2019). Classification of vestibular signs and examination techniques: nystagmus and nystagmus-like movements. *J. Vestib. Res.* 29, 57–87. doi: 10.3233/VES-190658
- Fetter, M., and Dichgans, J. (1996). Vestibular neuritis spares the inferior division of the vestibular nerve. *Brain* 119, 755–763. doi: 10.1093/brain/119.3.755
- Fife, T. D., Colebatch, J. G., Kerber, K. A., Brantberg, K., Strupp, M., Lee, H., et al. (2017). Practice guideline: cervical and ocular vestibular evoked myogenic potential testing: report of the guideline development, dissemination, and implementation Subcommittee of the American Academy of Neurology. *Neurology* 89, 2288–2296. doi: 10.1212/WNL.0000000000004690
- Lacour, M., Helmchen, C., and Vidal, P. P. (2016). Vestibular compensation: the neuro-otologist's best friend. *J. Neurol.* 263, S54–S64. doi: 10.1007/s00415-015-7903-4
- Le, T. N., Westerberg, B. D., and Lea, J. (2019). Vestibular neuritis: recent advances in etiology, diagnostic evaluation, and treatment. *Adv. Otorhinolaryngol.* 82, 87–92. doi: 10.1159/000490275
- Lee, J. Y., Park, J. S., and Kim, M. B. (2019). Clinical characteristics of acute vestibular neuritis according to involvement site. *Otol. Neurotol.* 40, 797–805. doi: 10.1097/MAO.0000000000002226
- Ling, X., Wu, Y. X., Feng, Y. F., Zhao, T. T., Zhao, G. P., Kim, J. S., et al. (2023). Spontaneous nystagmus with an upbeat component: central or peripheral vestibular disorders? *Front. Neurol.* 14:1106084. doi: 10.3389/fneur.2023.1106084
- Liu, W. Y., Chen, T. S., Wang, W., Xu, K. X., Li, S. S., Wen, C., et al. (2017). The analysis of the value of spontaneous nystagmus in peripheral vestibular hypofunction. *Lin Chung Er Bi Yan Hou Tou Jing Wai Ke Za Zhi* 31, 678–681. doi: 10.13201/j.issn.1001-1781.2017.09.007
- Liu, Y., Zhang, X., Deng, Q., Liu, Q., Wen, C., Wang, W., et al. (2022). The 3D characteristics of nystagmus in posterior semicircular canal benign paroxysmal positional vertigo. *Front. Neurosci.* 16:988733. doi: 10.3389/fnins.2022.988733
- Molnar, A., Jassoy, B. D., Maihoub, S., Mavrogeni, P., Tamás, L., and Szirmai, Á. (2023). Long-term follow-up of patients with vestibular neuritis by caloric testing and directional preponderance calculation. *Eur. Arch. Otorhinolaryngol.* 280, 1695–1701. doi: 10.1007/s00405-022-07660-9
- Paris, P., Charpiot, A., Veillon, F., Severac, F., and Djennaoui, I. (2022). Prevalence of cardiovascular risk factors in superior vestibular neuritis: a cross-sectional study following STROBE guidelines. *Eur. Ann. Otorhinolaryngol. Head Neck Dis.* 139, 194–197. doi: 10.1016/j.anorl.2022.01.002
- Professional Committee on Vertigo, Division of Neurology, Medical doctor Association Stroke and Vertigo Branch, Chinese Stroke Association (2020). Multidisciplinary experts' consensus on vestibular neuritis. *Chin J Geriatr.* 039, 985–994. doi: 10.3760/cma.j.issn.0254-9026.2020.09.005
- Psillas, G., Petrou, I., Printza, A., Sfakianaki, I., Binos, P., Anastasiadou, S., et al. (2022). Video head impulse test (vHIT): value of gain and refixation saccades in unilateral vestibular neuritis. *J. Clin. Med.* 11:3467. doi: 10.3390/jcm11123467
- Sando, I., Black, F. O., and Hemenway, W. G. (1972). Spatial distribution of vestibular nerve in internal auditory canal. *Ann. Otol. Rhinol. Laryngol.* 81, 305–314. doi: 10.1177/000348947208100301
- Strupp, M., Bisdorff, A., Furman, J., Hornibrook, J., Jahn, K., Maire, R., et al. (2022). Acute unilateral vestibulopathy/vestibular neuritis: diagnostic criteria. *J. Vestib. Res.* 32, 389–406. doi: 10.3233/VES-220201
- Wenyu, L., Taisheng, C., Wei, W., Xu, K. X., Li, S. S., Wen, C., et al. (2017). The analysis of the value of spontaneous nystagmus in peripheral vestibular hypofunction. *Lin Chung Er Bi Yan Hou Tou Jing Wai Ke Za Zhi* 31, 678–681. doi: 10.13201/j.issn.1001-1781.2017.09.007
- Xie, S., Chen, T., Deng, Q., Li, S. S., Mao, X., Wen, C., et al. (2021). Effects of vestibular spontaneous nystagmus on visual smooth pursuit function. *Zhonghua Er Bi Yan Hou Tou Jing Wai Ke Za Zhi* 56, 280–284. doi: 10.3760/cma.j.cn115330-20200325-00245
- Yagi, T., Koizumi, Y., and Sugizaki, K. (2010). 3D analysis of spontaneous nystagmus in early stage of vestibular neuritis. *Auris Nasus Larynx* 37, 167–172. doi: 10.1016/j.anl.2009.05.008
- Zhang, X., Bai, Y., Chen, T., Wang, W., Han, X., Li, S., et al. (2021). A show of Ewald's law: I horizontal semicircular canal benign paroxysmal positional vertigo. *Front. Neurol.* 12:632489. doi: 10.3389/fneur.2021.632489
- Zhang, X., Deng, Q., Liu, Q., Wen, C., Wang, W., and Chen, T. (2022). The horizontal and vertical components of nystagmus evoked by the supine roll test in horizontal semicircular canal canalolithiasis. *Front. Neurosci.* 16:957617. doi: 10.3389/fnins.2022.957617



OPEN ACCESS

EDITED BY

Sulin Zhan,
Huazhong University of Science and
Technology, China

REVIEWED BY

Takeshi Tsutsumi,
Tokyo Medical and Dental University, Japan
Jiying Zhou,
First Affiliated Hospital of Chongqing Medical
University, China

*CORRESPONDENCE

Tongxiang Diao
✉ tongx@foxmail.com
Lisheng Yu
✉ yulish68@163.com

RECEIVED 12 May 2023

ACCEPTED 18 August 2023

PUBLISHED 07 September 2023

CITATION

Chen Y, Zhao P, Ma X, Diao T and Yu L (2023)
Case report: MRI changes of the inner ear in an
MD patient with suspected immune
dysfunction.
Front. Neurol. 14:1220162.
doi: 10.3389/fneur.2023.1220162

COPYRIGHT

© 2023 Chen, Zhao, Ma, Diao and Yu. This is an
open-access article distributed under the terms
of the [Creative Commons Attribution License
\(CC BY\)](https://creativecommons.org/licenses/by/4.0/). The use, distribution or reproduction
in other forums is permitted, provided the
original author(s) and the copyright owner(s)
are credited and that the original publication in
this journal is cited, in accordance with
accepted academic practice. No use,
distribution or reproduction is permitted which
does not comply with these terms.

Case report: MRI changes of the inner ear in an MD patient with suspected immune dysfunction

Yurun Chen¹, Pengfei Zhao², Xin Ma¹, Tongxiang Diao^{1*} and
Lisheng Yu^{1*}

¹Department of Otolaryngology, Head and Neck Surgery, People's Hospital, Peking University, Beijing, China, ²Beijing Friendship Hospital, Capital Medical University, Beijing, China

Objectives: The primary objective of this study was to present the progressive changes from labyrinthitis to endolymphatic hydrops (EH) demonstrated in the inner ear MRI of a patient with MD and suspected immune dysfunction.

Patient: This 31-year-old male was diagnosed with MD and suspected autoimmune diseases.

Interventions: Immunosuppressants and biological agents.

Main outcomes measures: Inner ear MRI images.

Results: Changes in the patient's progress revealed that inner ear immune and inflammatory changes might induce EH, which may eventually turn into MD.

Conclusion: This case is the first documented case of MRI revealing progressive changes from inflammatory response to endolymphatic hydrops in the inner ear. It shows the correlation between MD and inflammation visually. It is of great significance to reveal the pathogenesis of MD to further assist in the guidance of treatment decision making.

KEYWORDS

Meniere's disease, immune and inflammatory responses, endolymphatic hydrops, MRI, pathophysiology

1. Introduction

Meniere's disease was first proposed by Prosper Menière in 1861 and is characterized by recurring spontaneous vertigo, fluctuating hearing loss, tinnitus, and aural fullness. The prevalence of MD is approximately 34–190 per 100,000 (1). Not all patients with MD showed every typical symptom at the early stage of onset. Approximately 50% of patients with MD sustained vertigo and hearing loss, 19% suffered only vertigo, and 26% presented only hearing loss (2). In this case, the patient first developed vertigo before the onset of fluctuating hearing loss, tinnitus, and aural fullness.

Studies have shown that the occurrence of Meniere's disease (MD) may be related to inflammation and immune dysfunction. In fact, as early as 1916, Wittmacck et al. proposed that some dizziness and imbalance diseases might be caused by infection based on temporal bone anatomy (3). Previous studies by our team have shown that MD patients are often associated with poorer mastoid pneumatization, which suggests that factors such as long-term drainage disorders and repeated inflammatory stimulation caused by anatomical variations may play an important role in the occurrence and development of MD (4).

Approximately one-third of patients with MD are accompanied with immune dysfunction (5). In 1986, Brooks et al. found that 54% of patients with MD had increased levels of immune complexes in their circulating blood. Several studies have described MD associated with autoimmune diseases such as rheumatoid arthritis, systemic lupus erythematosus, or psoriasis (6). Alleman et al. believed that this confirmed increase was caused by a local immune response in the endolymphatic sac, which originates from infection or allergy rather than from autoimmunity.

However, there remains a lack of direct evidence for the underlying pathophysiological mechanism of MD induced by immune and inflammatory responses. The changes of the inner ear demonstrated by MRI of the patient in this case intuitively demonstrated the progressive changes from labyrinthitis to endolymphatic hydrops (EH), which is of important clinical significance for not only validating the relationship between immune inflammatory response and MD, but also for providing a new direction to reveal the pathophysiology of MD and guiding its diagnosis and treatment.

2. Case report

A 31-year-old male presented to a physician with repeated episodes of rotational vertigo that lasted for a number of hours over the past 4 years (2017–09). He also reported nausea and vomiting with no tinnitus or hearing loss during the attack. Three years ago (2018–06), the patient started to experience left sided fluctuating tinnitus and sensorineural hearing loss (Table 1), accompanied by vertigo and aural fullness. He suffered attacks two or three times a week, lasting from 15 min to 2 h each. His past medical history was unremarkable, with no family history of dizziness or autoimmune disease.

There was no obvious abnormality in the video head impulse test (vHIT), while the caloric test showed left horizontal semicircular canal paresis (CP = 79%). This discrepancy indicates semicircular canal functions at normal head movement frequency and velocity ranges, but disfunctions at low frequency. No obvious abnormality was found in the electrocochleogram. No frequency of the left ear was elicited by distortion product otoacoustic emissions (DPOAE). Furthermore, ocular vestibular evoked myogenic potential (oVEMP) showed prolonged latency and low amplitude on the left-sided ear. Moreover, a lower amplitude on the left side was observed by cervical vestibular evoked myogenic potential (cVEMP).

The vHIT test is less sensitive for the detection of semicircular canal hypofunction than the caloric test (7). Considering all of the above, this patient was diagnosed with MD (1). Because the patient was less sensitive to vasodilators, flunarizine, and betahistine mesylate, but more sensitive to hormones, the immunologists believed that autoimmune diseases should be taken into consideration. After receiving immunosuppressants and biological agents, including tacrolimus, interleukin-2, cyclosporine, Rituxan, and Tocilizumab injections since March 2019, the patient reported that vertigo occurred less frequently. During the course of treatment, the immunologists attempted to reduce the dose of prednisone twice (2019-03, 2019-10).

However, after the reduction, the patient experienced vertigo similar to before the therapy. Thereafter, methylprednisolone and prednisone were used alternately up until now. After receiving glucocorticoids and immunosuppressant therapy, the patient was relieved from vertigo and stopped losing hearing.

The patient underwent inner ear MRI every 6 months since onset; all examinations were performed using the same apparatus. In March 2019, the left vestibular signal was higher than that in the contralateral in both T1WI (A1) and 3DT2FLAIR sequences, whereas it was lower in the water imaging sequence (A2), indicating a disruption of the blood labyrinth barrier caused by inflammatory or hemorrhagic changes (A3). In October 2019, the signal of the left vestibular in the T1WI sequence remained higher than that in the contralateral (B1). In the 3D-T2-FLAIR sequence, the signals of the left vestibular and vestibular nerve were higher than those of the right (B2). The differences between both sides became more remarkable, which suggested progression of the disease. In April 2020, the signals of the left vestibular and vestibular aqueduct remained higher than that of the contralateral in the 3D-T2-FLAIR sequence. Nevertheless, the signal differences decreased (C), indicating that inflammatory lesions had subsided. In December 2020, the left vestibular filling defect became larger under gadolinium angiography in the 3D-T2-FLAIR sequence, which was a sign of EH (D). In July 2021, under gadolinium angiography in the 3D-T2-FLAIR sequence, left-sided EH improved (E).

The inner ear MRI of the patient showed the progressive change from exudative inflammatory changes to EH. This revealed that inner ear immune and inflammatory changes might induce EH, which can eventually turn into MD.

3. Discussion

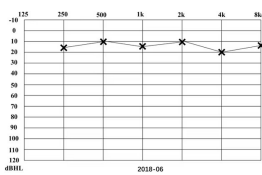
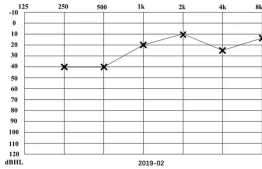

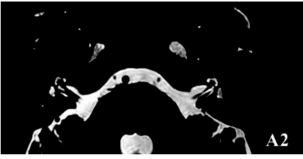
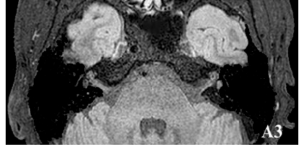
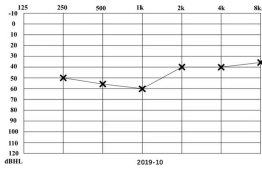
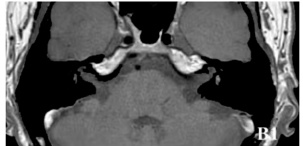
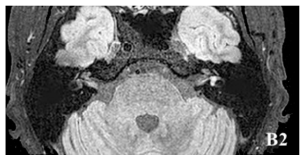


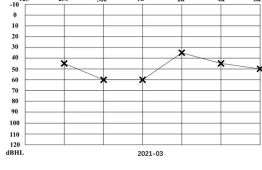
EH is currently believed to be the main pathophysiology of MD; approximately one-third of patients with MD may be associated with immune dysfunction (5). Frejo (8) divided unilateral and bilateral MD patients into five clinical subtypes. One of these is MD combined with autoimmune diseases. As for this patient's long course of disease, sensitivity to hormone and immunosuppressant therapy, and the rise in blood IgG4, immune diseases should be taken into consideration. However, there was no direct evidence on the pathological mechanism of how the immune inflammatory response induced MD. The inner ear MRI of this patient is the first documented case illustrating the progressive development from immune inflammatory changes to EH in the occurrence of MD. We speculate that local immune inflammatory responses in the inner ear can cause destruction of the blood-labyrinth barrier and labyrinthitis, can induce microcirculation disturbances, and can eventually lead to EH.

4. Conclusion

This case is the first documented case of MRI revealing the progressive changes from an inflammatory response to endolymphatic hydrops in the inner ear. It visually shows the correlation between MD and inflammation. It is of great significance to reveal the pathogenesis of MD, and this can further assist in the guidance of treatment decision making.

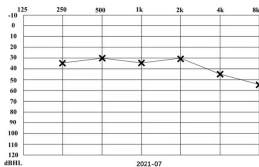
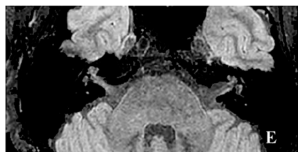
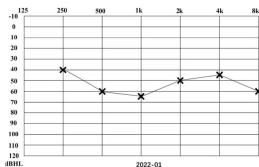
Abbreviations: MD, Meniere's disease; EH, Endolymphatic hydrops.

TABLE 1 The patient underwent Pure Tone Threshold Audiometry (PTA) and inner ear MRI since onset.

Date	Audiograms	MRI
2018-06		
2019-02		
2019-03		
		
2019-10		
		
2020-04		
2020-12		
2021-03		

(Continued)

TABLE 1 (Continued)

Date	Audiograms	MRI
2021-07		 <p>In July 2021, under gadolinium angiography in the 3D-T2-FLAIR sequence, left-sided EH improved (E).</p>
2022-01		

Data availability statement

The original contributions presented in the study are included in the article/supplementary material, further inquiries can be directed to the corresponding authors.

Ethics statement

Written informed consent was obtained from the individual(s) for the publication of any potentially identifiable images or data included in this article.

Author contributions

YC: data curation, formal analysis, and writing-original draft. PZ: data curation. XM: validation, supervision, and funding acquisition. TD: conceptualization, methodology, writing-review and editing, and funding acquisition. LY: project administration and funding acquisition. All authors contributed to the article and approved the submitted version.

Funding

This work was supported by Peking University People's Hospital Scientific Research Development Funds (RDL2021-14), Peking

University People's Hospital Scientific Research Development Funds (RDY2021-25), and the National Key Technologies Research and Development Program of China (2020YFC2005200).

Acknowledgments

The authors would like to express our sincere appreciation to this patient, whose unconditional cooperation and understanding of the treatment process have provided us with an opportunity to reach a deeper understanding of this disease.

Conflict of interest

The authors declare that the research was conducted in the absence of any commercial or financial relationships that could be construed as a potential conflict of interest.

Publisher's note

All claims expressed in this article are solely those of the authors and do not necessarily represent those of their affiliated organizations, or those of the publisher, the editors and the reviewers. Any product that may be evaluated in this article, or claim that may be made by its manufacturer, is not guaranteed or endorsed by the publisher.

References

- Lopez-Escamez JA, Carey J, Chung WH, Goebel JA, Magnusson M, Mandalà M, et al. Diagnostic criteria for Meniere's disease. *J Vestib Res.* (2015) 25:1–7. doi: 10.3233/VES-150549
- Schaaf H, Hesse G. Low frequency fluctuating hearing loss without labyrinthine vertigo—a genuine disease? A follow up study after 4 and 10 years. *HNO.* (2007) 55:630–7. doi: 10.1007/s00106-006-1495-3
- Derebery MJ, Berliner KI. Allergy and Ménière's disease. *Curr Allergy Asthma Rep.* (2007) 7:451–6. doi: 10.1007/s11882-007-0069-0
- Diao T, Han L, Jing Y, Wang Y, Ma X, Yu L, et al. The clinical characteristics and anatomical variations in patients with intractable unilateral Meniere's disease with and without migraine. *J Vestib Res.* (2021) 32:57–67. doi: 10.3233/VES-190755
- Greco A, Gallo A, Fusconi M, Marinelli C, Macri GF, De Vincentiis M. Meniere's disease might be an autoimmune condition? *Autoimmun Rev.* (2012) 11:731–8. doi: 10.1016/j.autrev.2012.01.004
- Flook M, Lopez Escamez JA. Meniere's disease: genetics and the immune system. *Curr Otorhinolaryngol Rep.* (2018) 6:24–31. doi: 10.1007/s40136-018-0182-8
- Park HJ, Migliaccio AA, Della Santina CC, Minor LB, Carey JP. Search-coil head-thrust and caloric tests in Ménière's disease. *Acta Otolaryngol.* (2005) 125:852–7. doi: 10.1080/00016480510033667
- Frejo L, Martin-Sanz E, Teggi R, Trinidad G, Soto-Varela A, Santos-Perez S, et al. Extended phenotype and clinical subgroups in unilateral Meniere disease: a cross-sectional study with cluster analysis. *Clin Otolaryngol.* (2017) 42:1172–80. doi: 10.1111/coa.12844



OPEN ACCESS

EDITED BY

Daogong Zhang,
Shandong Provincial ENT Hospital, China

REVIEWED BY

Alfonso Scarpa,
University of Salerno, Italy
Chenlu Zhu,
Lanzhou University Second Hospital, China

*CORRESPONDENCE

Lisheng Yu
✉ yulish68@163.com
Tongxiang Diao
✉ tongx@foxmail.com

†These authors have contributed equally to this work

RECEIVED 17 July 2023

ACCEPTED 10 October 2023

PUBLISHED 25 October 2023

CITATION

Qi R, Zhang J, Diao T and Yu L (2023) The auditory function in migraine model rats induced by postauricular nitroglycerin injection. *Front. Neurol.* 14:1259982. doi: 10.3389/fneur.2023.1259982

COPYRIGHT

© 2023 Qi, Zhang, Diao and Yu. This is an open-access article distributed under the terms of the [Creative Commons Attribution License \(CC BY\)](https://creativecommons.org/licenses/by/4.0/). The use, distribution or reproduction in other forums is permitted, provided the original author(s) and the copyright owner(s) are credited and that the original publication in this journal is cited, in accordance with accepted academic practice. No use, distribution or reproduction is permitted which does not comply with these terms.

The auditory function in migraine model rats induced by postauricular nitroglycerin injection

Rongxiang Qi, Jilei Zhang, Tongxiang Diao*† and Lisheng Yu*†

Department of Otolaryngology, Head and Neck Surgery, People's Hospital, Peking University, Beijing, China

Objective: The mechanism by which migraines produce inner ear-related symptoms is not well understood. Previous studies have found that the latency of auditory brainstem response (ABR) in animal models of migraine has changed, but the threshold has not changed significantly. Therefore, it is necessary to establish a better animal model with both migraine and hearing loss to explore the relationship between migraine and auditory function deeply.

Methods: In this study, the rat model of migraine was induced by postauricular injection of nitroglycerin (NTG), and the effect on the auditory function of the inner ear was explored by comparing with intraperitoneal injection of nitroglycerin. The rats were given the drug repeatedly on alternate days, a total of 5 dosing, with the body weight monitored during the drug administration. The tactile threshold of the rats' forepaw was measured using von-Frey filaments and auditory function was assessed by ABR.

Results: The results showed that the baseline tactile threshold of rats gradually decreased during the modeling process, and hyperalgesia appeared. Postauricular injection of NTG did not affect the weight gain of rats, while intraperitoneal injection of NTG showed slow or even negative weight gain. The ABR threshold of Click, 4 and 8 kHz of postauricular NTG injection rats increased, the latency was prolonged, and the ABR threshold in the right ear was higher than that in the left ear.

Conclusions: We demonstrated that postauricular injection of nitroglycerin may be safer and more effective than intraperitoneal injection of nitroglycerin in the process of creating rat migraine model without affecting the weight gain. Postauricular injection of nitroglycerin has more damage to the auditory function of rats. Therefore, the migraine model rat induced by postauricular injection of nitroglycerin may be a new model of cochlear migraine.

KEYWORDS

postauricular injection, intraperitoneal injection, auditory function, migraine model rat, cochlear migraine

1. Introduction

Migraine is a common neurological disease, which is characterized by paroxysmal, mostly unilateral, moderate to severe throbbing headache, often accompanied by photophobia, phonophobia, nausea and vomiting (1). According to the global burden of diseases 2016 study, migraine is the second most common neurological disability disease (2). Migraine patients can be accompanied by inner ear related symptoms such as vertigo, hearing loss,

tinnitus, hyperacusis, ear fullness, etc. The incidence of hearing loss in migraine patients ranges from 3.3 to 14% (3, 4); however, there are few studies using migraine animal models to explore the relationship between migraine and the inner ear function, especially those related to auditory function. Arakaki et al. (5) reported that the latency of IV, V, and VI waves of the ABR of the 8-kHz stimulus sound was significantly prolonged 2 h after nitroglycerin administration in the rat model of migraine. Therefore, to understand the association between migraine and inner ear hearing impairment deeply, it is necessary to establish a better animal models with both migraine-related manifestations and hearing loss.

Postauricular injection is a new method of drug administration. At present, postauricular injection of glucocorticoids is mainly used to treat inner ear diseases such as sudden deafness, tinnitus, and ear fullness. Previous studies have shown that postauricular injection has the advantages of being less invasive, convenient, and having high local cochlear drug concentrations (6, 7). Qiu et al. (8) used the anti-tumor drug cisplatin to explore the drug distribution characteristics after postauricular injection in animal experiments, the results showed that the systemic adverse reactions induced by cisplatin in the postauricular injection group and the intraperitoneal injection group were similar, and the postauricular injection of cisplatin could cause obvious damage to bilateral cochlear hair cells, and the damage of hair cells in the ipsilateral cochlea was significantly greater than that in the contralateral cochlea, postauricular injection of cisplatin also caused more damage to the hair cells of the ipsilateral cochlea than intraperitoneal injection, it is suggested that postauricular administration can achieve higher local drug concentration than systemic administration. In general, postauricular injection has the characteristics of high drug concentration in the inner ear of the administration side and drug distribution to the opposite inner ear and the whole body.

The nitroglycerin-induced migraine model is a classic experimental migraine model. The methods of nitroglycerin injection include intraperitoneal injection, intravenous injection and subcutaneous injection, and intraperitoneal injection is the most commonly used. So far, no relevant literature and reports on migraine animal models by postauricular injection of nitroglycerin have been retrieved. According to the distribution characteristics of drugs after postauricular injection, the migraine model rat was established by postauricular injection of nitroglycerin, so as to better study the correlation between migraine and the inner ear.

2. Material and methods

2.1. Animal subjects

Healthy male Wistar rats (7–8 weeks old, 200–250 g) were purchased from SPF Biotech Ltd (Beijing, China). The animals were housed under standard laboratory conditions: $20 \pm 4^\circ\text{C}$ ambient temperature with a relative humidity of $60 \pm 5\%$ and a 12-h light/dark cycle. All the animals had unlimited access to food and water. This study was approved by the Animal Ethics Committee of Peking University People's Hospital (Approval

Number: 2022PHE135), and animal care was performed in accordance with the Guide for the Care and Use of Laboratory Animals set by the China Association of Laboratory/Animal Care.

2.2. Experimental design

In this experiment, 45 Wistar rats were randomly assigned to four groups: group 1 ($n = 15$) received a postauricular injection of NTG (10 mg/kg) (PI-NTG) every other day for 9 days; group 2 ($n = 10$) received a postauricular injection of 0.9% saline (10 mL/kg) (PI-NS) every other day for 9 days; group 3 ($n = 10$) received a intraperitoneal injection of NTG (10 mg/kg) (II-NTG) every other day for 9 days; and group 4 ($n = 10$) received a intraperitoneal injection of 0.9% saline (10 mL/kg) (II-NS) every other day for 9 days. The body weight was monitored every other day for all rats. Forepaw sensitivity to mechanical stimulation was assessed using von Frey device 20 min before and 2 h after each dose for all rats. Five rats were randomly selected from group 1 to continue feeding for 14 days after the last dose, all remaining rats underwent ABR test 2 h after the last dose. After 14 days, the five rats from group 1 were assessed again for forepaw sensitivity to mechanical stimulation and underwent ABR tests.

2.3. Drug administration

The formula of NTG for injection was prepared as described previously (9). 5.0 mg/mL NTG (Beijing Yiming, China) was diluted with 0.9% saline to 1 mg/mL. Rats in the postauricular group were injected in the middle of the right postauricular groove. Rats in the intraperitoneal group were injected into the lower left quadrant of their abdomen.

2.4. Behavioral observation

The behavioral activities of the rats were observed and recorded before and after each administration. NTG-treated animals showed more anxiety-like behavior such as increased self-grooming and face rubbing behavior (10).

2.5. Measurement of forepaw thresholds after mechanical stimulation

As a surrogate measure of pain/pronociception, tactile sensitivity to stimulation with von Frey monofilaments (North Coast Medical, USA) within fore paw nociceptive circuits was measured using the up-down paradigm (11) as previously described in detail (12). The testing was performed with the rat placed in clear plexiglas chambers on a mesh floor. Rats were placed in the chambers for acclimatization 30–45 min prior to testing. Calculation of 50% withdrawal thresholds was done using the

free online calculator at https://bioapps.shinyapps.io/von_frey_app/ with application of inter-filament steps (13). Tactile sensitivity was measured at baseline and 120 min after each administration by a blinded experimenter.

2.6. Auditory brain stem response

ABR measurement was carried out in a sound-attenuating, electrically shielded booth located inside a sound-attenuating room. The rats were anesthetized with 10% chloral hydrate (4 mL/kg) injected intraperitoneal. ABR responses were recorded using subdermal needle electrodes. Needle electrodes were placed at the vertex (active), the test ear (reference), and the contralateral ear (ground) pinnae. Tucker Davis Technologies (TDT) System III hardware and SigGen/BioSig software (TDT, Alachua, FL USA) were used to present the stimulus and record responses. Click and 4, 8, 16, 24, and 32 kHz tone bursts were used as the auditory stimulant. Up to 1,024 responses were averaged for each stimulus level. Hearing thresholds were defined starting from 90 dB SPL, decreasing in 10 dB increments each time. Thresholds were interpolated between the lowest stimulus level where a response is observed, and 5 dB lower, where no response is observed. The latency time of I, II, III, IV, and V wave with 4 kHz 90 dB SPL tone bursts ABR waveform was recorded. Rats in the postauricular group tested both ears, while those in the intraperitoneal group only tested the right ear.

2.7. Statistical analysis

Descriptive data were presented as means and standard deviations (SD). Student's *t*-test was used for statistical comparisons between two groups. One-way or two-way ANOVA followed by *post-hoc* analysis with the Tukey test was used for statistical comparisons among groups. Mann Whitney *U*-test was selected for the non-parametric analysis. All statistical analyses were performed using SPSS software (version 27.0, IBM, USA), and statistical significance was set at $p < 0.05$.

3. Results

3.1. PI-NTG could induce migraine without affecting the animals' weight gain

The specific administration schedule is shown in Figure 1A. Behavioral manifestations related to migraine occurred after each administration of NTG. Chronic injection of NTG produced progressive basal hypersensitivity (Figure 1B) and acute allodynia (Figure 1C). However, abdominal pain, loss of appetite, and even diarrhea were observed in II-NTG rats, while no such phenomenon was observed in PI-NTG rats. During the modeling process, there was no significant difference in the body weight growth of rats in the PI-NTG group, the PI-NS group and the II-NS group ($p > 0.05$), while the body weight of rats in the II-NTG group increased slowly or even negatively, which was significantly different from other groups (Figure 1D; $p < 0.05$).

3.2. Compared with II-NTG group, PI-NTG rats showed more severe hearing loss

Compared with the II-NTG group, the ABR threshold of Click, 4 and 8 kHz in the PI-NTG injection group was increased (Table 1; $p < 0.05$), the latency was prolonged (Table 2; $p < 0.05$), and the ABR threshold in the right ear was higher than that in the left ear (Table 1; $p < 0.05$). There was no significant change in ABR threshold of rats in the II-NTG group, only the latency was prolonged.

3.3. Hearing loss was irreversible in PI-NTG group

Five rats in the PI-NTG group were selected and fed for 14 days after the last administration. The tactile threshold of forepaw and ABR were measured again. The results showed that the paw mechanical pain threshold basically returned to the state before administration on day 1. The ABR threshold and latency did not change significantly from the day after the last dose.

4. Discussion

The mechanism of migraine accompanied with inner ear dysfunction remains unclear. However, there are few basic researches on the relationship between migraine and inner ear function, especially animal experiments on the effect of migraine on auditory function. Previous studies have found that the latency of ABR in migraine animal models changes, but the threshold does not change significantly (5). Therefore, it is necessary to establish better animal models with both migraine and hearing loss, so as to understand the relationship between migraine and inner ear function deeply.

The results of this study show that it is feasible to establish a rat model of migraine by postauricular injection of nitroglycerin. Every time after postauricular injection of nitroglycerin, the rats showed the corresponding behavioral manifestations and hyperalgesia of migraine. Chronic intermittent administration can cause progressive, persistent hyperalgesia. The results of this study showed that the rats in the intraperitoneal injection of nitroglycerin group had poor appetite, reduced food intake, slow weight gain, or even negative growth, which was significantly different from the postauricular injection of nitroglycerin group. Compared with the intraperitoneal injection of nitroglycerin, postauricular injection of nitroglycerin is safer and has fewer systemic side effects. However, some rats with postauricular injection of nitroglycerin showed hair loss on the postauricular skin.

The results of this study show that postauricular injection of nitroglycerin can increase the ABR threshold and prolong the latency of ABR in rats, while intraperitoneal injection of nitroglycerin has no significant change in the ABR threshold of rats, only show prolonged latency, suggesting that the migraine model rat induced by postauricular injection of nitroglycerin is more likely to cause inner ear auditory function damage. The results of this study showed that the increase of ABR threshold in migraine model

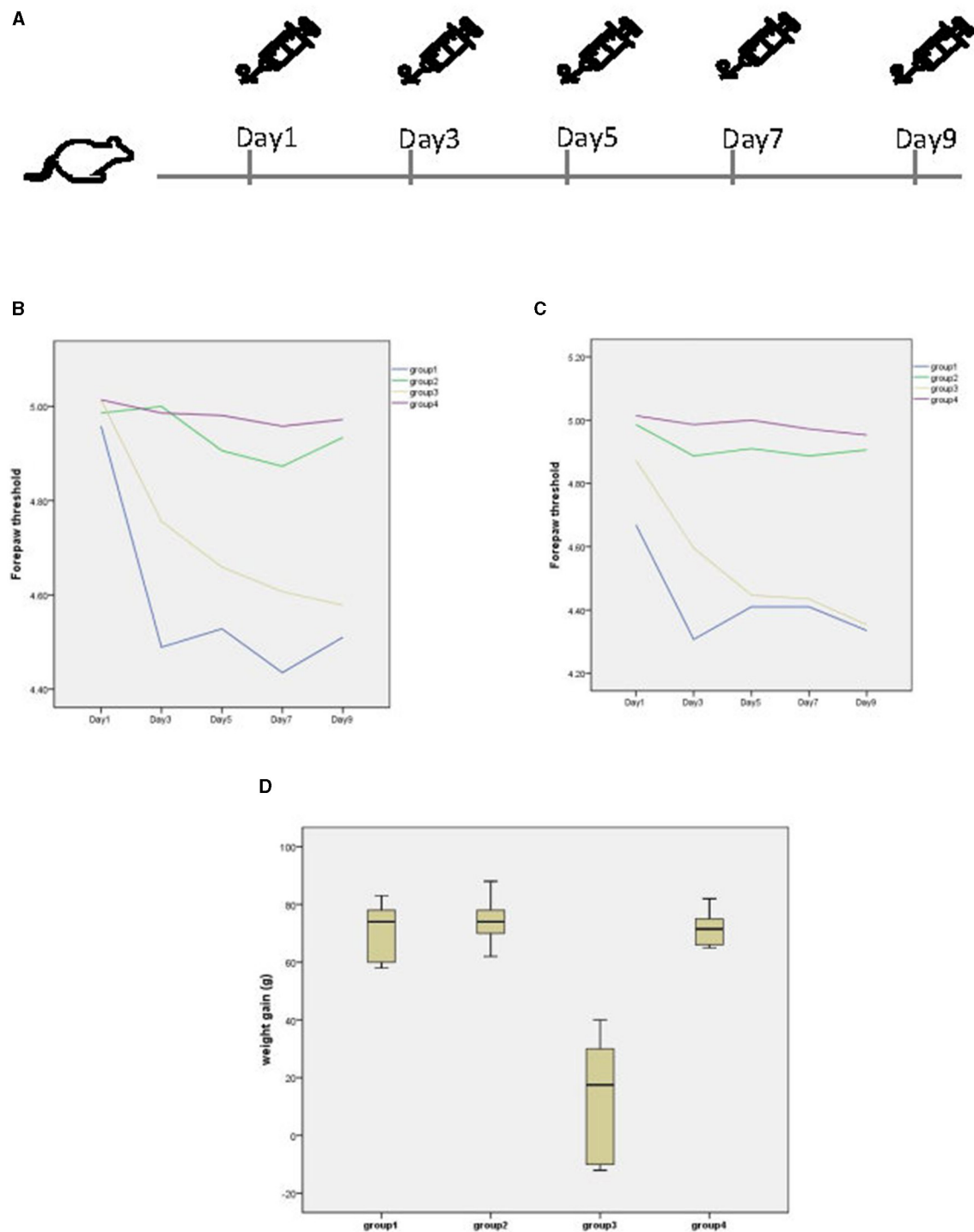


FIGURE 1

(A) Timeline of administration. (B) Basal and post-treatment tactile threshold (C) of forepaw were markedly decreased in a time dependent manner after NTG injection. (D) Body weight growth of each group, the weight gain is the weight on day 9 minus the weight on day 1. Group 1 ($n = 10$): postauricular NTG injection group; Group 2 ($n = 10$): postauricular saline injection group; Group 3 ($n = 10$): intraperitoneal NTG injection group; Group 4 ($n = 10$): intraperitoneal saline injection group.

rat induced by post-auricular injection of nitroglycerin mainly occurred in click and 4 kHz tone bursts. The increase of ABR threshold was also observed in 8 kHz tone bursts, but it was not as obvious as that in 4 kHz tone bursts. The ABR threshold of 16, 24, and 32 kHz tone bursts did not change. The results suggest

that the hearing changes in the migraine model rat induced by post-auricular injection of nitroglycerin mainly occur in the low frequency hearing, and the high frequency hearing is not impaired, which is consistent with the hearing changes in most migraine patients clinically. Shi et al. (14) studied the hearing of 166 patients

TABLE 1 ABR threshold (dB SPL) ($\bar{x} \pm s$).

	Group1 R	Group1 L	Group2 R	Group2 L	Group3 R	Group4 R
Click	39.50 \pm 3.69	32.00 \pm 2.58	30.00 \pm 0.00	30.00 \pm 0.00	23.00 \pm 2.58	21.00 \pm 2.11
4 k	33.50 \pm 3.38	28.50 \pm 5.30	25.00 \pm 0.00	25.00 \pm 0.00	18.00 \pm 2.58	16.00 \pm 2.11
8 k	22.00 \pm 4.22	17.00 \pm 4.22	17.00 \pm 2.58	17.00 \pm 2.58	10.00 \pm 0.00	10.00 \pm 0.00
16 k	10.00 \pm 0.00	10.00 \pm 0.00	10.00 \pm 0.00	10.00 \pm 0.00	10.00 \pm 0.00	10.00 \pm 0.00
24 k	10.00 \pm 0.00	10.00 \pm 0.00	10.00 \pm 0.00	10.00 \pm 0.00	10.00 \pm 0.00	10.00 \pm 0.00
32 k	10.00 \pm 0.00	10.00 \pm 0.00	10.00 \pm 0.00	10.00 \pm 0.00	10.00 \pm 0.00	10.00 \pm 0.00

Group 1 (n = 10): postauricular NTG injection group; Group 2 (n = 10): postauricular saline injection group; Group 3 (n = 10): intraperitoneal NTG injection group; Group 4 (n = 10): intraperitoneal saline injection group.

R, Right ear; L, Left ear.

TABLE 2 4 kHz 90 dB SPL tone bursts ABR latency (ms) ($\bar{x} \pm s$).

	Group1 R	Group1 L	Group2 R	Group2 L	Group3 R	Group4 R
I	1.38 \pm 0.02	1.31 \pm 0.06	1.31 \pm 0.03	1.31 \pm 0.04	1.33 \pm 0.02	1.29 \pm 0.05
II	2.26 \pm 0.16	2.05 \pm 0.16	2.15 \pm 0.12	2.07 \pm 0.07	2.13 \pm 0.06	2.03 \pm 0.11
III	3.00 \pm 0.25	2.70 \pm 0.12	2.77 \pm 0.18	2.70 \pm 0.08	2.79 \pm 0.07	2.64 \pm 0.10
IV	3.76 \pm 0.27	3.56 \pm 0.14	3.65 \pm 0.33	3.57 \pm 0.07	3.60 \pm 0.11	3.48 \pm 0.11
V	4.95 \pm 0.42	4.49 \pm 0.16	4.56 \pm 0.06	4.53 \pm 0.07	4.64 \pm 0.16	4.46 \pm 0.12

Group 1 (n = 10): postauricular NTG injection group; Group 2 (n = 10): postauricular saline injection group; Group 3 (n = 10): intraperitoneal NTG injection group; Group 4 (n = 10): intraperitoneal saline injection group.

R, Right ear; L, Left ear.

with vestibular migraine and found that the hearing impairment of VM patients was mainly manifested as low frequency hearing loss. Xue et al. (15) also found that patients with VM mainly presented with low-frequency hearing loss, and proposed that the history of migraine may be the cause of sudden low-frequency hearing loss.

The mechanism of migraine-related hearing loss is still unclear, and several theories have been proposed: (1) Migraine triggers vasospasm in the small arteries of the cochlea and labyrinth, which can induce endolymphatic hydrops (16). (2) Some inflammation and neurotransmitters involved in the pathogenesis of migraine affect the inner ear and central auditory system (17). (3) Ion channels expressed in both the inner ear and the brain may affect the peripheral and central auditory systems (18). The results of this study showed that the rat migraine model with postauricular injection of nitroglycerin was mainly characterized by low-frequency hearing loss, and there was no significant change in ABR hearing loss 14 days after administration. It was speculated that the rats in this model may have labyrinthitic hydrocephaly. Due to the limitation of experimental time and conditions, this subject was not further verified by electrocochleogram. In addition, the possibility of ototoxicity should be considered, but intraperitoneal administration of nitroglycerin did not change the ABR threshold of rats, and the relevant literature did not mention that nitroglycerin had ototoxicity.

In 2018, with the cochlear migraine first proposed by Lai et al. (19), Cochlear migraine entered the field of view of the population. Cochlear migraine is a disease that is clinically related to migraine and mainly produces moderate to severe auditory symptoms. The results of this study show that the migraine model rat

induced by postauricular injection of nitroglycerin accompanied with hearing loss, suggesting that this model is more inclined to cochlear migraine, and may be used as an animal model of cochlear migraine, it provides an important foundation for future clinical research.

5. Limitation

There were some limitations in our research. First, our study found that the migraine model rat induced by postauricular nitroglycerin injection was mainly characterized by low frequency hearing loss, and it was speculated that the inner ear of this migraine model rats might have hydrops of membranous labyrinth. However, due to the limitations of experimental time and conditions, this subject was not further verified by electrocochleogram, which is worthy of further study. Second, our study did not further explore the molecular mechanism of hearing loss in this model, which is well worth exploring. The last but not the least, we didn't have an effective mean of measuring vestibular function in rats to more fully evaluate inner ear function of this model.

6. Conclusion

In conclusion, we demonstrated that postauricular injection of nitroglycerin is a safer and more effective way to model migraine in rats than intraperitoneal injection. Postauricular injection of

nitroglycerin has more damage to the auditory function of rats. Therefore, the migraine model rat induced by postauricular injection of nitroglycerin may be a new model of cochlear migraine. The animal model of migraine established by our new method not only validates the effect of migraine on hearing, but also lays a foundation for future clinical research.

Data availability statement

The raw data supporting the conclusions of this article will be made available by the authors, without undue reservation.

Ethics statement

The animal study was approved by Animal Ethics Committee of Peking University People's Hospital. The study was conducted in accordance with the local legislation and institutional requirements.

Author contributions

RQ: Writing—original draft. JZ: Writing—review & editing. TD: Writing—review & editing. LY: Writing—review & editing.

References

- Olesen J. Headache Classification Committee of the International Headache Society (IHS). The international classification of headache disorders, 3rd edition. *Cephalalgia*. (2018) 38:1–211. doi: 10.1177/0333102417738202
- Johnson CO, Nguyen M, Alam T, Bannick MS, Beghi E, Blake N, et al. Global, regional, and national burden of neurological disorders, 1990–2016: a systematic analysis for the Global Burden of Disease Study 2016. *Lancet Neurol*. (2019) 18:439–58. doi: 10.1016/S1474-4422(19)30034-1
- Battista RA. Audiometric findings of patients with migraine-associated dizziness. *Otol Neurotol*. (2004) 25:987–92. doi: 10.1097/00129492-200411000-00021
- Dash AK, Panda N, Khandelwal G, Lal V, Mann SS. Migraine and audiovestibular dysfunction: is there a correlation? *Am J Otolaryngol*. (2008) 29:295–9. doi: 10.1016/j.amjoto.2007.09.004
- Arakaki XH, Galbraith G, Pikov V, Fonteh AN, Harrington MG. Altered brainstem auditory evoked potentials in a rat central sensitization model are similar to those in migraine. *Brain Res*. (2014) 1563:110–21. doi: 10.1016/j.brainres.2014.03.033
- Li J, Yu L, Xia R, Gao F, Luo W, Jing Y. Postauricular hypodermic injection to treat inner ear disorders: experimental feasibility study using magnetic resonance imaging and pharmacokinetic comparison. *J Laryngol Otol*. (2013) 127:239–45. doi: 10.1017/S0022215113000017
- Wang YX, Han L, Diao TX, Jing YY, Wang L, Zheng HW. A comparison of systemic and local dexamethasone administration: from perilymph/cochlea concentration to cochlear distribution. *Hear Res*. (2018) 370:1–10. doi: 10.1016/j.heares.2018.09.002
- Qiu K, Mao MZ, Deng D, Jiang CH, Li L, Zheng YB. Is postauricular injection a systemic or a topical route for inner ear drug delivery? *Hear Res*. (2022) 422:108570. doi: 10.1016/j.heares.2022.108570
- Greco R, Demartini C, Zanaboni AM, Tumelero E, Reggiani A, Misto A, et al. FAAH inhibition as a preventive treatment for migraine: a pre-clinical study. *Neurobiol Dis*. (2020) 134:104624. doi: 10.1016/j.nbd.2019.104624
- Chiara D, Rosaria G, Miriam F, Anna MZ, Cristina T. Modelling migraine-related features in the nitroglycerin animal model: trigeminal hyperalgesia is

Funding

The author(s) declare financial support was received for the research, authorship, and/or publication of this article. This work was supported by grants from the Peking University People's Hospital Scientific Research Development Funds (RDZH 2022-01).

Conflict of interest

The authors declare that the research was conducted in the absence of any commercial or financial relationships that could be construed as a potential conflict of interest.

Publisher's note

All claims expressed in this article are solely those of the authors and do not necessarily represent those of their affiliated organizations, or those of the publisher, the editors and the reviewers. Any product that may be evaluated in this article, or claim that may be made by its manufacturer, is not guaranteed or endorsed by the publisher.

- associated with affective status and motor behavior. *Physiol Behav*. (2022) 256:113956. doi: 10.1016/j.physbeh.2022.113956
- Christensen SLT, Petersen S, Kristensen DM, Olesen J, Munro G. Targeting CGRP via receptor antagonism and antibody neutralisation in two distinct rodent models of migraine-like pain. *Cephalalgia*. (2019) 39:151. doi: 10.1177/0333102419861726
- Chaplan SR, Bach FW, Pogrel JW, Chung JM, Yaksh TL. Quantitative assessment of tactile allodynia in the rat paw. *J Neurosci Methods*. (1994) 53:55–63. doi: 10.1016/0165-0270(94)90144-9
- Christensen SL, Hansen RB, Storm MA, Olesen J, Hansen TF, Ossipov M. Von Frey testing revisited: provision of an online algorithm for improved accuracy of 50% thresholds. *Eur J Pain*. (2020) 24:783–90. doi: 10.1002/ejp.1528
- Shi SM, Wang D, Ren TL, Wang WQ. Auditory manifestations of vestibular migraine. *Front Neurol*. (2022) 13:e944001. doi: 10.3389/fneur.2022.944001
- Xue JF, Ma X, Lin YJ, Shan HJ, Yu LS. Audiological findings in patients with vestibular migraine and migraine: history of migraine may be a cause of low-tone sudden sensorineural hearing loss. *Audiol Neurotol*. (2020) 25:209–14. doi: 10.1159/000506147
- Arslan Y, Arslan IB, Aydin H, Yagiz O, Tokucoglu F, Cukurova I. The etiological relationship between migraine and sudden hearing loss. *Otol Neurotol*. (2017) 38:1411–4. doi: 10.1097/MAO.0000000000001617
- Kirkim G, Mutlu B, Olgun Y, Tanriverdzade T, Keskinoglu P, Guneri EA. Comparison of audiological findings in patients with vestibular migraine and migraine. *Turk Arch Otorhinolaryngol*. (2017) 55:158–61. doi: 10.5152/tao.2017.2609
- Radtke A, von Brevern M, Neuhauser H, Hottenrott T, Lempert T. Vestibular migraine: long-term follow-up of clinical symptoms and vestibulo-cochlear findings. *Neurology*. (2012) 79:1607–14. doi: 10.1212/WNL.0b013e31826e264f
- Lai JT, Liu TC. Proposal for a new diagnosis for cochlear migraine. *JAMA Otolaryngol Head Neck Surg*. (2018) 144:185–6. doi: 10.1001/jamaoto.2017.2427



OPEN ACCESS

EDITED BY

Sulin Zhang,
Huazhong University of Science and
Technology, China

REVIEWED BY

Alfarghal Mohamad,
National Guard Hospital, Saudi Arabia
Enrico Armato,
University of Padua, Italy
Ricardo Daniel D'Albora,
Universidad de la República, Uruguay

*CORRESPONDENCE

Tzu-Pu Chang
✉ neurochang0617@gmail.com

RECEIVED 25 October 2023

ACCEPTED 29 November 2023

PUBLISHED 15 December 2023

CITATION

Chen C-C, Bery AK and Chang T-P (2023) Weak
nystagmus in the dark persists for months after
acute unilateral vestibular loss.
Front. Neurol. 14:1327735.
doi: 10.3389/fneur.2023.1327735

COPYRIGHT

© 2023 Chen, Bery and Chang. This is an
open-access article distributed under the terms
of the [Creative Commons Attribution License
\(CC BY\)](https://creativecommons.org/licenses/by/4.0/). The use, distribution or reproduction
in other forums is permitted, provided the
original author(s) and the copyright owner(s)
are credited and that the original publication in
this journal is cited, in accordance with
accepted academic practice. No use,
distribution or reproduction is permitted which
does not comply with these terms.

Weak nystagmus in the dark persists for months after acute unilateral vestibular loss

Chih-Chung Chen^{1,2,3}, Anand K. Bery⁴ and Tzu-Pu Chang^{5,6*}

¹Dizziness and Balance Disorder Center, Taipei Medical University–Shuang Ho Hospital, New Taipei City, Taiwan, ²Taipei Neuroscience Institute, Taipei Medical University, New Taipei City, Taiwan, ³Department of Neurology, School of Medicine, College of Medicine, Taipei Medical University, Taipei, Taiwan, ⁴Division of Neuro-Visual and Vestibular Disorders, Department of Neurology, The Johns Hopkins Hospital, Baltimore, MD, United States, ⁵Department of Neurology/Neuro-medical Scientific Center, Taichung Tzu Chi Hospital, Buddhist Tzu Chi Medical Foundation, Taichung, Taiwan, ⁶Department of Neurology, School of Medicine, Tzu Chi University, Hualien, Taiwan

Background: Weak nystagmus with fixation removed can be seen both in normal individuals and in recovery from a unilateral vestibular insult, thus its clinical significance is unclear in patients with dizziness. We thus sought to compare features of nystagmus at various stages following unilateral vestibular loss (UVL).

Methods: We enrolled thirty consecutive patients after acute UVL with impaired vestibulo-ocular reflex (VOR) gain. The patients were allocated into three groups according to time from onset of symptoms: acute (1–7 days), subacute (8–30 days), and chronic (>30 days). Patients underwent video-oculography (with and without fixation) and video head impulse testing (vHIT) to determine VOR gain. We examined the relationships amongst SPV, VOR gain, and time from symptom onset across groups.

Results: There were 11, 10, and 9 patients in the acute, subacute, and chronic stages of UVL, respectively. With visual fixation, only 8 patients (26.7%) demonstrated nystagmus, all from the acute group. With fixation removed, 26 patients (86.7%) exhibited spontaneous nystagmus, including 90.9%, 90%, and 77.8% of the patients from the acute, subacute, and chronic groups, respectively. Horizontal nystagmus was paralytic (i.e., fast phase contralesional) in 25 (96.7%) cases. Horizontal SPV was negatively correlated with logarithm of time from onset to examination ($r = -0.48$, $p = 0.007$) and weakly negatively correlated with ipsilesional VOR gain ($r = -0.325$, $p = 0.08$).

Conclusion: In the subacute or chronic stages of UVL, paralytic nystagmus with fixation removed persisted at a low intensity. Therefore, weak nystagmus in the dark may have diagnostic value in chronic dizziness.

KEYWORDS

nystagmus, vestibular, video-oculography, vertigo, dizziness

Introduction

Nystagmus is an involuntary “to and fro movement” of the eyes, which can be highly localizing in patients with acute dizziness and vertigo. One common cause of vertigo is acute unilateral vestibular loss (UVL), for example from vestibular neuritis. Unilateral vestibular loss (UVL) typically presents with horizontal-predominant nystagmus with the fast phase toward the contralesional side (1).

Vestibular recovery following unilateral vestibular loss is a dynamic process. The spontaneous nystagmus, which often starts strong, gradually gets weaker with time as vestibular compensation begins. One technique to enhance detection of subtle nystagmus at the bedside is to remove fixation (i.e., to remove the stationary visual signal that can suppress VOR and inhibit nystagmus). Conventional teaching is that removing visual fixation only enhances peripheral nystagmus (2). However, studies have also demonstrated that some central nystagmus can be enhanced by removing visual fixation (3, 4).

In clinical settings, various tools are used to remove visual fixation, such as the penlight cover test (5), occlusive ophthalmoscopy (6), optical Frenzel goggles, video-infrared goggles examination, and video-oculography (VOG). Among them, VOG systems that employ infrared goggles can completely remove visual fixation.

The clinical significance of weak nystagmus with removal of fixation (i.e., in the dark) remains unclear. Studies have demonstrated that some healthy individuals present with weak spontaneous or positional nystagmus in the dark (7, 8). This finding in normal subjects can make it difficult to interpret the relevance of low-intensity nystagmus, particularly those with a slow-phase velocity (SPV) of $<3^\circ/\text{s}$ (9).

To date, most studies have focused on ocular motor signs during the acute stage of vertigo (10, 11), rather than the subacute or chronic phases (12). In clinical practice, however, patients often present after the acute phase. We therefore need better data on nystagmus intensity in the subacute and chronic phases of peripheral loss (ideally, a clinical cut-point that can help determine whether a given weak nystagmus is likely to represent recovering vestibular loss versus a normal finding).

In the present study, we investigated the direction and intensity of nystagmus in patients who presented at differing time-points after (initially acute) UVL. We sought to determine (i) how commonly weak nystagmus persists in the dark after acute UVL and (ii) whether weak nystagmus has localizing value (i.e., can it predict the lesion side?).

Method

We retrospectively reviewed consecutive patients who presented to our outpatient department for dizziness or vertigo between July 2019 and June 2021. All patients underwent structured histories, complete neurological and oto-neurological examinations, and video-infrared goggles examination (with skull vibration and head-shaking as provocative maneuvers for nystagmus). All underwent VOG (including quantitative nystagmus measurement) and video head impulse testing (vHIT) simultaneously, which was recorded using a VOG/vHIT system (EyeSeeCam; Middelfart, Denmark). Brain MRI was performed when focal neurological signs or central vestibular signs were identified. The patients who experienced acute vestibular syndrome at onset of dizziness and had a VOR gain of <0.8 on one side during vHIT were included for subsequent analysis. Patients with central vestibulopathy confirmed by MRI (i.e., a structural lesion) were excluded from this study. Patients who took any vestibular suppressant in the 48 h prior to vestibular testing were excluded. Patients who underwent vestibular rehabilitation before

VOG examination were similarly excluded. The present study was performed in accordance with the ethical standards set forth in the 1964 Declaration of Helsinki and its subsequent amendments, and it was approved by the Institutional Review Board of the Research Ethics Committee of Taichung Tzu Chi Hospital (REC109-64).

During VOG examination, spontaneous nystagmus with and without visual fixation was recorded when the patients sat upright with their heads in neutral position and straight-ahead gaze. The presence or absence of nystagmus was determined by a subspecialty-trained vestibular neurologist (TPC) on the basis of VOG traces and videos. When nystagmus was present, the SPVs of the horizontal and vertical components were calculated. The lesion side was determined through vHIT, where which the lesioned VOR gain was defined as <0.8 . On the basis of the time from symptom onset to VOG and vHIT, the included patients' UVL were classified as being in the acute (1–7 days), subacute (8–30 days), or chronic (>30 days) stage. We compared the SPVs of nystagmus across the acute, subacute, and chronic stages. We also measured the relationships (i) between SPV and VOR gain, (ii) between SPV and time from onset to examination, and (iii) between VOR gain and time from onset to examination.

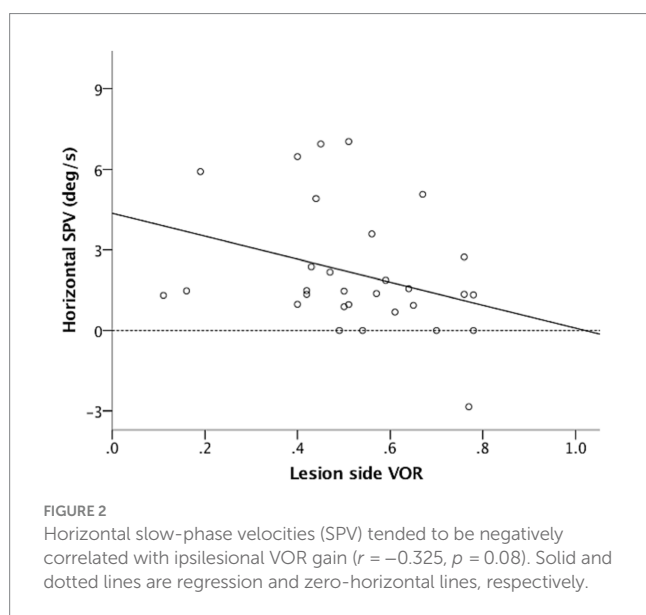
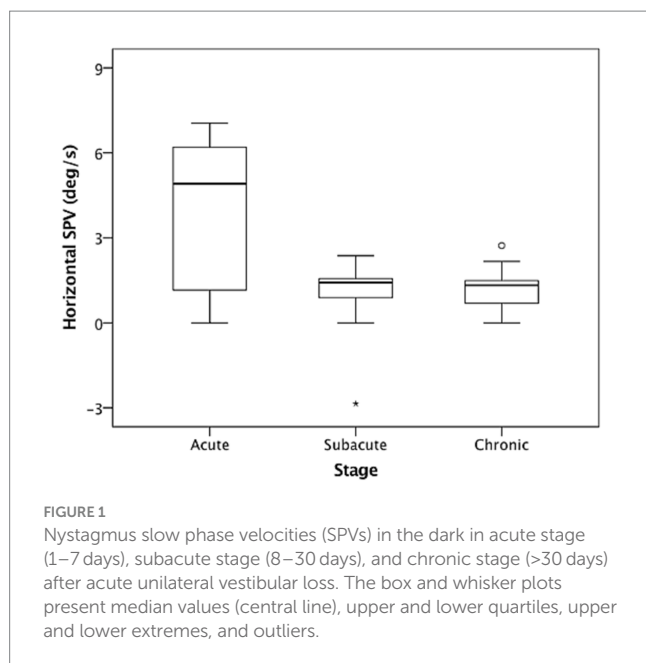
Descriptive statistics were applied to the collected demographic data and the data on the prevalence of nystagmus at various stages of UVL. Mann–Whitney U test was performed to compare the SPVs between stage groups. Pearson's correlation coefficients were calculated to determine the correlations between SPV, VOR gain, and the time from onset to examination.

Results

Thirty patients with UVL were included in our study. Among the included patients, 18 (60%) were male, their mean age was 54.1 years (range, 32–76 years), 16 (53.3%) had right vestibular loss, and 14 had left vestibular loss. The etiologies comprised acute unilateral vestibulopathy/vestibular neuritis ($n = 25$), Ramsay Hunt syndrome ($n = 3$), and acute unilateral audio-vestibular loss ($n = 2$). None of the included patients had middle ear symptoms or prior history of middle ear diseases.

On the basis of the timing of VOG and vHIT examinations relative to symptom onset, 11, 10, and 9 patients were determined to be in the acute stage (1–7 days), subacute stage (8–30 days), and chronic stage (>30 days) of UVL, respectively. The mean time from onset of vestibular syndrome to exam was 4.1 days in acute stage, 21.1 days in subacute stage, and 192.3 days in chronic stage (range 2–409 days). All included patients were symptomatic (i.e., had dizziness or vertigo) at the time of examination. With visual fixation, 8 patients (72.7%) in the acute stage had spontaneous nystagmus (mean horizontal SPV, $0.76^\circ/\text{s}$), whereas none in the subacute or chronic stage presented with spontaneous nystagmus.

In the dark (i.e., without fixation), 26 of the included patients (86.7%) had spontaneous nystagmus, including 90.9%, 90%, and 77.8% of the patients in the acute stage, subacute stage, and chronic stage, respectively. Among the included patients, 25 (96.7%) presented with paralytic nystagmus, in which the fast phase was directed toward the contralesional side. One patient displayed recovery nystagmus in which the fast phase was directed toward the



ipsilesional side. Quantitative analysis revealed that the mean horizontal SPVs were $3.93^\circ/\text{s}$, $0.95^\circ/\text{s}$, and $1.19^\circ/\text{s}$ in the acute stage, subacute stage, and chronic stage, respectively. The distribution is presented in Figure 1. The SPV tended to be higher in the acute stage (acute vs. subacute, $p = 0.06$; acute vs. chronic, $p = 0.04$, Mann–Whitney U test), but not different between subacute and chronic stages ($p = 0.84$, Mann–Whitney U test). The horizontal SPV was negatively correlated with the ipsilesional VOR gain but not to a significant level ($r = -0.325$, $p = 0.08$; Figure 2). The horizontal SPV was not correlated with the time from onset to examination ($r = -0.202$, $p = 0.28$). However, it was negatively correlated with the logarithm of time ($r = -0.48$, $p = 0.007$). Most SPV values recorded in the first week (63.6%) were greater than $3^\circ/\text{s}$. Thereafter, the recorded SPVs decreased sharply. However, most of the nystagmus

in the subacute and chronic stages persisted at a low intensity (SPV, $0.69^\circ/\text{s}$ – $2.73^\circ/\text{s}$). Three patients still had nystagmus 1 year after vertigo onset. Weak paralytic nystagmus (SPV, $0.69^\circ/\text{s}$) was observed for up to 409 days (Figure 3) in one case.

Of the 30 included patients, 10 (33.3%) also had vertical components to their nystagmus. All vertical components were upbeating (vertical SPV, $0.73^\circ/\text{s}$ – $5.66^\circ/\text{s}$), and 70% of the upbeat-component nystagmus cases were in patients seen in the acute stage. Among the patients with provoked nystagmus, 28 had skull vibration-induced nystagmus, and 27 had head-shaking-induced nystagmus. All provoked nystagmus was paralytic (i.e., with fast phase directed toward the contralesional side).

Only one patient with left vestibular neuritis had recovery nystagmus, which was observed 8 days after vertigo onset. This spontaneous nystagmus was left-beating. By contrast, the patient's skull vibration-induced and head-shaking nystagmus were right-beating.

Discussion

In the present study, we investigated nystagmus characteristics in patients who were at different stages following onset of unilateral vestibular loss. Nystagmus with fixation disappeared beyond 1 week of symptom onset of vestibular loss. By contrast, most patients continued to demonstrate weak nystagmus (SPV $< 3^\circ/\text{s}$) in the absence of fixation (in other words, in the dark) for months. Notably, this faint nystagmus was still observed in 3 patients who were examined more than 1 year after onset. The longest interval was 409 days. Of the 26 cases with nystagmus, 25 exhibited nystagmus beating away from the lesion side, indicating the presence of paralytic nystagmus. Several patients (36.4%) in the acute stage only exhibited weak nystagmus (SPV $< 3^\circ/\text{s}$) even when examinations were conducted in the absence of fixation.

A number of compensatory mechanisms begin soon after a vestibular insult and may be attributed to either static vestibular compensation or vestibular restoration (i.e., recovery of vestibular hair cells or the vestibular nerve) (13). These processes cause spontaneous nystagmus to decay over time following acute vestibular injury. Rodents can achieve complete static vestibular compensation in 1 week (14), and cats can complete this process in 6 weeks (15, 16). By contrast, the time required to complete static compensation varies widely across human individuals. An early study by Matsuzaki et al. indicated that the spontaneous nystagmus of most people completely disappeared within 1 month after vestibular neuritis (17). However, Matsuzaki used optical Frenzel goggles, which could not completely remove visual fixation. In a study that used infrared goggles to block fixation, only 2 of 20 patients exhibited weak spontaneous nystagmus at 3 months after symptom onset, and only 1 still had nystagmus 1 year after onset (12). However, 35% of patients in that study had reversal of their canal paresis by calorics, suggesting that a part of their nystagmus disappeared because of vestibular restoration. Another long-term follow-up study reexamined 18 patients 7–8 years after the onset of vestibular neuritis, and it reported that 7 (38.9%) patients still displayed weak spontaneous nystagmus, which was identified through electro-oculography (18). Caloric testing revealed that among the 18

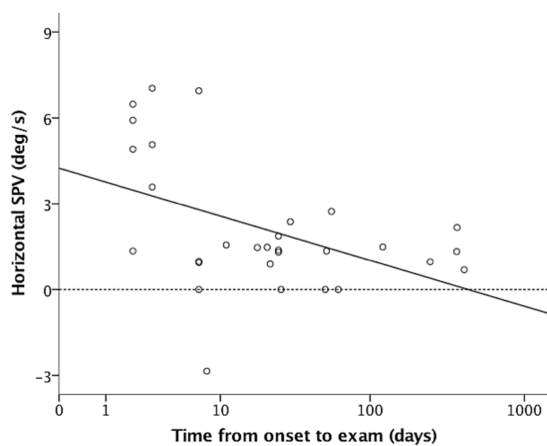


FIGURE 3
Nystagmus weakened rapidly after acute stage unilateral vestibular loss and was maintained at a low intensity ($0.69^{\circ}/s$ and $2.73^{\circ}/s$). Horizontal slow-phase velocity (SPV) was negatively correlated with logarithm of time from onset to examination ($r = -0.48$, $p = 0.007$). X-axis scale is logarithmic. Solid and dotted lines are regression and zero-horizontal lines.

patients, 10 (55.6%) exhibited vestibular restoration and eight did not. In contrast to the aforementioned studies, the patients included in our study all exhibited incomplete vestibular restoration (as indicated by their vHIT results) at the time of enrollment. Consequently, 25 (83.3%) of the included patients presented with paralytic nystagmus and only one patient had recovery nystagmus. Our study demonstrated that when vestibular restoration is incomplete, static vestibular compensation is usually insufficient to completely overcome imbalances, resulting in residual weak nystagmus in the dark. This weak spontaneous nystagmus reflects the patients' inability to establish stable static compensation and is associated with the chronic dizziness of these patients. Interestingly, there may have been a plateau of static compensation in these patients since the SPV was similar in subacute and chronic patients (in other words, nystagmus did not weaken further beyond the subacute phase). A prospective, longitudinal study with repeated measurement of SPV in the same patients is required to examine the existence of this plateau.

With the development of video oculomotor recording systems, infrared goggles can be effectively used to detect weak nystagmus. However, the clinical relevance of weak nystagmus is still being debated. In a study, portable VOG with fixation blocking revealed a high prevalence (30.7%) of low-velocity spontaneous nystagmus in 100 healthy individuals (7). This finding also corresponds to those of several other studies, which detected weak nystagmus (SPV, $0.7^{\circ}/s$ – $5.0^{\circ}/s$) in some healthy individuals (8, 19, 20). Collectively, these literature findings contribute to the ongoing debate about the clinical relevance of weak nystagmus. The present study showed that most patients in the subacute and chronic stages following unilateral vestibular loss had persisting low-intensity nystagmus that could only be detected with fixation removal. Another similar study examined 22 patients 2 months after acute vestibular neuritis and found that ten manifested weak nystagmus (SPV, $0^{\circ}/s$ – $3^{\circ}/s$) (21). If weak nystagmus is clinically nonsignificant, the directions of

nystagmus should be evenly distributed between the ipsilesional and contralesional sides. Our study indicated that 96.2% of the nystagmus cases beat toward the contralesional side (i.e., were paralytic nystagmus), demonstrating that weak nystagmus in UVL is likely clinically significant and an indicator of the lesion side. There is likely an overlap in the range of intensity of nystagmus between physiologic nystagmus and the weak, but clinically significant, nystagmus seen in the subacute and chronic stages following unilateral loss. Thus, for patients with the correct history (onset of dizziness weeks to months prior), weak nystagmus should be carefully examined for, including with removal of visual fixation. For clinical settings without specialized equipment (e.g., infrared video-oculography or optical Frenzels), fixation can be easily removed at the bedside by means of the penlight-cover test, or by occlusive ophthalmoscopy (5, 6). Because of the overlap in nystagmus intensity, it is hard to distinguish weak pathological nystagmus from physiologic nystagmus simply using an SPV cut-off. Instead, the presence and intensity of nystagmus should be considered within the broader clinical context (clinical history, vestibular findings, ocular motor signs). Together, these features help identify when weak nystagmus may be pathologic and/or provide useful diagnostic information. If its clinical relevance remains undetermined, the weak nystagmus should be closely followed up to observe how the nystagmus changes over time.

Our study has several limitations. First, it was not a longitudinal study, and included patients were not individually followed up at multiple time points to monitor changes in nystagmus. Second, our study was a retrospective study with a small sample size. Prospective studies with larger sample sizes are needed to confirm our findings.

Conclusion

Nystagmus with visual fixation may begin to disappear by as soon as 1 week after onset of acute unilateral vestibular loss. By contrast, nystagmus in the dark persisted at a low intensity for months, and in most cases the direction was consistent with the expected paralytic nystagmus (i.e., contralesional). Therefore, although subtle nystagmus in the dark is not always pathological, it can be of clinical significance in patients with chronic dizziness and should not be overlooked.

Data availability statement

The raw data supporting the conclusions of this article will be made available by the authors, without undue reservation.

Ethics statement

The studies involving humans were approved by the Institutional Review Board of the Research Ethics Committee of Taichung Tzu Chi Hospital (REC109-64). The studies were conducted in accordance with the local legislation and institutional requirements. Written informed consent for participation was not required from the participants or the participants' legal guardians/next of kin because this is a retrospective study.

Author contributions

C-CC: Data curation, Formal analysis, Methodology, Writing – original draft. AB: Writing – review & editing. T-PC: Conceptualization, Data curation, Formal analysis, Funding acquisition, Methodology, Supervision, Writing – original draft, Writing – review & editing.

Funding

The author(s) declare financial support was received for the research, authorship, and/or publication of this article. This study is funded by TCMF-A 111-07(112), Buddhist Tzu Chi Medical Foundation.

References

1. Leigh JR, Zee DS. *The neurology of eye movements*. 5th ed. Oxford: Oxford University Press (2015).
2. Baloh RW, Honrubia V. *Clinical neurophysiology of the vestibular system*. New York: Oxford University Press (2001).
3. Mantokoudis G, Wyss T, Zamaro E, Korda A, Wagner F, Sauter TC, et al. Stroke prediction based on the spontaneous nystagmus suppression test in dizzy patients: a diagnostic accuracy study. *Neurology*. (2021) 97:e42–51. Epub 2021/05/15. doi: 10.1212/WNL.00000000000012176
4. Bery AK, Wang CF, Gold DR, Chang TP. The fixation suppression test can uncover vertical nystagmus of central origin in some patients with dizziness. *Neurol Sci*. (2021) 42:5343–52. Epub 2021/10/27. doi: 10.1007/s10072-021-05676-3
5. Newman-Toker DE, Sharma P, Chowdhury M, Clemons TM, Zee DS, Della Santina CC. Penlight-cover test: a new bedside method to unmask nystagmus. *J Neurol Neurosurg Psychiatry*. (2009) 80:900–3. doi: 10.1136/jnnp.2009.174128
6. Zee DS. Ophthalmoscopy in examination of patients with vestibular disorders. *Ann Neurol*. (1978) 3:373–4. Epub 1978/04/01. doi: 10.1002/ana.410030422
7. Young AS, Rosengren SM, D'Souza M, Bradshaw AP, Welgampola MS. Nystagmus characteristics of healthy controls. *J Vestib Res*. (2020) 30:345–52. Epub 2020/12/09. doi: 10.3233/VES-200022
8. Bisdorff AR, Sancovic S, Debatisse D, Bentley C, Gresty MA, Bronstein AM. Positional nystagmus in the dark in normal subjects. *Neuro-Ophthalmology*. (2000) 24:283–90. doi: 10.1076/0165-8107(200008)2411-VFT283
9. von Brevern M, Zeise D, Neuhauser H, Clarke AH, Lempert T. Acute migrainous vertigo: clinical and oculographic findings. *Brain*. (2005) 128:365–74. Epub 2004/12/17. doi: 10.1093/brain/awh351
10. Carmona S, Martinez C, Zalazar G, Moro M, Batuecas-Caletrio A, Luis L, et al. The diagnostic accuracy of truncal ataxia and hints as cardinal signs for acute vestibular syndrome. *Front Neurol*. (2016) 7:125. doi: 10.3389/fneur.2016.00125
11. Kattah JC, Talkad AV, Wang DZ, Hsieh YH, Newman-Toker DE. Hints to diagnose stroke in the acute vestibular syndrome: three-step bedside oculomotor examination more sensitive than early MRI diffusion-weighted imaging. *Stroke*. (2009) 40:3504–10. Epub 2009/09/19. doi: 10.1161/STROKEAHA.109.551234
12. Choi KD, Oh SY, Kim HJ, Koo JW, Cho BM, Kim JS. Recovery of vestibular imbalances after vestibular neuritis. *Laryngoscope*. (2007) 117:1307–12. Epub 2007/07/03. doi: 10.1097/MLG.0b013e31805c08ac
13. Lacour M, Helmchen C, Vidal PP. Vestibular compensation: the neuro-otologist's best friend. *J Neurol*. (2016) 263:S54–64. doi: 10.1007/s00415-015-7903-4
14. Darlington CL, Smith PF. Molecular mechanisms of recovery from vestibular damage in mammals: recent advances. *Prog Neurobiol*. (2000) 62:313–25. Epub 2000/06/17. doi: 10.1016/s0304-0082(00)00002-2
15. Lacour M, Tighilet B. Plastic events in the vestibular nuclei during vestibular compensation: the brain orchestration of a “Deafferentation” code. *Restor Neurol Neurosci*. (2010) 28:19–35. doi: 10.3233/RNN-2010-0509
16. Borel L, Lopez C, Peruch P, Lacour M. Vestibular syndrome: a change in internal spatial representation. *Neurophysiol Clin*. (2008) 38:375–89. doi: 10.1016/j.neucli.2008.09.002
17. Matsuzaki M, Kamei T. Stage-assessment of the progress of continuous vertigo of peripheral origin by means of spontaneous and head-shaking nystagmus findings. *Acta Otolaryngol Suppl*. (1995) 519:188–90. doi: 10.3109/00016489509121900
18. Bergenius J, Perols O. Vestibular neuritis: a follow-up study. *Acta Otolaryngol*. (1999) 119:895–9. doi: 10.1080/00016489950180243
19. Levo H, Aalto H, Petheri HT. Nystagmus measured with video-oculography: methodological aspects and normative data. *ORL J Otorhinolaryngol Relat Spec*. (2004) 66:101–4. doi: 10.1159/000079327
20. Van Der Stappen A, Wuyts FL, Van De Heyning PH. Computerized electronystagmography: normative data revisited. *Acta Otolaryngol*. (2000) 120:724–30. Epub 2000/12/01. doi: 10.1080/000164800750000243
21. Park H, Hong SC, Shin J. Clinical significance of vibration-induced nystagmus and head-shaking nystagmus through follow-up examinations in patients with vestibular neuritis. *Otol Neurotol*. (2008) 29:375–9. doi: 10.1097/MAO.0b013e318169281f

Conflict of interest

The authors declare that the research was conducted in the absence of any commercial or financial relationships that could be construed as a potential conflict of interest.

Publisher's note

All claims expressed in this article are solely those of the authors and do not necessarily represent those of their affiliated organizations, or those of the publisher, the editors and the reviewers. Any product that may be evaluated in this article, or claim that may be made by its manufacturer, is not guaranteed or endorsed by the publisher.



OPEN ACCESS

EDITED BY

Nicolas Perez-Fernandez,
University of Navarra Clinic, Spain

REVIEWED BY

Marcos Rossi-Izquierdo,
Lucas Augusti University Hospital, Spain
Sun-Uk Lee,
Korea University Medical Center,
Republic of Korea
Fernando Gananca,
Federal University of São Paulo, Brazil

*CORRESPONDENCE

Lisa van Stiphout
✉ lisa.van.stiphout@mumc.nl

RECEIVED 06 October 2023

ACCEPTED 29 November 2023

PUBLISHED 19 December 2023

CITATION

van Stiphout L, Szmulewicz DJ, Guinand N,
Fornos AP, Van Rompaey V and
van de Berg R (2023) Bilateral vestibulopathy: a
clinical update and proposed diagnostic
algorithm.
Front. Neurol. 14:1308485.
doi: 10.3389/fneur.2023.1308485

COPYRIGHT

© 2023 van Stiphout, Szmulewicz, Guinand,
Fornos, Van Rompaey and van de Berg. This is
an open-access article distributed under the
terms of the [Creative Commons Attribution
License \(CC BY\)](https://creativecommons.org/licenses/by/4.0/). The use, distribution or
reproduction in other forums is permitted,
provided the original author(s) and the
copyright owner(s) are credited and that the
original publication in this journal is cited, in
accordance with accepted academic practice.
No use, distribution or reproduction is
permitted which does not comply with these
terms.

Bilateral vestibulopathy: a clinical update and proposed diagnostic algorithm

Lisa van Stiphout^{1*}, David J. Szmulewicz^{2,3}, Nils Guinand⁴,
Angélica Pérez Fornos⁴, Vincent Van Rompaey^{5,6} and
Raymond van de Berg¹

¹Department of Otorhinolaryngology and Head and Neck Surgery, Division of Balance Disorders, School for Mental Health and Neuroscience, Maastricht University Medical Center, Maastricht, Netherlands, ²Royal Victorian Eye and Ear Hospital, University of Melbourne, Melbourne, VIC, Australia, ³Bionics Institute, Melbourne, VIC, Australia, ⁴Service of Otorhinolaryngology Head and Neck Surgery, Department of Clinical Neurosciences, Geneva University Hospitals, Geneva, Switzerland, ⁵Department of Otorhinolaryngology, Head and Neck Surgery, Antwerp University Hospital, Antwerp, Belgium, ⁶Faculty of Medicine and Health Sciences, University of Antwerp, Antwerp, Belgium

Bilateral vestibulopathy (BVP) is characterized by its heterogeneous and chronic nature with various clinical presentations and multiple etiologies. This current narrative review reflects on the main insights and developments regarding clinical presentation. In addition, it proposes a new diagnostic algorithm, and describes available and potential future therapeutic modalities.

KEYWORDS

bilateral vestibulopathy, clinical update, diagnostic algorithm, diagnosis, review, vestibular impairment, vestibulopathy

1 Background

Bilateral vestibulopathy (BVP) was first described in 1936 in patients with Menière's disease who had been managed with bilateral vestibular neurectomy (1, 2). BVP has also been known as Dandy syndrome (after the neurosurgeon who performed 907 vestibular neurectomies), bilateral vestibular hypofunction, bilateral vestibular impairment, bilateral vestibular areflexia and bilateral vestibular loss (3–5). The Consensus document of the Classification Committee of the Bárány Society (2017) recommends “bilateral vestibulopathy” as the preferred term (6). As the variation in the terms for BVP imply, it is defined by a bilaterally reduced or absent function of the vestibular end organs and/or nerves, ganglia, the vestibular root entry zone and/or the brain, which negatively impacts vestibular functioning resulting in symptoms of impaired gaze stabilization and imbalance (7). The reported prevalence varies from 28 to 81 per 100,000 people. However, this is believed to be a significant under estimation based on misdiagnosis (8–12). This is partly caused by the heterogeneous presentation of the disorder, with its various clinical characteristics and multiple etiologies (5, 7, 13, 14). BVP negatively impacts quality of life and the socio-economic burden of BVP is substantial, due to work-related disability and health service utilization (8, 15–17). Here we offer an evidence-based approach for the clinician in approaching the patient with a potential BVP.

2 Clinical characteristics

2.1 Etiology

BVP may be the result of over 20 different etiologies (Table 1) (7). Nonetheless, the reported percentages of idiopathic BVP vary between 20 and 75% (7, 14, 19–21). The more common causes of BVP are genetic disorders (e.g., DFNA9), ototoxicity exposure (e.g., aminoglycosides antibiotics, chemotherapy), and infectious causes (e.g., meningitis). Less frequently, BVP may be caused by bilateral Menière's Disease, trauma, auto-immune disease [e.g., Cogan's syndrome, Autoimmune Inner Ear Disease (AIED)], and neurodegenerative disorders [e.g., Cerebellar Ataxia with Neuronopathy and Vestibular Areflexia Syndrome (CANVAS)] (19, 22, 23). BVP may also be a component of peripheral neuropathy [e.g., Chronic Inflammatory Demyelinating Polyradiculoneuropathy (CIDP) and Charcot–Marie Tooth (CMT) disease], congenital syndromes (e.g., Usher and Turner syndromes) and Wernicke's encephalopathy (19, 24). Furthermore, an association between vestibular migraine and the development of BVP has been described (7, 25). Largely depending on etiology, BVP can have a rapid or slowly progressive onset (mostly due to ototoxicity and genetic causes respectively). BVP can also develop following recurrent episodes of vertigo, as is particularly seen in patients with bilateral (sequential or consecutive) Menière's Disease (7).

2.2 Symptoms

Two of the main physical symptoms of BVP are movement-induced blurred vision (oscillopsia) and unsteadiness when walking or standing which often worsens on uneven ground or in darkness. These symptoms are primarily due to impaired vestibular-ocular and

vestibular-spinal reflexes (6). Furthermore, BVP may be associated with cognitive and emotional symptoms such as difficulties with performing dual tasks, impaired concentration, forgetfulness, reduced spatial orientation, anxiety, anger, and sadness (26–29).

Neither vertigo nor abnormal nystagmus are typical symptoms of BVP as both are generally related to an acute asymmetry in vestibular function (i.e., an acute unilateral vestibulopathy) and are in general not caused by a symmetrical decrease in vestibular function (30). The exception here is bilateral sequential vestibulo-ocular reflex (VOR) reduction. In other words, vertigo and nystagmus can be related to the underlying etiology of BVP (e.g., Menière's disease), but are generally not a sign of BVP itself.

In particular the unsteadiness can be difficult to recognize as balance control is a multisensory process (31–33). Compensation via sensory reweighting plays a key role in attempted recovery from BVP. In this process, the remaining senses such as vision, somatosensory input (e.g., pressure perception) and proprioception are preferentially utilized (34). As a result of sensory reweighting, many spatiotemporal gait parameters do not differ between BVP patients and healthy controls at their preferred walking speed. However, BVP patients do tend to walk with an increased cadence (35). When testing gait at fixed walking speeds, gait parameters such as step length and step width variability differ significantly to those of healthy controls (33). Sensory reweighting also explains why certain complaints worsen in situations where other sensory inputs are less effective, such as worsening of unsteadiness in poorly lit environments. This phenomenon offers a partial explanation for the higher incidence of falls and severe fall-related injuries in the BVP population (18, 36–38). In addition, loss of somatosensory input (in particular from the soles of the feet) also increases unsteadiness and is a proven risk factor for falls in BVP patients (39). Other risk factors for falls include advanced age, a decline in cognitive resources and having a sedentary lifestyle (38).

TABLE 1 Etiologies of bilateral vestibulopathy (18, 19).

Idiopathic	
Genetic	DFNA9, DFNA11, DFNA15, DFNB4, mutation chromosome 5q, 6q, 11q, 22q Muckle Wells (NLPR3)
Toxic/metabolic	Antibiotics (particularly aminoglycosides), furosemide, amiodarone, aspirin, chemotherapeutics (e.g., cisplatin), immunotherapy (e.g., immune checkpoint inhibitors), anti-epileptic drugs (particularly aromatic anti-epileptic drugs), alcohol, styrene poisoning, combination non-steroidal anti-inflammatory drugs with penicillin
Infectious	Meningitis, syphilis, Lyme disease, bilateral vestibular neuritis (Herpes Simplex Virus), Herpes zoster, rubella
Other ear pathology	Bilateral Menière's disease, otosclerosis, bilateral labyrinthitis, cholesteatoma, vestibular atelectasis, presbyvestibulopathy
Trauma	Head trauma, iatrogenic (e.g., bilateral Cochlear Implant, local radiotherapy)
Autoimmune	Cogan's syndrome, Susac syndrome, Sarcoidosis, Granulomatosis with polyangiitis, Sjögren syndrome, inflammatory bowel disease, Behçet's disease, celiac disease, polyarteritis nodosa, antiphospholipid syndrome, Anti-GQ1b antibody syndrome, Autoimmune Inner Ear Disease, other systemic diseases
Neuropathies	Guillain-Barre Syndrome (GBS), and Chronic Inflammatory Demyelinating Polyradiculoneuropathy (CIDP), Charcot–Marie Tooth (CMT) disease, Fabry's disease
Neurodegenerative	CANVAS, Friedreich Ataxia, multiple system atrophy, SCA3, SCA6, SCA27B,
Congenital/syndromal	Usher, Turner, enlarged vestibular aqueduct syndrome, Alport syndrome, coloboma-heart-atresia-retarded-genital-ear (CHARGE) syndrome
Vascular	Vertebrobasilar dolichoectasia
Tumors	Bilateral vestibular schwannoma, Neurofibromatosis type 2, metastasis, lymphoma
Other	Auditory neuropathy spectrum disorders, superficial siderosis, hypothyroidism, vitamin B12 deficiency, folate deficiency, vestibular migraine, Wernicke's encephalopathy.

Due to the absence of standardized and validated Patient Reported Outcome Measures (PROMs) capable of capturing the subjective severity and burden of the complete spectrum of BVP symptoms, the Bilateral Vestibulopathy Questionnaire (BVQ) was recently developed. The BVQ serves as a comprehensive tool for assessing the spectrum of BVP symptoms and its impact on daily life, in order to quantify treatment efficacy and improve clinical decision making (40, 41).

3 Physical examination and laboratory assessment

Physical and laboratory assessment in BVP patients mainly focuses on two aspects: (1) identifying the presence or absence of central vestibular signs (e.g., gaze evoked nystagmus, downbeat nystagmus, dysmetria, etc.), and (2) confirming BVP.

3.1 Physical examination

In identifying central vestibular signs, it is advised to perform cerebellar testing, including oculomotor examination, evaluation of coordination (e.g., finger-to-nose test for identifying dysmetria, rapid alternating movements for identifying dysdiadochokinesia) and evaluation of gait and posture. As abnormalities in oculomotor functioning may be the first signs of central pathology, oculomotor examination should always be performed (42). The Head Impulse Test (HIT) is sensitive in identification of severe BVP, particularly when performed by an expert (43). However, false-negative results may be found in the presence of covert saccades, mild BVP and when the HIT is performed by less experienced clinicians (5, 43, 44). Another key oculomotor test is the visually enhanced VOR (VVOR), which is specific for the combination of BVP and cerebellar impairment. The VVOR is performed by turning a patient's head slowly side-to-side while the patient fixates at an earth-fixed target (e.g., the clinicians nose). The VVOR is abnormal in case the ensuing eye movements are broken-up or saccadic, rather than smooth. The VVOR is a simple, brief and reproducible bedside test (45). In addition to oculomotor examination and the HIT, Romberg's test (including Romberg in tandem or Romberg on foam rubber) and evaluation for neuropathy is recommended (39, 46, 47).

3.2 Laboratory assessment

The Consensus document of the Classification Committee of the Bárány Society describes the diagnostic criteria for BVP as summarized in Table 2 (6). Regarding the three objective VOR test measurements (Table 2, part C), both caloric testing and horizontal vHIT appear to be more sensitive for detecting impairment of vestibular function than the torsion swing test (rotatory chair testing). The latter proved to be most sensitive in measuring residual vestibular function (19). When performing the vHIT, it is important to be aware that the sensitivity may depend on the type of device used, as vHIT systems are not yet standardized across different manufacturers (48). In addition to the HIT, the Suppression Head Impulse Paradigm (SHIMP) was introduced as a diagnostic tool for identifying VOR alterations in BVP patients. The advantage of SHIMP is that it

TABLE 2 Diagnostic criteria for bilateral vestibulopathy, as described by the Bárány Society (6).

A. Chronic vestibular syndrome with the following symptoms	1 Unsteadiness when walking or standing plus at least one of 2 or 3
	2 Movement-induced blurred vision or oscillopsia during walking or quick head/body movements and/or
	3 Worsening of unsteadiness in darkness and/or on uneven ground
B. No symptoms while sitting or lying down under static conditions	
C. Bilaterally reduced or absent angular VOR function documented by	- Bilaterally pathological horizontal angular VOR gain <0.6, measured by the video-HIT or scleral-coil technique and/or
	- Reduced caloric response (sum of bithermal max. Peak SPV on each side <6°/sec) and/or
	- Reduced horizontal angular VOR gain <0.1 upon sinusoidal stimulation on a rotatory chair (0.1Hz, Vmax = 50°/sec) and a phase lead >68 degrees (time constant <5sec).
D. Not better accounted for by another disease	

significantly reduces covert saccades (49, 50), which might allow for more reliable VOR gain calculation. However, a recent study in BVP patients showed that the clinical benefit of SHIMP compared to HIT was marginal, given that both paradigms successfully detected BVP in the majority of patients (93%) (50). Despite the comparable diagnostic capabilities of SHIMP and HIT, the former, characterized as a 'covert saccade killer', may serve as a viable alternative in clinical settings where access to a vHIT-system is unavailable (50). In order to facilitate the most efficient diagnostic workflow, it is worth considering to first perform vHIT (due to the lower patient burden), followed by caloric testing, before performing the torsion swing test. In this way, the test battery can be discontinued as soon as the patient meets one of the diagnostic test criteria.

Other possible vestibular function measurements are cervical and ocular Vestibular Evoked Myogenic Potentials (c- and oVEMPs). However, various studies have found a high degree of variability in VEMP responses within BVP populations, and more importantly, there remains a lack of certainty regarding whether isolated bilateral impairment of both otolith organs causes significant disability (19, 51, 52). Therefore, c- and oVEMPs are as yet not included in the Bárány diagnostic criteria as a definite stand-alone diagnostic modality in BVP.

Several outcome measures are available for quantifying the functional manifestations of BVP. The functional HIT (fHIT) proved to be a feasible test for evaluating oscillopsia by testing the Dynamic Visual Acuity (DVA) (53). Another assessment complementary to the fHIT, is testing the DVA while walking on a treadmill, which is strongly related to activities of daily living and therefore has significant ecological validity (54, 55). Unfortunately, the DVA while walking on a treadmill cannot always be performed in elderly patients, as increased age in combination with BVP leads to a higher drop out rate during test performance (54). Lastly, the vestibular system contributes to detecting self-motion. Earlier research showed that self-motion perception is significantly decreased in patients with BVP compared to control subjects, and therefore self-motion perception could also be considered as a functional outcome measure in the future (56–58).

4 Proposal of a diagnostic algorithm for BVP

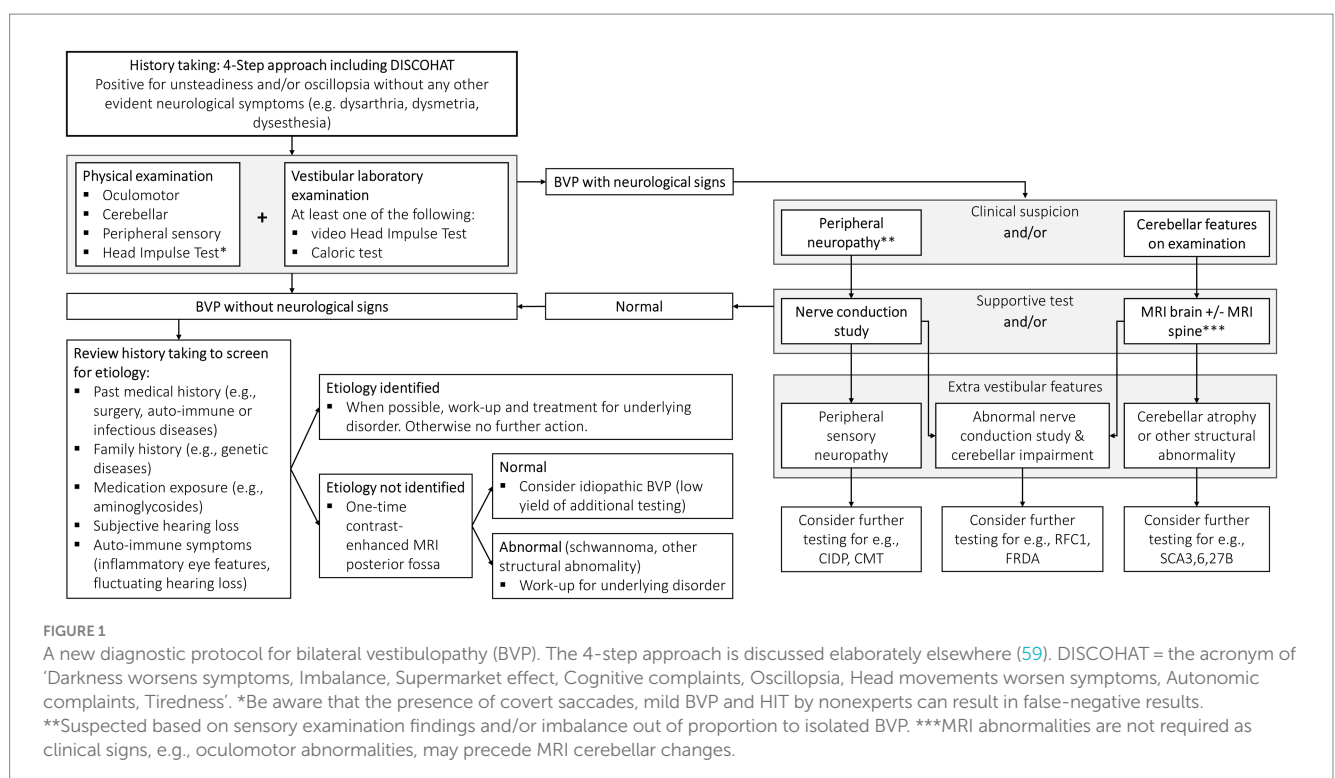
Establishing the diagnosis of BVP is often delayed. To facilitate a prompt, accurate and robust diagnostic process, a new protocol has been proposed based on the current knowledge summarized in this narrative review (Figure 1). The diagnostic process for vestibular disorders starts with an adequate medical history. A tool for improving history taking is the 4-step approach which focuses on: (1) potential attacks of vertigo and/or dizziness, (2) potential chronic vestibular symptoms, (3) any additional functional, psychological or psychiatric co-morbidities, and taken together leading to (4) a comprehensive differential diagnosis (59). Regarding episodes of vertigo or dizziness attacks in the context of BVP principally depends on etiology (e.g., positive history taking for experiencing vertigo attacks in a patient with bilateral Menière's Disease). Chronic symptoms are however always present in BVP and can be summarized according to the DISCOHAT acronym (worsening of symptoms in Darkness and/or uneven ground, Imbalance, Supermarket effect, Cognitive complaints, Oscillopsia, Head movements worsen symptoms, Autonomic complaints, and Tiredness), with a particular focus on imbalance/unsteadiness and oscillopsia (60).

In every patient with a positive history for imbalance/unsteadiness and/or oscillopsia without any other neurological symptoms (e.g., dysarthria, dysmetria, dysesthesia), a thorough physical examination focused on oculomotor testing, HIT, cerebellar testing, and testing for neuropathy is indicated. This is all necessary in order to identify patients with combined peripheral and central neurological disorders such as CANVAS or the recently described Spinocerebellar Ataxia Type 27B (SCA27B) (7, 61). Oculomotor abnormalities such as broken-up visual pursuit, gaze-evoked nystagmus and abnormal saccades to target, point to pathology of the cerebellum and its

connections (62). In addition to oculomotor signs, other localizing abnormalities observed during examination include cerebellar dysarthria, often described as 'slurred' or 'drunken' speech, as well as limb ataxia, such as the presence of an intention tremor during the finger-to-nose test. These clinical manifestations are frequently encountered in cases of cerebellar impairment (63).

In addition to the physical examination, at least one vestibular laboratory examination to objectify the vestibular function must be performed, preferably by means of a vHIT or caloric test (5). vHIT is favored over HIT as it provides a calculated VOR gain and recognizes the influence of covert saccades and other eye movement abnormalities (5). Regarding caloric testing, it is important to irrigate with at least 250 mL of water for a duration of 30s for both cold (30°C) and warm (44°C) irrigations with a 5-min stimulus interval between irrigations. Furthermore, it is necessary to not only look for a potential asymmetry (%) but also evaluate absolute caloric values (°/sec). The torsion swing test is less suitable to use as a single diagnostic tool since it appears to be less sensitive for detecting vestibular impairment as compared to vHIT and the caloric test (7, 19). Therefore, the torsion swing test is not included in the diagnostic algorithm.

Where history, physical examination and vestibular function tests lead to a BVP diagnosis without neurological involvement, the next step is attempting to identify the etiology (Figure 1, lower left side of the flow chart). Important information includes past medical history (e.g., surgery, auto-immunity, infectious diseases such as Lyme disease or syphilis), family history (genetic disorders), use of medication (ototoxicity), subjective hearing loss and auto-immune symptoms (including those of inflammatory eye disease and fluctuating hearing loss). Where a treatable etiology is identified (e.g., autoimmune or infectious disease), then this obviously becomes the clinical priority. Where the etiology remains idiopathic, a one-time contrast-enhanced MRI of the posterior fossa is advised because of the relatively high



yield of positive findings (e.g., vestibular schwannoma). Contrast-enhanced MRI scans are preferred over non-contrast MRI scans as they increase the detection rate of small schwannomas, particularly intralabyrinthine ones, which may be missed by radiologists who are less familiar with intralabyrinthine pathology (64). Blood tests are not routinely advised because of the low yield (7).

Where history, physical examination, and vestibular function tests lead to a BVP diagnosis in combination with neurological signs, the next step is the evaluation of peripheral sensory neuropathy and/or cerebellar features by performing clinical tests such as a nerve conduction study and/or a MRI scan (Figure 1, right side of the flow chart).

Regarding peripheral neuropathy, studies show that up to 53 percent of patients with a peripheral neuropathy also suffer from vestibular hypofunction (65). Conditions where this combination is seen, include Chronic Inflammatory Demyelinating Polyradiculoneuropathy (CIDP), Charcot-Marie Tooth (CMT) disease, Guillain-Barre Syndrome (GBS), neurosarcoidosis and other inflammatory and inherited diseases (noting that diseases such as GBS, CIDP and neurosarcoidosis require treatment which may be lifesaving) (66–71). Therefore, further testing for, e.g., CIDP and CMT needs to be considered in cases of bilateral vestibulopathy accompanied by abnormal nerve conduction studies indicating a peripheral sensory neuropathy.

Regarding cerebellar features, BVP is increasingly identified as an extracerebellar feature of the many cerebellar ataxias, including the most common sporadic and inherited diseases such as idiopathic late-onset cerebellar ataxia (ILOCA), idiopathic Cerebellar Ataxia with Bilateral Vestibulopathy (iCABV), spinocerebellar ataxia (SCA) 3 and 6, Friedreich ataxia (FRDA), Cerebellar Ataxia, Neuronopathy, Vestibular Areflexia syndrome (CANVAS)/*RFC1*-related disease, and most recently SCA27B (*FGF14* GAA expansion) (23, 61, 72–76). Where cerebellar signs on examination, or MRI changes such as atrophy are found (with or without sensory peripheral neuropathy), further testing for the above-mentioned etiologies is advised. It is important to bear in mind that cerebellar signs on examination (particularly oculomotor abnormalities) may be seen well before MRI changes are found. In other words, the normal appearance of the cerebellum on MRI scanning does not exclude cerebellar impairment, especially in the earlier stages of cerebellar disease (77).

5 Treatment

Unfortunately, to date, the prognosis for recovery of vestibular function is poor (14). Detailed patient counseling and education with a focus on explaining the cause of the symptoms is therefore of great importance.

Vestibular rehabilitation therapy remains the mainstay of treatment for vestibular hypofunction. Exercise-based vestibular rehabilitation is aimed at (1) adaptation and (2) substitution. Adaptation is the process by which the gain of the vestibular reflexes are increased, while substitution (or sensory reweighting) involves strategies to utilize alternate modalities in place of the vestibular hypofunction (78). The reported efficacy of vestibular rehabilitation in BVP differs. Two independent systematic reviews found moderate to strong evidence supporting the utility of vestibular rehabilitation

in BVP in improving gaze and postural stability and improving overall functional status (79, 80). Additionally, vestibular rehabilitation was found to significantly reduce the number of falls in patients with combined BVP and cerebellar impairment (81). Sensory reweighting (substitution) is however limited since other somatosensory systems cannot fully compensate for the elaborate function of the vestibular system. In particular, the somatosensory system is not able to respond as rapidly as the VOR, the vestibulo-spinal reflex, and the vestibulo-colic reflex. As a result, the balance system as a whole lacks the speed and automatism provided by an intact vestibular system (82). In other words, a BVP patient is less able to reflexively react to balance perturbations. Sensory substitution devices aim to substitute the loss of vestibular input by administering tactile or auditory stimulation which may result in some degree of improvement in balance control (83–85). However, it is important to note that these devices are unable to replace the rapid vestibular reflexes.

Other therapeutic approaches, such as noisy galvanic vestibular stimulation, aim to enhance the residual vestibular function. Previous studies indicated that noisy galvanic vestibular stimulation improves postural and gait stability in patients with BVP (86–88). This treatment strategy will probably offer the most benefit in patients with residual vestibular function (e.g., similar to the functionality of hearing aids: hearing aids can augment the hearing performance only in the presence of residual hearing).

An artificial balance organ, the vestibular implant, directly stimulates the peripheral vestibular nerve and therefore does not depend on the presence of residual vestibular function (89, 90). Vestibular implant research to date demonstrated partial recovery of the VOR and the vestibulo-colic reflex, and hence, rapid vestibular responses are achievable (89, 91–93). This approach appears promising since the functional improvements closely match the expectations of BVP patients regarding vestibular implant treatment (94, 95).

6 Conclusion

The knowledge of BVP has grown expansively since its first description in 1936. The proposed diagnostic algorithm facilitates in-clinic assessment and diagnosis. In addition to the vestibular rehabilitation, therapeutic modalities currently under development hold significant promise.

Author contributions

LS: Conceptualization, Methodology, Writing – original draft, Writing – review & editing. DS: Writing – review & editing. NG: Writing – review & editing. AF: Writing – review & editing. VR: Writing – review & editing. RB: Conceptualization, Methodology, Supervision, Writing – review & editing.

Funding

The author(s) declare that no financial support was received for the research, authorship, and/or publication of this article.

Conflict of interest

The authors declare that the research was conducted in the absence of any commercial or financial relationships that could be construed as a potential conflict of interest.

The author(s) declared that they were an editorial board member of Frontiers, at the time of submission. This had no impact on the peer review process and the final decision.

References

- Dandy WE. The surgical treatment of Meniere's disease. *Surg Gynecol Obstet.* (1941) 72:421–5.
- Ward BK, Tarnutzer AA. Editorial: bilateral Vestibulopathy - current knowledge and future directions to improve its diagnosis and treatment. *Front Neurol.* (2018) 9:762–2. doi: 10.3389/fneur.2018.00762
- Alarcón AV, Hidalgo LO, Arévalo RJ, Diaz MP. Labyrinthectomy and vestibular Neurectomy for intractable vertiginous symptoms. *Int Arch Otorhinolaryngol.* (2017) 21:184–90. doi: 10.1055/s-0037-1599242
- Hain TC, Cherchi M, Yacovino DA. Bilateral vestibular loss. *Semin Neurol.* (2013) 33:195–203. doi: 10.1055/s-0033-1354597
- van de Berg R, van Tilburg M, Kingma H. Bilateral vestibular hypofunction: challenges in establishing the diagnosis in adults. *ORL J Otorhinolaryngol Relat Spec.* (2015) 77:197–218. doi: 10.1159/000433549
- Strupp M, Kim JS, Murofushi T, Straumann D, Jen JC, Rosengren SM, et al. Bilateral vestibulopathy: diagnostic criteria consensus document of the classification Committee of the Barany Society. *J Vestib Res.* (2017) 27:177–89. doi: 10.3233/VES-170619
- Lucieir F, Vonk P, Guinand N, Stokroos R, Kingma H, van de Berg R. Bilateral vestibular hypofunction: insights in etiologies, clinical subtypes, and diagnostics. *Front Neurol.* (2016) 7:26. doi: 10.3389/fneur.2016.00026
- Guinand N, Boselie F, Guyot JP, Kingma H. Quality of life of patients with bilateral vestibulopathy. *Ann Otol Rhinol Laryngol.* (2012) 121:471–7. doi: 10.1177/000348941212100708
- Miffon M, Guyot JP. Difficulties faced by patients suffering from Total bilateral vestibular loss. *ORL J Otorhinolaryngol Relat Spec.* (2015) 77:241–7. doi: 10.1159/000433553
- Piper KS, Juhl CB, Andersen HE, Christensen J, Søndergaard K. Prevalence of bilateral vestibulopathy among older adults above 65 years on the indication of vestibular impairment and the association with dynamic gait index and dizziness handicap inventory. *Disabil Rehabil.* (2022) 45:1220–8. doi: 10.1080/09638288.2022.2057603
- Vibert D, Liard P, Häusser R. Bilateral idiopathic loss of peripheral vestibular function with normal hearing. *Acta Otolaryngol.* (1995) 115:611–5. doi: 10.3109/00016489509139375
- Ward BK, Agrawal Y, Hoffman HJ, Carey JP, Della Santina CC. Prevalence and impact of bilateral vestibular hypofunction: results from the 2008 US National Health Interview Survey. *JAMA Otolaryngol Head Neck Surg.* (2013) 139:803–10. doi: 10.1001/jamaoto.2013.3913
- Tarnutzer AA, Bockisch CJ, Buffone E, Weber KP. Hierarchical cluster analysis of Semicircular Canal and otolith deficits in bilateral Vestibulopathy. *Front Neurol.* (2018) 9:244. doi: 10.3389/fneur.2018.00244
- Zingler VC, Weintz E, Jahn K, Huppert D, Cnyrim C, Brandt T, et al. Causative factors, epidemiology, and follow-up of bilateral vestibulopathy. *Ann N Y Acad Sci.* (2009) 1164:505–8. doi: 10.1111/j.1749-6632.2009.03765.x
- Grill E, Strupp M, Müller M, Jahn K. Health services utilization of patients with vertigo in primary care: a retrospective cohort study. *J Neurol.* (2014) 261:1492–8. doi: 10.1007/s00415-014-7367-y
- Kovacs E, Wang X, Grill E. Economic burden of vertigo: a systematic review. *Heal Econ Rev.* (2019) 9:1–14. doi: 10.1186/s13561-019-0258-2
- Wang X, Strobl R, Holle R, Seidl H, Peters A, Grill E. Vertigo and dizziness cause considerable more health care resource use and costs: results from the KORA FF4 study. *J Neurol.* (2019) 266:2120–8. doi: 10.1007/s00415-019-09386-x
- Dobbels B, Lucieir F, Mertens G, Gilles A, Moyaert J, van de Heyning P, et al. Prospective cohort study on the predictors of fall risk in 119 patients with bilateral vestibulopathy. *PLoS One.* (2020) 15:e0228768. doi: 10.1371/journal.pone.0228768
- van Stiphout L, Pleshkov M, Lucieir F, Dobbels B, Mavrodiev V, Guinand N, et al. Patterns of vestibular impairment in bilateral Vestibulopathy and its relation to etiology. *Front Neurol.* (2022) 13:856472. doi: 10.3389/fneur.2022.856472
- Sun DQ, Ward BK, Semenov YR, Carey JP, Della Santina CC. Bilateral vestibular deficiency: quality of life and economic implications. *JAMA Otolaryngol Head Neck Surg.* (2014) 140:527–34. doi: 10.1001/jamaoto.2014.490

Publisher's note

All claims expressed in this article are solely those of the authors and do not necessarily represent those of their affiliated organizations, or those of the publisher, the editors and the reviewers. Any product that may be evaluated in this article, or claim that may be made by its manufacturer, is not guaranteed or endorsed by the publisher.

- Tarnutzer AA, Bockisch CJ, Buffone E, Weiler S, Bachmann LM, Weber KP. Disease-specific sparing of the anterior semicircular canals in bilateral vestibulopathy. *Clin Neurophysiol.* (2016) 127:2791–801. doi: 10.1016/j.clinph.2016.05.005
- Greco A, De Virgilio A, Gallo A, Fusconi M, Ruoppolo G, Turchetta R, et al. Idiopathic bilateral vestibulopathy: an autoimmune disease? *Autoimmun Rev.* (2014) 13:1042–7. doi: 10.1016/j.autrev.2014.08.035
- Szmulewicz DJ, McLean CA, MacDougall HG, Roberts L, Storey E, Halmagyi GM. CANVAS an update: clinical presentation, investigation and management. *J Vestib Res.* (2014) 24:465–74. doi: 10.3233/ves-140536
- Kattah JC. Clinical characteristics and etiology of bilateral vestibular loss in a cohort from Central Illinois. *Front Neurol.* (2018) 9:46. doi: 10.3389/fneur.2018.00046
- Wester JL, Ishiyama A, Ishiyama G. Recurrent vestibular migraine Vertigo attacks associated with the development of profound bilateral Vestibulopathy: a case series. *Otol Neurotol.* (2017) 38:1145–8. doi: 10.1097/mao.0000000000001486
- Brandt T, Schautzer F, Hamilton DA, Brüning R, Markowitsch HJ, Kalla R, et al. Vestibular loss causes hippocampal atrophy and impaired spatial memory in humans. *Brain.* (2005) 128:2732–41. doi: 10.1093/brain/awh617
- Dobbels B, Mertens G, Gilles A, Claes A, Moyaert J, van de Berg R, et al. Cognitive function in acquired bilateral Vestibulopathy: a cross-sectional study on cognition, hearing, and vestibular loss. *Front Neurosci.* (2019) 13:340. doi: 10.3389/fnins.2019.00340
- Lucieir F, Duijn S, Van Rompaey V, Perez Fornos A, Guinand N, Guyot JP, et al. Full Spectrum of reported symptoms of bilateral Vestibulopathy needs further investigation - a systematic review. *Front Neurol.* (2018) 9:352. doi: 10.3389/fneur.2018.00352
- Schöberl F, Pradhan C, Grosch M, Brendel M, Jostes F, Obermaier K, et al. Bilateral vestibulopathy causes selective deficits in recombining novel routes in real space. *Sci Rep.* (2021) 11:2695. doi: 10.1038/s41598-021-82427-6
- Strupp M, Arbusow V. Acute vestibulopathy. *Curr Opin Neurol.* (2001) 14:11–20. doi: 10.1097/00019052-200102000-00003
- Bronstein AM. Multisensory integration in balance control. *Handb Clin Neurol.* (2016) 137:57–66. doi: 10.1016/B978-0-444-63437-5.00004-2
- Jahn K, Strupp M, Schneider E, Dieterich M, Brandt T. Visually induced gait deviations during different locomotion speeds. *Exp Brain Res.* (2001) 141:370–4. doi: 10.1007/s002210100884
- McCrum C, Lucieir F, van de Berg R, Willems P, Pérez Fornos A, Guinand N, et al. The walking speed-dependency of gait variability in bilateral vestibulopathy and its association with clinical tests of vestibular function. *Sci Rep.* (2019) 9:18392. doi: 10.1038/s41598-019-54605-0
- Medendorp WP, Alberts B, Verhagen WIM, Koppen M, Selen LPJ. Psychophysical evaluation of sensory reweighting in bilateral Vestibulopathy. *Front Neurol.* (2018) 9:377. doi: 10.3389/fneur.2018.00377
- Herssens N, Saeyns W, Vereeck L, Meijer K, van de Berg R, Van Rompaey V, et al. An exploratory investigation on spatiotemporal parameters, margins of stability, and their interaction in bilateral vestibulopathy. *Sci Rep.* (2021) 11:6427. doi: 10.1038/s41598-021-85870-7
- Herssens N, Dobbels B, Moyaert J, Van de Berg R, Saeyns W, Halleman A, et al. Paving the way toward distinguishing fallers from non-fallers in bilateral Vestibulopathy: a wide pilot observation. *Front Neurol.* (2021) 12:611648. doi: 10.3389/fneur.2021.611648
- Herssens N, How D, van de Berg R, McCrum C. Falls among people with bilateral Vestibulopathy: a review of causes, incidence, injuries, and methods. *JAMA Otolaryngol Head Neck Surg.* (2022) 148:187–92. doi: 10.1001/jamaoto.2021.3673
- Wuehr M, Decker J, Schenkel F, Jahn K, Schniepp R. Impact on daily mobility and risk of falling in bilateral vestibulopathy. *J Neurol.* (2022) 269:5746–54. doi: 10.1007/s00415-022-11043-9
- Schniepp R, Schlick C, Schenkel F, Pradhan C, Jahn K, Brandt T, et al. Clinical and neurophysiological risk factors for falls in patients with bilateral vestibulopathy. *J Neurol.* (2017) 264:277–83. doi: 10.1007/s00415-016-8342-6
- van Stiphout L, Hossein I, Kimmman M, Whitney SL, Ayiotis A, Strupp M, et al. Development and content validity of the bilateral Vestibulopathy questionnaire. *Front Neurol.* (2022) 13:852048. doi: 10.3389/fneur.2022.852048

41. van Stiphout L, Rolfes J, Waardenburg S, Kimman M, Guinand N, Perez Fornos A, et al. Construct validity and reliability of the bilateral Vestibulopathy questionnaire (BVQ). *Front Neurol.* (2023) 14:1221037. doi: 10.3389/fneur.2023.1221037
42. Kattah JC, Talkad AV, Wang DZ, Hsieh YH, Newman-Toker DE. HINTS to diagnose stroke in the acute vestibular syndrome: three-step bedside oculomotor examination more sensitive than early MRI diffusion-weighted imaging. *Stroke.* (2009) 40:3504–10. doi: 10.1161/strokeaha.109.551234
43. Yip CW, Glaser M, Frenzel C, Bayer O, Strupp M. Comparison of the bedside head-impulse test with the video head-impulse test in a clinical practice setting: a prospective study of 500 outpatients. *Front Neurol.* (2016) 7:58. doi: 10.3389/fneur.2016.00058
44. Machner B, Erber K, Choi JH, Trillenber P, Sprenger A, Helmchen C. Usability of the head impulse test in routine clinical practice in the emergency department to differentiate vestibular neuritis from stroke. *Eur J Neurol.* (2021) 28:1737–44. doi: 10.1111/ene.14707
45. Szmulewicz DJ, MacDougall HG, Storey E, Curthoys IS, Halmagyi MG. A novel quantitative bedside test of balance function: the video visually enhanced Vestibulo-ocular reflex (VVOR) (S19.002). *Neurology.* (2014) 82:S19–S1002.
46. Petersen JA, Straumann D, Weber KP. Clinical diagnosis of bilateral vestibular loss: three simple bedside tests. *Ther Adv Neurol Disord.* (2013) 6:41–5. doi: 10.1177/1756285612465920
47. Zwergal A, Feil K, Schniepp R, Strupp M. Cerebellar dizziness and vertigo: etiologies, diagnostic assessment, and treatment. *Semin Neurol.* (2020) 40:087–96. doi: 10.1055/s-0039-3400315
48. Van Dooren TS, Starkov D, Lucieer FMP, Vermorken B, Janssen AML, Guinand N, et al. Comparison of three video head impulse test systems for the diagnosis of bilateral vestibulopathy. *J Neurol.* (2020) 267:256–64. doi: 10.1007/s00415-020-10060-w
49. Manzari L, De Angelis S, Princi A.A., Galeoto G, Tramontano M. The clinical use of the suppression head impulse paradigm in patients with vestibulopathy: a systematic review. *Healthcare (Basel).* (2022) 10. doi: 10.3390/healthcare10071182
50. van Dooren T, Starkov D, Lucieer F, Dobbels B, Janssen M, Guinand N, et al. Suppression Head Impulse Test (SHIMP) versus Head Impulse Test (HIMP) When Diagnosing Bilateral Vestibulopathy. *J Clin Med.* (2022) 11. doi: 10.3390/jcm11092444
51. Rosengren SM, Welgampola MS, Taylor RL. Vestibular-evoked myogenic potentials in bilateral Vestibulopathy. *Front Neurol.* (2018) 9:252. doi: 10.3389/fneur.2018.00252
52. Zingler VC, Weintz E, Jahn K, Botzel K, Wagner J, Huppert D, et al. Saccular function less affected than canal function in bilateral vestibulopathy. *J Neurol.* (2008) 255:1332–6. doi: 10.1007/s00415-008-0887-6
53. Van Dooren T, Lucieer F, Duijn S, Janssen A, Guinand N, Perez Fornos A, et al. The functional head impulse test to assess oscillopsia in bilateral vestibulopathy. *Front Neurol.* (2019) 10:365. doi: 10.3389/fneur.2019.00365
54. Starkov D, Snelders M, Lucieer F, Janssen A, Pleshkov M, Kingma H, et al. Bilateral vestibulopathy and age: experimental considerations for testing dynamic visual acuity on a treadmill. *J Neurol.* (2020) 267:265–72. doi: 10.1007/s00415-020-10249-z
55. Starkov D, Strupp M, Pleshkov M, Kingma H, van de Berg R. Diagnosing vestibular hypofunction: an update. *J Neurol.* (2021) 268:377–85. doi: 10.1007/s00415-020-10139-4
56. Merfeld DM, Priesol A, Lee D, Lewis RF. Potential solutions to several vestibular challenges facing clinicians. *J Vestib Res.* (2010) 20:71–7. doi: 10.3233/ves-2010-0347
57. Priesol AJ, Valko Y, Merfeld DM, Lewis RF. Motion perception in patients with idiopathic bilateral vestibular hypofunction. *Otolaryngol Head Neck Surg.* (2014) 150:1040–2. doi: 10.1177/0194599814526557
58. van Stiphout L, Lucieer F, Pleshkov M, Van Rompaey V, Widdershoven J, Guinand N, et al. Bilateral vestibulopathy decreases self-motion perception. *J Neurol.* (2021) 269:5216–28. doi: 10.1007/s00415-021-10695-3
59. van de Berg R, Kingma H. History taking in non-acute vestibular symptoms: a 4-step approach. *J Clin Med.* (2021) 10:5726. doi: 10.3390/jcm10245726
60. Paredis S, van Stiphout L, Remmen E, Strupp M, Gerards M-C, Kingma H, et al. DISCOHAT: an acronym to describe the Spectrum of symptoms related to bilateral Vestibulopathy. *Front Neurol.* (2021) 12:771650. doi: 10.3389/fneur.2021.771650
61. Rafehi H, Read J, Szmulewicz DJ, Davies KC, Snell P, Fearnley LG, et al. An intronic GAA repeat expansion in FGF14 causes the autosomal-dominant adult-onset ataxia SCA50/ATX-FGF14. *Am J Hum Genet.* (2023) 110:105–19. doi: 10.1016/j.ajhg.2022.11.015
62. Kheradmand A, Zee D. Cerebellum and ocular motor control. *Front Neurol.* (2011) 2:53. doi: 10.3389/fneur.2011.00053
63. Bodranghien F, Bastian A, Casali C, Hallett M, Louis ED, Manto M, et al. Consensus paper: revisiting the symptoms and signs of cerebellar syndrome. *Cerebellum.* (2016) 15:369–91. doi: 10.1007/s12311-015-0687-3
64. Salzman KL, Childs AM, Davidson HC, Kennedy RJ, Shelton C, Harnsberger HR. Intralabyrinthine schwannomas: imaging diagnosis and classification. *AJNR Am J Neuroradiol.* (2012) 33:104–9. doi: 10.3174/ajnr.A2712
65. Samaha M, Katsarkas A. Vestibular impairment in peripheral sensory neuropathies. *J Otolaryngol.* (2000) 29:299–301.
66. Akdal G, Tanriverdizade T, Şengün İ, Bademkiran F, Koçoğlu K, Yüceyar AN, et al. Vestibular impairment in chronic inflammatory demyelinating polyneuropathy. *J Neurol.* (2018) 265:381–7. doi: 10.1007/s00415-017-8712-8
67. Blanquet M, Petersen JA, Palla A, Veraguth D, Weber KP, Straumann D, et al. Vestibulo-cochlear function in inflammatory neuropathies. *Clin Neurophysiol.* (2018) 129:863–73. doi: 10.1016/j.clinph.2017.11.025
68. Bradshaw MJ, Pawate S, Koth LL, Cho TA, Gelfand JM. Neurosarcoidosis: pathophysiology, diagnosis, and treatment. *Neuro Neuroimmunol Neuroinflamm.* (2021) 8:e1084. doi: 10.1212/nxi.0000000000001084
69. Frohman EM, Tusa R, Mark AS, Cornblath DR. Vestibular dysfunction in chronic inflammatory demyelinating polyneuropathy. *Ann Neurol.* (1996) 39:529–35. doi: 10.1002/ana.410390415
70. Nadol JB Jr, Hedley-Whyte ET, Amr SS, JT OAM, Kamakura T. Histopathology of the inner ear in Charcot-Marie-Tooth syndrome caused by a missense variant (p.Thr65Ala) in the MPZ gene. *Audiol Neurotol.* (2018) 23:326–34. doi: 10.1159/000495176
71. Szmulewicz DJ, Waterston JA. Two patients with audiovestibular sarcoidosis. *J Clin Neurosci.* (2012) 19:158–61. doi: 10.1016/j.jocn.2011.07.020
72. Fahey MC, Cremer PD, Aw ST, Millist L, Todd MJ, White OB, et al. Vestibular, saccadic and fixation abnormalities in genetically confirmed Friedreich ataxia. *Brain.* (2008) 131:1035–45. doi: 10.1093/brain/awn323
73. Gordon CR, Joffe V, Vainstein G, Gadoth N. Vestibulo-ocular areflexia in families with spinocerebellar ataxia type 3 (Machado-Joseph disease). *J Neurol Neurosurg Psychiatry.* (2003) 74:1403–6. doi: 10.1136/jnnp.74.10.1403
74. Huh YE, Kim JS, Kim HJ, Park SH, Jeon BS, Kim JM, et al. Vestibular performance during high-acceleration stimuli correlates with clinical decline in SCA6. *Cerebellum.* (2015) 14:284–91. doi: 10.1007/s12311-015-0650-3
75. Ishai R, Seyyedi M, Chancellor AM, McLean CA, Rodriguez ML, Halmagyi GM, et al. The pathology of the vestibular system in CANVAS. *Otol Neurotol.* (2021) 42:e332–40. doi: 10.1097/mao.0000000000002985
76. Szmulewicz D. Combined central and peripheral degenerative vestibular disorders: CANVAS, idiopathic cerebellar Ataxia with bilateral Vestibulopathy (CABV) and other differential diagnoses of the CABV phenotype. *Curr Otorhinolaryngol Rep.* (2017) 5:167–74. doi: 10.1007/s40136-017-0161-5
77. Szmulewicz DJ, Waterston JA, Halmagyi GM, Mossman S, Chancellor AM, McLean CA, et al. Sensory neuropathy as part of the cerebellar ataxia neuropathy vestibular areflexia syndrome. *Neurology.* (2011) 76:1903–10. doi: 10.1212/WNL.0b013e31821d746e
78. Herdman SJ. Role of vestibular adaptation in vestibular rehabilitation. *Otolaryngol Head Neck Surg.* (1998) 119:49–54. doi: 10.1016/s0194-5998(98)70195-0
79. McDonnell MN, Hillier SL. Vestibular rehabilitation for unilateral peripheral vestibular dysfunction. *Cochrane Database Syst Rev.* (2015) 1:CD005397. doi: 10.1002/14651858.CD005397.pub4
80. Porciuncula F, Johnson CC, Glickman LB. The effect of vestibular rehabilitation on adults with bilateral vestibular hypofunction: a systematic review. *J Vestib Res.* (2012) 22:283–98. doi: 10.3233/ves-120464
81. Hassannia F, Misale P, Sulway S, Olmos GV, Dabiri S, Ranalli P, et al. Effectiveness of vestibular rehabilitation therapy in patients with idiopathic cerebellar Ataxia with bilateral Vestibulopathy (iCABV). *J Vestib Res.* (2022) 32:479–85. doi: 10.3233/ves-210058
82. Lucieer FMP, Van Hecke R, van Stiphout L, Duijn S, Perez-Fornos A, Guinand N, et al. Bilateral vestibulopathy: beyond imbalance and oscillopsia. *J Neurol.* (2020) 267:241–55. doi: 10.1007/s00415-020-10243-5
83. Basta D, Rossi-Izquierdo M, Wonneberger K, Brugnera C, Bittar RSM, Greters ME, et al. Individualized Vibrotactile neurofeedback training in patients with chronic bilateral Vestibulopathy. *Brain Sci.* (2023) 13:1219. doi: 10.3390/brainsci13081219
84. Dozza M, Chiari L, Horak FB. Audio-biofeedback improves balance in patients with bilateral vestibular loss. *Arch Phys Med Rehabil.* (2005) 86:1401–3. doi: 10.1016/j.apmr.2004.12.036
85. Kingma H, Felipe L, Gerards MC, Gerits P, Guinand N, Perez-Fornos A, et al. Vibrotactile feedback improves balance and mobility in patients with severe bilateral vestibular loss. *J Neurol.* (2019) 266:19–26. doi: 10.1007/s00415-018-9133-z
86. Fujimoto C, Egami N, Kawahara T, Uemura Y, Yamamoto Y, Yamasoba T, et al. Noisy galvanic vestibular stimulation sustainably improves posture in bilateral Vestibulopathy. *Front Neurol.* (2018) 9:900. doi: 10.3389/fneur.2018.00900
87. Iwasaki S, Fujimoto C, Egami N, Kinoshita M, Togo F, Yamamoto Y, et al. Noisy vestibular stimulation increases gait speed in normals and in bilateral vestibulopathy. *Brain Stimul.* (2018) 11:709–15. doi: 10.1016/j.brs.2018.03.005
88. Wuehr M, Decker J, Schniepp R. Noisy galvanic vestibular stimulation: an emerging treatment option for bilateral vestibulopathy. *J Neurol.* (2017) 264:81–6. doi: 10.1007/s00415-017-8481-4
89. Chow MR, Ayiotis AI, Schoo DP, Gimmon Y, Lane KE, Morris BJ, et al. Posture, gait, quality of life, and hearing with a vestibular implant. *N Engl J Med.* (2021) 384:521–32. doi: 10.1056/NEJMoa2020457

90. van de Berg R, Guinand N, Nguyen TA, Ranieri M, Cavuscens S, Guyot JP, et al. The vestibular implant: frequency-dependency of the electrically evoked vestibulo-ocular reflex in humans. *Front Syst Neurosci.* (2014) 8:255. doi: 10.3389/fnsys.2014.00255
91. Fornos AP, van de Berg R, Armand S, Cavuscens S, Ranieri M, Cretallaz C, et al. Cervical myogenic potentials and co-ntrolled postural responses elicited by a prototype vestibular implant. *J Neurol.* (2019) 266:33–41. doi: 10.1007/s00415-019-09491-x
92. Guinand N, Van de Berg R, Cavuscens S, Stokroos R, Ranieri M, Pelizzzone M, et al. Restoring visual acuity in dynamic conditions with a vestibular implant. *Front Neurosci.* (2016) 10:577. doi: 10.3389/fnins.2016.00577
93. Starkov D, Guinand N, Lucieer F, Ranieri M, Cavuscens S, Pleshkov M, et al. Restoring the high-frequency dynamic visual acuity with a vestibular implant prototype in humans. *Audiol Neurotol.* (2019) 25:91–5. doi: 10.1159/000503677
94. Stultiens JJA, Lewis RF, Phillips JO, Boutabla A, Della Santina CC, Glueckert R, et al. The next challenges of vestibular implantation in humans. *J Assoc Res Otolaryngol.* (2023) 24:401–12. doi: 10.1007/s10162-023-00906-1
95. van Stiphout L, Lucieer F, Guinand N, Pérez Fornos A, van de Berg M, Van Rompaey V, et al. Bilateral vestibulopathy patients' perspectives on vestibular implant treatment: a qualitative study. *J Neurol.* (2021) 269:5249–57. doi: 10.1007/s00415-021-10920-z



OPEN ACCESS

EDITED BY

Leonardo Manzari,
MSA ENT Academy Center, Italy

REVIEWED BY

Luigi Califano,
A.O. San Pio Benevento, Italy
Xin-Da Xu,
Fudan University, China

*CORRESPONDENCE

Xiaokai Yang
✉ yakeworld@126.com

[†]These authors share first authorship

RECEIVED 30 October 2023

ACCEPTED 07 December 2023

PUBLISHED 21 December 2023

CITATION

Chen X, Mao J, Ye H, Fan L, Tong Q, Zhang H, Wu C and Yang X (2023) The effectiveness of the modified Epley maneuver for the treatment of posterior semicircular canal benign paroxysmal positional vertigo. *Front. Neurol.* 14:1328896. doi: 10.3389/fneur.2023.1328896

COPYRIGHT

© 2023 Chen, Mao, Ye, Fan, Tong, Zhang, Wu and Yang. This is an open-access article distributed under the terms of the [Creative Commons Attribution License \(CC BY\)](#). The use, distribution or reproduction in other forums is permitted, provided the original author(s) and the copyright owner(s) are credited and that the original publication in this journal is cited, in accordance with accepted academic practice. No use, distribution or reproduction is permitted which does not comply with these terms.

The effectiveness of the modified Epley maneuver for the treatment of posterior semicircular canal benign paroxysmal positional vertigo

Xiaosu Chen^{1†}, Jiesheng Mao^{1†}, Hua Ye¹, Luping Fan², Qiaowen Tong¹, Hehui Zhang¹, Chengcheng Wu¹ and Xiaokai Yang^{1*}

¹Neurology Department, Third Affiliated Hospital of Shanghai University, Wenzhou Third Clinical Institute Affiliated to Wenzhou Medical University, Wenzhou People's Hospital, Wenzhou, China,

²Rehabilitation Department, Third Affiliated Hospital of Shanghai University, Wenzhou Third Clinical Institute Affiliated to Wenzhou Medical University, Wenzhou People's Hospital, Wenzhou, China

Objective: To compare the repositioning effect of the modified Epley maneuver and the traditional Epley maneuver for posterior semicircular canal benign paroxysmal positional vertigo (PC-BPPV).

Methods: Sixty-five patients with unilateral PC-BPPV were randomly divided into two groups. The control group received the traditional Epley maneuver, while the experimental group received the modified Epley maneuver, which prolonged the time in the healthy side lying position and the final bowing position. The number of successful repositions after one, two, and three attempts and the total number of successful repositions were recorded and compared between the two groups. A BPPV virtual simulation model was used to analyze the mechanism of the modified Epley maneuver.

Results: The first repositioning success rate of the experimental group was significantly higher than that of the control group (85% vs. 63%, $p = 0.040$). The experimental group achieved 100% repositioning success rate after two attempts, while the control group needed three attempts to reach 86% repositioning success rate. Four cases in the control group experienced canal switching during the repositioning process, while none in the experimental group did. The BPPV virtual simulation model showed that the modified Epley maneuver could facilitate the passage of otoliths through the posterior arm of the posterior semicircular canal, especially through the location of obstruction.

Conclusion: The modified Epley maneuver is more effective than the traditional Epley maneuver in improving the single repositioning success rate and reducing the canal switching rate for PC-BPPV. This study provides a new option for the treatment of BPPV.

KEYWORDS

BPPV, otoconia, Epley maneuver, nystagmus, simulation

1 Introduction

Benign paroxysmal positional vertigo (BPPV) stands out as a prevalent cause of peripheral vertigo, constituting 17–42% of reported cases (1). Manifesting as brief episodes of vertigo and nystagmus, BPPV is triggered by alterations in head position relative to gravity, such as lying down, turning over, or standing up (2). The prevailing pathophysiological understanding attributes BPPV to the detachment of otoconia from the utricular macula, migrating into one or more semicircular canals. This migration disrupts normal endolymph flow and induces abnormal stimulation of the cupula (3). BPPV is further categorized based on the involved semicircular canal, with posterior canal BPPV (PC-BPPV) being the most prevalent, accounting for 80% of cases (4).

Diagnosis relies predominantly on patient history and positional tests, such as the Dix-Hallpike test for PC-BPPV and the supine roll test for horizontal canal BPPV (HC-BPPV) (5). Treatment primarily revolves around repositioning maneuvers, aiming to relocate otoconia from the affected semicircular canal back to the utricle through a series of head movements (6). The widely adopted Epley maneuver, introduced by John Epley in 1992 (6, 7), has demonstrated efficacy and safety for PC-BPPV, with success rates ranging from 63.65 to 98% after one or more attempts (8).

Despite its success, some patients exhibit poor response or canal switching, converting PC-BPPV to HC-BPPV during or after the maneuver (9). Factors contributing to these challenges remain not fully elucidated, potentially involving anatomical variations, membranous canal stenosis, otolith adhesion, otolith re-entry, incorrect diagnosis, or inadequate repositioning techniques (10). Consequently, modifications to the Epley maneuver have been proposed to enhance efficacy and reduce adverse effects, including head shaking, prolonged postural holding, or hastened head movements (11). However, these modifications may introduce limitations such as increased complexity, discomfort, or an elevated risk of canal switching (12).

This study introduces a novel modification to the Epley maneuver for PC-BPPV, incorporating a BPPV virtual simulation model. Our modification involves extending the retention time in the healthy lateral position and the final low head position, facilitating the passage of otoliths through the posterior arm of the posterior semicircular canals, especially through obstructed regions. We hypothesize that our modified Epley maneuver can enhance the single repositioning success rate for PC-BPPV compared to the traditional Epley maneuver. To test this hypothesis, we conducted a randomized controlled trial involving 65 patients with unilateral PC-BPPV, comparing repositioning outcomes between the modified and control groups. Additionally, we utilized a BPPV virtual simulation model to analyze the mechanism underlying our modified Epley maneuver. The aim of this study is to provide a promising treatment option for PC-BPPV, especially for refractory PC-BPPV.

2 Materials and methods

2.1 Sample size calculation and endpoints

The sample size calculation centered on the primary endpoint—the first repositioning success rate, defined as the absence of vertigo and nystagmus after a single attempt of the repositioning maneuver. Assuming a baseline first repositioning success rate of 70% for the traditional Epley maneuver, we anticipated a 20% increase with the modified Epley maneuver. With a significance level of 0.05 and a

power of 0.8, the calculated sample size was 28 patients in each group. To account for potential dropouts (estimated at 10%), the sample size was increased to 32 patients per group. Secondary endpoints included the number of repositioning attempts for successful reduction, canal switching rate, repositioning time, and patient tolerance.

2.2 Ethical considerations

Approval for the study was obtained from the ethical committee of Wenzhou People's Hospital (KY-2022-080). The study adhered to the principles of good clinical practice (ICH-GCP), the Declaration of Helsinki, and national laws and regulations regarding clinical studies. Written informed consent was obtained from eligible patients, or in cases of incapacity, approval was sought from a legally acceptable representative (see Table 1).

2.3 Subjects

Patients diagnosed with unilateral posterior semicircular canal BPPV at Wenzhou People's Hospital from January 2022 to October 2022 were included. Inclusion criteria comprised patients aged 20 to 80 years exhibiting vertigo episodes lasting no more than 60 s triggered by a change in head direction relative to gravity. Diagnosis was confirmed through the Dix-Hallpike maneuver, with delayed torsional upbeat nystagmus lasting no more than 60 s. No nystagmus induced by the supine roll test or torsional nystagmus evoked by the supine roll test and cannot be attributed to other diseases (13).

Exclusion criteria encompassed an inability to complete physical therapy due to language comprehension or compliance issues, involvement of horizontal or multiple semicircular canals, and the presence of severe cervical spondylosis, cardiac arrhythmia, heart failure, movement disorders, or upper gastrointestinal bleeding, history suggestive of alternate peripheral or central vestibular disorders including vestibular neuritis, Ménière's disease, migrainous vertigo, etc., torsional upbeat nystagmus lasting >60 s provoked by the Dix-Hallpike maneuver suggestive of cupulolithiasis (13). A computer-generated randomization sequence divided the 65 eligible patients into the Control and Experimental groups, ensuring no statistically significant baseline imbalances between the two groups ($p > 0.05$) as confirmed by a balance test utilizing standardized mean difference (SMD) (14, 15).

2.4 Equipment

The G-Force swivel chair system (Figure 1) has a high accuracy and stability for nystagmus detection and recording, with spatial and temporal resolution of 640*480@60 Hz (16). The system we have developed also generates a BPPV virtual simulation model based on the patient's nystagmus data and repositioning maneuver parameters, which can be used to visually analyze the movement of the otolith in the semicircular canal (17).

2.5 Repositioning maneuver

Figure 2 illustrates the structure of the semicircular. Figure 3 illustrates the operational flow of the Epley maneuver and modified

TABLE 1 Comparison of baseline information of the 2 groups of patients.

Characteristic	Control group	Experimental group	$\chi^2/t/Z$	P
Male/Cases (%)	10(31)	9(27)	0.124	0.724
Age/Years	51.59 ± 14.74	7.09 ± 14.3	1.254	0.932
History of vestibular disease/Cases(%)	8(25)	14(42)	2.203	0.138
Disease duration/d	20.69 ± 64.0	6.27 ± 8.0	1.769	0.077
Right posterior semicircular canal/Cases(%)	16(50)	20(61)	0.740	0.390
Left posterior semicircular canal/Cases(%)	16(50)	13(39)	0.740	0.390
Combined Hypertension/Cases(%)	10(31)	8(24)	0.398	0.528
Combine Diabetes/Cases(%)	3(9)	3(9)	0	1
The duration of the latency time/Seconds	0.875 ± 2.091	0.909 ± 2.777	0.056	0.478
Time of nystagmus/Seconds	16.375 ± 8.354	15.485 ± 7.041	0.465	0.322



FIGURE 1
The G-Force swivel chair system.

Epley maneuver. The Control group underwent the traditional Epley maneuver (Figure 3), while the experimental group received the novel modified Epley maneuver (Figure 3). The operations are as follows:

Right Epley repositioning maneuver. (A) The patient was in an upright position (B) The patient's head was allowed to turn 45° to the right side (C) The patient was allowed to lie down quickly, supine, with head tilted back 30° and the position was maintained for 1 min. (D1) Turn the head 90° to the left side, keeping the head tilted back and maintained for 1 min. (D2) Turn the head 90 to the left side, keeping the head flat or tilted back, and maintained for 1 min. (E1) Return to the sitting position and lowered the head 30° and held it for 5 min.

Novel modified right Epley repositioning maneuver. (A) The patient was in an upright position. (B) The patient's head was allowed

to turn 45° to the right side. (C) The patient was allowed to lie down quickly, supine, with head tilted back 30° and the position was maintained for 1 min. (D3) Turn the head 135° to the left side with the healthy side lying down and maintained for 5 min. (E2) Return to the sitting position and lowered the head 60° and held it for 5 min.

2.6 Observed indicators

The Dix-Hallpike maneuver, performed 5 min after the first repositioning, evaluated the repositioning effect. Patients without vertigo and nystagmus were considered cured. If vertigo and nystagmus persisted or transformed into other BPPV types, the repositioning was deemed ineffective. Each group underwent a maximum of 3 repositioning attempts, with evaluation after 5 min each time. The observed indicators included the success rate of the repositioning maneuvers (1st, 2nd, and 3rd) and the incidence of canal switching.

2.7 BPPV virtual simulation model

A BPPV virtual simulation model was employed to visualize and analyze otolith movement during traditional and modified Epley maneuvers (17). Developed using Unity 3D software (version 2020.3) and the NVIDIA physics engine, the model simulated head movements and postural changes based on maneuver parameters (17). Real patient nystagmus data from the G-Force swivel chair system were used for calibration and validation, generating realistic and dynamic images of otolith movement in the semicircular canal under varying head positions (16, 18, 19).

2.8 Statistical analysis

Data analysis utilized SPSS 22.0 software, with measurement data expressed as $x \pm s$. The t-test compared the age of the two groups, while the Mann-Whitney U test compared disease duration due to non-normal distribution. χ^2 was employed for comparing patient history of vestibular disease, gender, underlying disease, laterality of the involved semicircular canal, and repositioning effect, with a significance level set at $\alpha = 0.05$.

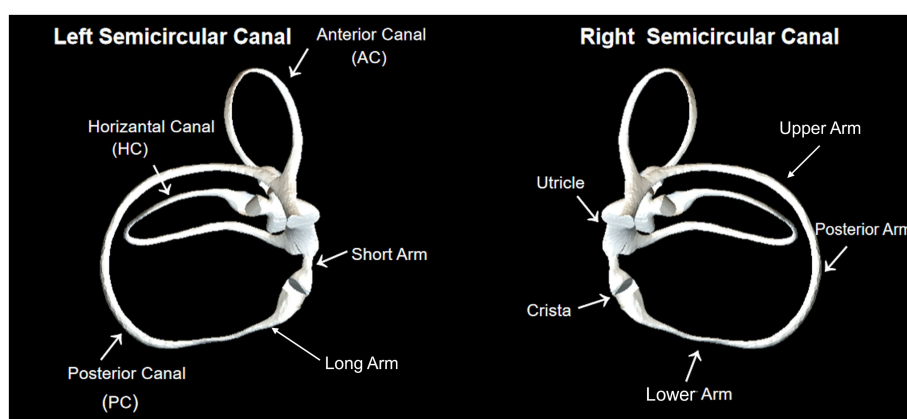


FIGURE 2

The structure of the semicircular canal shows the anterior, horizontal, and posterior canals. By using the crista as a boundary, the semicircular canal is divided into short and long arms. Besides, the long arm is divided into lower, posterior and upper parts.

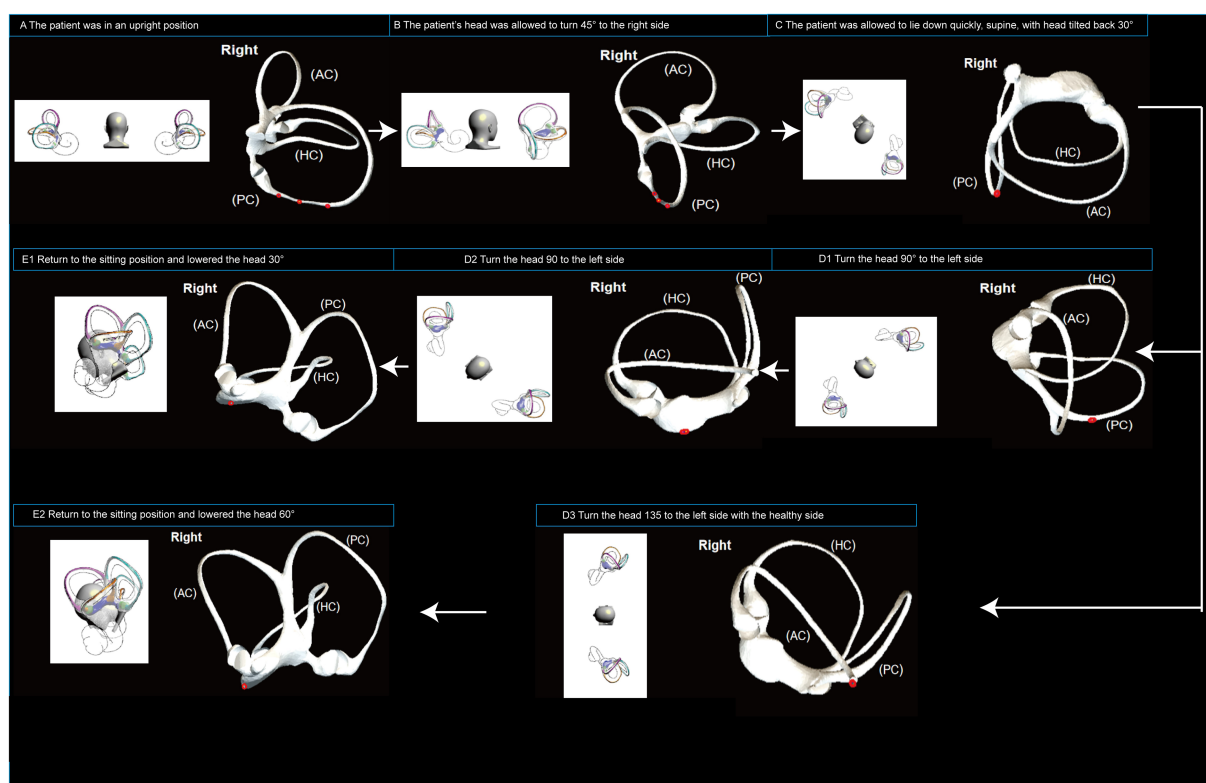


FIGURE 3

Operational flowchart of the right Epley maneuver and the modified right Epley maneuver. The left side shows the schematic diagram of the head position and the right side shows the corresponding virtual simulation model of the right semicircular canal. Red dots represent otoliths. AC: anterior semicircular canal; HC: horizontal semicircular canal; PC: posterior semicircular canal.

3 Results

3.1 Repositioning outcomes

In the Control group, the traditional Epley maneuver successfully repositioned 32 cases. Among these, 20 cases were successfully repositioned on the first attempt, accounting for 63%.

Additionally, 6 cases were successfully repositioned on the second attempt (19%), and 2 cases required three attempts for successful repositioning (6%). Unfortunately, 4 cases in the Control group were converted into horizontal semicircular canals, constituting 13% of the cases.

In the experimental group, the modified Epley maneuver successfully repositioned 33 cases. Of these, 28 cases were

TABLE 2 Comparison of the repositioning effect of the 2 groups of patients.

Group	n	Number of first successful repositions/ Cases(%)	Number of second successful repositions / Cases(%)	Number of third successful repositions/ Cases(%)	Total number of failed repositions/ Cases (%)	Total number of successful repositions/ Cases (%)
Control group	32	20(63)	6(19)	2(6)	4(13)	28(86)
Experimental group	33	28(85)	5(15)	0(0)	0(0)	33(100)
χ^2		4.201	0	0	0	2.498
<i>p</i>		0.040	1	1	1	0.114

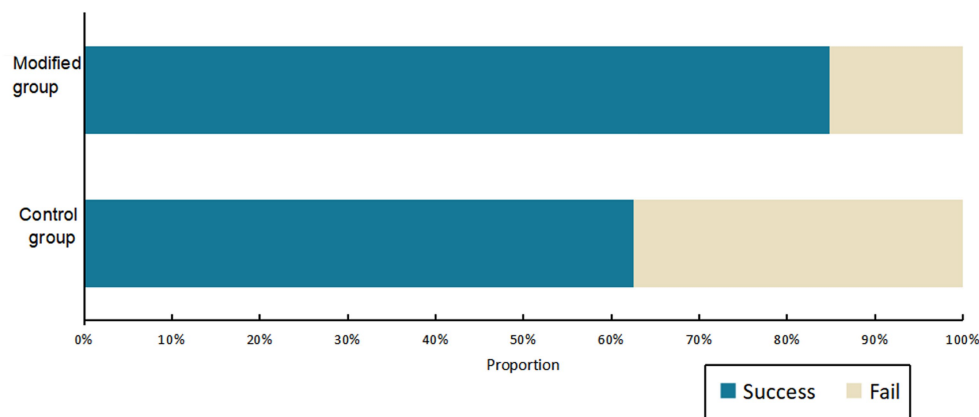


FIGURE 4

The success rate of first repositioning. The success rate was significantly higher in the experimental group than in the Control group. (χ^2 test: $p < 0.05$).

successfully repositioned on the first attempt, constituting 85%. Moreover, 5 cases were successfully repositioned on the second attempt (15%) (see Table 2). The first repositioning success rate in the experimental group was significantly different from that of the Control group, with the experimental group showing superior performance ($\chi^2 = 4.201$, $p = 0.040$) (see Figure 4). Importantly, in the experimental group, resulting in a 100% success rate after two repositioning attempts, while in the Control group, two cases required triple repositioning maneuvers for success. Furthermore, no canal switching occurred in the experimental group. Despite these variations, there was no significant difference in the total repositioning success rate between the two groups ($\chi^2 = 2.498$, $p = 0.114$).

3.2 BPPV virtual simulation model

The BPPV simulation model illustrated that during the head-down position of the Epley maneuver, the otoliths in the posterior semicircular canal entered the utricle via the common duct (see Figure 5). In the supine position, the otoliths in the posterior semicircular canal were prone to deposition in the posterior arm (see Figure 6).

Upon direct transfer of the patient to the healthy side lateral position after the supine position, the simulation model demonstrated that the otolith in the obstructed position moved away from the ampulla. Subsequently, under the influence of gravity, the otolith left

the posterior semicircular canal and entered the common crus. This position was found to be more conducive for the otolith to slide into the common duct (see Figure 7). Drawing on clinical experience, extending the retention time in the lateral position of the healthy side to 5 min was deemed sufficient for the otolith to effectively enter the common duct.

4 Discussion

The Epley maneuver, a widely utilized repositioning technique for posterior canal benign paroxysmal positional vertigo (PC-BPPV), may encounter challenges such as ineffectiveness or canal switching.

In this study, we introduce a novel modified Epley maneuver and analyze its mechanism using the BPPV virtual simulation model.

This modification involved prolonging the time in the healthy side lying position and the final bowing position. Our findings indicate that the modified Epley maneuver significantly enhanced the single repositioning success rate and reduced the incidence of canal switching in PC-BPPV when compared to the traditional Epley maneuver.

Several factors contribute to the failure or complication of the Epley maneuver for PC-BPPV (10), including anatomical variations, membranous canal stenosis, otolith adhesion, otolith re-entry, incorrect diagnosis, and inadequate repositioning technique (2, 20–23).

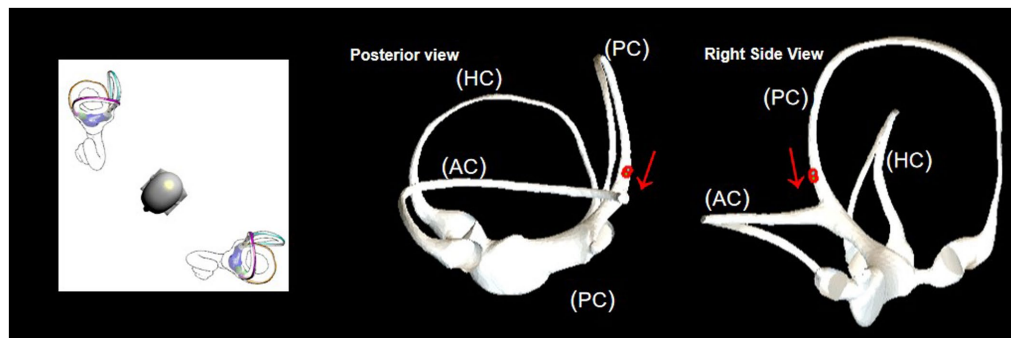


FIGURE 5

In the head-downward position of the Epley maneuver, the otoliths in the posterior semicircular canal enter the utricle through the common duct. The red arrow represents the direction of otolith advancement.

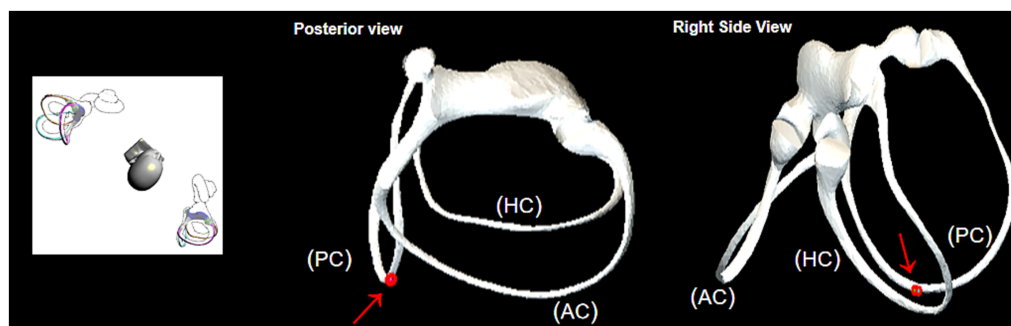


FIGURE 6

Position of otolith deposition in the supine position. The red arrow indicates where the otolith is obstructed.

- 1) Anatomical variations of the affected semicircular canal, such as semicircular canal fistula or fracture, which may prevent the complete discharge of otoliths or debris in the expected direction during the head movements (20).
- 2) Membranous canal stenosis, which may occur when the otoliths or debris partially adhere to the membranous semicircular canal, especially the common crus, causing a narrowing of the lumen and impeding the expulsion of the remaining otoliths or debris (21).
- 3) Otolith adhesion, which may occur when the otoliths or debris adhere to the cupula or ampulla of the affected semicircular canal, making them resistant to gravity and head movements (22).
- 4) Otolith re-entry, which may occur when the otoliths or debris that have entered the utricle fall off again and re-enter the semicircular canal, either the same one or a different one, causing recurrent or converted BPPV (23).
- 5) Incorrect diagnosis, which may occur when the affected side or canal is misidentified, leading to inappropriate repositioning maneuvers or false negative results (2).
- 6) Inadequate repositioning technique, which may occur when the head movements are not performed with sufficient speed, angle, or duration, or when the postural holding time is too short, leading to incomplete relocation of otoliths or debris (2).

Notably, some patients exhibited no significant movement of otoliths or debris during the head-down position of the Epley maneuver, suggesting an obstruction in the posterior arm of the posterior semicircular canal. This obstruction hindered otolith movement into the utricle, leading to vertigo upon returning to the sitting position. To validate this observation, we utilized a BPPV virtual simulation model, demonstrating that extending the time in the healthy side lying position facilitated otolith movement through the posterior arm, preventing their return to the ampulla and subsequent vertigo.

The model illustrated an obstruction in the posterior arm during the head-down position, impeding otolith passage through the common crus (Figure 5). Transitioning to the healthy side lying position facilitated otolith movement away from the ampulla, aiding their entry into the common crus (Figure 7). Extending the postural holding time in this position enhanced otolith passage through the posterior semicircular canals, particularly past the site of obstruction, preventing their dislodgment.

In a randomized controlled trial involving 65 unilateral PC-BPPV patients, our modified Epley maneuver demonstrated a significant improvement in the single repositioning success rate (85%) compared to the traditional Epley maneuver (63%). Additionally, the canal switching rate was reduced to 0% in the experimental group compared to 13% in the control group, indicating the efficacy and safety of our modification.

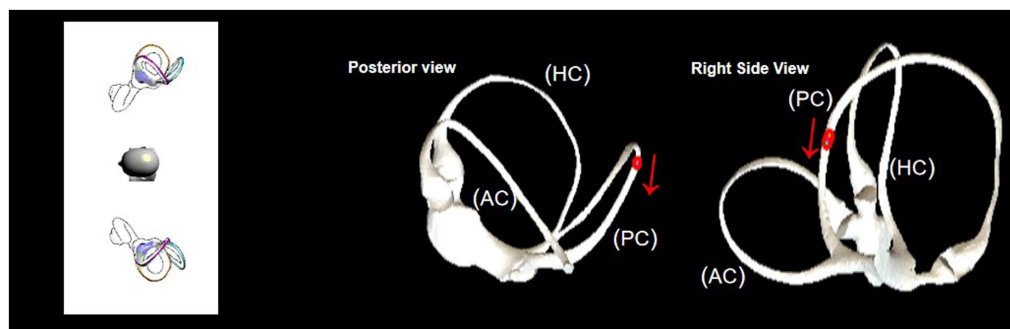


FIGURE 7

Observation of otolith passage through the obstructed position in the healthy side lying position. The red arrow represents the direction of otolith advancement.

Comparisons with other modified Epley maneuvers from existing studies reveal varying success rates. The Semont maneuver achieved success rates of 72–84% and 92–93% after one and two maneuvers, respectively (24, 25). The Modified Epley Maneuver achieved success rates of 76.2–83% and 92–95.2% after one and two maneuvers (25, 26). A shorter variant of Epley's treatment is the so-called Quick Liberatory Rotation, based on the same principles and technique as Gans maneuver (27), achieved success rates of 81 and 96% after one and two maneuvers, respectively (27, 28).

Our modified Epley maneuver demonstrated a one-maneuver success rate of 85% and a two-maneuver success rate of 100%, suggesting its efficacy in achieving superior treatment outcomes.

In summary, our modified Epley maneuver effectively addresses challenges associated with PC-BPPV by overcoming obstructions in the posterior arm, resulting in more efficient and safer otolith relocation to the utricle. While various modifications of the Epley maneuver have shown improvements, our modification significantly reduces the need for repeated maneuvers, potentially enhancing treatment adherence in BPPV patients.

Despite these promising findings, our study has limitations, including a relatively small sample size that may impact the generalizability of results. Additionally, our study did not encompass patients with bilateral or multiple canal involvement, necessitating further investigation to assess the applicability and efficacy of our modified Epley maneuver for these cases.

5 Conclusion

The utilization of the BPPV virtual simulation model emerges as a valuable tool for both studying and refining repositioning maneuvers in benign paroxysmal positional vertigo (BPPV). In particular, the modified Epley maneuver, applicable to patients with posterior semicircular canal BPPV, even those with semicircular canal obstruction, extends the duration of the healthy side lying position. This extension proves beneficial in facilitating the expulsion of otoliths. Our study contributes a novel treatment approach for patients with posterior canal BPPV, particularly those with refractory cases, offering a promising therapeutic option.

Data availability statement

The original contributions presented in the study are included in the article/supplementary material, further inquiries can be directed to the corresponding author.

Author contributions

XC: Conceptualization, Formal analysis, Funding acquisition, Investigation, Methodology, Project administration, Resources, Software, Visualization, Writing – original draft. JM: Conceptualization, Formal analysis, Investigation, Methodology, Resources, Software, Writing – original draft. HY: Data curation, Formal analysis, Investigation, Software, Visualization, Writing – original draft. LP: Data curation, Formal analysis, Investigation, Software, Visualization, Writing – original draft. QT: Data curation, Methodology, Resources, Software, Visualization, Writing – original draft. HZ: Formal analysis, Investigation, Methodology, Software, Visualization, Writing – original draft. CW: Supervision, Validation, Writing – review & editing. XY: Conceptualization, Funding acquisition, Project administration, Resources, Software, Supervision, Validation, Visualization, Writing – review & editing.

Funding

The author(s) declare financial support was received for the research, authorship, and/or publication of this article. This work was financially supported by the Wenzhou Science and Technology Bureau [Y20220823].

Conflict of interest

The authors declare that the research was conducted in the absence of any commercial or financial relationships that could be construed as a potential conflict of interest.

Publisher's note

All claims expressed in this article are solely those of the authors and do not necessarily represent those of their affiliated

organizations, or those of the publisher, the editors and the reviewers. Any product that may be evaluated in this article, or claim that may be made by its manufacturer, is not guaranteed or endorsed by the publisher.

References

1. von Brevern M, Radtke A, Lezius F, Feldmann M, Ziese T, Lempert T, et al. Epidemiology of benign paroxysmal positional vertigo: a population based study. *J Neurol Neurosurg Psychiatry*. (2007) 78:710–5. doi: 10.1136/jnnp.2006.100420
2. Bhattacharyya N, Gubbels SP, Schwartz SR, Edlow JA, El-Kashlan H, Fife T, et al. Clinical practice guideline: benign paroxysmal positional vertigo (update). *Otolaryngol Head Neck Surg*. (2017) 156:S1–S47. doi: 10.1177/0194599816689660
3. Kim JS, Zee DS. Clinical practice. Benign paroxysmal positional vertigo. *N Engl J Med*. (2014) 370:1138–47. doi: 10.1056/NEJMcp1309481
4. Prokopakis EP, Chimona T, Tsagournisakis M, Christodoulou P, Hirsch BE, Lachanas VA, et al. Benign paroxysmal positional vertigo: 10-year experience in treating 592 patients with canalith repositioning procedure. *Laryngoscope*. (2005) 115:1667–71. doi: 10.1097/01.mlg.0000175062.36144.b9
5. Fife TD, Iverson DJ, Lempert T, Furman JM, Baloh RW, Tusa RJ, et al. Practice parameter: therapies for benign paroxysmal positional vertigo (an evidence-based review): report of the quality standards Subcommittee of the American Academy of neurology. *Neurology*. (2008) 70:2067–74. doi: 10.1212/01.wnl.0000313378.77444.ac
6. Epley JM. The canalith repositioning procedure: for treatment of benign paroxysmal positional vertigo. *Otolaryngol Head Neck Surg*. (1992) 107:399–404. doi: 10.1177/019459989210700310
7. Hilton MP, Pinder DK. The Epley (canalith repositioning) manoeuvre for benign paroxysmal positional vertigo. *Cochrane Database Syst Rev*. (2014):CD003162. doi: 10.1002/14651858.CD003162.pub3
8. AlMohiza MA. Effects of Epley procedure on BPPV patients: a systematic review of randomized controlled trials. *European Review for Medical & Pharmacological Sciences*. (2023) 27:7409–15. doi: 10.26355/eurrev_202308_33392
9. Lin GC, Basura GJ, Wong HT, Heidenreich KD. Canal switch after canalith repositioning procedure for benign paroxysmal positional vertigo: case report and literature review. *Acta Otolaryngol Suppl*. (2010) 563:28–31. doi: 10.1002/lary.23315
10. Kim JS, Oh SY, Lee SH, Kang JH, Kim DU, Jeong SH, et al. Randomized clinical trial for apogeotropic horizontal canal benign paroxysmal positional vertigo. *Neurology*. (2012) 78:159–66. doi: 10.1212/WNL.0b013e31823fcd26
11. Li JC, Li CJ, Epley J, Weinberg L. Cost-effective management of benign positional vertigo using canalith repositioning. *Otolaryngol Head Neck Surg*. (2000) 122:334–9. doi: 10.1007/mhn.2000.100752
12. Anagnostou, E, Stamboulis, E, and Kararizou, E. Canal conversion after repositioning procedures: comparison of Semont and Epley maneuver. *J. Neurol*. (2014) 261: 866–869. doi: 10.1007/s00415-014-7290-2
13. von Brevern M, Bertholon P, Brandt T, Fife T, Imai T, Nuti D, et al. Benign paroxysmal positional vertigo: diagnostic criteria. *J Vestib Res*. (2015) 25:105–17. doi: 10.3233/VES-150553
14. Pauwels, S, Casters, L, Lemkens, N, Lemmens, W, Meijer, K, Meyns, P, et al. Gait and Falls in Benign Paroxysmal Positional Vertigo: A Systematic Review and Meta-analysis. *J Neurol Phys Ther*. (2023) 47:127–138. doi: 10.1097/NPT.0000000000000438
15. Li, W, Sun, J, Zhao, Z, Xu, J, Wang, H, Ding, R, et al. Efficacy of Epley's maneuver plus betahistine in the management of PC-BPPV: a systematic review and meta-analysis. *Medicine*. (2023) 10:e33421. doi: 10.1097/MD.00000000000033421
16. Wang, W, Yan, S, Zhang, S, Han, R, Li, D, Liu, Y, et al. Clinical Application of Different Vertical Position Tests for Posterior Canal-Benign Paroxysmal Positional Vertigo-Cupulolithiasis. *Front. Neurol*. (2022) 13:930542. doi: 10.3389/fneur.2022.930542
17. Wu, S, Li, J, Zhou, M, and Yang, X. Simulation study of canal switching in BPPV. *Front. Neurol*. (2022) 13:944703. doi: 10.3389/fneur.2022.944703
18. Liu, R, Zheng, J, Dong, H, iang, D, He, G, Wen, Y, et al. Analysis of reduction effect of the evoked nystagmus in the non-affect side during Dix-Hallpike or Roll-test in unilateral posterior semicircular canal benign paroxysmal positional vertigo[J]. *Lin Chuang er bi yan hou tou jing wai ke za zhi*. (2020) 34: 1027–1029. doi: 10.13201/j.issn.2096-7993.2020.11.016
19. Li Y, Yang X. Design and analysis of HSC-BPPV diagnostic maneuver based on virtual simulation. *Front Neurol*. (2023) 14:1132343. doi: 10.3389/fneur.2023.1132343
20. Pace-Balzan A, Rutka JA. Non-ampullary plugging of the posterior semicircular canal for benign paroxysmal positional vertigo. *The Journal of Laryngology & Otolaryngology*. (1991) 105:901–6. doi: 10.1017/S0022215100117785
21. Yetiser S. A new variant of Posterior Canal benign paroxysmal positional vertigo: a Nonampullary or common crus Canalolithiasis. *Case reports in otolaryngology*. (2015) 2015:816081:1–4. doi: 10.1155/2015/816081
22. Schratzenstaller B, Wagner-Manslau C, Alexiou C, Arnold W. High-resolution three-dimensional magnetic resonance imaging of the vestibular labyrinth in patients with atypical and intractable benign positional vertigo. *Orl*. (2001) 63:165–77. doi: 10.1159/000055734
23. Dispenza F, De Stefano A, Costantino C, et al. Canal switch and re-entry phenomenon in benign paroxysmal positional vertigo: difference between immediate and delayed occurrence. *Acta Otorhinolaryngol Ital*. (2015) 35:116–20.
24. Semont, A, Freyss, G, and Vitte, E. Curing the BPPV with a liberatory maneuver. *Adv Otorhinolaryngol*. (1988) 42:290–3. doi: 10.1159/000416126
25. Califano L, Capparuccia PGG, Di Maria D, Melillo MG, Villari D. Treatment of benign paroxysmal positional vertigo of posterior semicircular canal by "quick Liberatory rotation manoeuvre". *Acta Otorhinolaryngol Ital*. (2003) 23:161–7.
26. Parnes LS, Price-Jones RG. Particle repositioning maneuver for benign paroxysmal positional vertigo. *Annals of Otolaryngology & Laryngology*. (1993) 102:325–31. doi: 10.1177/000348949310200501
27. Califano L. "Comparison between Epley and Gans repositioning Maneuvers for Posterior Canal BPPV: a randomized controlled trial": is really "Gans" repositioning Maneuver the original one? *Ann Indian Acad Neurol*. (2023) 26:565. doi: 10.4103/aian.aian_407_23
28. Roberts RA, Gans RE, Montaudo RL. Efficacy of a new treatment maneuver for posterior canal benign paroxysmal positional vertigo. *J Am Acad Audiol*. (2006) 17:598–604. doi: 10.3766/jaaa.17.8.6



OPEN ACCESS

EDITED BY

Hubertus Axer,
Jena University Hospital, Germany

REVIEWED BY

Kemar E. Green,
Johns Hopkins Medicine, United States
Ana Isabel Cisneros-Gimeno,
University of Zaragoza, Spain

*CORRESPONDENCE

Wei Wang
✉ wwei1106@hotmail.com
Taisheng Chen
✉ fch_cts@sina.com

RECEIVED 15 October 2023

ACCEPTED 12 December 2023

PUBLISHED 04 January 2024

CITATION

Huang X, Zhang X, Deng Q, Li S, Liu Q,
Wen C, Wang W and Chen T (2024) Three-
dimensional characteristics of nystagmus
induced by low frequency in semicircular
canals of healthy young people.
Front. Neurosci. 17:1321906.
doi: 10.3389/fnins.2023.1321906

COPYRIGHT

© 2024 Huang, Zhang, Deng, Li, Liu, Wen,
Wang and Chen. This is an open-access
article distributed under the terms of the
[Creative Commons Attribution License
\(CC BY\)](https://creativecommons.org/licenses/by/4.0/). The use, distribution or reproduction
in other forums is permitted, provided the
original author(s) and the copyright owner(s)
are credited and that the original publication
in this journal is cited, in accordance with
accepted academic practice. No use,
distribution or reproduction is permitted
which does not comply with these terms.

Three-dimensional characteristics of nystagmus induced by low frequency in semicircular canals of healthy young people

Xiaobang Huang^{1,2,3,4,5}, Xueqing Zhang^{1,2,3,4,5},
Qiaomei Deng^{1,2,3,4,5}, Shanshan Li^{1,2,3,4,5}, Qiang Liu^{1,2,3,4,5},
Chao Wen^{1,2,3,4,5}, Wei Wang^{1,2,3,4,5*} and Taisheng Chen^{1,2,3,4,5*}

¹Department of Otorhinolaryngology Head and Neck Surgery, Tianjin First Central Hospital, Tianjin, China, ²Institute of Otolaryngology of Tianjin, Tianjin, China, ³Key Laboratory of Auditory Speech and Balance Medicine, Tianjin, China, ⁴Key Medical Discipline of Tianjin (Otolaryngology), Tianjin, China, ⁵Quality Control Centre of Otolaryngology, Tianjin, China

Objective: The study aimed to analyze the three-dimensional characteristics of nystagmus induced by different semicircular canal combinations in healthy young people, and to determine the reference range of nystagmus slow phase velocity (SPV) and its asymmetry.

Materials and methods: Fifty-two healthy volunteers (26 males and 26 females, aged 17–42 years, average 23.52 ± 6.59), were recruited to perform the manual triaxial rotation testing with a 3D-Videonystagmography (3D-VNG) device (VertiGoggles (ZT-VNG-II), Shanghai ZEHNIT Medical Technology Co., Ltd., Shanghai, China) using a 0.3 Hz prompt beat and a 90° amplitude, respectively. The induced nystagmus around the Z-, X-, and Y-axes were recorded in the yaw, pitch, and roll planes. The directions and slow phase velocities of the horizontal, vertical, and torsional components of the induced nystagmus under different semicircular canal combinations (the left lateral and right lateral semicircular canal combination, bilateral anterior semicircular canals, bilateral posterior semicircular canals combination, and the anterior and posterior semicircular canals combination of each ear), as well as their asymmetry, were taken as the observation indexes to analyze the characteristics of the nystagmus vectors of different combinations.

Results: Fifty-two healthy volunteers had no spontaneous nystagmus. The characteristic nystagmus was induced by the same head movement direction in all three axial rotation tests. The SPVs of the left and right nystagmus were $44.45 \pm 15.75^\circ/\text{s}$ and $43.79 \pm 5.42^\circ/\text{s}$, respectively, when the subjects' heads were turned left or right around the Z-axis (yaw). The SPVs of vertically upward and downward nystagmus were $31.67 \pm 9.46^\circ/\text{s}$ and $30.01 \pm 9.20^\circ/\text{s}$, respectively, when the subjects' heads were pitched around the X-axis (pitch). The SPVs of torsional nystagmus, with the upper poles of the eyes twisting slowly to the right and left ears (from the participant's perspective), were $28.99 \pm 9.20^\circ/\text{s}$ and $28.35 \pm 8.17^\circ/\text{s}$, respectively, when the subjects' heads were turned left or right around the Y-axis (roll). There was no significant difference in the SPVs of nystagmus induced by the same rotation axis in two opposite directions ($p > 0.05$). The reference ranges for the slow phase velocities (SPVs) of nystagmus induced by the triaxial

rotation testing were as follows: For the Z-axis (yaw), the SPVs were 13.58–75.32°/s for leftward head rotation and 13.56–74.02°/s for rightward head rotation. For the X-axis (pitch), the SPVs were 13.13–50.21°/s for upward head nystagmus and 11.98–48.04°/s for downward head nystagmus. For the Y-axis (roll), the SPVs were 10.97–47.02°/s for the left-sided head rotation and 12.34–44.35°/s for the right-sided head rotation.

Conclusion: This study clarified the three-dimensional characteristics of nystagmus induced by different semicircular canal combinations in healthy young people. It also established a preliminary reference range of SPVs and SPV asymmetry of nystagmus induced by the vertical semicircular canal. It can further provide a basis for the mechanism of semicircular canal-induced nystagmus and the traceability of nystagmus in patients with otogenic vertigo. It is shown that the portable 3D-VNG eye mask can be used for the manual triaxial rotation testing to achieve the evaluation of the low-frequency angular vestibulo-ocular reflex (aVOR) function of the vertical semicircular canal, which is convenient, efficient, and practical.

KEYWORDS

nystagmus, vertical semicircular canal, rotation test, 3D-VNG, SPV, nystagmus direction

1 Introduction

Peripheral vestibular spontaneous and induced nystagmus serve as objective signs of asymmetric input from the same plane semicircular canals or different semicircular canal combinations between the two ears. These are crucial for the diagnosis, treatment, rehabilitation, and evaluation of otogenic vertigo. It can be horizontal, horizontally torsional, or vertically torsional (von Brevern et al., 2015; Strupp et al., 2022). The characteristics of peripheral vestibular nystagmus abide by Ewald's law, but this law is limited to a single semicircular canal effect in animals. Previous studies have also shown that the characteristics of nystagmus in BPPV-Canalolithiasis represent the manifestation of Ewald's law in a single semicircular canal effect (single canal mode) (Zhang et al., 2021). If two or more semicircular canals or different combinations of semicircular canals get impaired, their detailed nystagmus characteristics (Eggers et al., 2019) are rarely reported. The evaluation of semicircular canal function is a major aspect of the evaluation of vestibular function in patients with vertigo and balance disorders. At present, there are many clinical evaluation methods for the lateral semicircular canal, including the caloric test (0.003 Hz), head shaking test (2 Hz), rotation test (SHAT, 0.01–3 Hz), active rotation test VAT (2–6 Hz), passive rotation test, the video head impulse test (vHIT), (2–5 Hz), etc., involving low-frequency, medium-frequency, and high-frequency functional area detection, with a wide frequency coverage. However, there are few evaluation techniques for the vertical semicircular canal. In 1963, Robinson proposed the magnetic sclera search coil system (Eibenberger et al., 2016), which quickly became the recognized standard for accurately recording eye movement. In 1964, Suzuki et al. (1964) conducted animal experiments, surgically implanting electrodes to stimulate the ampullary nerve of the vertical semicircular canal, and observed the eye movement of four different animals with photographic records. In 1988, Halmagyi and Curthoys (1988) introduced this technology to evaluate the function of the lateral semicircular canal. It was subsequently adopted to evaluate the function

of the vertical semicircular canals, thereby evolving into a reliable method for recording the three-dimensional eye movement. In 1996, Fetter and Dichgans (1996) studied the three-dimensional characteristics of spontaneous nystagmus and nystagmus induced by rotation of the semicircular canal in different planes, as well as the dynamic characteristics of the lateral, anterior, and posterior semicircular canals (vestibulo-ocular reflex, VOR) in patients with “vestibular neuritis” by using the magnetic sclera search coil technology. They also conducted vector analysis. Despite its effectiveness, the invasive and costly nature of this technology limited its widespread use from 1988 to 2008 (Halmagyi et al., 2017). In 1988, Halmagyi and Curthoys first reported the HIT technology (Halmagyi and Curthoys, 1988; Curthoys et al., 2023). In 2009, MacDougall (MacDougall et al., 2009) further developed this into a noninvasive variant (vHIT) to detect the lateral semicircular canal abnormalities. By 2013, vHIT could objectively and quantitatively detect high-frequency (2–5 Hz) aVOR injury of the six semicircular canals (MacDougall et al., 2013). Since then, detecting the vertical semicircular canal mainly relies on vHIT and VAT, both of which focus on the high-frequency functional area. In 2001, Iida (Iida et al., 2001) proposed a stimulation method for the vertical semicircular canal by using the head position of 60° backward and 45° left/right inclination. However, this method is only suitable for mechanism exploration, rather than clinical application due to its limited practicality. In the same year, Young (Young et al., 2001) used 3D-VNG (Ulmer, France Synapsys) to conduct the three-dimensional analysis of post-caloric nystagmus in different postures. In 2003, Morita (Morita et al., 2003) explored a method for detecting the vertical semicircular canal abnormalities using different head positions during the traditional low-frequency swivel chair rotation around the vertical axis. However, due to the need for a large swivel chair or invasive technology, as well as the age limitation and difficulty in controlling the head position, the method was deemed impractical. Recently, 3D-VNG has attracted broad attention (Liu et al., 2022). However, it is limited to the three-dimensional nystagmus record and analysis in the caloric test,

positional test, and the evaluation of low–medium frequency of aVOR function of the lateral semicircular canal during the rotation tests. In the early stage, our research center initially applied 3D-VNG to analyze the characteristics and mechanism of nystagmus in benign paroxysmal positional vertigo (BPPV) (Liu et al., 2022). This analysis proved that BPPV was the embodiment of Ewald's law in humans, and can be used as a nystagmus model for the single semicircular canal under single-factor stimulation (Zhang et al., 2021). However, otogenic vertigo diseases usually involve two or more semicircular canals. Therefore, a more comprehensive and effective method is necessary for multi-frequency evaluation of the semicircular canal system. In this study, a portable 3D-VNG eye mask was used to investigate the feasibility of low-frequency aVOR-induced nystagmus in the vertical semicircular canal. The aim was to record and analyze the directions and slow phase velocity (SPV) characteristics of horizontal, vertical, and torsional components of low-frequency aVOR-induced nystagmus of each semicircular canal and different semicircular canal combinations under different axial stimuli via the 3D-VNG, to provide a basis for the mechanism of semicircular canal induced nystagmus and tracing nystagmus in patients with otogenic vertigo. It can also provide a more convenient, efficient, and practical approach for low-frequency measurement technology of all semicircular canals.

2 Materials and methods

2.1 Participants

From July to September 2023, 52 healthy young volunteers were recruited to record the three-dimensional nystagmus using 3D-Videonystagmography (3D-VNG) in the Department of Otorhinolaryngology, Tianjin Institute of Otorhinolaryngology, and Tianjin Key Laboratory of Auditory Speech and Balance Medicine in Tianjin First Central Hospital. All participants provided informed consent before being included in the study. This study has been approved by the Ethics Committee of Tianjin First Central Hospital.

2.2 Methods

There were 52 healthy volunteers (26 males and 26 females, aged 17–42 years, average 23.52 ± 6.59). They all declared no medical history of tinnitus, deafness, dizziness, vertigo, or equilibrium disorders. None of the participants exhibited any cochlear, vestibular, or ophthalmic symptoms or clinical signs, including covert or overt strabismus. Using a 3D-VNG meter (VertiGoggles (ZT-VNG-II), Shanghai ZEHNT Medical Technology Co., Ltd., Shanghai, China), the same physician performed the manual triaxial rotation testing on volunteers, who were seated upright in the examination chair and wore a 3D-VNG eye mask with two high-resolution and high-frequency cameras recording their binocular movements, respectively. After calibration, the spontaneous nystagmus was recorded first. Thereafter, the triaxial passive rotation test was performed with a prompt beat sound of 0.3 Hz and a total amplitude of 90° rotation (referring to the following study procedure below) (Figure 1). The eye-tracking windows and the eye-tracking curves were used to detect nystagmus, including its direction. Employing different semicircular canal combinations, the characteristics of nystagmus vectors were

analyzed by observing the directions, SPVs, and asymmetry of different horizontal, vertical, and torsional components of nystagmus.

2.3 Study procedure

The head was turned left and right in the yaw plane around the vertical axis (Z) to stimulate the left and right lateral semicircular canals, respectively (Figure 1, Row A). The head was pitched around the interauricular axis (X) along the pitch plane to stimulate the combination of the anterior semicircular canals of both ears and the combination of the posterior semicircular canals of both ears (double-canal mode), respectively (Figure 1, Row B). The head was tilted to the left and right in the roll plane around the anterior and posterior axis, namely the nasal occipital axis (Y), and the anterior and posterior semicircular canal combination of each ear was stimulated (double-canal mode), respectively (Figure 1, Row C). Then, the induced nystagmus of the passive rotation around the Z, X, and Y axes were recorded.

The asymmetry of induced nystagmus SPV was calculated based on the formulae:

- 1 SPV asymmetry in horizontal nystagmus induced by the left and right lateral semicircular canals:
 - $| (L_{\text{left}} - L_{\text{right}}) / (L_{\text{left}} + L_{\text{right}}) | * 100\%$
 - $= | (SPV_{\text{YawL}} - SPV_{\text{YawR}}) / (SPV_{\text{YawL}} + SPV_{\text{YawR}}) | * 100\%$
- 2 SPV asymmetry in vertical nystagmus induced by bilateral anterior semicircular and bilateral posterior semicircular canals combination:
 - $| [(A_{\text{left}} + A_{\text{right}}) - (P_{\text{left}} + P_{\text{right}})] / [A_{\text{left}} + A_{\text{right}} + P_{\text{left}} + P_{\text{right}}] | * 100\%$
 - $= | (SPV_{\text{PitchA}} - SPV_{\text{PitchP}}) / (SPV_{\text{PitchA}} + SPV_{\text{PitchP}}) | * 100\%$
- 3 SPV asymmetry in torsional nystagmus induced by bilateral anterior and posterior semicircular canals combination:
 - $| [(A_{\text{left}} + P_{\text{left}}) - (A_{\text{right}} + P_{\text{right}})] / [A_{\text{left}} + P_{\text{left}} + A_{\text{right}} + P_{\text{right}}] | * 100\%$
 - $= | [(SPV_{\text{RollL}} - SPV_{\text{RollR}})] / [SPV_{\text{RollL}} + SPV_{\text{RollR}}] | * 100\%$

2.4 Analysis

IBM SPSS Statistics 21 (IBM SPSS, Turkey) was used for statistical analyses. The quantitative data were presented as mean \pm SD values and plotted using GraphPad Prism version 10 (GraphPad, San Diego, CA, United States). A p value < 0.05 was considered statistically significant. The two-sided reference range was ± 1.96 SD and the single-sided reference range was ± 1.65 SD.

3 Results

3.1 Demographic characteristics

A total of 52 healthy young volunteers were enrolled, including 26 males and 26 females, aged 17–42 years (average 23.52 ± 6.59). The age range of males was 17–42 years (average 22.12 ± 6.61), while that for the females was 18–37 years (average 24.92 ± 6.39). No significant difference in age was observed between groups ($p > 0.05$).

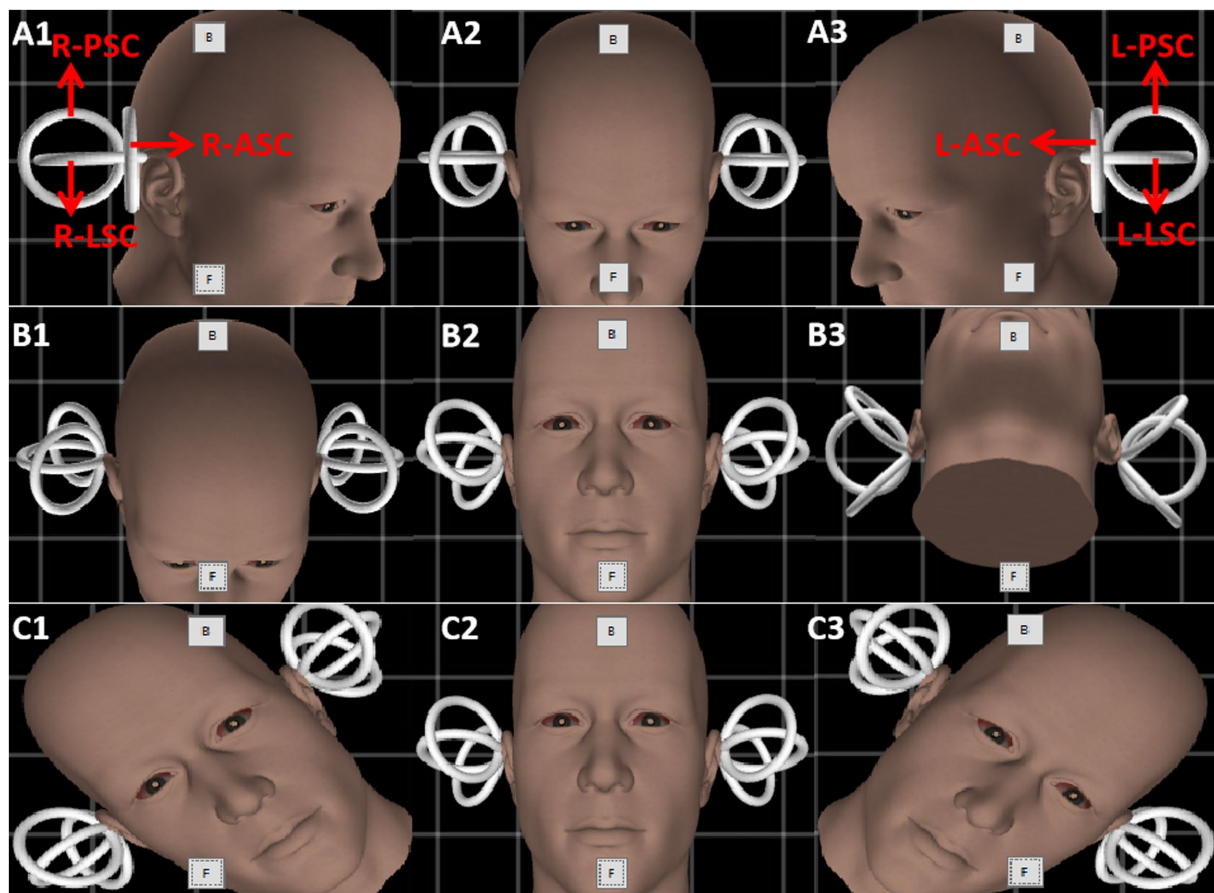


FIGURE 1

The schematic diagram of the triaxial rotation testing. Gray boxes named “B” and “F” are the buttons to calibrate the gyroscope in every picture. Row (A–C) indicate the rotation protocol of three planes (yaw, pitch, and roll). The amplitude of rotation in each direction is 45 degrees. Red arrows depict the six semicircular canals of both inner ears. L-PSC, left-posterior semicircular canal; R-PSC, right-posterior semicircular canal; L-LSC, left-lateral semicircular canal; R-LSC, right-lateral semicircular canal; L-ASC, left-anterior semicircular canal; R-ASC, right-anterior semicircular canal.

3.2 Characteristics of nystagmus induced by triaxial rotation testing

None of the 52 healthy young volunteers exhibited spontaneous nystagmus (Figure 2). The direction of nystagmus induced by triaxial rotation test mirrored the direction of head movement. The SPVs of left-to-right horizontal nystagmus induced by the left and right turning of the head around the Z-axis (yaw) were $44.45 \pm 15.75^\circ/\text{s}$ and $43.79 \pm 15.42^\circ/\text{s}$, respectively, with no vertical or torsional components observed. The SPVs of vertical downward-to-upward nystagmus induced by turning the head in the same direction around the X-axis (pitch) were $30.01 \pm 9.20^\circ/\text{s}$ and $31.67 \pm 9.46^\circ/\text{s}$, respectively, without obvious horizontal or torsional components. The left and right biases around the Y axis (roll) induced the upper pole of the eye to twist fast toward the subject's left ear, with the nystagmus SPV recorded as $28.99 \pm 9.20^\circ/\text{s}$, while the SPV for the upper pole of the eye twisting fast to the subject's right ear was $28.35 \pm 8.17^\circ/\text{s}$, accompanied by a slight horizontal component and no obvious vertical component. The average SPVs of the two-directional nystagmus induced by rotation around the Z-axis (yaw), X-axis (pitch), and Y-axis (roll) were $44.12 \pm 15.51^\circ/\text{s}$, $30.84 \pm 9.32^\circ/\text{s}$, and $28.67 \pm 8.66^\circ/\text{s}$, respectively. A significant difference was observed in the average SPVs of the

nystagmus induced by rotation around the Z-axis (yaw) compared with those induced by rotation around the X-axis (pitch) and Y-axis (roll) ($p < 0.001$) (Figure 3A). Among them, the SPV of the three-directional nystagmus induced by rotation around the Z-axis (yaw) was the largest, with the ratio of $\text{SPV}_{\text{Yaw}} : \text{SPV}_{\text{Pitch}}$ and $\text{SPV}_{\text{Yaw}} : \text{SPV}_{\text{Roll}}$ of about 3:2, while that of $\text{SPV}_{\text{Pitch}} : \text{SPV}_{\text{Roll}}$ of about 1:1 (Figure 3B). No significant difference was found in the SPVs of nystagmus induced in different genders and between the aforementioned groups ($p > 0.05$). Similarly, there was no significant difference in the SPVs of the two-directional nystagmus induced by rotating around the same axis ($p > 0.05$).

The reference ranges for SPVs of nystagmus induced by the triaxial rotation testing were as follows:

- For the left-directional rotation around the Z-axis (yaw): (13.58–75.32) $^\circ/\text{s}$.
- For the right-directional rotation around the Z-axis (yaw): (13.57–74.02) $^\circ/\text{s}$.
- For the up-directional rotation around the X-axis (pitch): (13.13–50.21) $^\circ/\text{s}$.
- For the down-directional rotation around the X-axis (pitch): (11.98–48.04) $^\circ/\text{s}$.

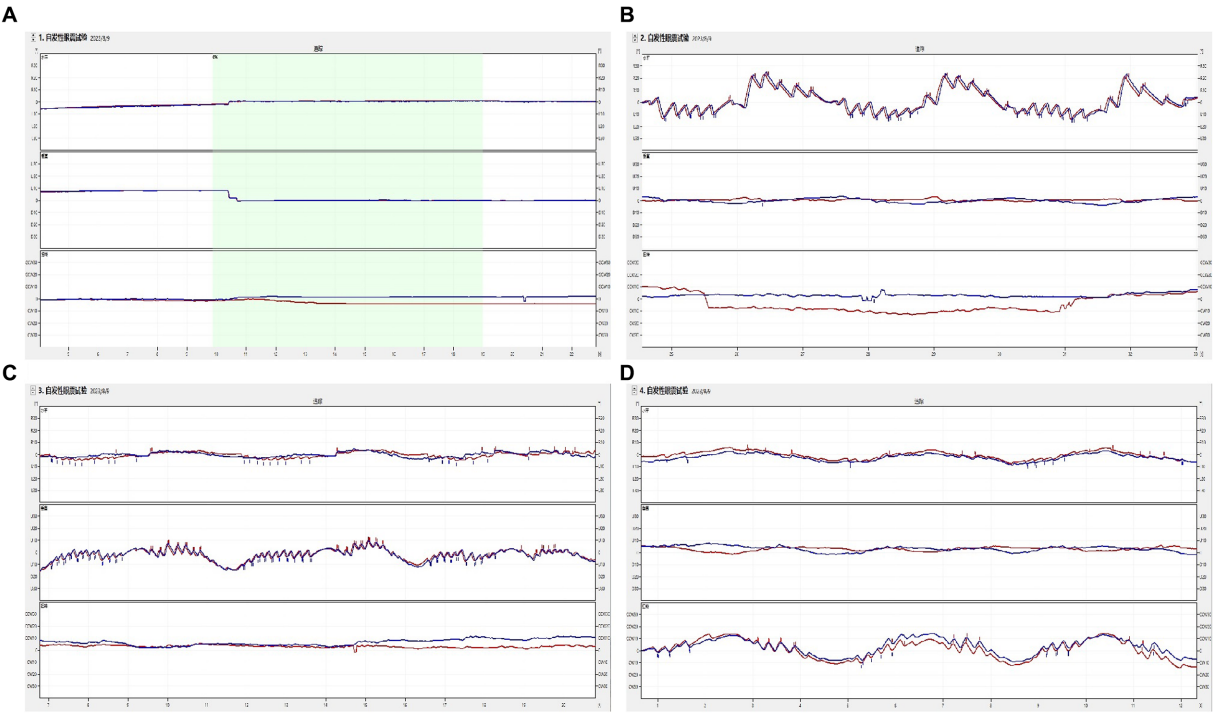


FIGURE 2
The induced nystagmus by the triaxial rotation testing. The movements of two eyes are displayed from top to bottom in the order of horizontal, vertical, and torsional components, with red lines for the right eye and blue for the left eye. The upward direction of each trace indicates the right, up, and upper pole of the eye beating slowly toward the left ear from the subject's perspective. **(A)** spontaneous nystagmus. The spontaneous nystagmus (SN) of a participant was negative and remained negative after fixation. **(B)** The head was turned left and right in the yaw plane around the vertical axis (Z). When the physician rotated the subject's head left to right back and forth at the yaw plane, horizontally left and right nystagmus appeared. **(C)** The head was pitched around the interauricular axis (X) along the pitch plane. When the physician rotated the subject's head up and down back and forth at the pitch plane, vertically up and down nystagmus appeared. **(D)** The head was rolled to the left and right side around the nasal occipital axis (Y) at the roll plane. When the physician rotated the subject's head left to right back and forth at the roll plane, torsional (upper pole of the eye beating toward the right/left ear from the subject's perspective) nystagmus appeared.

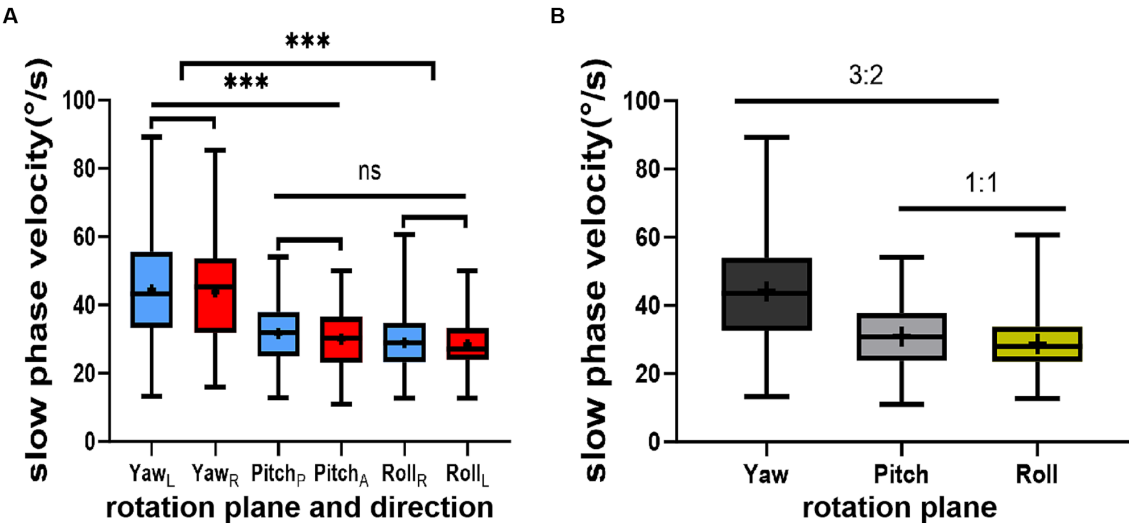


FIGURE 3
This figure illustrates the results of the triaxial rotation tests. **(A)** depicts the relationship among the slow phase velocities (SPVs) of nystagmus induced by these tests. **(B)** presents the ratios of SPVs of nystagmus induced by the same tests. The direction of nystagmus is indicated as left/right, upward/downward, or Right/Left (the upper pole of the eye beating toward the right/left ear (from the participant's perspective)). The red color represents positive-direction nystagmus or right semicircular canals, while blue signifies negative-direction nystagmus or left semicircular canals. The horizontal (black), vertical (gray), and torsional (yellow) components of nystagmus are also depicted. Statistical significance is denoted as follows: "***" for $p < 0.001$ and "ns" for not significant.

TABLE 1 The direction and SPV of induced nystagmus in 52 subjects.

Rotation plane	Yaw		Pitch		Roll	
Direction	Left	Right	Upward	Downward	Right	Left
Sex (M:F)	1:1	1:1	1:1	1:1	1:1	1:1
M* SPV (°/s)	42.81 ± 13.63	43.31 ± 12.28	31.78 ± 8.27	30.72 ± 7.53	28.11 ± 6.80	27.80 ± 7.41
F* SPV (°/s)	46.08 ± 17.73	44.27 ± 18.27	31.56 ± 10.68	29.30 ± 10.72	29.87 ± 11.17	28.89 ± 8.97
Both SPV (°/s)	44.45 ± 15.75	43.79 ± 15.42	31.67 ± 9.46	30.01 ± 9.20	28.99 ± 9.20	28.35 ± 8.17
RV _{SPV} (°/s)	(13.58, 75.32)	(13.57, 74.02)	(13.13, 50.21)	(11.98, 48.04)	(10.97, 47.02)	(12.34, 44.35)
SPV (°/s)	44.12 ± 15.51		30.84 ± 9.32		28.67 ± 8.66	
RV _{SPV} (°/s)	(13.72–74.52)		(12.57–49.11)		(11.7–45.64)	

Both, male and female; M, male; F, female; * $p > 0.05$; left/right, upward/downward, right/left (upper pole of the eye beating toward the right/left ear (from the participant's perspective), the direction of nystagmus; SPV, slow phase velocity; RV, reference value of slow phase velocity.

TABLE 2 The induced nystagmus SPV asymmetry of multiaxial rotation test and its reference value in 52 subjects.

Rotation plane	Yaw	Pitch	Roll	P – value
SPV asymmetry (%)	11.8 ± 9.1	15.1 ± 13.0	10.8 ± 7.8	0.140**
RV _{SPV Asymmetry} (%)	(0, 26.8)	(0, 36.6)	(0, 23.7)	/

** $p > 0.05$; SPV, slow phase velocity; RV_{SPV Asymmetry}, reference value of slow phase velocity asymmetry; '/', no value.

- For the left-directional rotation around the Y-axis (roll): (10.97–47.02) °/s.
- For the right-directional rotation around the Y-axis (roll): (12.34–44.35) °/s.

The reference ranges of SPVs of horizontal nystagmus induced by rotation around the Z-axis (yaw), vertical nystagmus induced by rotation around the X-axis (pitch), and rotational nystagmus induced by rotation around the Y-axis (roll) were 13.72–74.52°/s, 12.57–49.11°/s and 11.7–45.64°/s, respectively (Table 1).

3.3 The asymmetry of induced nystagmus SPVs and its reference range by triaxial rotation testing

SPV asymmetry for the nystagmus induced by the triaxial rotation testing was 11.8 ± 9.1% for yaw, 15.1 ± 13.0% for pitch, and 10.8 ± 7.8% for roll, respectively (Table 2).

4 Discussion

4.1 Three-dimensional characteristics and clinical significance of the low-frequency induced nystagmus of each semicircular canal in healthy young people

The detection of vertical semicircular canal function has posed a significant challenge in clinical vestibular medicine. The traditional sine harmonic acceleration (SHA) around the vertical axis is limited to detecting the aVOR function in the low-frequency region of the lateral semicircular canal. Although vHIT can detect all six semicircular canals, it only detects the aVOR function in the high-frequency region of each semicircular canal (Liu et al., 2023; Ramaioli

et al., 2023). Despite many studies (Baloh et al., 1986; Iida et al., 2001; Young et al., 2001) have explored methods to detect the low-frequency region of the vertical semicircular canal, their clinical applicability remains limited due to the high cost, invasiveness, age restrictions, and difficulties of head position control.

In this study, a 3D-VNG eye mask was used to perform the manual triaxial rotation testing focusing on the vertical semicircular canal. The results showed no statistical significance when comparing SPVs of nystagmus induced by two opposite directions of the same rotation. This suggests that this portable manual triaxial rotation testing could consistently stimulate nystagmus to the same extent in two opposite directions of the same rotation axis, with equivalent nystagmus SPVs. This aligns with the characteristics of vestibular function examination, where equal physiological stimulation can induce an equal effect, which can provide a reliable reference for future studies on the mechanism and location of damage in the different vertical semicircular canals at low frequencies. This study also showed that the type of nystagmus is contingent on the plane of head movement: the horizontal nystagmus was primarily observed with left and right head turns in the yaw plane, the vertical nystagmus with head tilts in the pitch plane, and the torsional nystagmus (accompanied with a slight horizontal component) mainly with left and right head turns in the roll plane. The SPVs of induced nystagmus in the yaw plane were the largest, followed by the pitch plane, while the roll plane was the smallest. The SPV ratio for yaw plane to pitch plane-induced nystagmus was approximately 3:2, while that for pitch plane to roll plane-induced nystagmus was approximately 1:1. The reasons for the mild horizontal component of nystagmus induced by the left and right head deviation in the roll plane and the unequal SPV in the three planes may be due to off-axis stimulation of the vertical semicircular canal. This aligns with reports by Benson et al. (1989) and Allred and Clark (2023) suggesting a higher perception threshold for the vertical semicircular canal than that for the lateral semicircular canal. In 1979 and 2023, it was reported that when the rotation axis is not parallel to the gravitational acceleration vector, the effect of the

velocity storage mechanism diminishes or disappears (Raphan et al., 1979; Allred and Clark, 2023). This characteristic was also observed in this study. In 1988, Lafortune et al. (1988) studied the effect of otoliths organ-mediated activity induced by triaxial active head position changes coupled with human horizontal velocity storage on optokinetic afternystagmus (OKAN) in 16 subjects. They found that OKAN was inhibited along the pitch or roll plane but enhanced along the yaw plane, suggesting a potential correlation.

In 2003, Morita (Morita et al., 2003) stimulated the vertical semicircular canal by tilting the head back 60° and rotating it 45° from the sagittal plane to either side. The findings revealed that the vertical semicircular canal function was less affected by the velocity storage mechanism than the lateral semicircular canal function. These results are consistent with previous research (Liu et al., 2022), and the relationship between nystagmus SPVs (3:2 and 1:1) is consistent with the physiological characteristics of the semicircular canals. In addition, this study established the reference ranges for SPVs induced by the triaxial rotation testing: the SPV reference ranges for the left and right horizontal nystagmus induced by the left and right rotation around the Z-axis (yaw) were 13.58–75.32°/s and 13.56–74.02°/s, respectively. The SPV reference ranges of the vertical upward and downward nystagmus induced by head elevation and head bowing around the X-axis (pitch) were 13.13–50.21°/s and 11.98–48.04°/s, respectively. For the left/right rotation induced by head tilt around the Y-axis (roll) (from the subject's perspective), the reference range for normal nystagmus SPV was 10.97–47.02°/s and 12.34–44.35°/s, respectively. The mean values of SPV asymmetry induced by the triaxial rotation around the Z-axis (yaw), X-axis (pitch), and Y-axis (roll) were 11.8 ± 9.1%, 15.1 ± 13.0%, and 10.8 ± 7.8%, respectively, with no statistical significance ($p = 0.140$). The reference ranges of one side were 0, 26.8%, 0, 36.6%, and 0, 23.7%, respectively. The above normal reference ranges can provide a reliable reference for quantitative analysis of the low-frequency damage of different vertical semicircular canals. The asymmetric reference range for SPV of induced nystagmus by the pitch plane rotation is larger than those of nystagmus induced in the yaw and roll planes, which may be related to the effect of receiving the same stimulation in the anterior and posterior semicircular canals. Aw et al. (1998) stimulated the three semicircular canals by caloric tests and found that the induced nystagmus of the lateral semicircular canal was the strongest, and the SPV for the induced nystagmus of the anterior and posterior semicircular canal was 30% and 10%, respectively. The difference between this report and our study results may be due to the different stimulation frequencies of the two methods or the simultaneous stimulation of the two anterior and two posterior semicircular canals in this study.

Modern diagnosis and treatment of vertigo put forward higher requirements for the recording of eye movements. To align with the evolution of big data and intelligence in vertigo diagnosis and treatment, a study (Kattah and Newman-Toker, 2022; Parker et al., 2022) on big data of vertigo telemedicine was conducted in the United States in recent years. However, it was unsuccessful due to the lack of a reliable eye movement recording system. This study, following the description method of nystagmus presented by the Barany Association in 2019 (Eggers et al., 2019), applied a portable 3D-VNG eye mask to carry out the low-frequency manual triaxial rotation testing on each semicircular canal and different semicircular canal combinations. We analyzed the SPV characteristics of induced

nystagmus and discussed the application of this method for detecting the lateral semicircular canal. We also evaluated the feasibility of the low-frequency aVOR-induced nystagmus in the vertical semicircular canal. The results of this study show that the manual triaxial rotation testing can be used to evaluate the function of the low-frequency aVOR of the semicircular canals. Specifically, the horizontal nystagmus, induced by rotation around the Z-axis (yaw), can distinguish the damaged side of the left and right lateral semicircular canals. Rotation around the X-axis (pitch) induces vertical nystagmus, which identifies the anterior and posterior semicircular canals. This, in combination with rotation around the Y-axis (roll), identifies the left and right vertical semicircular canals, thereby localizing damage to the vertical semicircular canal. The damage of any one of the vertical semicircular canals can be deduced from the SPV of nystagmus induced by the combinations of “double anterior + double posterior” semicircular canals and “anterior + posterior on each side” semicircular canals by rotating in the pitch plane and roll plane, respectively. For example, nystagmus induced by rotation along the pitch plane is characterized by a smaller SPV for the vertical downward nystagmus compared to that of the vertical upward nystagmus $[(LA + RA) < (LP + RP)]$. Nystagmus induced by rotation along the roll plane shows a smaller SPV for the right-rotatory nystagmus compared to that of the left-rotatory nystagmus $[(RA + RP) < (LA + LP)]$, suggesting damage to the right anterior (RA) semicircular canal, and vice versa. Similarly, the function of the right anterior/right posterior semicircular canal and the left anterior/left posterior semicircular canal can be evaluated separately based on the SPV characteristics of the nystagmus induced by rotation along the pitch and roll planes (referring to the formula below). The results of our study show the characteristics of nystagmus induced by different semicircular canal combinations, which can help to provide objective support for tracing the injury localization of one or two semicircular canals, especially vertical semicircular canals, and further provide objective quantified big data and machine learning algorithms of AI technology for otogenic disease in the future.

The damage of every one of the vertical semicircular canals can be deduced based on the formula:

$$\begin{aligned} 1 \quad RA^{\text{loss}} &\Rightarrow [(LA + RA^{\text{loss}}) < (LP + RP)] + [(RA^{\text{loss}} + RP) < (LA + LP)]; \\ 2 \quad LP^{\text{loss}} &\Rightarrow [(LA + RA) < (LP^{\text{loss}} + RP)] + [(RA + RP) < (LA + LP^{\text{loss}})]; \\ 3 \quad LA^{\text{loss}} &\Rightarrow [(LA^{\text{loss}} + RA) < (LP + RP)] + [(RA + RP) < (LA^{\text{loss}} + LP)]; \\ 4 \quad RP^{\text{loss}} &\Rightarrow [(LA + RA) < (LP + RP^{\text{loss}})] + [(RA + RP^{\text{loss}}) < (LA + LP)]. \end{aligned}$$

4.2 Mechanism analysis of the low-frequency induced nystagmus of each semicircular canal

The test results showed that turning the head around the Z-axis (yaw) stimulates the left and right lateral semicircular canals, inducing left and right horizontal nystagmus, respectively. Pitching the head around the X-axis (pitch) stimulates the combination of the anterior semicircular canals of both ears and the combination of the posterior semicircular canals of both ears (double-canal mode), inducing vertical downward and upward nystagmus. Rolling the head around the Y-axis (roll) to the left and the right stimulates the anterior and posterior semicircular canals (double-canal mode) of each ear,

respectively, inducing significant torsional nystagmus. Given that the lateral semicircular canal is at a physiological angle of 30° to the ground, the torsional nystagmus was accompanied by a mild horizontal nystagmus. The direction and SPV characteristics of nystagmus induced by the triaxial rotation testing were analyzed. The SPV induced by nystagmus in two opposite directions of the same rotation axis was not statistically significant. This suggests that this portable manual triaxial rotation testing can achieve consistent results, namely that an equal amount of induced nystagmus SPV is induced by an equal of stimulation in two opposite directions around the same rotation axis. The test exhibits the characteristic where an equal amount of physiological stimulation induces an equal amount of effect (Figure 2).

4.3 Mechanism analysis

4.3.1 When the head rotates to the left around the Z-axis (yaw), the bilateral lateral semicircular canal aligns with the plane of rotation. Consequently, the endolymph fluid in the left lateral (LL) semicircular canal flows to the ampullary crest, producing excitatory stimulation, while, in the right lateral (RL) semicircular canal, it flows away, producing inhibitory stimulation. This excites the left lateral (LL) semicircular canal, activating the left medial rectus (MR) and the right lateral rectus (LR), producing a combined effect to produce a slow-phase eye movement to the right (the fast phase of nystagmus in the opposite direction). Similarly, when the head rotates to the right around the Z-axis (yaw), the bilateral lateral semicircular canal aligns with the rotation plane. Thereafter, the endolymph fluid in the right lateral (RL) semicircular canal flows to the ampulla crest, producing excitatory stimulation, while, in the left lateral (LL) semicircular canal, it flows away, producing inhibitory stimulation. This excites the right lateral (RL) semicircular canal, activating the right medial rectus (MR) and left lateral rectus (LR), producing a combined effect that results in a slow phase movement of the eye to the left (opposite to the nystagmus fast phase).

4.3.2 When the head rotates downward around the X-axis (pitch), a combined equal excitation of both the left anterior (LA) and right anterior (RA) semicircular canals activates bilateral superior rectus (SR) and oblique muscles, causing purely upward slow phases as the torsional components from each canal cancel each other out (purely downward fast phases of nystagmus). Similarly, when the head rotates upward around the X-axis (pitch), a combined equal excitation of both the left posterior (LP) and right posterior (RP) semicircular canals activates bilateral inferior rectus (IR) and oblique muscles, causing purely downward slow phases as the torsional components from each canal cancel each other out (purely upward fast phases of nystagmus). Clinically, bilateral anterior or posterior injuries are rare, but this study induced pure vertical upward or downward nystagmus through the combination of bilateral anterior and bilateral posterior semicircular canals in healthy individuals, further suggesting that pure vertical nystagmus is often caused by damage to the vestibular center.

4.3.3 When the head deflects to the left around the Y-axis (roll), the bilateral anterior and posterior (LA + LP + RA + RP) vertical semicircular canals enter the rotation plane, the endolymph fluid in the left anterior (LA) and posterior (LP) vertical semicircular canals flows away from the ampullary crest, producing a joint excitatory stimulus. The endolymph fluid in the right anterior (RA) and posterior

(RP) vertical semicircular canal flows toward the ampullary crest, producing a combined inhibitory stimulus. This excites the left anterior (LA) canal, activating the right inferior oblique (IO) (large), right superior rectus (SR), left superior oblique (SO), and left superior rectus (SR) (large). Excitation of the left posterior (LP) semicircular canal excitation activates the right inferior oblique muscle (IO), right inferior rectus (IR) (large), left superior oblique muscle (SO) (large), and left inferior rectus (IR). The vertical components of the left vertical semicircular canal up and down cancel each other out, resulting in a slow phase movement of the upper pole of the eye twisting to the right ear (from the subject's perspective). This produces nystagmus in which the upper pole of the eye twists to the left ear (from the subject's perspective) or purely clockwise nystagmus (from the physician's perspective). Similarly, when the head deflects to the right around the Y-axis (roll), both the bilateral anterior and posterior (LA + LP + RA + RP) vertical semicircular canals align with the rotation plane. The endolymph fluid in the right anterior (RA) and posterior (RP) vertical semicircular canal flows away from the ampullary crest, producing a joint excitatory stimulus. Conversely, in the left anterior (LA) and posterior (LP) vertical semicircular canal, the endolymph fluid flows toward the ampullary crest, producing a joint inhibitory stimulus. Excitation of the right anterior (RA) semicircular canal activates the left inferior oblique (IO) (large), left superior rectus (SR), right superior oblique (SO), and right superior rectus (SR) (large). Excitation of the right posterior (RP) semicircular canal activates the left inferior oblique (IO), left inferior rectus (IR) (large), right superior oblique (SO) (large), and right inferior rectus (IR). Thereafter, the vertical components of the right vertical semicircular canal up and down cancel each other out, resulting in a slow phase movement of the upper pole of the eye to the left ear (from the subject's perspective). This produces nystagmus in which the upper part of the eye moves to the right ear (from the subject's perspective) or pure counterclockwise nystagmus (from the physician's perspective).

4.4 Limitations and further research

This study's observations were limited to healthy young people; further research is needed to extend these findings to other age groups. Although rotation in the left anterior/right posterior semicircular canal conjugate plane is the most effective stimulation of the vertical canal, this study did not adopt this stimulation method due to the effect of pupillary exposure on the 3D nystagmus recording. Further research should focus on overcoming these limitations and improving the 3D recording of nystagmus in different head positions. Multi-frequency, multi-axial vertical semicircular canal induction test represents a promising direction for future research. Portable binocular 3D-VNG, which may be facilitated in bedside examination or as an in-home vestibular event monitor to capture intermittent events for later analysis (Young et al., 2019), makes it possible for telemedicine and AI diagnosis based on bid data in the future.

5 Conclusion

In summary, the manual triaxial rotation testing, facilitated by a portable 3D-VNG eye mask, effectively induces the characteristic

nystagmus, and enables the evaluation of the vertical semicircular canal's low-frequency aVOR function. This method is convenient, efficient, and practical. Moreover, it elucidates the three-dimensional characteristics of nystagmus induced by different semicircular canal combinations in healthy young people. The reference range for the SPV of the vertical semicircular canal-induced nystagmus and its asymmetric reference range in healthy young people were preliminarily obtained. These findings provide a basis for the traceability of nystagmus in patients with otogenic vertigo and pave the way for further research on the mechanism of semicircular canal-induced nystagmus, baseline evaluation of various otogenic vertigo diseases, precision diagnosis, and treatment rehabilitation as well as big data telemedicine.

Data availability statement

The original contributions presented in the study are included in the article/supplementary material, further inquiries can be directed to the corresponding author/s.

Ethics statement

The studies involving humans were approved by the Ethics Committee of Tianjin First Central Hospital, China. The studies were conducted in accordance with the local legislation and institutional requirements. Written informed consent for participation in this study was provided by the participants' legal guardians/next of kin.

Author contributions

XH: Formal analysis, Investigation, Methodology, Writing – original draft, Writing – review & editing, Software. XZ: Data curation,

Formal analysis, Writing – review & editing. QD: Investigation, Writing – review & editing. SL: Investigation, Writing – review & editing. QL: Investigation, Writing – review & editing. CW: Investigation, Writing – review & editing. WW: Conceptualization, Funding acquisition, Methodology, Project administration, Resources, Supervision, Writing – review & editing. TC: Conceptualization, Funding acquisition, Methodology, Project administration, Resources, Supervision, Writing – review & editing.

Funding

The author(s) declare financial support was received for the research, authorship, and/or publication of this article. This study was supported by the Tianjin Key Medical Discipline Construction Project (TJYXZDXK-046A), Tianjin Applied Basic Research Multiple Investment Fund Project (21JCQNJC01780), and Tianjin Health Research Project (TJWJ2022QN027 and TJSJMYXYC-D2-021).

Conflict of interest

The authors declare that the research was conducted in the absence of any commercial or financial relationships that could be construed as a potential conflict of interest.

Publisher's note

All claims expressed in this article are solely those of the authors and do not necessarily represent those of their affiliated organizations, or those of the publisher, the editors and the reviewers. Any product that may be evaluated in this article, or claim that may be made by its manufacturer, is not guaranteed or endorsed by the publisher.

References

- Allred, A. R., and Clark, T. K. (2023). Vestibular perceptual thresholds for rotation about the yaw, roll, and pitch axes. *Exp. Brain Res.* 241, 1101–1115. doi: 10.1007/s00221-06570-4
- Aw, S. T., Haslwanter, T., Fetter, M., Heimberger, J., and Todd, M. J. (1998). Contribution of the vertical semicircular canals to the caloric nystagmus. *Acta Otolaryngol.* 118, 618–627. doi: 10.1080/00016489850183089
- Baloh, R. W., Honrubia, V., Yee, R. D., and Jacobson, K. (1986). Vertical visual-vestibular interaction in normal human subjects. *Exp. Brain Res.* 64, 400–406. doi: 10.1007/BF00340476
- Benson, A. J., Hutt, E. C., and Brown, S. F. (1989). Thresholds for the perception of whole body angular movement about a vertical axis. *Aviat. Space Environ. Med.* 60, 205–213. PMID: 2712798.
- Curthoys, I. S., McGarvie, L. A., MacDougall, H. G., Burgess, A. M., Halmagyi, G. M., Rey-Martinez, J., et al. (2023). A review of the geometrical basis and the principles underlying the use and interpretation of the video head impulse test (vHIT) in clinical vestibular testing. *Front. Neurol.* 14:1147253. doi: 10.3389/fneur.2023.1147253
- Eggers, S. D. Z., Bisdorff, A., von Brevin, M., Zee, D. S., Kim, J. S., Perez-Fernandez, N., et al. (2019). Classification of vestibular signs and examination techniques: nystagmus and nystagmus-like movements. *J. Vestib. Res.* 29, 57–87. doi: 10.3233/VES-190658
- Eibenberger, K., Eibenberger, B., Roberts, D. C., Haslwanter, T., and Carey, J. P. (2016). A novel and inexpensive digital system for eye movement recordings using magnetic scleral search coils. *Med. Biol. Eng. Comput.* 54, 421–430. doi: 10.1007/s11517-015-1326-3
- Fetter, M., and Dichgans, J. (1996). Vestibular neuritis spares the inferior division of the vestibular nerve. *Brain* 119, 755–763. doi: 10.1093/brain/119.3.755
- Halmagyi, G. M., Chen, L., MacDougall, H. G., Weber, K. P., McGarvie, L. A., and Curthoys, I. S. (2017). The video head impulse test. *Front. Neurol.* 8:258. doi: 10.3389/fneur.2017.00258
- Halmagyi, G. M., and Curthoys, I. S. (1988). A clinical sign of canal paresis. *Arch. Neurol.* 45, 737–739. doi: 10.1001/archneur.1988.00520310043015
- Iida, M., Hitouji, K., and Takahashi, M. (2001). Vertical semicircular canal function: a study in patients with benign paroxysmal positional Vertigo. *Acta Otolaryngol. Suppl.* 545, 35–37. PMID: 11677738. doi: 10.1080/000164801750388072
- Kattah, J. C., and Newman-Toker, D. E. (2022). Video-Oculography to guide neuroimaging for dizziness and Vertigo. *JAMA Otolaryngol. Head Neck Surg.* 148, 474–475. doi: 10.1001/jamaoto.2022.0330
- Lafortune, S. H., Ireland, D. J., and Jell, R. M. (1988). Effect of active head movements about the pitch, roll, and yaw axes on human optokinetic afternystagmus. *Can. J. Physiol. Pharmacol.* 66, 689–696. doi: 10.1139/y88-110
- Liu, Y., Leng, Y., Zhou, R., Liu, J., Wang, H., Xia, K., et al. (2023). Discrepancies of video head impulse test results in patients with idiopathic sudden sensorineural hearing loss with vertigo and vestibular neuritis. *Front. Neurosci.* 17:1102512. doi: 10.3389/fnins.2023.1102512
- Liu, Y., Zhang, X., Deng, Q., Liu, Q., Wen, C., Wang, W., et al. (2022). The 3D characteristics of nystagmus in posterior semicircular canal benign paroxysmal positional vertigo. *Front. Neurosci.* 16:988733. doi: 10.3389/fnins.2022.988733
- MacDougall, H. G., McGarvie, L. A., Halmagyi, G. M., Curthoys, I. S., and Weber, K. P. (2013). The video head impulse test (vHIT) detects vertical semicircular canal dysfunction. *PLoS One* 8:e61488. doi: 10.1371/journal.pone.0061488

- MacDougall, H. G., Weber, K. P., McGarvie, L. A., Halmagyi, G. M., and Curthoys, I. S. (2009). The video head impulse test: diagnostic accuracy in peripheral vestibulopathy. *Neurology* 73, 1134–1141. doi: 10.1212/WNL.0b013e3181bacf85
- Morita, M., Imai, T., Kazunori, S., Takeda, N., Koizuka, I., Uno, A., et al. (2003). A new rotational test for vertical semicircular canal function. *Auris Nasus Larynx* 30, 233–237. doi: 10.1016/S0385-8146(03)00098-1
- Parker, T. M., Badihian, S., Hassoon, A., Saber Tehrani, A. S., Farrell, N., Newman-Toker, D. E., et al. (2022). Eye and head movement recordings using smartphones for telemedicine applications: measurements of accuracy and precision. *Front. Neurol.* 13:789581. doi: 10.3389/fneur.2022.789581
- Ramaioli, C., Steinmetzer, T., Brietzke, A., Meyer, P., Xuan, R. P., Schneider, E., et al. (2023). Assessment of vestibulo-ocular reflex and its adaptation during stop-and-go car rides in motion sickness susceptible passengers. *Exp. Brain Res.* 241, 1523–1531. doi: 10.1007/s00221-023-06619-4
- Raphan, T., Matsuo, V., and Cohen, B. (1979). Velocity storage in the vestibulo-ocular reflex arc (VOR). *Exp. Brain Res.* 35, 229–248. doi: 10.1007/BF00236613
- Strupp, M., Bisdorff, A., Furman, J., Hornibrook, J., Jahn, K., Maire, R., et al. (2022). Acute unilateral vestibulopathy/vestibular neuritis: diagnostic criteria. *J. Vestib. Res.* 32, 389–406. doi: 10.3233/VES-220201
- Suzuki, J. I., Cohen, B., and Bender, M. B. (1964). Compensatory eye movements induced by vertical Semicircular Canal stimulation. *Exp. Neurol.* 9, 137–160. doi: 10.1016/0014-4886(64)90013-5
- von Brevern, M., Bertholon, P., Brandt, T., Fife, T., Imai, T., Nuti, D., et al. (2015). Benign paroxysmal positional vertigo: diagnostic criteria. *J. Vestib. Res.* 25, 105–117. doi: 10.3233/VES-150553
- Young, Y. H., Chiang, C. W., and Wang, C. P. (2001). Three-dimensional analysis of post-caloric nystagmus caused by postural change. *Acta Otolaryngol. Suppl.* 121, 69–72. doi: 10.1080/000164801750388153
- Young, A. S., Lechner, C., Bradshaw, A. P., MacDougall, H. G., Black, D. A., Halmagyi, G. M., et al. (2019). Capturing acute vertigo: a vestibular event monitor. *Neurology* 92, e2743–e2753. doi: 10.1212/WNL.0000000000007644
- Zhang, X., Bai, Y., Chen, T., Wang, W., Han, X., Li, S., et al. (2021). A show of Ewald's law: I horizontal semicircular canal benign paroxysmal positional vertigo. *Front. Neurol.* 12:632489. doi: 10.3389/fneur.2021.632489



OPEN ACCESS

EDITED BY

Sulin Zhang,
Huazhong University of Science and
Technology, China

REVIEWED BY

Toshihisa Murofushi,
Teikyo University Mizonokuchi Hospital,
Japan
Leonardo Manzari,
MSA ENT Academy Center, Italy

*CORRESPONDENCE

F. Lucieer
✉ f.lucieer@gmail.com

RECEIVED 11 November 2023

ACCEPTED 31 January 2024

PUBLISHED 21 February 2024

CITATION

Lucieer F, van der Lubbe M, van Stiphout L,
Janssen M, Van Rompaey V, Devocht E,
Perez-Fornos A, Guinand N and van de
Berg R (2024) Multi-frequency VEMPs
improve detection of present otolith
responses in bilateral vestibulopathy.
Front. Neurol. 15:1336848.
doi: 10.3389/fneur.2024.1336848

COPYRIGHT

© 2024 Lucieer, van der Lubbe, van Stiphout,
Janssen, Van Rompaey, Devocht, Perez-
Fornos, Guinand and van de Berg. This is an
open-access article distributed under the
terms of the [Creative Commons Attribution
License \(CC BY\)](https://creativecommons.org/licenses/by/4.0/). The use, distribution or
reproduction in other forums is permitted,
provided the original author(s) and the
copyright owner(s) are credited and that the
original publication in this journal is cited, in
accordance with accepted academic
practice. No use, distribution or reproduction
is permitted which does not comply with
these terms.

Multi-frequency VEMPs improve detection of present otolith responses in bilateral vestibulopathy

F. Lucieer^{1*}, M. van der Lubbe¹, L. van Stiphout¹, M. Janssen²,
V. Van Rompaey³, E. Devocht¹, A. Perez-Fornos⁴, N. Guinand⁴
and R. van de Berg¹

¹Division of Balance Disorders, Department of Otorhinolaryngology, Head and Neck Surgery, Maastricht University Medical Centre, Maastricht, Netherlands, ²Department of Methodology and Statistics, Care and Public Health Research Institute, Maastricht University, Maastricht, Netherlands, ³Department of Otorhinolaryngology and Head and Neck Surgery, Antwerp University Hospital, Faculty of Medicine and Health Sciences, University of Antwerp, Antwerp, Belgium, ⁴Service of Otorhinolaryngology Head and Neck Surgery, Department of Clinical Neurosciences, Geneva University Hospitals, Geneva, Switzerland

Objective: To investigate whether multi-frequency Vestibular Evoked Myogenic Potential (VEMP) testing at 500, 750, 1,000, and 2,000 Hz, would improve the detection of present dynamic otolith responses in patients with bilateral vestibulopathy (BV).

Methods: Prospective study in a tertiary referral center. BV patients underwent multi-frequency VEMP testing. Cervical VEMPs and ocular VEMPs were recorded with the Neuro-Audio system (v2010, Neurosoft, Ivanovo, Russia). The stimuli included air-conducted tone bursts of 500, 750, 1,000, and 2,000 Hz, at a stimulation rate of 13 Hz. Outcome measures included the percentage of present and absent VEMP responses, and VEMP thresholds. Outcomes were compared between frequencies and type of VEMPs (cVEMPs, oVEMPs). VEMP outcomes obtained with the 500 Hz stimulus, were also compared to normative values obtained in healthy subjects.

Results: Forty-nine BV patients completed VEMP testing: 47 patients completed cVEMP testing and 48 patients completed oVEMP testing. Six to 15 % more present VEMP responses were obtained with multifrequency testing, compared to only testing at 500 Hz. The 2,000 Hz stimulus elicited significantly fewer present cVEMP responses (right and left ears) and oVEMP responses (right ears) compared to the other frequencies ($p \leq 0.044$). Using multi-frequency testing, 78% of BV patients demonstrated at least one present VEMP response in at least one ear. In 46% a present VEMP response was found bilaterally. BV patients demonstrated a significantly higher percentage of absent VEMP responses and significantly higher VEMP thresholds than healthy subjects, when corrected for age ($p \leq 0.002$). Based on these results, a pragmatic VEMP testing paradigm is proposed, taking into account multi-frequency VEMP testing.

Conclusion: Multi-frequency VEMP testing improves the detection rate of present otolith responses in BV patients. Therefore, multi-frequency VEMPs should be considered when evaluation of (residual) otolith function is indicated.

KEYWORDS

bilateral vestibulopathy (BV), vestibular evoked myogenic potential (VEMP), multi-frequency, vestibular, cVEMP, oVEMPs, otolith

Introduction

Bilateral vestibulopathy (BV) is a chronic disorder in which the vestibular function is bilaterally severely reduced or absent (1). It has many etiologies, varying from toxic (e.g., gentamicin ototoxicity), infectious (e.g., meningitis) and genetic (e.g., DFNA9), to inner ear disease (e.g., Menière's disease, auto-immune inner ear disease) and neurodegenerative disease (e.g., CANVAS) (2). BV patients report a spectrum of symptoms, of which chronic unsteadiness and/or oscillopsia are most frequently reported (3, 4). These symptoms often result in a decreased quality of life and a high socio-economic burden on society (4, 5). BV can be diagnosed using the diagnostic criteria of the Bárány Society. These criteria include a chronic vestibular syndrome with symptoms of unsteadiness when walking or standing (possibly combined with oscillopsia), and a bilaterally reduced or absent angular vestibulo-ocular reflex function. This latter should be documented by at least one of the following three tests: video Head Impulse Test, caloric test or rotatory chair test (6). Currently, only lateral semicircular canal function is included in the diagnostic criteria of BV, not otolith function. This implies that in patients diagnosed with BV, otolith function can still be present (7–9).

Vestibular evoked myogenic potentials (VEMPs) measure dynamic otolith function by stimulating the Type I hair cells at the striola (10, 11). VEMPs are electromyographic responses to air-conducted sound or bone-conducted vibration of the skull, which most likely reflect otolith function. Two types of VEMPs can be measured: cervical VEMPs (cVEMP) and ocular VEMPs (oVEMP). Cervical VEMPs comprise inhibitory responses from the ipsilateral sternocleidomastoid muscle, mainly evaluating function of the saccule. Ocular VEMPs comprise excitatory responses from the contralateral inferior oblique extra-ocular muscle, mainly evaluating function of the utricle. The testing paradigm and interpretation of VEMPs are difficult to standardize (12). Since VEMP response characteristics (amplitude, latency, threshold) depend on, e.g., stimulus type, muscle-contraction and age, each laboratory should obtain its own normative data. However, even after correcting for differences in muscle contraction, variability in VEMPs can be large in normal subjects (13).

In BV, VEMPs vary widely. BV can lead to reduced or absent VEMP responses, but in a significant number of patients VEMPs are within the normal range (7–9). The number of reduced, absent or present VEMPs in BV patients differs between studies. This most likely reflects the heterogeneity of testing paradigms, outcome measures and patient populations used in these studies (7). For example, some etiologies like aminoglycoside toxicity might be associated with otolith abnormalities (14). Moreover, it remains difficult to perfectly understand VEMPs in BV due to the large variability in normal subjects. After all, VEMPs might be reduced due to BV, but still be within the “broad” normal range, leading to false negative results (7). Additionally, age significantly affects VEMPs, resulting in a high rate of absent responses in normal subjects above the age of 60 years (12). Since the age of the BV population is relatively high (8), an absent VEMP response in a BV patient might reflect age, BV, testing paradigm, or a combination of these factors. In these patients, the influence of BV in the observed VEMP responses remains unknown. Furthermore, as stated above, otolith function is not included in the diagnostic criteria of BV. Patients with disorders predominantly affecting otolith function, might therefore be missed and not included in BV studies (7, 15, 16).

It was previously found that different acoustic stimulus frequencies, evoke different VEMP responses (17). For example, cVEMP responses in the affected ears of patients with Menière's disease, demonstrate a significantly higher cVEMP threshold at tone bursts of 500 Hz than at 1,000 Hz, compared to normal subjects (18, 19). This implies that “frequency tuning” exists in the vestibular system. This “frequency tuning” is also affected by age. In young normal adults, the largest VEMP responses are obtained around 500 Hz. In older adults (≥ 60 years), the largest VEMP responses are more often obtained at 750 and 1,000 Hz in the majority of cases. It was therefore recommended to test 750 and 1,000 Hz tone burst frequencies, in case absent responses are found at 500 Hz (20).

In the last decades, a novel treatment was proposed to treat BV: the vestibular implant. This is a (not yet clinically available) strategy to partially restore vestibular function by stimulating the vestibular nerves, using surgically implanted electrodes (21–23). The electrodes can be implanted inside or close to the semicircular canals (24, 25), or inside the otolith organs (26). Surgically positioning electrodes in a semicircular canal or otolith organ, can destroy the (residual) function of that specific organ. Consequently, otolith implantation is currently only considered in case of bilaterally absent cVEMP and oVEMP responses (27). In BV subjects it is therefore imperative to understand, before considering vestibular implantation, whether otolith function is present or not. However, previous VEMP studies in BV patients mainly tested at 500 Hz (8, 9, 14). This might imply that some BV patients that were considered to have absent VEMP responses, might have had preserved VEMPs at other test frequencies.

The objective of this study was therefore to investigate whether multi-frequency VEMP testing (500, 750, 1,000, and 2,000 Hz) would improve the detection of present otolith responses in BV patients.

Methods

Patient population

The patient population was previously described (4, 28–33). In short, BV patients who were previously diagnosed according to the diagnostic criteria of the Bárány Society (6) at Maastricht University Medical Center, were included in this prospective study. Adult BV patients were invited for a testing day that also involved examinations related to other BV studies (4, 28–33). BV patients who were not able to undergo the detailed audiovestibular testing, or who did not want to talk about one of the investigated topics (e.g., psychological symptoms), or who were not able to stop vestibulo-suppressive medication, were excluded from this study.

VEMP testing

Cervical VEMPs and oVEMPs were recorded with the Neuro-Audio system (v2010, Neurosoft, Ivanovo, Russia) and self-adhesive electrodes (Blue sensor, Ambu, Denmark). For cVEMPs, the recording electrodes were placed on the sternocleidomastoid muscles and the reference electrode on the sternum. For oVEMPs, the recording electrodes were placed on the orbital margin inferior to both eyes, and the reference electrode approximately 2 cm below them. For both c- and oVEMPs, the ground electrode was placed on the forehead (8).

The order of testing was randomized for VEMP type (cVEMP and oVEMP) and for stimulation side (right ear and left ear).

Cervical VEMPs were measured in supine position. The head was flexed 30° and turned away from the stimulation side. A monitor (v2010, Neurosoft, Ivanovo, Russia) provided visual feedback to the patient regarding sternocleidomastoid muscle contraction. Patients were instructed to control muscle contraction between 65 and 205 μ V. This was indicated on the monitor as a meter which should be held in a green area. Red areas on the monitor indicated contractions which were too low or too high. Two-hundred electromyography traces with muscle contraction between 65 and 205 μ V were required (8). Cervical VEMPs were elicited with air-conducted tone bursts, provided by inserted earphones. The stimuli included air-conducted tone bursts of 500, 750, 1,000, and 2,000 Hz. A Blackman gating window was used with a two cycle rise/fall without a plateau. The resulting rise time was 4.00 ms at 500 Hz, 2.66 ms at 750 Hz, 2.00 ms at 1,000 Hz, and 1.00 ms at 2,000 Hz. Thirteen Hertz was chosen as stimulation rate, to decrease testing time (34). Furthermore, no significant difference was found regarding present and absent cVEMP and oVEMP responses, when comparing normative VEMP data of 5 and 13 Hz (500 Hz air-conducted tone bursts) obtained in our vestibular laboratory ($p \geq 0.063$).

Ocular VEMPs were also measured in supine position. Patients were instructed to keep their eyes fixed on a target which was located 30 degrees behind their head on the ceiling of the examination room. This achieved superomedial gaze. The same stimulus parameters were used as for cVEMPs, but for oVEMPs a minimum of 300 electromyography traces were required (8).

A staircase approach was adopted to determine VEMP thresholds. Steps of 5 dB SPL were used, which started at 130 dB SPL. The threshold was defined as the lowest sound level that elicited detectable P1 and N1 peaks. A trial repetition was performed to confirm the absence of P1 and N1 peaks at the sound level just below threshold (8). Stimulation was not corrected for conductive hearing loss, since no significant conductive hearing loss was present in any of the patients, as tested by audiometry (Interacoustics Affinity audiometer and Easidata software). All tested ears demonstrated ≤ 20 dB air-bone gaps at all tested frequencies. The median air-bone gaps of right and left ears separately, were 5 dB for each tested frequency.

To obtain normative data for our vestibular laboratory, normative cVEMP data was obtained in 51 healthy subjects (29 women, mean age 47 years, standard deviation 20 years). Normative oVEMP data was obtained in 48 healthy subjects (27 women, mean age 49 years, standard deviation 19 years).

Statistical analysis

Data were analyzed using SPSS Statistics 28 for Windows. VEMP outcome measures included the percentage of present and absent VEMP responses, and VEMP thresholds. A VEMP response was considered present, in case a response could be obtained (regardless of the absolute threshold). A VEMP response was considered absent, in case no response could be obtained at the highest stimulus level. Regarding thresholds, the sound level (dB SPL) was used as input for the statistical analysis. In case of an absent response, a (hypothetical) sound level of 140 dB SPL was used. This number was chosen to facilitate conservative calculations, since it was very close to the highest tested sound level (130 dB SPL).

The Cochran's Q test was used to determine whether the proportion of patients who had a VEMP response differed across the 4 stimulus frequencies. In case of a significant Cochran's Q test, *post hoc* paired analyses were carried out using multiple McNemar's tests. Since every BV patient was tested at multiple frequencies, the assumption of independence was violated. Therefore, the relationship between stimulus frequency (500, 750, 1,000, and 2,000 Hz) and VEMP sound level threshold (dB SPL) was investigated using marginal linear regression analyses with unstructured covariance matrix of the residuals. The effect of stimulus frequency was adjusted for ear (left, right), age, gender and starting side of the threshold measurements (left, right ear). In addition, to test for a possible differential effect, the interaction between frequency and ear was first included in the model and removed again if it was not significant (top-down strategy). Linear regression analysis was applied to compare the mean threshold levels (dB SPL) between BV patients and healthy controls adjusted for age. To compare the BV patients and controls with respect to the occurrence of a present VEMP response after correction for age, logistic regression was performed. Mean differences in threshold levels and odds ratios for no present VEMP response were reported as BV patients compared to healthy controls. The α -value was set to 0.05. In case of multiple comparisons, Bonferroni correction was applied. Two-sided Bonferroni corrected (exact) *p*-values were reported, unless stated otherwise.

Ethical considerations

This study was performed in accordance with the Declaration of Helsinki (amended version 2013). Approval was obtained from the ethical committee of Maastricht University Medical.

Center (NL52768.068.15/METC). All subjects provided written informed consent.

Results

Patient characteristics

Forty-nine BV patients underwent multi-frequency VEMP testing in this study. This included 24 women (49%). Mean age of all patients was 60 years (minimum 21 years, maximum 79 years). Etiologies included ototoxicity (22%), infectious (16%), genetic (14%), Menière's disease (6%), metabolic (4%) and auto-immune disease (2%). The etiology in approximately 35% of patients remained idiopathic. Forty-seven patients completed cVEMP testing and 48 patients completed oVEMP testing. In total, multi-frequency cVEMPs and oVEMPs could both be obtained in 46 patients. Reasons for not completing multi-frequency VEMP testing in all patients included: tiredness ($n = 1$), neck pain ($n = 1$) and equipment failure ($n = 1$).

Presence of multi-frequency VEMP responses in BV patients

Figures 1A,B present the percentages of present cVEMP and oVEMP responses in BV patients, classified by stimulus frequency. Regarding cVEMPs, it can be observed that a present cVEMP was

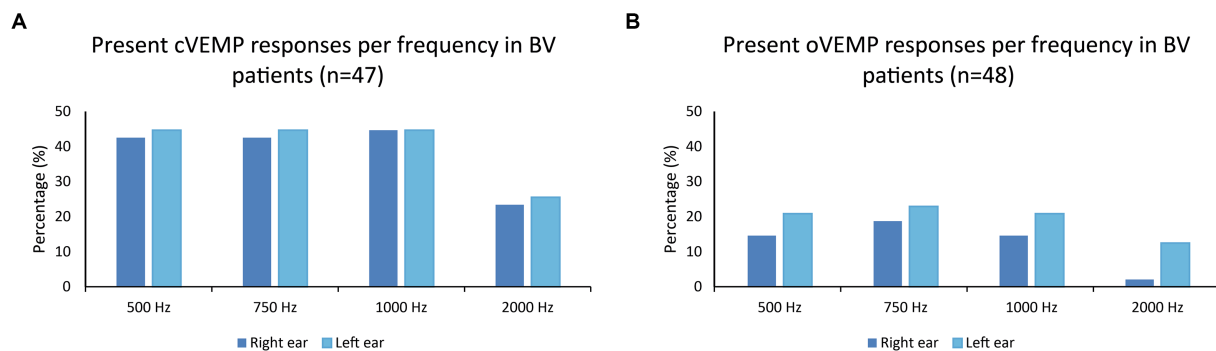


FIGURE 1
(A,B) Percentages of present cVEMP and oVEMP responses in BV patients, classified by stimulus frequency (500, 750, 1,000, and 2,000 Hz).

found in more than 40% of the patients for the frequencies 500 to 1,000 Hz. This was significantly lower for 2,000 Hz compared to the other frequencies (right ears: $p \leq 0.009$; left ears: $p = 0.018$). Marginal regression analysis showed that cervical VEMP thresholds were significantly higher at 2,000 Hz in both ears of the BV patients ($p < 0.001$). Regarding oVEMPs, the percentage of present VEMP responses was significantly lower for all frequencies compared to cVEMP in right ears (one-sided p -values ≤ 0.012). This was not the case for all frequencies in left ears: $p = 0.040$ (500 Hz), $p = 0.012$ (750 Hz), $p = 0.052$ (1,000 Hz), $p = 0.360$ (2,000 Hz). Present oVEMP responses were found in 15–23% for the frequencies 500 Hz to 1,000 Hz, and in less than 13% for 2,000 Hz (Figure 1B). Two-thousand Hertz elicited significantly fewer present oVEMP responses compared to the other frequencies in the right ears ($p \leq 0.044$), but not in the left ears. However, marginal regression analysis did not show a significant relationship between the stimulation frequency and the oVEMP threshold values in both ears. The frequencies eliciting present VEMP responses differed between patients: not all patients with, e.g., a present VEMP response at 500 Hz, also showed a present VEMP response at 750 Hz. Patients with at least one present VEMP response, demonstrated (on average) present VEMP responses at 3.0 and 2.7 frequencies for cVEMP (right and left ears respectively), and at 2.4 and 2.3 frequencies for oVEMP (right and left ears respectively). The percentage of patients with at least one present VEMP response was therefore higher than the percentages found in Figure 1 (see also Table 1).

Detection of present otolith function in BV: multi-frequency vs. 500 Hz stimulus

Table 1 illustrates that, in the same BV population, more present otolith responses were found when using multi-frequency stimuli compared to only testing at 500 Hz. This was significant for cVEMP and oVEMP responses obtained in left ears, but not in right ears (Table 1). The difference in present responses between multi-frequency and 500 Hz stimulation could increase up to 15% when considering each ear separately (cVEMPs, left ears). Additionally, 70% of patients demonstrated a cVEMP response in at least one ear, and 35% of patients demonstrated an oVEMP response in at least one ear (Table 1). A bilaterally present VEMP response was found in 40% (cVEMP) and 19% (oVEMP) of the patients.

In some ears, a VEMP response was found at only one frequency, despite multifrequency testing (Table 2). This was the case in the minority of ears and did not always involve 500 Hz. For example, in 6% of the left ears, a cVEMP response was only present at 1,000 Hz.

Multi-frequency VEMPs: cVEMPs and oVEMPs combined

Forty-six BV patients completed both cVEMP and oVEMP testing, sufficient for analysis. Seventy-eight percent of these patients showed at least one present cVEMP or oVEMP response, in at least one ear. It was found that in 46% of BV patients, bilateral VEMP responses were found in cVEMP, or oVEMP, or both. However, this latter was only the case in 15% of the patients (Table 3).

VEMP responses (500 Hz stimulus): BV patients vs. healthy subjects

VEMP responses (500 Hz stimulus) of the BV patients were compared to VEMP responses of healthy subjects. Cervical VEMP responses (right and left ears) were significantly more absent in BV patients compared to healthy subjects (Odds Ratio ≥ 4.462 , $p \leq 0.002$). Furthermore, mean thresholds of cVEMP responses (right and left ears) were significantly different in BV patients compared to healthy subjects (mean difference BV patients compared to healthy controls of ≥ 7.698 dB SPL, $p \leq 0.001$). Ocular VEMP responses (right and left ears) were also significantly more absent in BV patients compared to healthy subjects (Odds Ratio ≥ 8.885 , $p < 0.001$). The mean thresholds of oVEMP responses in BV patients compared to healthy controls (right and left ears) were significantly different as well (mean difference BV patients compared to healthy controls of ≥ 9.379 dB SPL, $p < 0.001$). In summary, BV patients demonstrated a significantly higher percentage of absent VEMP responses and significantly higher VEMP thresholds than healthy subjects, when corrected for age.

Discussion

This study investigated whether multi-frequency VEMP testing (500, 750, 1,000, and 2,000 Hz) would improve the detection of present

otolith responses in BV patients, compared to only testing at 500 Hz. It was demonstrated that more present otolith responses were obtained with multi-frequency testing. Present cVEMPs were more often present than present oVEMPs. Most present VEMP responses were found when testing at 500, 750, and 1,000 Hz, while 2,000 Hz resulted in fewer present VEMP responses and (for cVEMPs) significantly higher thresholds. These results show that multi-frequency VEMP testing should be considered in BV patients, in case evaluation of (residual) otolith function is indicated.

Multi-frequency VEMP testing improves the detection of present VEMP responses in BV patients, emphasizing the need to test “beyond” the 500 Hz stimulus. These findings are congruent with previous literature in healthy subjects, in which it was illustrated that 500 Hz is not always the best frequency for VEMP testing (20). This results from “frequency-tuning” of the vestibular system, in which different acoustic stimulus frequencies evoke different VEMP responses. Frequency-tuning is patient specific, since it might depend on multiple factors. These factors include, among others: etiology, stage of disease, age, and stimulation paradigm (18, 20). Since multi-frequency VEMP testing improves the detection of present VEMP responses in BV patients, it might be somehow analogous to ice water caloric testing (1). After all, multi-frequency VEMPs and ice water calorics can both be used to detect residual function in case no responses are obtained in the “routine tests” (respectively 500 Hz VEMPs and bithermal caloric testing). Furthermore, this study showed that fewer present VEMP responses and (for cVEMPs) significantly higher thresholds were found when testing at 2,000 Hz. This was expected, since in healthy subjects 2,000 Hz has also less robust responses and significantly higher thresholds than the other tested frequencies (35). This might not directly imply that VEMP testing at 2,000 Hz should be abandoned completely: one ear only demonstrated a 2,000 Hz oVEMP response, without any responses at the other tested frequencies (oVEMPs and cVEMPs). Future research should be conducted to investigate whether testing at other frequencies is beneficial.

Present VEMP responses were frequent in this BV population. Seventy-eight percent demonstrated at least one present VEMP

response in at least one ear, and in 46% a present VEMP response was found bilaterally. A high percentage of present VEMP responses in BV patients is consistent with previous studies. However, direct comparison is difficult because of different BV populations, stimulation paradigms and outcome measures. Nevertheless, these results illustrate two important aspects. First, BV is currently a diagnosis based on lateral semicircular canal function: it does not include vertical semicircular canal function, or otolith function as measured by VEMPs (6, 9, 14). This implies that patients with predominantly affected vertical semicircular canal and/or otolith function, might be missed (7, 15, 16, 36). However, diagnosing (isolated) otolith dysfunction is still challenging. The clinical presentation of otolith dysfunction is not yet well understood and no consensus has been reached on this possible clinical entity (37–39). After all, absent VEMP responses are not necessarily causally related to vestibular symptoms, and do not rule out involvement of other structures (37). It would therefore be advised to further investigate the possible clinical entity of otolith dysfunction (38). Secondly, this study shows that VEMP responses are often still present in BV patients. On-the-one-hand this may imply that otolith function is relatively spared in BV patients compared to lateral semicircular canal function. It could be hypothesized that, e.g., otoliths are less affected by certain vestibular disorders. On-the-other-hand it might have nothing to do with otoliths being less affected than semicircular canals, but with VEMP testing itself. It could be hypothesized that VEMPs are relatively stronger stimuli to the otoliths than, e.g., bithermal caloric testing or video head impulse testing to the semicircular canals. In other words: although otolith function might be affected, a response remains present due to the strong nature of the stimulus. As a result, a present VEMP response is obtained, while hypofunction of the lateral semicircular canals is detected by the caloric test and/or video head impulse test. Additionally, VEMPs are considered to test Type 1 hair cells, while the caloric test might mainly test Type 2 hair cells (10). A dissociation between these tests could therefore also result from a difference in affected hair cell type. Furthermore, the interpretation

TABLE 1 Present VEMP responses: multi-frequency vs. only the 500 Hz stimulus in BV patients.

	cVEMP (n = 47)		oVEMP (n = 48)	
	Multi-frequency	500 Hz	Multi-frequency	500 Hz
Present response(s): right ear	51%	43%	21%	15%
Present response(s): left ear	60%	45% *	33%	21% *
Present response(s): at least one ear	70%	57% *	35%	23% *
Present response(s): both ears	40%	30% *	19%	13%
All tested frequencies present (500–2,000 Hz)	15%	N/A	2%	N/A

Multifrequency VEMP response(s) are classified as present, in case at least one tested frequency demonstrated a present response. Multi-frequency included VEMP testing at 500, 750, 1,000, and 2,000 Hz. N/A, not applicable. *Significant difference between multi-frequency testing and only testing at 500 Hz (one-sided value of $p < 0.05$).

TABLE 2 Multi-frequency testing: percentage of ears with a VEMP response at only one frequency.

	cVEMP (n = 47), only present response at:				oVEMP (n = 48), only present response at:			
	500 Hz	750 Hz	1,000 Hz	2,000 Hz	500 Hz	750 Hz	1,000 Hz	2,000 Hz
Present response: right ear	4%	0%	2%	0%	2%	2%	0%	0%
Present response: left ear	4%	4%	6%	0%	4%	2%	0%	2%

of the tests may play a role. VEMPs are currently not able to detect subtle changes in otolith function, even with good normative data (7). This results from the large range of normal responses in healthy subjects (7). Therefore, except for superior semicircular canal dehiscence syndrome (40), VEMPs are clinically often interpreted as an “on–off” response: response are considered present or absent (27). It is however not justified to compare tests with different outcomes: categorical “on–off” (VEMPs) vs. numerical (e.g., caloric test slow phase eye velocities, video-head impulse test vestibulo-ocular reflex gain). For example, in cases with reduced (but still minimally present) otolith and lateral semicircular canal function, a reduced but present VEMP response might be obtained. This would then be classified as “normal.” The numerical outcomes of the caloric test and/or video head impulse would indicate a reduced function. These tests would then be classified as “abnormal.” However, if the caloric test and video head impulse test would be interpreted based on just the presence of a response, these tests would have also been classified as “normal” (e.g., a video head impulse test gain of 0.4 is still a response). Therefore, the dissociation between otolith and lateral semicircular canal findings in BV patients, should be interpreted with care. It might even be incorrect to state that, e.g., otolith function would be less affected than lateral semicircular canal function in BV patients.

Nevertheless, this study demonstrates that the diagnostic criteria of bilateral vestibulopathy should be revised in the future. A more detailed classification could be considered, taking into account all 10

vestibular sensors, not only the lateral semicircular canals. This might facilitate a detailed classification. For example, categories could vary from abnormal vestibular responses in all vestibular sensors, to isolated abnormal responses such as selective vertical canal or otolith impairment (10, 36).

In this study, the presence of present cVEMP responses was higher than present oVEMP responses. Air-conducted cVEMPs are therefore superior to air-conducted oVEMPs to detect present VEMP responses in BV patients. This does not necessarily indicate that, e.g., saccular function is less affected than utricular function. After all, these findings are not consistent with previous literature, in which saccular and utricular function were almost equally affected (14). Most likely, this can mainly be attributed to the stimulation paradigm: air-conducted sound (this study) vs. bone conducted vibration. Bone conducted vibration produces more reliable oVEMP responses than air-conducted sound (12). This implies that the oVEMP findings in this study probably underestimate the presence of present oVEMP responses in BV patients. It was aimed to use bone-conducted vibration in this study, but long lasting equipment failure unfortunately prevented this study from using bone-conducted vibration. Nevertheless, the objective of this study was to investigate the application of multi-frequency stimulation. This could still be accomplished, but these findings are only applicable to air-conducted stimulation.

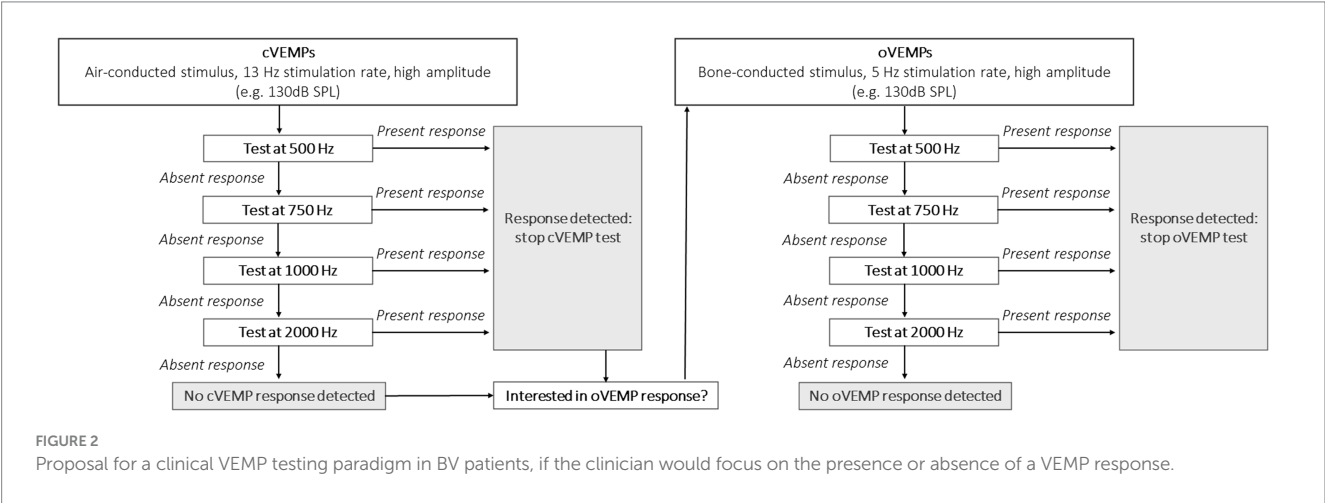
BV patients demonstrated a significantly higher percentage of absent VEMP responses and significantly higher VEMP thresholds than healthy subjects, when corrected for age. This shows that VEMP responses can be significantly affected in BV patients. Unfortunately, as stated above, the large range of normal responses in healthy subjects does not allow to detect subtle changes in otolith function (7, 12). Therefore, VEMPs are mainly interpreted as an “on–off” response in BV patients (27). Taking these limitations and the results of this study into account, a pragmatic VEMP testing paradigm could be proposed for BV patients, if the clinician would only be interested in the presence or absence of a VEMP response. This paradigm is illustrated in Figure 2.

Its concept focuses on obtaining a relatively quick insight in VEMP responses: start testing at a high sound pressure level (e.g., 130 dB SPL) to maximize the detection rate; use a 13 Hz stimulus rate to minimize testing time (cVEMPs); use multi-frequency testing to improve detection rate; stop when one frequency shows a present

TABLE 3 Bilaterally present multi-frequency VEMP responses (n = 46).

	Percentage of BV patients
Present bilateral responses: cVEMP	41%
Present bilateral responses: oVEMP	20%
Present bilateral responses: cVEMP or oVEMP or both	46%
Present bilateral responses: cVEMP and oVEMP	15%

Multifrequency VEMP response(s) are classified as present, in case at least one tested frequency demonstrated a present response. Multi-frequency included VEMP testing at 500, 750, 1,000, and 2,000 Hz.



response since presence of a VEMP response has been demonstrated. It should be noted that testing at 2,000 Hz may be optional. After all, only one ear demonstrated a present VEMP response at 2,000 Hz, without any responses at the other frequencies (Table 2: oVEMP, left ear). The proposed frequencies in this paradigm are based on this study, and other frequencies (e.g., 1,500 Hz) were not tested. Therefore, other frequencies could also be included. Additionally, based on previous literature it would be proposed to use a bone-conducted stimulus for oVEMP testing (12). However, the reliability of a 13 Hz stimulus for a bone-conducted stimulus should still be determined and therefore a 5 Hz stimulus would still be preferred for oVEMPs.

Limitations

BV is a heterogeneous disorder and VEMP responses depend on many factors (e.g., age). This implies that findings of this study are restricted to this specific study population.

Conclusion

Multi-frequency VEMP testing improves the detection rate of present otolith responses in BV patients. Therefore, multi-frequency VEMPs should be considered when evaluation of (residual) otolith function is indicated.

Data availability statement

The raw data supporting the conclusions of this article will be made available by the authors, without undue reservation.

Ethics statement

The studies involving humans were approved by Ethical Committee of Maastricht University Medical Center (NL52768.068.15/METC). The studies were conducted in accordance with the local legislation and institutional requirements. The participants provided their written informed consent to participate in this study.

References

- van de Berg R, van Tilburg M, Kingma H. Bilateral vestibular hypofunction: challenges in establishing the diagnosis in adults. *ORL J. Otorhinolaryngol Relat. Spec.* (2015) 77:197–218. doi: 10.1159/000433549
- Lucieer F, Vonk P, Guinand N, Stokroos R, Kingma H, van de Berg R. Bilateral vestibular hypofunction: insights in etiologies, clinical subtypes, and diagnostics. *Front. Neurol.* (2016) 7:26. doi: 10.3389/fneur.2016.00026
- Lucieer F, Duijn S, Van Rompaey V, Perez Fornos A, Guinand N, Guyot JP, et al. Full Spectrum of reported symptoms of bilateral Vestibulopathy needs further investigation—a systematic review. *Front. Neurol.* (2018) 9:352. doi: 10.3389/fneur.2018.00352
- Lucieer FMP, Van Hecke R, van Stiphout L, Duijn S, Perez-Fornos A, Guinand N, et al. Bilateral vestibulopathy: beyond imbalance and oscillopsia. *J. Neurol.* (2020) 267:241–55. doi: 10.1007/s00415-020-10243-5
- Sun DQ, Ward BK, Semenov YR, Carey JP, Della Santina CC. Bilateral vestibular deficiency: quality of life and economic implications. *JAMA Otolaryngol. Head Neck Surg.* (2014) 140:527–34. doi: 10.1001/jamaoto.2014.490
- Strupp M, Kim J, Murofushi T, Straumann D, Jen JC, Rosengren SM, et al. Bilateral vestibulopathy: Diagnostic criteria consensus document of the classification committee of the barany society. *J Vestib Res Equilib Orientat.* (2017). doi: 10.3233/VES-170619
- Rosengren SM, Welgampola MS, Taylor RL. Vestibular-evoked myogenic potentials in bilateral Vestibulopathy. *Front. Neurol.* (2018) 9:252. doi: 10.3389/fneur.2018.00252
- van Stiphout L, Pleshkov M, Lucieer F, Dobbels B, Mavrodiev V, Guinand N, et al. Patterns of vestibular impairment in bilateral Vestibulopathy and its relation to etiology. *Front. Neurol.* (2022) 13:856472. doi: 10.3389/fneur.2022.856472
- Zingler VC, Weintz E, Jahn K, Botzel K, Wagner J, Huppert D, et al. Saccular function less affected than canal function in bilateral vestibulopathy. *J. Neurol.* (2008) 255:1332–6. doi: 10.1007/s00415-008-0887-6
- Curthoys IS, Burgess AM, Manzari L. The evidence for selective loss of Otolithic function. *Semin. Neurol.* (2020) 40:33–9. doi: 10.1055/s-0039-3402064
- Curthoys IS. Concepts and physiological aspects of the otolith organ in relation to electrical stimulation. *Audiol. Neurotol.* (2020) 25:25–34. doi: 10.1159/000502712

Author contributions

FL: Conceptualization, Investigation, Methodology, Visualization, Writing – original draft, Writing – review & editing, Data curation, Formal analysis, Project administration, Resources. ML: Investigation, Writing – review & editing, Formal analysis. LS: Writing – review & editing. MJ: Formal analysis, Methodology, Writing – review & editing. VR: Writing – review & editing. ED: Writing – review & editing. AP-F: Writing – review & editing. NG: Writing – review & editing. RB: Conceptualization, Data curation, Formal analysis, Funding acquisition, Methodology, Supervision, Validation, Visualization, Writing – original draft, Writing – review & editing.

Funding

The authors declare financial support was received for the research, authorship, and/or publication of this article. This study was supported by MED-EL (Innsbruck, Austria). The funder was not involved in the study design, collection, analysis, interpretation of data, the writing of this article, or the decision to submit it for publication.

Conflict of interest

The authors declare that the research was conducted in the absence of any commercial or financial relationships that could be construed as a potential conflict of interest.

The authors declared that they were an editorial board member of Frontiers, at the time of submission. This had no impact on the peer review process and the final decision.

Publisher's note

All claims expressed in this article are solely those of the authors and do not necessarily represent those of their affiliated organizations, or those of the publisher, the editors and the reviewers. Any product that may be evaluated in this article, or claim that may be made by its manufacturer, is not guaranteed or endorsed by the publisher.

12. Starkov D, Strupp M, Pleshkov M, Kingma H, van de Berg R. Diagnosing vestibular hypofunction: an update. *J. Neurol.* (2021) 268:377–85. doi: 10.1007/s00415-020-10139-4
13. van de Berg R, Rosengren S, Kingma H. Laboratory examinations for the vestibular system. *Curr. Opin. Neurol.* (2018) 31:111–6. doi: 10.1097/WCO.0000000000000526
14. Agrawal Y, Bremova T, Kremmyda O, Strupp M. Semicircular canal, saccular and utricular function in patients with bilateral vestibulopathy: analysis based on etiology. *J. Neurol.* (2013) 260:876–83. doi: 10.1007/s00415-012-6724-y
15. Fujimoto C, Murofushi T, Chihara Y, Suzuki M, Yamasoba T, Iwasaki S. Novel subtype of idiopathic bilateral vestibulopathy: bilateral absence of vestibular evoked myogenic potentials in the presence of normal caloric responses. *J. Neurol.* (2009) 256:1488–92. doi: 10.1007/s00415-009-5147-x
16. Fujimoto C, Murofushi T, Sugawara K, Chihara Y, Ushio M, Yamasoba T, et al. Bilateral vestibulopathy with dissociated deficits in the superior and inferior vestibular systems. *Ann. Otol. Rhinol. Laryngol.* (2012) 121:383–8. doi: 10.1177/000348941212100604
17. Murofushi T, Matsuzaki M, Wu CH. Short tone burst-evoked myogenic potentials on the sternocleidomastoid muscle: are these potentials also of vestibular origin? *Arch. Otolaryngol. Head Neck Surg.* (1999) 125:660–4. doi: 10.1001/archotol.125.6.660
18. Noij KS, Herrmann BS, Guinan JJ Jr, Rauch SD. Cervical vestibular evoked myogenic potentials in Meniere's disease: a comparison of response metrics. *Otol. Neurotol.* (2019) 40:e215–24. doi: 10.1097/MAO.0000000000002092
19. Rauch SD, Zhou G, Kujawa SG, Guinan JJ, Herrmann BS. Vestibular evoked myogenic potentials show altered tuning in patients with Meniere's disease. *Otol. Neurotol.* (2004) 25:333–8. doi: 10.1097/00129492-200405000-00022
20. Piker EG, Jacobson GP, Burkard RF, McCaslin DL, Hood LJ. Effects of age on the tuning of the cVEMP and oVEMP. *Ear Hear.* (2013) 34:e65–73. doi: 10.1097/AUD.0b013e31828fc9f2
21. Guinand N, van de Berg R, Cavuscens S, Stokroos RJ, Ranieri M, Pelizzone M, et al. Vestibular implants: 8 years of experience with electrical stimulation of the vestibular nerve in 11 patients with bilateral vestibular loss. *ORL J. Otorhinolaryngol. Relat. Spec.* (2015) 77:227–40. doi: 10.1159/000433554
22. van de Berg R, Guinand N, Nguyen TA, Ranieri M, Cavuscens S, Guyot JP, et al. The vestibular implant: frequency-dependency of the electrically evoked vestibulo-ocular reflex in humans. *Front Syst Neurosci.* (2014) 8:255. doi: 10.3389/fnsys.2014.00255
23. van de Berg R, Guinand N, Ranieri M, Cavuscens S, Khoa Nguyen TA, Guyot JP, et al. The vestibular implant input interacts with residual natural function. *Front. Neurol.* (2017) 8:644. doi: 10.3389/fneur.2017.00644
24. van de Berg R, Guinand N, Guyot JP, Kingma H, Stokroos RJ. The modified ampullar approach for vestibular implant surgery: feasibility and its first application in a human with a long-term vestibular loss. *Front. Neurol.* (2012) 3:18. doi: 10.3389/fneur.2012.00018
25. Kos MI, Feigl G, Anderhuber F, Wall C, Fasel JH, Guyot JP. Transcanal approach to the singular nerve. *Otol. Neurotol.* (2006) 27:542–6. doi: 10.1097/00129492-200606000-00017
26. Ramos de Miguel A, Falcon Gonzalez JC, Ramos MA. Vestibular response to electrical stimulation of the otolith organs. Implications in the development of a vestibular implant for the improvement of the sensation of Gravito-inertial accelerations. *J Int Adv Otol.* (2017) 13:154–61. doi: 10.5152/iao.2017.4216
27. van de Berg R, Ramos A, van Rompaey V, Bisdorff A, Perez-Fornos A, Rubinstein JT, et al. The vestibular implant: opinion statement on implantation criteria for research. *J. Vestib. Res.* (2020) 30:213–23. doi: 10.3233/VES-200701
28. van Stiphout L, Lucieer F, Pleshkov M, Van Rompaey V, Widdershoven J, Guinand N, et al. Bilateral vestibulopathy decreases self-motion perception. *J. Neurol.* (2022) 269:5216–28. doi: 10.1007/s00415-021-10695-3
29. van Dooren T, Starkov D, Lucieer F, Dobbels B, Janssen M, Guinand N, et al. Suppression head impulse test (SHIMP) versus head impulse test (HIMP) when diagnosing bilateral Vestibulopathy. *J. Clin. Med.* (2022) 11:2444. doi: 10.3390/jcm11092444
30. van Dooren TS, Lucieer FMP, Duijn S, Janssen AML, Guinand N, Perez Fornos A, et al. The functional head impulse test to assess Oscillopsia in bilateral Vestibulopathy. *Front. Neurol.* (2019) 10:365. doi: 10.3389/fneur.2019.00365
31. van Dooren TS, Starkov D, Lucieer FMP, Vermorken B, Janssen AML, Guinand N, et al. Comparison of three video head impulse test systems for the diagnosis of bilateral vestibulopathy. *J. Neurol.* (2020) 267:256–64. doi: 10.1007/s00415-020-10060-w
32. Starkov D, Snelders M, Lucieer F, Janssen AML, Pleshkov M, Kingma H, et al. Bilateral vestibulopathy and age: experimental considerations for testing dynamic visual acuity on a treadmill. *J. Neurol.* (2020) 267:265–72. doi: 10.1007/s00415-020-10249-z
33. van Stiphout L, Lucieer F, Guinand N, Perez Fornos A, van de Berg M, Van Rompaey V, et al. Bilateral vestibulopathy patients' perspectives on vestibular implant treatment: a qualitative study. *J. Neurol.* (2022) 269:5249–57. doi: 10.1007/s00415-021-10920-z
34. van Tilburg MJ, Herrmann BS, Guinan JJ Jr, Rauch SD. Increasing the stimulation rate reduces cVEMP testing time by more than half with no significant difference in threshold. *Otol. Neurotol.* (2016) 37:933–6. doi: 10.1097/MAO.0000000000001096
35. Noij KS, Herrmann BS, Guinan JJ Jr, Rauch SD. Toward optimizing cVEMP: 2,000-Hz tone bursts improve the detection of Superior Canal dehiscence. *Audiol. Neurotol.* (2018) 23:335–44. doi: 10.1159/000493721
36. Murofushi T, Monobe H, Ushio M. Isolated bilateral posterior semicircular canal hypofunction: comparison with bilateral vestibulopathy. *Acta Otolaryngol.* (2023) 143:687–91. doi: 10.1080/00016489.2023.2253270
37. De Chua KW, Yuen HW, Low D, Kamath S. Proposal on the diagnostic criteria of definite isolated otolith dysfunction. *J Audiol Otol.* (2021) 25:59–60. doi: 10.7874/jao.2020.00535
38. Suh MW, Murofushi T. Response: proposed diagnostic criteria for definite isolated otolith dysfunction. *J Audiol Otol.* (2021) 25:61–3. doi: 10.7874/jao.2020.00661
39. Park HG, Lee JH, Oh SH, Park MK, Suh MW. Proposal on the diagnostic criteria of definite isolated otolith dysfunction. *J Audiol Otol.* (2019) 23:103–11. doi: 10.7874/jao.2018.00374
40. Ward BK, van de Berg R, van Rompaey V, Bisdorff A, Hullar TE, Welgampola MS, et al. Superior semicircular canal dehiscence syndrome: diagnostic criteria consensus document of the committee for the classification of vestibular disorders of the Barany society. *J. Vestib. Res.* (2021) 31:131–41. doi: 10.3233/VES-200004



OPEN ACCESS

EDITED BY

Sulin Zhang,
Huazhong University of Science and
Technology, China

REVIEWED BY

Jianyong Chen,
Shanghai Jiao Tong University, China
Jun Wang,
Huazhong University of Science and
Technology, China

*CORRESPONDENCE

Dan Deng
✉ 878720578@qq.com

RECEIVED 09 October 2023

ACCEPTED 18 March 2024

PUBLISHED 09 April 2024

CITATION

Liu S, Zhang L, Deng D and Luo W (2024)
Associations between benign paroxysmal
positional vertigo and seven mental disorders:
a two-sample Mendelian randomization
study. *Front. Neurol.* 15:1310026.
doi: 10.3389/fneur.2024.1310026

COPYRIGHT

© 2024 Liu, Zhang, Deng and Luo. This is an
open-access article distributed under the
terms of the [Creative Commons Attribution
License \(CC BY\)](#). The use, distribution or
reproduction in other forums is permitted,
provided the original author(s) and the
copyright owner(s) are credited and that the
original publication in this journal is cited, in
accordance with accepted academic practice.
No use, distribution or reproduction is
permitted which does not comply with these
terms.

Associations between benign paroxysmal positional vertigo and seven mental disorders: a two-sample Mendelian randomization study

Shihan Liu¹, Lingli Zhang², Dan Deng^{3*} and Wenlong Luo¹

¹Department of Otorhinolaryngology, The Second Affiliated Hospital of Chongqing Medical University, Chongqing, China, ²Department of Otorhinolaryngology, Central Hospital Affiliated to Chongqing University of Technology, Chongqing, China, ³Department of Eye and ENT, Chongqing Maternal and Child Health Care Hospital, Chongqing, China

Background: The association between benign paroxysmal positional vertigo (BPPV) and various mental disorders is still controversial. This study used the Mendelian randomization (MR) method to clarify the correlation between BPPV and seven mental disorders (bipolar disorder, depression, anxiety disorder, schizophrenia, suicidality, neuroticism, and mood swings) to aid in the exploration of BPPV complications and prevention and early treatment of mental disorders.

Methods: The datasets for BPPV and seven mental disorders were obtained from genome-wide association studies (GWASs). Two-sample MR was used to analyze the correlation between exposure (BPPV) and various outcomes (bipolar disorder, depression, anxiety disorder, schizophrenia, suicidality, neuroticism, and mood swings). A reverse MR study was also performed. The inverse variance weighting (IVW) method, the MR-Egger method, the simple mode method, the weighted mode method, and the weighted median method were selected.

Results: The MR analysis and the reverse MR analysis results did not reveal significant associations between BPPV and bipolar disorder, depression, anxiety disorder, schizophrenia, suicidal tendencies, neuroticism, and mood swings. Interestingly, neuroticism (IVW: OR = 1.142, 95% CI: 1.059–1.231, $P = 0.001$; P-MR-PRESSO adjustment = 0.0002) and mood swings (IVW: OR = 3.119, 95% CI: 1.652–5.884, $P = 0.0004$) may have a significant association with BPPV. After MR-PRESSO adjustment, there was no horizontal pleiotropy or heterogeneity, and a significant association between neuroticism, mood swings, and BPPV has still been suggested.

Conclusion: We conducted MR analysis on genetic data from European populations and discovered a causal relationship between BPPV and the seven mental disorders. Our research findings suggest that BPPV may not have a significant causal relationship with bipolar disorder, depression, anxiety disorder, schizophrenia, or suicidal tendencies. However, neuroticism and mood swings may be risk factors for BPPV.

KEYWORDS

Mendelian randomization, benign paroxysmal positional vertigo, mental disorders, neuroticism, mood swings

1 Introduction

Benign paroxysmal positional vertigo (BPPV) is the most common cause of vertigo, and 24.1% of patients with dizziness/vertigo have BPPV (1). The underlying mechanism of BPPV may be the displacement of degenerate otoliths into the semicircular canal, resulting in increased sensitivity to head movement, which induces paroxysmal positional vertigo (2). The lifetime incidence of BPPV is as high as 2.4% (3), and BPPV seriously affects the quality of life in affected individuals (4), increases their risk of falls, and reduces their walking speed (5). BPPV has caused a significant medical burden worldwide (6). Therefore, exploring the impact of BPPV on the incidence of other diseases would be highly helpful for informing personalized treatment and improving patient prognosis.

At present, increased attention has been given to mental disorders worldwide. Approximately one in five people experience a common mental disorder in a year (7). Mental disorders lead to a serious decline in the participation rate of affected individuals in the social labor force, and the high cost of treatment seriously affects their quality of life in the later stages of the illness (8, 9). Multiple diseases or behaviors are thought to contribute to an increased prevalence of mental disorders (10–12). Therefore, identifying the risk factors for mental disorders could facilitate early intervention for individuals affected, thereby reducing the impact of mental disorders on both patients and society.

Although vertigo caused by BPPV can be resolved by the implementation of repeated canalith repositioning procedure (CRP), symptoms of vertigo and positional nystagmus in the patient often return (13). However, some studies have suggested that the clinical features of paroxysmal vertigo may induce various mental disorders in patients with BPPV. At present, whether BPPV can increase the risk of various mental disorders in patients is still controversial, and related studies are rare. A cohort study from Taiwan, China, suggested that chronic stress due to paroxysmal vertigo may increase the risk of BPPV-related suicide (14). A survey of the incidence of BPPV in all patients with mood disorders in Korea revealed that mood disorders may be significantly associated with BPPV (15). A recent meta-analysis suggested that BPPV may increase the risk of anxiety, but no significant association between BPPV and depression was found. There were few relevant studies included in this meta-analysis, and the sample size was small; therefore, further research is needed to determine the associations between BPPV and anxiety and depression (16). Similar to anxiety and depression, bipolar disorder and schizophrenia are also common mental disorders (17), and no relevant studies have explored the associations between bipolar disorder and schizophrenia and BPPV. A lower neuroticism score and stable emotions play a certain role in mental health (18, 19). However, recurrent progression of vertigo may lead to greater neuroticism and mood swings in patients (20).

Many studies have explored the association between mental disorders and diseases through Mendelian randomization (MR) (11, 21). MR is used to clarify the association between two traits. Genetic variants are included as instrumental variables. Single-nucleotide polymorphisms (SNPs) are identified from independent genome-wide association study (GWAS) datasets and are subjected

to association analysis as instrumental variables (22). The advantages of MR include avoiding the limitations of traditional observational research and eliminating the interference of various confounding factors in the study as much as possible so that the research results have greater credibility. MR studies have improved the statistical power to infer causal relationships between diseases (23). This study aimed to analyze the relationship between BPPV and seven mental disorders (bipolar disorder, depression, anxiety disorder, schizophrenia, suicidality, neuroticism, and mood swings) by using the MR method to clarify whether there is a correlation between BPPV and seven mental disorders. Neuroticism and the presence of mood swings are considered risk factors for mental disorders; therefore, these factors were included in this study to explore the correlation between BPPV and neuroticism and mood swings. The association between BPPV and mental disorders is clarified to improve the timeliness and targeting of the prevention and treatment of both conditions.

2 Methods

2.1 Data sources

In this study, a two-sample MR analysis was used to analyze the relationship between exposure (BPPV) and various outcomes (bipolar disorder, depression, anxiety disorder, schizophrenia, suicidality, neuroticism, and mood swings). Reverse MR was applied to analyze the correlation between exposure (bipolar disorder, depression, anxiety disorder, schizophrenia, suicidality, neuroticism, and mood swings) and an outcome (BPPV). The GWAS datasets used in this study were all obtained from the IEU GWAS database (<https://gwas.mrcieu.ac.uk/>), from which the datasets for BPPV and bipolar disorder, depression, anxiety, schizophrenia, suicidality, neuroticism, and mood swings were selected. The BPPV dataset was collected from the FinnGen database, which includes genomic and health data collected from 500,000 Finnish biobanks to determine the genetic basis of the disease. The IEU database has obtained the BPPV dataset from the FinnGen database R5 version. The diagnosis criteria in the FinnGen database are based on the Tenth Revision of the International Statistical Classification of Diseases and Related Health Problems (ICD-10). The diagnosis of BPPV requires meeting the diagnostic criteria with the code H81.1 according to the ICD-10. Depression, anxiety disorders, suicidality, neuroticism, and mood swing-related datasets were collected from the UK Biobank, which includes genetic information obtained from more than 500,000 participants from all over the UK. The bipolar disorder and schizophrenia dataset was derived from a GWAS database of patients with bipolar disorder and schizophrenia (24, 25). Detailed information on the GWAS data sources used in our study is provided in Table 1.

2.2 Selection of instrumental variables

The SNPs were selected from the GWAS dataset based on the following conditions: 1. The significance in genome-wide studies to prevent the inclusion of fewer SNPs ($P < 5 \times 10^{-6}$ was selected as the screening criterion). 2. No linkage disequilibrium was detected

TABLE 1 The GWAS data sources.

Phenotype	Data source	PMID	Cases	Controls	Sample size	Ancestry
BPPV	FinnGen		3,834	209,582	213,416	European
Bipolar disorder	Stahl, E et al.	31043756	20,352	31,358	51,710	European
Depression	Ben Elsworth et al.		26,595	436,338	462,933	European
Anxiety disorders	Ben Elsworth et al.		6,410	456,523	462,933	European
Schizophrenia	Trubetskoy V et al.	35396580	52,017	75,889	127,906	European
Suicidality	Neale laboratory		2,658	2,275	4,933	European
Neuroticism	Ben Elsworth et al.				374,323	European
Mood swings	Ben Elsworth et al.		204,412	247,207	451,619	European

BPPV, benign paroxysmal positional vertigo.

between any of the SNPs to preserve SNP independence ($r^2 < 0.001$ and 10,000 kb). 3. SNPs with an F-statistic < 10 were excluded as they were considered weak instrumental variables. Plus-strand allele inference was then attempted using palindromic allele frequencies.

2.3 Mendelian randomization analysis

The inverse variance weighting (IVW), MR-Egger, simple mode, weighted mode, and weighted median methods were used for data evaluation. IVW obtained a total estimate of the effect of exposure on the outcome by combining the causal estimate of the Wald ratio for each IV, and IVW was used as the primary analysis method (26). The non-zero intercept values shown by the MR-Egger method were mainly used to examine horizontal pleiotropy (27). The weighted median gives an accurate estimate based on the assumption that at least 50% of IVs are effective (28). The simple mode, weighted mode, and weighted median methods were mainly used to verify the reliability and stability of the results. Causality was assessed using the odds ratio (OR) and 95% confidence interval (95% CI) to determine the significance. To strengthen the reliability of this study, the significance was set at 0.05/7 (0.007) according to the Bonferroni correction method.

The MR-Egger method was used to obtain intercept values to evaluate horizontal pleiotropy. The Q-statistic from Cochran's IVW was then used to investigate the impact of heterogeneity. The results of pleiotropic and heterogeneous MR-PRESSO analysis were obtained to remove outlier SNPs from the group and recalculate the MR results.

MR analysis was performed using the TwoSampleMR package in R version 4.2.3 (<http://www.r-project.org>) (29). The TwoSampleMR package enables online analysis of the association between exposure and outcome datasets through the IEU database.

3 Results

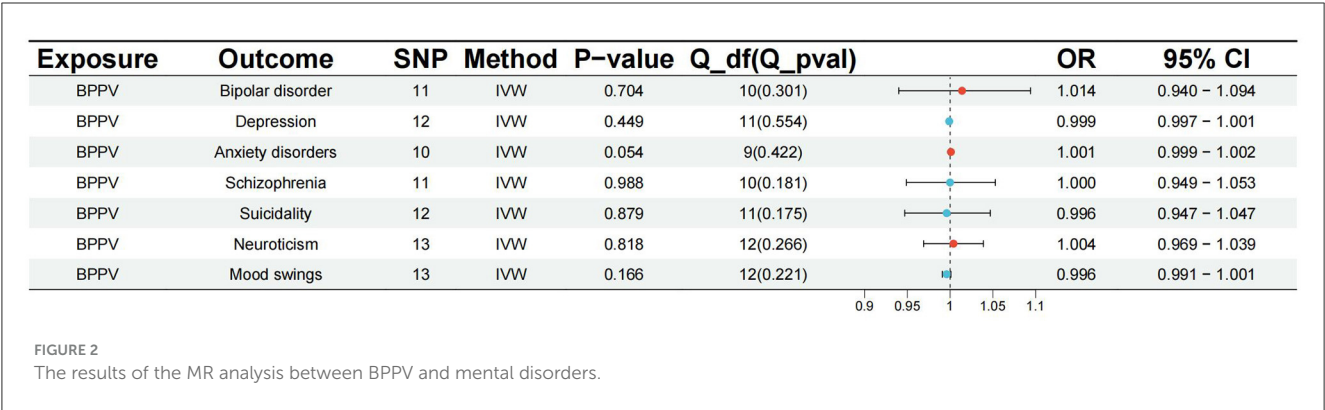
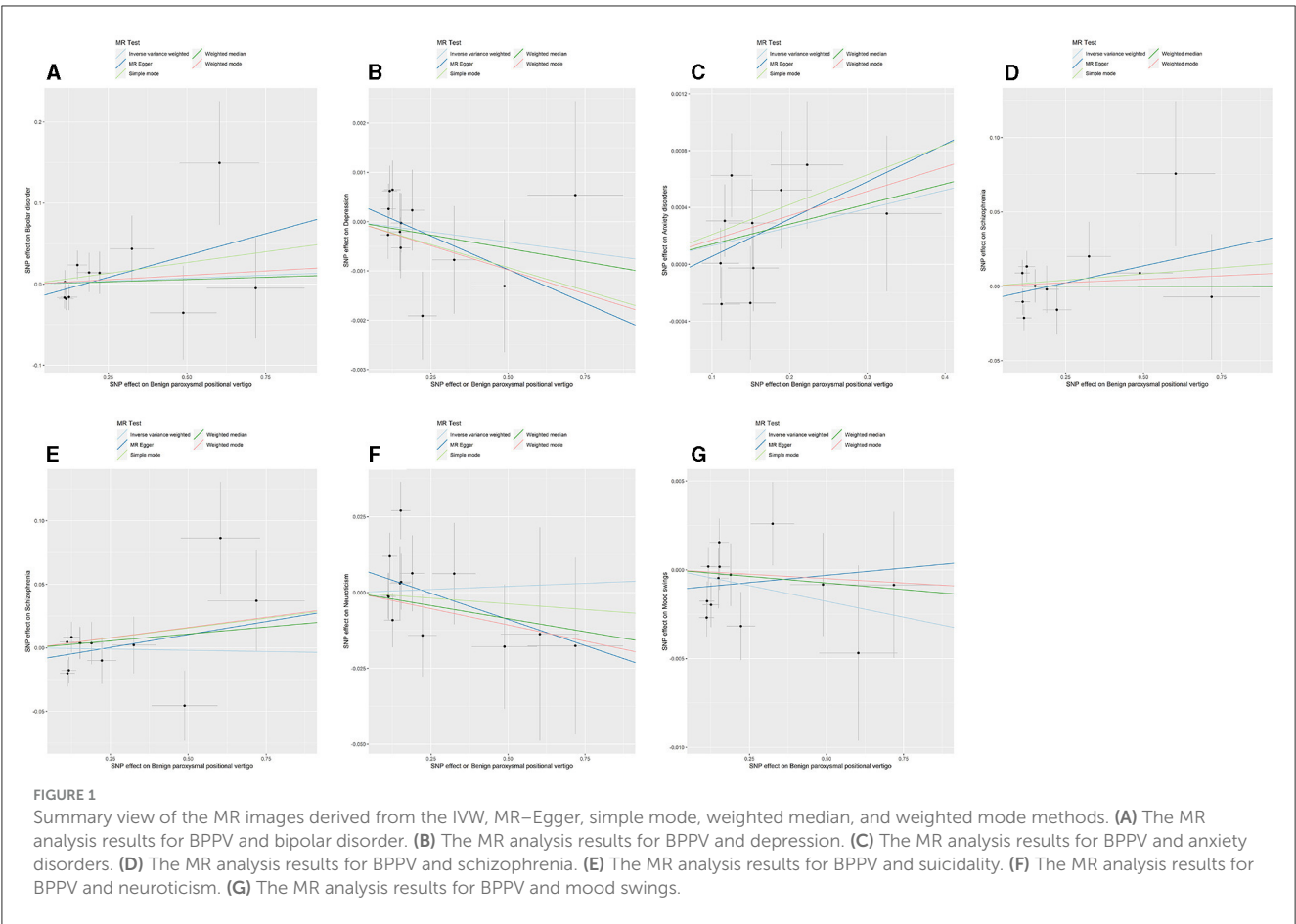
3.1 The results of MR analysis between BPPV and seven mental disorders

The p -value of $<5 \times 10^{-6}$ was selected as the screening criterion for BPPV-related SNPs. After screening based on the

screening criteria, MR analysis was performed, and the F -statistics of the SNPs included in the analysis were all found to be >10 , indicating that they were all strong instrumental variables (Supplementary material). All heterogeneity analyses showed results that $p > 0.05$, which suggested that there was no heterogeneity in the results. No horizontal pleiotropy was found in any of the MR-Egger analyses ($P > 0.05$). The results suggested that there was no significant association between BPPV and bipolar disorder (IVW: OR = 1.014, 95% CI: 0.940–1.094, $P = 0.704$), depression (IVW: OR = 0.999, 95% CI: 0.997–1.001, $P = 0.449$), anxiety disorders (IVW: OR = 1.001, 95% CI: 0.999–1.002, $P = 0.054$), schizophrenia (IVW: OR = 1.000, 95% CI: 0.949–1.053, $P = 0.988$), suicidality (IVW: OR = 0.996, 95% CI: 0.947–1.047, $P = 0.879$), neuroticism (IVW: OR = 1.004, 95% CI: 0.969–1.039, $P = 0.818$), and mood swings (IVW: OR = 0.996, 95% CI: 0.991–1.001, $P = 0.166$) (Figures 1, 2). The detailed analysis results are shown in Table 2.

3.2 The results of MR analysis between seven mental disorders and BPPV

The p -value of $<5 \times 10^{-6}$ was selected as the screening criterion for seven mental disorder-related SNPs. After screening based on the criteria, MR analysis was performed, and the F -statistics of the SNPs included in the analysis were all found to be >10 , indicating strong instrumental variables (Supplementary material). No significant association was found in the reverse MR of bipolar disorder (IVW: OR = 1.004, 95% CI: 0.938–1.074, $P = 0.902$), depression (IVW: OR = 6.995, 95% CI: 0.069–7.004E+02, $P = 0.408$, P-MR-PRESSO adjustment = 0.147), anxiety (IVW: OR = 3.529E-04, 95% CI: 1.037E-10–1.200E+03, $P = 0.300$), schizophrenia (IVW: OR = 0.994, 95% CI: 0.944–1.045, $P = 0.809$), suicidality (IVW: OR = 0.975, 95% CI: 0.730–1.301, $P = 0.864$), and BPPV. Neuroticism (IVW: OR = 1.142, 95% CI: 1.059–1.231, $P = 0.001$; P-MR-PRESSO adjustment = 0.0002) and mood swings (IVW: OR = 3.119, 95% CI: 1.652–5.884, $P = 0.0004$) were significantly associated with BPPV. Horizontal pleiotropy and heterogeneity were detected in the reverse MR analysis of patients with depression and BPPV, and heterogeneity was detected in the inverse variance MR analysis of patients with neuroticism and BPPV. MR analysis was performed again after MR-PRESSO adjustment, and the results showed a lack of horizontal pleiotropy



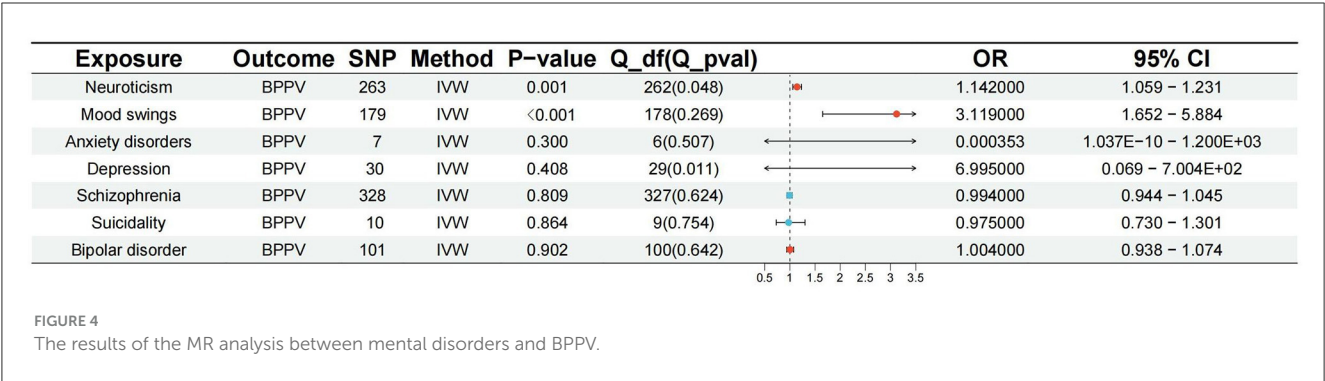
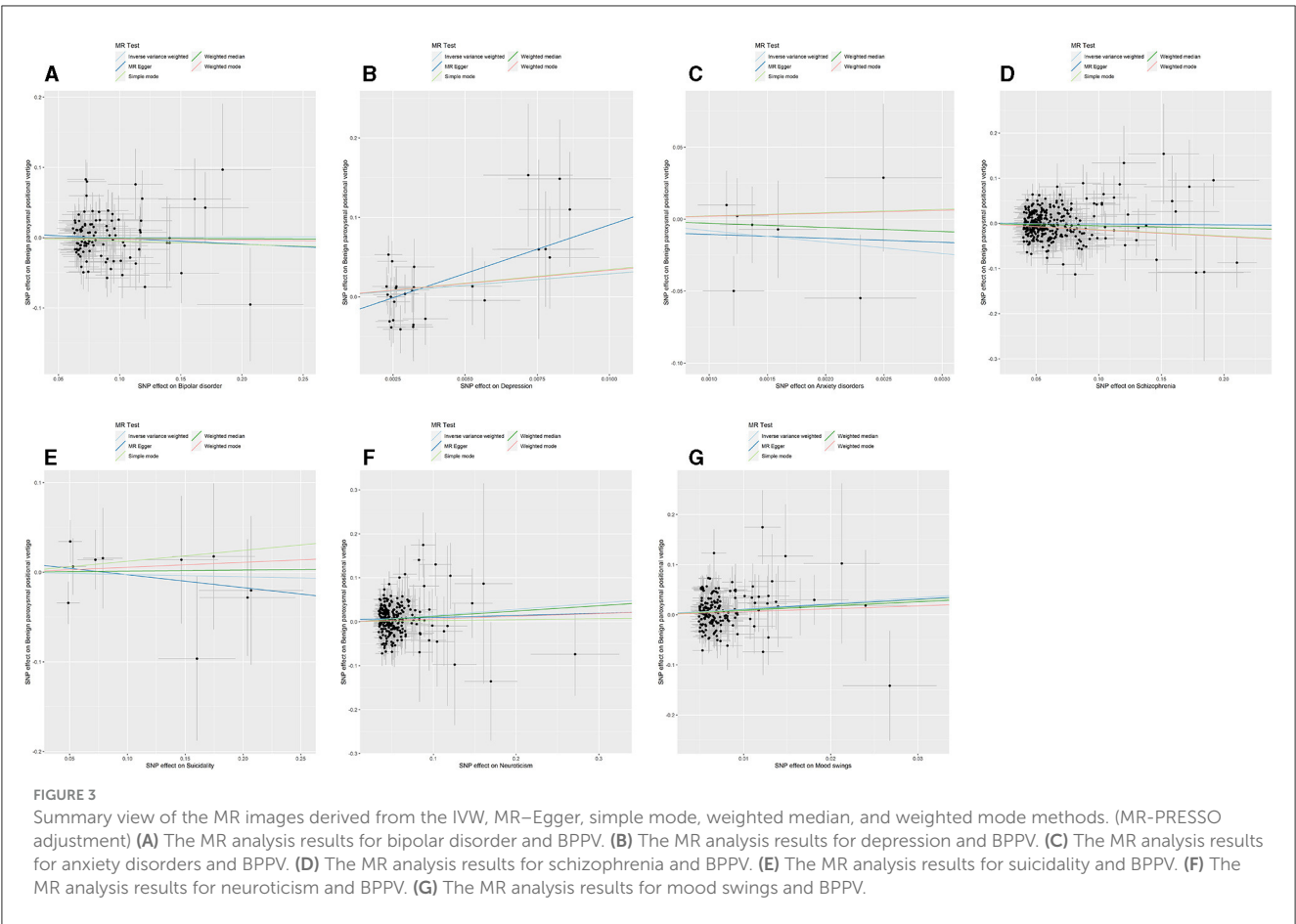
and heterogeneity (Figures 3, 4). The detailed analysis results are shown in Table 3.

4 Discussion

In this study, the MR method was used to assess the association between BPPV and seven mental disorders. The results showed that BPPV was not significantly associated with bipolar disorder, depression, anxiety disorders, schizophrenia, or suicidality. Reverse MR analysis indicated that bipolar disorder, depression, anxiety, schizophrenia, and suicidality were not significantly associated

with BPPV, while higher neuroticism scores and mood swings may promote the occurrence and development of BPPV. Analyses of horizontal pleiotropy and heterogeneity after MR-PRESSO adjustment did not reveal significant differences, which suggests the reliability of the results.

In related studies analyzing patients with BPPV in Korea, it was found that the risk of developing mood disorders in BPPV patients was significantly greater than that in healthy people (15). The degree of anxiety and depression may reflect the probability of residual dizziness after canalith repositioning (30). At present, the associations between BPPV and anxiety and depression have been studied the most. A recent meta-analysis of



23 studies and 2,902 patients showed that there was a significant association between BPPV and anxiety, but the association between BPPV and depression still needs to be further studied (16). Yang et al. conducted an analysis of 72,569 patients with peripheral vestibular disorders and 217,707 healthy controls in Taiwan and reported that suicidal attempts were strongly associated with BPPV, Meniere's disease, and vestibular neuritis; however, due to the uncertainty of other suicide risk factors, the association between these conditions needs to be further studied (14), and other studies have shown results similar to those in our analyses. Kalderon et al. analyzed the clinical data of 18 patients with BPPV and 18 healthy controls and reported that there may be no difference in anxiety between patients with BPPV and healthy controls (31).

In our research, no relevant clinical studies on BPPV or bipolar disorder or schizophrenia were found, and the association between BPPV and the relevance of bipolar disorder and schizophrenia may require further exploration. Psychological distress has been shown to predict the severity of vestibular dysfunction to a certain extent (32). Neuroticism and mood swings, which are common psychological factors (33), may also have a certain effect on BPPV. Several clinical studies have confirmed our results from other perspectives (20, 34, 35). Our results are inconsistent with the results of several clinical analyses, possibly due to the lack of reliability of the results due to the unmeasured confounding factors that often appear in clinical studies of mental disorders or BPPV. Therefore, the results of clinical studies cannot fully reflect the

TABLE 2 Results of the MR analysis of BPPV and mental disorders.

Exposure	Outcome	SNP	Method	OR	95% CI	P-value	Q_df (Q_pval)
BPPV	Bipolar disorder	11	MR Egger	1.113	0.968–1.281	0.165	9 (0.404)
			Weighted median	1.011	0.916–1.116	0.822	
			IVW	1.014	0.940–1.094	0.704	10 (0.301)
			Simple mode	1.054	0.893–1.245	0.543	
			Weighted mode	1.021	0.866–1.205	0.802	
BPPV	Depression	12	MR Egger	0.997	0.992–1.001	0.246	10 (0.554)
			Weighted median	0.998	0.995–1.001	0.478	
			IVW	0.999	0.997–1.001	0.449	11 (0.554)
			Simple mode	0.998	0.993–1.002	0.465	
			Weighted mode	0.998	0.994–1.001	0.345	
BPPV	Anxiety disorders	10	MR Egger	1.002	0.998–1.007	0.291	8 (0.361)
			Weighted median	1.001	0.999–1.003	0.119	
			IVW	1.001	0.999–1.002	0.054	9 (0.422)
			Simple mode	1.002	0.999–1.004	0.186	
			Weighted mode	1.001	0.999–1.004	0.212	
BPPV	Schizophrenia	11	MR Egger	1.046	0.944–1.159	0.406	9 (0.190)
			Weighted median	0.999	0.937–1.066	0.994	
			IVW	1.000	0.949–1.053	0.988	10 (0.181)
			Simple mode	1.016	0.915–1.129	0.763	
			Weighted mode	1.009	0.926–1.099	0.835	
BPPV	Suicidality	12	MR Egger	1.041	0.947–1.145	0.418	10 (0.194)
			Weighted median	1.022	0.962–1.085	0.476	
			IVW	0.996	0.947–1.047	0.879	11 (0.175)
			Simple mode	1.031	0.933–1.139	0.552	
			Weighted mode	1.032	0.934–1.140	0.540	
BPPV	Neuroticism	13	MR Egger	0.966	0.905–1.030	0.321	11 (0.329)
			Weighted median	0.983	0.940–1.027	0.443	
			IVW	1.004	0.969–1.039	0.818	12 (0.266)
			Simple mode	0.993	0.927–1.062	0.832	
			Weighted mode	0.979	0.924–1.036	0.475	
BPPV	Mood swings	13	MR Egger	1.002	0.992–1.011	0.742	11 (0.263)
			Weighted median	0.999	0.992–1.004	0.647	
			IVW	0.996	0.991–1.001	0.166	12 (0.221)
			Simple mode	0.999	0.988–1.009	0.857	
			Weighted mode	0.999	0.989–1.008	0.838	

BPPV, Benign paroxysmal positional vertigo.

association between these diseases. We used the MR method at the level of genetic analysis to determine the relationship between the two parameters (mental disorders and BPPV), ruling out various confounding factors, and thus improved the reliability of the results (36).
Due to the influence of various factors on the mechanism of BPPV, there may be no significant association between several

mental disorders and this disease. Neuroticism and mood swings are more likely to be the risk factors for BPPV compared to other mental disorders. However, the mechanism by which neuroticism and mood swings, as common psychological distress factors, affect the occurrence and development of BPPV is still unclear, and local inflammation due to abnormal psychology could promote the development of BPPV (37, 38). Psychological stress can trigger

TABLE 3 Results of the MR analysis of mental disorders and BPPV.

Exposure	Outcome	SNP	Method	OR	95% CI	P-value	Q_df (Q_pval)	P-value (MR-PRESSON after adjustment)
Bipolar disorder	BPPV	101	MR Egger	0.924	0.675–1.264	0.622	99 (0.623)	
			Weighted median	0.992	0.898–1.095	0.882		
			IVW	1.004	0.938–1.074	0.902	100 (0.642)	
			Simple mode	0.953	0.732–1.240	0.723		
			Weighted mode	0.983	0.764–1.263	0.892		
Depression	BPPV	30	MR Egger	3.419E+07	3.733E+3–3.131E+12	0.006	28 (0.097)	0.028
			Weighted median	17.253	0.089–3.318E+03	0.288		0.293
			IVW	6.995	0.069–7.004E+02	0.408	29 (0.011)	0.147
			Simple mode	39.385	4.942E-04–3.139E+06	0.529		0.543
			Weighted mode	39.385	2.188E-03–7.090E+05	0.468		0.502
Anxiety disorders	BPPV	7	MR Egger	0.065	4.480E-28–9.384E+24	0.933	5 (0.385)	
			Weighted median	0.058	2.737E-11–1.214E+08	0.794		
			IVW	3.529E-04	1.037E-10–1.200E+03	0.300	6 (0.507)	
			Simple mode	9.836	3.593E-12–2.691E+13	0.881		
			Weighted mode	7.861	2.101E-12–2.941E+13	0.894		
Schizophrenia	BPPV	328	MR Egger	0.978	0.809–1.181	0.819	326 (0.609)	
			Weighted median	0.948	0.878–1.023	0.171		
			IVW	0.994	0.944–1.045	0.809	327 (0.624)	
			Simple mode	0.870	0.667–1.134	0.306		
			Weighted mode	0.864	0.672–1.109	0.253		
Suicidality	BPPV	10	MR Egger	0.866	0.497–1.509	0.626	8 (0.690)	
			Weighted median	1.012	0.684–1.496	0.951		
			IVW	0.975	0.730–1.301	0.864	9 (0.754)	
			Simple mode	1.130	0.648–1.968	0.677		
			Weighted mode	1.057	0.630–1.770	0.839		
Neuroticism	BPPV	263	MR Egger	1.042	0.760–1.427	0.798	261 (0.046)	0.757
			Weighted median	1.126	1.012–1.251	0.028		0.026
			IVW	1.142	1.059–1.231	0.001	262 (0.048)	0.0002
			Simple mode	1.034	0.730–1.463	0.851		0.902
			Weighted mode	1.066	0.768–1.480	0.701		0.716

(Continued)

TABLE 3 (Continued)

Exposure	Outcome	SNP	Method	OR	95% CI	P-value	Q_df (Q_pval)	P-value (MR-PRESSO after adjustment)
Mood swings	BPPV	179	MR Egger	2.713	0.195–37.608	0.458	177 (0.252)	
			Weighted median	2.357	0.928–5.979	0.071		
			IVW	3.119	1.652–5.884	0.0004	178 (0.269)	
			Simple mode	2.648	0.145–48.330	0.512		
			Weighted mode	1.795	0.132–24.352	0.661		

BPPV, Benign paroxysmal positional vertigo. Bold values indicates that *P*-values are significant.

a systemic stress response, leading to an inflammatory reaction. This regulation of an inflammatory reaction may serve a protective function in the short term, but sustained chronic inflammation stimulation may affect the functioning of the balance receptors in the inner ear, ultimately promoting the development of BPPV (39). Additionally, neuroticism and mood swings may enhance neural network activity, thereby affecting patients' visual balance control (40). Stable visual perception is crucial for individuals with BPPV (41). Further exploration of the relevant mechanisms is needed in the future. A deeper understanding of these mechanisms will aid in the development of more effective treatment strategies and preventive measures for BPPV.

Although our results suggest that there is no significant association between BPPV and five mental disorders (bipolar disorder, depression, anxiety disorder, schizophrenia, and suicidality), BPPV may have some influence on the occurrence and development of the five mental disorders. The underlying mechanisms of BPPV and mental disorders are complex. It is possible that long-term repeated harmful physical stimuli, such as chronic pain, may lead to emotional changes in patients, which may induce mental disorders (42). It has been suggested that somatic imbalance, spatial orientation disorder, nausea, and vomiting caused by recurrent vertigo attacks lead to secondary psychological distress (43). It has also been hypothesized that the cerebellar and vestibular systems play complementary roles in emotion regulation and that long-term maladaptation to the environment may lead to anxiety and depression (44, 45). Hemispheric lateralization may link vestibular systems to systems that process emotions (46). The chronic physical stress caused by BPPV will also continue to affect the hypothalamic–pituitary–adrenal (HPA) axis (47), and disorders of the HPA axis may affect mood in individuals (48). The exploration of the mechanisms underlying the correlation between neuroticism and mood swings and BPPV merits further study because of the association between BPPV and mental disorders, which may be significant for guiding future research on the underlying mechanisms of the associations between psychological states and BPPV.

To date, no MR study has examined the association between BPPV and mental disorders. We used MR analysis in this study to avoid the bias caused by confounding factors and sample size difficulties that occur in traditional clinical research. The reliability and accuracy of the study were improved. MR analysis

strengthened the causal relationship and reduced the probability of confounding and reverse causality. This study has some limitations. Because the datasets were obtained from a public database and the patients were of European ancestry, the results of this study were not necessarily generalizable to other regions or ethnic groups. Although we did not find horizontal pleiotropy after adjustment for MR-PRESSO, we cannot completely rule out that horizontal pleiotropy affected the generalizability of our results. Since the datasets used in this study were obtained from a public database, we cannot classify the sample population by age and sex or analyze their correlation more precisely. Although the findings of the study established a causal relationship between BPPV and neuroticism and mood swings, future research should involve additional design interventions targeting the risk factors for BPPV to aid in the development of better prevention for the recurrence of BPPV.

5 Conclusion

In summary, the results of the two-sample MR analysis revealed that BPPV was not significantly associated with five mental disorders (bipolar disorder, depression, anxiety disorders, schizophrenia, and suicidality). Neuroticism and mood swings are more likely to be the risk factors for BPPV. Therefore, we need to pay more attention to the psychological distress in BPPV patients, and we need to treat BPPV and prevent its recurrence. The association between BPPV and mental disorders is clarified to improve the early prevention and treatment of mental disorders and BPPV in clinical research. The findings of this study will help to improve the comprehensive medical management of patients with mental disorders and BPPV in clinical practice and contribute to further revealing the underlying mechanisms of mental disorders and BPPV.

Data availability statement

The original contributions presented in the study are included in the article/Supplementary material, further inquiries can be directed to the corresponding author.

Ethics statement

Ethical review and approval was not required for the study on human participants in accordance with the local legislation and institutional requirements. Written informed consent from the patients/participants or patients/participants' legal guardian/next of kin was not required to participate in this study in accordance with the national legislation and the institutional requirements.

Author contributions

SL: Conceptualization, Data curation, Software, Visualization, Writing – original draft. LZ: Investigation, Methodology, Project administration, Supervision, Writing – review & editing. DD: Project administration, Supervision, Visualization, Writing – review & editing, Conceptualization, Funding acquisition. WL: Project administration, Supervision, Visualization, Writing – review & editing.

Funding

The author (s) declare that no financial support was received for the research, authorship, and/or publication of this article.

References

- Kim HJ, Lee JO, Choi JY, Kim JS. Etiologic distribution of dizziness and vertigo in a referral-based dizziness clinic in South Korea. *J Neurol*. (2020) 267:2252–9. doi: 10.1007/s00415-020-09831-2
- Imai T, Inohara H. Benign paroxysmal positional vertigo. *Auris Nasus Larynx*. (2022) 49:737–47. doi: 10.1016/j.anl.2022.03.012
- von Brevern M, Radtke A, Lezius F, Feldmann M, Ziese T, Lempert T, et al. Epidemiology of benign paroxysmal positional vertigo: a population based study. *J Neurol Neurosurg Psychiatry*. (2007) 78:710–5. doi: 10.1136/jnnp.2006.100420
- Lindell E, Kollen L, Johansson M, Karlsson T, Ryden L, Falk Erhag H, et al. Benign paroxysmal positional vertigo: a systematic review and meta-analysis. *J Arch Otorhinolaryngol*. (2021) 278:1637–44. doi: 10.1007/s00405-020-06357-1
- Pauwels S, Casters L, Lemkens N, Lemmens W, Meijer K, Meyns P, et al. Gait and falls in benign paroxysmal positional vertigo: a systematic review and meta-analysis. *J Neurol Phys Ther*. (2023) 47:127–38. doi: 10.1097/NPT.0000000000000438
- Kim HJ, Park J, Kim JS. Update on benign paroxysmal positional vertigo. *J Neurol*. (2021) 268:1995–2000. doi: 10.1007/s00415-020-10314-7
- Steel Z, Marnane C, Iranpour C, Chey T, Jackson JW, Patel V, et al. The global prevalence of common mental disorders: a systematic review and meta-analysis 1980–2013. *Int J Epidemiol*. (2014) 43:476–93. doi: 10.1093/ije/dyu038
- Schofield DJ, Shrestha RN, Percival R, Passey ME, Callander EJ, Kelly SJ. The personal and national costs of mental health conditions: impacts on income, taxes, government support payments due to lost labour force participation. *BMC Psychiatry*. (2011) 11:72. doi: 10.1186/1471-244X-11-72
- Christensen MK, Lim CCW, Saha S, Plana-Ripoll O, Cannon D, Presley F, et al. The cost of mental disorders: a systematic review. *Epidemiol Psychiatr Sci*. (2020) 29:e161. doi: 10.1017/S204579602000075X
- Howard LM, Oram S, Galley H, Trevillion K, Feder G. Domestic violence and perinatal mental disorders: a systematic review and meta-analysis. *PLoS Med*. (2013) 10:e1001452. doi: 10.1371/journal.pmed.1001452
- Cai J, Wei Z, Chen M, He L, Wang H, Li M, et al. Socioeconomic status, individual behaviors and risk for mental disorders: a Mendelian randomization study. *Eur Psychiatry*. (2022) 65:e28. doi: 10.1192/j.eurpsy.2022.18
- Sun X, Liu B, Liu S, Wu DJH, Wang J, Qian Y, et al. Sleep disturbance and psychiatric disorders: a bidirectional Mendelian randomisation study. *Epidemiol Psychiatr Sci*. (2022) 31:e26. doi: 10.1017/S2045796021000810
- Hilton MP, Pinder DK. The Epley (canalith repositioning) manoeuvre for benign paroxysmal positional vertigo. *Cochrane Database Syst Rev*. 2014:CD003162. doi: 10.1002/14651858.CD003162.pub3
- Yang TH, Xirasagar S, Cheng YF, Chen CS, Lin HC. Does peripheral vestibular disorder increase the risk of attempted suicide: a retrospective cohort study. *J Affect Disord*. (2023) 341:12–6. doi: 10.1016/j.jad.2023.08.110
- Kim SK, Hong SM, Park IS, Lee HJ, Park B, Choi HG. Mood disorders are associated with increased risk of BPPV: a national sample cohort. *Laryngoscope*. (2021) 131:380–5. doi: 10.1002/lary.28638
- Yeo BSY, Toh EMS, Lim NE, Lee RS, Ho RCM, Tam WWS, et al. Association of benign paroxysmal positional vertigo with depression and anxiety—a systematic review and meta-analysis. *Laryngoscope*. (2023). doi: 10.1002/lary.30957
- Baxter AJ, Patton G, Scott KM, Degenhardt L, Whiteford HA. Global epidemiology of mental disorders: what are we missing? *PLoS ONE*. (2013) 8:e65514. doi: 10.1371/journal.pone.0065514
- Safer DJ. Mood swing and mood stabilizer: how specific are these terms? *Bipolar Disord*. (2010) 12:685–90. doi: 10.1111/j.1399-5618.2010.00870.x
- Ormel J, Jeronimus BF, Kotov R, Riese H, Bos EH, Hankin B, et al. Neuroticism and common mental disorders: meaning and utility of a complex relationship. *Clin Psychol Rev*. (2013) 33:686–97. doi: 10.1016/j.cpr.2013.04.003
- Trinidade A, Harman P, Stone J, Staab JP, Goebel JA. Assessment of potential risk factors for the development of persistent postural-perceptual dizziness: a case-control pilot study. *Front Neurol*. (2020) 11:601883. doi: 10.3389/fneur.2020.601883
- Zhong H, Huan X, Jiao K, He S, Wen Z, Zhao R, et al. Causal relationships between mood instability and autoimmune diseases: a mendelian randomization analysis. *Autoimmun Rev*. (2023) 22:103214. doi: 10.1016/j.autrev.2022.103214
- Birney E. Mendelian Randomization. *Cold Spring Harb Perspect Med*. (2022) 12:a041302. doi: 10.1101/cshperspect.a041302
- Pierce BL, Burgess S. Efficient design for Mendelian randomization studies: subsample and 2-sample instrumental variable estimators. *Am J Epidemiol*. (2013) 178:1177–84. doi: 10.1093/aje/kwt084
- Stahl EA, Breen G, Forstner AJ, McQuillin A, Ripke S, Trubetskoy V, et al. Genome-wide association study identifies 30 loci associated with bipolar disorder. *Nat Genet*. (2019) 51:793–803. doi: 10.1038/s41588-019-0397-8

Conflict of interest

The authors declare that the research was conducted in the absence of any commercial or financial relationships that could be construed as a potential conflict of interest.

Publisher's note

All claims expressed in this article are solely those of the authors and do not necessarily represent those of their affiliated organizations, or those of the publisher, the editors and the reviewers. Any product that may be evaluated in this article, or claim that may be made by its manufacturer, is not guaranteed or endorsed by the publisher.

Supplementary material

The Supplementary Material for this article can be found online at: <https://www.frontiersin.org/articles/10.3389/fneur.2024.1310026/full#supplementary-material>

25. Trubetskoy V, Pardinas AF Qi T, Panagiotaropoulou G, Awasthi S, Bigdeli TB, et al. Mapping genomic loci implicates genes and synaptic biology in schizophrenia. *Nature*. (2022) 604:502–8. doi: 10.1038/s41586-022-04434-5
26. Burgess S, Butterworth A, Thompson SG. Mendelian randomization analysis with multiple genetic variants using summarized data. *Genet Epidemiol*. (2013) 37:658–65. doi: 10.1002/gepi.21758
27. Burgess S, Thompson SG. Interpreting findings from Mendelian randomization using the MR-Egger method. *Eur J Epidemiol*. (2017) 32:377–89. doi: 10.1007/s10654-017-0255-x
28. Bowden J, Davey Smith G, Haycock PC, Burgess S. Consistent estimation in mendelian randomization with some invalid instruments using a weighted median estimator. *Genet Epidemiol*. (2016) 40:304–14. doi: 10.1002/gepi.21965
29. Hemani G, Zheng J, Elsworth B, Wade KH, Haberland V, Baird D, et al. The MR-Base platform supports systematic causal inference across the human genome. *Elife*. (2018) 7:e34408. doi: 10.7554/eLife.34408
30. Sun J, Ma X, Yang Y, He K, Wang W, Shen J, et al. Associations between cognition, anxiety, depression, and residual dizziness in elderly people with BPPV. *Front Aging Neurosci*. (2023) 15:1208661. doi: 10.3389/fnagi.2023.1208661
31. Kalderon L, Chaimoff M, Katz-Leurer M. The distinction between state and trait anxiety levels in patients with BPPV in comparison with healthy controls. *Front Psychol*. (2022) 13:1055467. doi: 10.3389/fpsyg.2022.1055467
32. Probst T, Dinkel A, Schmid-Mühlbauer G, Radziej K, Limburg K, Pieh C, et al. Psychological distress longitudinally mediates the effect of vertigo symptoms on vertigo-related handicap. *J Psychosom Res*. (2017) 93:62–8. doi: 10.1016/j.jpsychores.2016.11.013
33. Schick RR, Yaksh TL, Roddy DR, Go VL. Release of hypothalamic cholecystokinin in cats: effects of nutrient and volume loading. *Am J Physiol*. (1989) 256:R248–54. doi: 10.1152/ajpregu.1989.256.1.R248
34. Staab JP, Rohe DE, Eggers SD, Shepard NT. Anxious, introverted personality traits in patients with chronic subjective dizziness. *J Psychosom Res*. (2014) 76:80–3. doi: 10.1016/j.jpsychores.2013.11.008
35. Wolf J, Sattel H, Limburg K, Lahmann C. From illness perceptions to illness reality? Perceived consequences and emotional representations relate to handicap in patients with vertigo and dizziness. *J Psychosom Res*. (2020) 130:109934. doi: 10.1016/j.jpsychores.2020.109934
36. Sekula P, Del Greco MF, Pattaro C, Kottgen A. Mendelian randomization as an approach to assess causality using observational data. *J Am Soc Nephrol*. (2016) 27:3253–65. doi: 10.1681/ASN.2016010098
37. Koc A. Benign paroxysmal positional vertigo: is it really an otolith disease? *J Int Adv Otol*. (2022) 18:62–70. doi: 10.5152/iao.2022.21260
38. Chistyakov DV, Astakhova AA, Sergeeva MG. Resolution of inflammation and mood disorders. *Exp Mol Pathol*. (2018) 105:190–201. doi: 10.1016/j.yexmp.2018.08.002
39. Rohleder N. Stress and inflammation - The need to address the gap in the transition between acute and chronic stress effects. *Psychoneuroendocrinology*. (2019) 105:164–71. doi: 10.1016/j.psyneuen.2019.02.021
40. Passamonti L, Riccelli R, Lacquaniti F, Staab JP, Indovina I. Brain responses to virtual reality visual motion stimulation are affected by neurotic personality traits in patients with persistent postural-perceptual dizziness. *J Vestib Res*. (2018) 28:369–78. doi: 10.3233/VES-190653
41. Nair MA, Mulavara AP, Bloomberg JJ, Sangi-Haghighi H, Cohen HS. Visual dependence and spatial orientation in benign paroxysmal positional vertigo. *J Vestib Res*. (2018) 27:279–86. doi: 10.3233/VES-170623
42. Racine M. Chronic pain and suicide risk: a comprehensive review. *Prog Neuropsychopharmacol Biol Psychiatry*. (2018) 87(Pt B):269–80. doi: 10.1016/j.pnpbp.2017.08.020
43. Brandt T, Dieterich M. 'Excess anxiety' and 'less anxiety': both depend on vestibular function. *Curr Opin Neurol*. (2020) 33:136–41. doi: 10.1097/WCO.0000000000000771
44. Hilber P. The role of the cerebellar and vestibular networks in anxiety disorders and depression: the internal model hypothesis. *Cerebellum*. (2022) 21:791–800. doi: 10.1007/s12311-022-01400-9
45. Elyoseph Z, Geisinger D, Zaltzman R, Hartman TG, Gordon CR, Mintz M. The overarching effects of vestibular deficit: imbalance, anxiety, and spatial disorientation. *J Neurol Sci*. (2023) 451:120723. doi: 10.1016/j.jns.2023.120723
46. Bednarczuk NF, Casanovas Ortega M, Fluri AS, Arshad Q. Vestibulo-cortical hemispheric dominance: the link between anxiety and the vestibular system? *Eur J Neurosci*. (2018) 47:1517–24. doi: 10.1111/ejn.13948
47. Herman JP, McKlveen JM, Ghosal S, Kopp B, Wulsin A, Makinson R, et al. Regulation of the hypothalamic-pituitary-adrenocortical stress response. *Compr Physiol*. (2016) 6:603–21. doi: 10.1002/cphy.c150015
48. Wingfield K, Wolf OT. HPA axis alterations in mental disorders: impact on memory and its relevance for therapeutic interventions. *CNS Neurosci Ther*. (2011) 17:714–22. doi: 10.1111/j.1755-5949.2010.00207.x

Frontiers in Neurology

Explores neurological illness to improve patient care

The third most-cited clinical neurology journal explores the diagnosis, causes, treatment, and public health aspects of neurological illnesses. Its ultimate aim is to inform improvements in patient care.

Discover the latest Research Topics

[See more →](#)

Frontiers

Avenue du Tribunal-Fédéral 34
1005 Lausanne, Switzerland
frontiersin.org

Contact us

+41 (0)21 510 17 00
frontiersin.org/about/contact

